

NOVEL REGULATORS OF EPITHELIAL-TO-MESENCHYMAL
TRANSFORMATION IN CARDIOGENESIS ARE IDENTIFIED
THROUGH NEXT-GENERATION SEQUENCING

By

Daniel Morris DeLaughter

Dissertation

Submitted to the Faculty of the
Graduate School of Vanderbilt University
in partial fulfillment of the requirements
for the degree of

DOCTOR OF PHILOSOPHY

In

Cell and Developmental Biology

August 2013

Nashville, TN

Approved:

Professor Joey V. Barnett

Professor H. Scott Baldwin

Professor Christopher V. E. Wright

Professor Antonis K. Hatzopoulos

Professor Guoqiang Gu

For my Mother, Father, and Family

ACKNOWLEDGEMENTS

First, I thank the sources of funding that have allowed me the opportunity to attend graduate school and pursue my Ph.D research. In particular, I thank the Vanderbilt University Medical Center Program in Developmental Biology for awarding me the Developmental Biology Training Grant (T32 HD007502-12, T32 HD007502-13). I thank the Systems-based Consortium for Organ Design and Engineering (NIH U54 092551) overseen by Dick Moss which provided excellent opportunities to pursue an interdisciplinary research project and was instrumental in shaping how I view the potential of collaborative science.

I would like to thank the members of my committee, Chris Wright, Guoqiang Gu, and Antonis Hatzopoulos, for their advice and perspective. In particular, I am grateful to the chair of my committee, Chris Wright, for keeping me focused.

To my mentors Scott Baldwin and Joey Barnett, I thank you for your time and immense patience. I am infinitely grateful and deeply cherish the opportunities and unique perspectives that were provided. In particular, the attitude, enthusiasm, and willingness to take time to teach me you both displayed was exceedingly helpful in my growth as a scientist.

I thank the current and former members of the Baldwin laboratory for providing their expert advice and fellowship. Thank you Chris Brown, Kel Vin Woo, Paige Debenedittis, LeShana Saint-Jean, Kevin Tompkins, Kim Roberts, and Kate Violette.

I would like to specifically thank former members of the Barnett laboratory who made this work possible. Thank you Todd Townsend, Joseph Douglas Love, and Jon Soslow. I thank Jamille Robinson, who performed the NF-κB inhibitor experiment presented in Chapter II (Figure 13H) and provided considerable help when troubleshooting the collagen gel assay. Cyndi Hill's work with the epicardial cell culture system

was of immense help, providing key data validating a candidate signaling pathway identified in epicardial cells and is presented in Chapter III (Figure 24B-C).

I extend a heartfelt thanks to my collaborator Jon Seidman and the members of his laboratory whose assistance was fundamental to progress of my PhD work. I thank Danos Christodoulou, who designed and oversaw the RNA-seq methodology used in Chapter II and III. His kindness and constant willingness to provide advice was instrumental in moving my research forward. I would also like to thank Josh Gorham who was also of great assistance in generating the RNA-seq data sets.

Finally, I would like to thank my family for their faith and constant support. To my siblings, who from an early age toughened me up to deal with the slings and arrows (and noogies) of outrageous fortune, I give my heartfelt thanks and back away cautiously. In particular, I thank my brother, Andy, who always allowed me to bounce ideas off of him no matter how odd and fostered my curiosity. To my godson Nathan, I have enjoyed watching you grow up into a fine young man. Most of all, to my mother and father who have encouraged my academic and other pursuits from an early age I give my sincerest thanks. Your stability has helped me through many hard times and without it I would not be here today. Mom, Dad, thank you.

TABLE OF CONTENTS

	Page
DEDICATION.....	ii
ACKNOWLEDGEMENTS.....	iii
LIST OF FIGURES.....	vii
LIST OF TABLES.....	ix
LIST OF ABBREVIATIONS.....	x
Chapter	
I. INTRODUCTION	
Cardiovascular Disease.....	1
Epithelial-to-Mesenchmal Transformation in Development.....	4
EMT in Valvulogenesis.....	6
Formation of the Endocardial Cushions.....	8
Endocardial Cell Transformation.....	9
In Vitro Artioventricular Cushion Assay.....	11
What can <i>In Vitro</i> Results Tell Us About <i>In Vivo</i> Phenotypes?....	19
VIC Function in Valve Remodeling.....	22
Unique Functions for the Ventricular Endocardium.....	29
Summary of Valve Development.....	31
EMT in Coronary Vessel Development.....	32
Formation of the Epicardium.....	32
The Fate of EPDCs.....	33
Formation of Coronary Vessels.....	35
Signaling Pathways Regulating Epicardial EMT.....	37
TGFB Signaling in Coronary Vessel Development.....	37
Summary.....	43
II. SPATIAL TRANSCRIPTIONAL PROFILE OF THE CHICK AND MOUSE ENDOCARDIAL CUSHIONS IDENTIFY NOVEL REGULATORS OF ENDOCARDIAL EMT <i>IN VITRO</i>	
Introduction.....	45
Experimental Methods.....	48
Results.....	55
Defining a Spatial Transcriptional Profile of the Developing Heart Tube.....	55
Gene Ontology Analysis of Cushion-Enriched Genes.....	59
Gene Regulatory Network (GRN) Analysis of Cushion-Enriched Genes.....	63
Identification of Gene Candidates for Functional Analysis.....	66
Selection and Validation of Signaling Pathway	

Identified by GRN Analysis.....	72
Discussion.....	73
III. TRANSCRIPTIONAL PROFILING OF CULTURED, EMBRYONIC EPICARDIAL CELLS IDENTIFIES NOVEL GENES AND SIGNALING PATHWAYS REGULATED BY TGFBR3 <i>IN VITRO</i>	
Introduction.....	80
Experimental Methods.....	85
Results.....	90
Transcriptional profiles of <i>Tgfbr3^{+/+}</i> and <i>Tgfbr3^{-/-}</i> cells confirm epicardial cell identity and ligand response.....	90
Dysregulation of gene expression in epicardial cells lacking <i>TGFβR3</i>	93
NF-κB signaling is dysregulated in <i>Tgfbr3^{-/-}</i> epicardial cells <i>in vitro</i>	104
Discussion.....	105
IV. SUMMARY AND CONCLUSIONS.....	111
Appendix	
A. HH18 CHICK GENES WITH >1.25-FOLD HIGHER EXPRESSION IN AVC AND OFT COMPARED TO VEN.....	122
B. E11.0 MOUSE GENES WITH >1.25-FOLD HIGHER EXPRESSION IN AVC AND OFT COMPARED TO VEN.....	135
C. GO ANALYSIS OF HH18 CHICK GENES WITH 2-FOLD HIGHER EXPRESSION IN AVC AND OFT COMPARED TO VEN.....	141
D. GO ANALYSIS OF E11.0 MOUSE GENES WITH >1.25-FOLD HIGHER EXPRESSION IN AVC AND OFT COMPARED TO VEN.....	142
E. GENES >2-FOLD DYSREGULATED BETWEEN <i>TGFBR3^{+/+}</i> AND <i>TGFBR3^{-/-}</i> EPICARDIAL CELLS AFTER VEH INCUBATION.....	144
F. GENES >2-FOLD DYSREGULATED BETWEEN <i>TGFBR3^{+/+}</i> AND <i>TGFBR3^{-/-}</i> EPICARDIAL CELLS AFTER <i>TGFβ1</i> INCUBATION.....	160
G. GENES >2-FOLD DYSREGULATED BETWEEN <i>TGFBR3^{+/+}</i> AND <i>TGFBR3^{-/-}</i> EPICARDIAL CELLS AFTER <i>TGFβ2</i> INCUBATION.....	174
H. GENES >2-FOLD DYSREGULATED BETWEEN <i>TGFBR3^{+/+}</i> AND <i>TGFBR3^{-/-}</i> EPICARDIAL CELLS AFTER <i>BMP2</i> INCUBATION.....	189
REFERENCES.....	206

LIST OF FIGURES

Figure	Page
1. Endocardial cell populations exhibit functional heterogeneity during tubular heart morphogenesis.....	7
2. Viral gene transfer into the endocardium of the tubular heart	15
3. Comparison of <i>Tgfb3^{+/+}</i> and <i>Tgfb3^{-/-}</i> epicardial cell proliferation, apoptosis, and invasion <i>in vitro</i>	41
4. Spatial transcriptional profile of heart identifies cushion-enriched genes.....	49
5. Variability in RNA-seq data sets.....	50
6. Comparison of differential gene expression between E11.0 biological replicates.....	51
7. Spatial expression of select genes in the HH18 chick and E11.0 mouse heart tube	57
8. Spatial transcriptional profile of heart identifies cushion-enriched genes.....	60
9. Gene ontology, predicted protein location, and protein function of >2-fold cushion-enriched genes.....	61
10. Gene ontology, predicted protein location, and protein function of >1.25 cushion-enriched genes	62
11. Gene regulatory networks generated from cushion-enriched-gene lists identifies known regulators of endocardial EMT.....	64
12. Confirmation of cushion-enriched gene expression in E11.0 hearts.....	67
13. Candidate genes are required for endocardial EMT <i>in vitro</i>	69
14. Quantification of siRNA Knockdown	71
15. <i>Tgfb3^{-/-}</i> epicardial cells have dysregulated proliferation, apoptosis, and invasion.....	84

16. Immortalized epicardial cells undergo loss of epithelial character.....	87
17. Variability of RNA-seq data sets	88
18. Comparison of differential gene expression between biological replicates...	89
19. <i>Tgfbr3^{+/+}</i> and <i>Tgfbr3^{-/-}</i> epicardial RNA-seq datasets confirm cell identity and differential ligand response.....	92
20. RNA-seq analysis identifies genes dysregulated in <i>Tgfbr3^{-/-}</i> epicardial cells.....	94
21. Gene regulatory network analysis identifies NF-κB signaling as a central node after TGFβ1 or BMP2 incubation.....	98
22. Gene regulatory network analysis identifies NF-κB signaling as a central node after TGFβ1 or VEH incubation.....	101
23. Genes downstream of NF-κB signaling dysregulated with loss of <i>Tgfbr3</i> in epicardial cells <i>in vitro</i>	102
24. <i>Tgfbr3^{-/-}</i> epicardial cells fail to activate the NF-κB signaling pathway.....	103

LIST OF TABLES

Table	Page
1. Selected genes with valve formation defects <i>in vivo</i> in mouse knockout models.....	7
2. Primers Used to Confirm Gene Knockdown	53
3. siRNA Construct Sequences.....	54
4. Collagen Gel Assay Counting Data	54
5. Primers Used to Generate ISH Probes.....	55
6. Genes >2-fold Enriched in Chick or Mouse Cushions Previously Implicated in Cushion Development.....	58
7. Genes >2-fold Enriched in Both Chick and Mouse Cushions	75
8. GO Analysis of Genes >2-fold Differentially Expressed Between Genotypes Unique to Specific Ligand Incubation Groups.....	97

LIST OF ABBREVIATIONS

°C	Degrees Celsius
β-Arrestin2	Beta-arrestin2
β-gal	Beta-galactosidase
µM	micromolar
µL	microliter
ALK	Activin Receptor-Like Kinases
AVC	Atrioventricular
BMP	Bone Morphogenetic Protein
BSA	Bovine Serum Albumin
CHD	Congenital Heart Disease
CHST3	Carbohydrate (chondroitin 6) Sulfotransferase 3
COL	Collagen
Cre	Cre Recombinase
DAPI	4',6-diamidino-2-phenylindole
DORV	Double Outlet Right Ventricle
E	Embryonic
EPDC	Epicardially-Derived Cell
EMT	Epithelial-Mesenchymal Transformation
ES	Embryonic stem
FBS	Fetal Bovine Serum
FGF	Fibroblast Growth Factor
FGFR	Fibroblast Growth Factor Receptor
FOX	Forkhead box
GFP	Green Fluorescent Protein

GIPC	GAIP-interacting protein, C terminus
GRN	Gene Regulatory Network
HA	Hyaluronic Acid
HAPLN1	Hyaluronic acid and proteoglycan link protein 1
HAS2	Hyaluronic acid synthase 2
HH	Hamburger-Hamilton
ID1	Inhibitor of DNA binding 1
ID3	Inhibitor of DNA binding 2
IκB	Inhibitor of kappa B protein
IKK	I kappa B kinase
M	Molar
MAP	Mitogen Activated Protein
MATN4	Matrilin 4
MEIS2	Myeloid ecotropic viral integration site 2 homolog
ml	milliliter
mRNA	messenger Ribonucleic Acid
NF-κB	Nuclear Factor- kappa B
ng	nanograms
OFT	Outflow Tract
oligo	oligonucleotide
PAR6	Par-6 partitioning defective 6 homolog gamma
PBS	Phosphate Buffered Saline
PCR	Polymerase Chain Reaction
PDGF	Platelet-Derived Growth Factor
PDGFR	Platelet-Derived Growth Factor Receptor
PECAM	Platelet Endothelial Cell Adhesion Molecule

PFA	Paraformaldehyde
PI3K	Phosphoinositol 3 Kinase
pM	picomolar
R-	Receptor
RA	Retinoic Acid
RALDH2	Retinaldehyde dehydrogenase
RHOA	Ras homolog gene family member A
RNA	Ribonucleic Acid
RNA-seq	Ribonucleic Acid Sequencing
RT	Room Temperature
qRT-PCR	Quantitative Reverse Transcriptase Polymerase Chain Reaction
SEAP	Secreted Alkaline Phosphotase
SLUG	Snail homolog 2
SMURF1	Smad ubiquitination regulatory factor1
SM22 α	Smooth Muscle 22 alpha
SMaA	Smooth Muscle alpha Actin
SNAI1	Snail homolog 1
SOX	SRY-box containing gene 9
TBX	T-box
TGF β	Transforming Growth Factor Beta
TGF β R1	Type I TGF β receptor
TGF β R2	Type II TGF β receptor
TGF β R3	Type III TGF β receptor
TRAF6	TNF Receptor-associated Factor 6, E3 ubiquitin protein ligase

TWIST1	Twist homolog 1
VCAM-1	Vascular Cell Adhesion Molecule
VCAN	Versican
VEGF	Vascular Endothelial Growth Factor
VEGFR	Vascular Endothelial Growth Factor Receptor
VEN	Ventricle
VIC	Valvular Interstitial Cell
WNT	Wingless Type
WT-1	Wilm's Tumor-1
ZO-1	Zonula Occludins-1

CHAPTER I

INTRODUCTION

Cardiovascular Disease

Cardiovascular disease is the leading cause of death in the world whose incidence has increased in the last 20 years (Lozano, Naghavi et al. 2012; Go, Mozaffarian et al. 2013), with over 2000 people dying of cardiovascular disease every day in the United States alone (Go, Mozaffarian et al. 2013). Cardiovascular disease is a heterogeneous complaint compromising a wide spectrum of conditions that includes, but is not limited to, valvular heart disease, coronary heart disease, cardiomyopathy, hypertension, cerebral vascular disease, and arrhythmia. Valvular heart disease comprises a significant proportion of cardiovascular disease in children and adults, affecting an estimated 2.5% of the population of the United States (Go, Mozaffarian et al. 2013). In adults, disease may result from valvular injury as a result of infection (Connolly, Crary et al. 1997), pharmacological therapy (Mylonakis and Calderwood 2001), or tumorigenesis (Robiolio, Rigolin et al. 1995). Together, these factors result in over 100,000 Americans a year undergoing surgery to repair or replace heart valves (Roger, Go et al. 2012). As the population becomes older and as the risk factors associated with adult valvular disease become more prevalent, the incidence of valvular heart disease is expected to

rise and remain a major public health concern (Lozano, Naghavi et al. 2012; Go, Mozaffarian et al. 2013).

Coronary heart disease is a major source of mortality in the United States and is associated with 1 of every 6 deaths (Lloyd-Jones, Adams et al. 2010). Coronary heart disease arises from a failure of the coronary vessels to supply sufficient circulation to the cardiac muscle, resulting in ischemic injury referred to as myocardial infarction. While advances in therapeutic and reperfusion strategies have improved survival rates in patients with myocardial infarction (Parikh, Gona et al. 2009), survivors have increased the pool of patients at risk of developing heart failure (Lewis, Moye et al. 2003). The overwhelming incidence of coronary heart disease requires renewed efforts to understand this disease process and develop new therapeutic modalities that may increase the efficiency of repair and preclude later disease progression.

Congenital Heart Disease and Cardiac Repair

Congenital Heart Disease (CHD), which includes defects in valvular and coronary vessel development, occurs in 1 out of 100 live births and is responsible for ten percent of infant deaths per year (Loffredo 2000; Barnett and Desgrosellier 2003; Hauser 2005). Ninety percent of children with CHD now live to adulthood due to the surgical and medical advances of the past half century (Khairy, Hosn et al. 2008). As a result, adults now represent the largest age group with CHD, but because they are a relatively new class of patient, treatment

approaches are as yet unclear (Doetschman T 2012). Also, it is now well recognized that there is a developmental basis to adult cardiovascular disease (Doetschman T 2012). Currently, it is thought that the homeostatic and repair functions present in adults may use many of the same mechanisms involved in the original development and remodeling of these tissues. Indeed, several lines of evidence support the importance of developmental processes in cardiac repair and cardiac response to injury (reviewed (von Gise and Pu 2012)). Evidence includes a demonstrated role of the epicardium in myocardial repair (Limana, Capogrossi et al. 2011; Vieira and Riley 2011) after injury in response to insults such as resection (Lepilina, Coon et al. 2006; Major and Poss 2007; Kikuchi, Gupta et al. 2011) or ischemia (Zhou, Honor et al. 2011). After coronary ligation in mice, the epicardium undergoes specific morphological alterations and begins to express angiogenic factors (Zhou, Honor et al. 2011). Coronary ligation stimulates re-expression of the embryonic epicardial markers *Raldh2*, *Tbx18*, & *Wt1* (Zhou, Honor et al. 2011) as epicardial cells and epicardially derived cells (EPDCs) begin to divide and increase in number. These epicardial cells lose epithelial character (EC) (Zhou, Honor et al. 2011) and express markers of EMT (van Wijk, Gunst et al. 2012). EPDC's were found to differentiate along myofibroblast/fibroblast and smooth muscle lineages, assumed perivascular locations, and potently stimulated blood vessel formation in angiogenesis assays (Zhou, Honor et al. 2011). Whether these EPDCs subsequently invade into the myocardium is still controversial. Two different studies using viral labeling reported cell invasion in response to injury suggesting that some cells may

invade into the myocardium (Limana, Zacheo et al. 2007; Gittenberger-de Groot, Winter et al. 2010). These investigators also reported the generation of additional cell types by the epicardium, most notably myocardium. There are conflicting studies that label epicardial cells in mice using *Wt1*^{creERT2} (Zhou, Honor et al. 2011) or *Wt1*^{cre} (van Wijk, Gunst et al. 2012) that either disagree and agree with the invasion and myocardial differentiation of EPDCs after injury respectively. Although some results vary, together these studies establish that in response to cardiac injury the activated epicardium re-expresses developmental markers, undergoes EMT, and secretes angiogenic factors.

Epithelial-to-Mesenchymal Transformation in Development

Epithelial-to-Mesenchymal Transformation (EMT) is an important process in development (Lim and Thiery 2012), and occurs during key steps in both valvular (DeLaughter, Saint-Jean et al. 2011) and coronary vessel development (von Gise and Pu 2012). EMT arises when an epithelial cell undergoes a morphological and phenotypic transition from an epithelial cell into a motile mesenchymal cell (Kalluri 2009). Mesenchymal cells may then undergo Mesenchymal-to-Epithelial Transformation (MET) to generate secondary epithelial cell populations during organogenesis. In this manner EMT is a process that generates cell diversity during development. EMT is also important in adults, regulating cancer progression and metastasis, tissue regeneration, and fibrosis (reviewed (Kalluri and Weinberg 2009)). Despite the importance of EMT the signaling pathways regulating EMT are still incompletely understood.

Specific morphological and molecular cellular processes must necessarily occur during EMT if an epithelial cell is to transitions into a mesenchymal cell (Zeisberg and Neilson 2009). Briefly, the initial steps of EMT involve the loss of apical-basal polarity as tight-junctions and other adhesion complexes are disassembled (Enciso, Gratzinger et al. 2003; Ma, Lu et al. 2005). This adhesion complexes, particularly E-cadherin, and loss of EC is thought to be mediated by transcription factors associated with EMT whose expression is normally seen in transitioning cells. These transcriptional repressors include *Goosecoid*, *Lef1*, *Snai1*, *Slug*, *Twist1*, *Zeb1*, and *Zeb2* among others (Timmerman, Grego-Bessa et al. 2004; Niessen, Fu et al. 2008; Shelton and Yutzey 2008). These changes result in a major reorganization of the cytoskeleton, which morphologically can be viewed as rounded epithelial cells becoming elongate and assuming a mesenchymal phenotype. The expression of mesenchymal markers, which may include *Smooth Muscle α -Actin* (*SM α A*), is indicative of this change in cytoskeleton organization (Nakajima, Mironov et al. 1997). Other mesenchymal or fibroblast markers can be upregulated during EMT, including *Cnn1* and *Fsp1*(Zeisberg and Neilson 2009). Expression of a particular mesenchymal marker is dependent on the cells and the cellular context where EMT occurs. For example, cells undergoing EMT during a fibrotic event often express *Fsp1* whereas cells undergoing EMT during gastrulation do not initially express *Fsp1*(Strutz, Okada et al. 1995). A fundamental function of EMT is to make motile cells, and as such the migration or invasion of cells into a substrate after EMT is an important functional indicator that EMT has occurred. Together, loss of

EC, through a switching of adhesion complexes and cytoskeletal reorganization, and invasion into a substrate are key landmarks in defining whether a cell has undergone EMT.

Understanding the upstream signaling events which promote these processes in EMT has provided fundamental insights into organogenesis, including valvulogenesis and coronary vessel development.

EMT in Valvulogenesis

After the primitive heart tubes fuse in a cranial to caudal process, the heart undergoes looping, bringing the common atria superior to the common ventricle (DeRuiter, Poelmann et al. 1992). The tubular heart at this point is comprised of two concentric layers of epithelium: the outer myocardial layer and the inner endocardial layer (Figure 1A). In between these layers is an acellular, gel-like matrix, the cardiac jelly. At Hamburger-Hamilton (HH) stage 14 (Hamburger and Hamilton 1951) in the chick or E9.0 in the mouse the cardiac jelly in the regions of the atrioventricular (AV) canal and the distal outflow tract (OFT) expands to form the endocardial cushions. A pivotal step in valvulogenesis occurs when a subpopulation of endocardial cells overlaying the endocardial cushions undergo EMT (Figure 1B). The resulting mesenchymal cells populate the cardiac cushions and by multiple methods aid in the formation of the valves and septa of the adult heart (reviewed (Aikawa, Whittaker et al. 2006; Butcher and Markwald 2007)). Therefore, it is important to understand the signaling

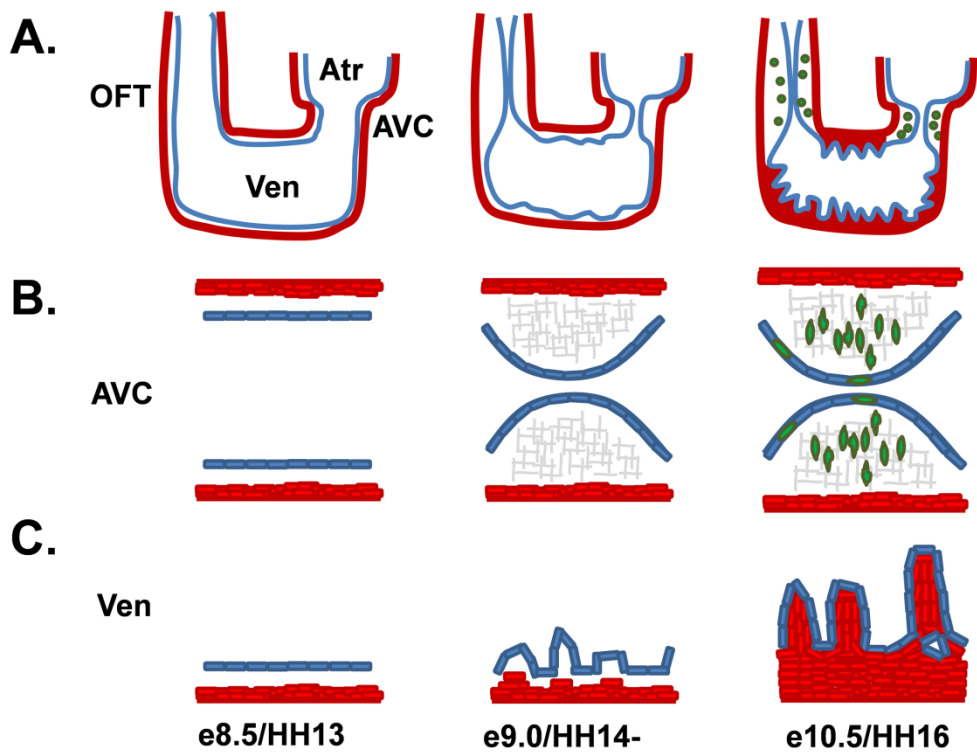


Figure 1: Endocardial cell populations exhibit functional heterogeneity during tubular heart morphogenesis. **A.** At e8.5/HH13, the u-shaped tubular heart is comprised of an outer layer of Myocardium (Red) and an inner layer of Endocardium (blue) with a layer of cardiac jelly in between. It possesses a common outflow tract (OFT), ventricle (Ven), atria (Atr) and atrioventricular canal (AVC), the region between the atria and ventricle. **B.** By e9.0/HH14- swellings of ECM restricted to the AVC and OFT form the endocardial cushions. Endocardial cells in the AVC initiate EMT soon afterwards, while the OFT endocardium undergo EMT at a later stage. By e10.5/HH16 endocardial cells overlaying the cushions undergo EMT and invade cardiac jelly. **C.** The ventricular endocardium does not undergo EMT at this time, rather it begins the complicated process of trabeculation around this time. The atrial endocardium undergoes neither EMT or trabeculation at this time.

pathways regulating endocardial EMT, but the developmental context, the endocardial cushions, and the heterogeneity observed between the endocardium of the cushions endocardium and the non-transforming ventricular endocardium.

Formation of the Endocardial Cushions

The endocardium displays functional heterogeneity during both the formation of the endocardial cushions and subsequent endocardial EMT. The first sign of this endocardial cell heterogeneity is seen in the initial formation of the endocardial cushions. The expansion of the endocardial cushions is due to the myocardial secretion of a glycosaminoglycan rich matrix which includes hyaluronic acid, versican and collagen I (Manasek 1970; Manasek, Reid et al. 1973). Injection of hyaluronanidase into the cushions of chick embryos to cause breakdown of hyaluronic acid caused cushion formation to fail (Baldwin and Solursh 1989). These data were confirmed in the mouse by the inactivation of hyaluronan synthase 2 (*Has2*), which is specific to the cushion forming regions in the heart, to eliminate hyaluronic acid synthesis. Targeting *Has2* precludes endocardial cushion formation and subsequent valve development (Camenisch, Spicer et al. 2000). Similarly, disruption of *Cspg2*, which encodes the Extracellular Matrix (ECM) protein Versican, yields a similar phenotype wherein the endocardial cushions are absent from the tubular heart among other heart defects (Mjaatvedt, Yamamura et al. 1998). Thus, the ECM of the endocardial cushions is distinct from that of the adjacent ventricle and atria.

The signals which induce cushion formation are incompletely described, but include Bmp, Wnt and Notch signaling pathways (Lyons, Pelton et al. 1990; Schubert, Mootoosamy et al. 2002; Timmerman, Grego-Bessa et al. 2004). *Bmp2* is expressed in the AV and OFT myocardium prior to cushion expansion, starting at E8.5 (Sugi, Yamamura et al. 2004). Mouse embryos with myocardial specific deletion of *Bmp2* lack AV cushions, have decreased Has2 expression corresponding with decreased ECM deposition, and possess AV myocardium patterning defects (Ma, Lu et al. 2005). Notch has also been shown to be required for endocardial cushion formation. Mice with deletions of *Notch1* or its associated transcription factor RBPJk lack cushions (Timmerman, Grego-Bessa et al. 2004). Inhibition of canonical Wnt signaling by overexpression of the Wnt antagonist Dickkopf-1 in zebrafish or by endothelial β -catenin deletion in mice prevents cushion tissue formation, while expansion of Wnt signaling with β -catenin in zebrafish or Wnt9A overexpression in chick expand the domain of the endocardial cushions (Hurlstone, Haramis et al. 2003; Liebner, Cattelino et al. 2004; Person, Garriock et al. 2005). These data identify Wnt signaling as a regulator of endocardial cell heterogeneity. The ultimate inductive signal that specifies and induces cushion formation, and the identity of the associated endocardium, is unknown.

Endocardial Cell Transformation

Immediately after cushion formation at HH14⁺/E9.5, factors secreted by the myocardium induce a subpopulation of endocardial cells overlying the cardiac

cushions to undergo EMT. The criteria for determining if an endocardial cell has undergone EMT are derived from the morphological and molecular events which occur if an epithelial cell in a sheet is to transition into a mesenchymal cell. Briefly, the apical-basal polarity of the endothelial cells is lost as tight-junctions and other adhesion complexes are disassembled. VE-cadherin and PECAM-1, important in endothelial cell-cell adhesion, are downregulated during the initial steps of EMT and their loss is associated with the loss of the endothelial phenotype (Enciso, Gratzinger et al. 2003; Ma, Lu et al. 2005). The downregulation of cadherins and other adhesion complexes is thought to be mediated by transcription factors associated with EMT whose expression is normally seen in transitioning cells. These transcriptional repressors include snai1, slug, twist1, and goosecoid among others (Timmerman, Grego-Bessa et al. 2004; Niessen, Fu et al. 2008; Shelton and Yutzey 2008). Loss of tight junctions and cell-cell adhesion cause a major reorganization of the cytoskeleton, which morphologically can be viewed as endothelial cells losing their rounded, ‘cobblestone’ appearance and becoming elongate. The expression of Smooth Muscle α -Actin (SMA) is a hallmark of cushion EMT and indicative of this change in cytoskeleton organization (Nakajima, Mironov et al. 1997). During this process the transformed cells in the endocardial cushions also lose markers of endocardial cushion identity such as Nfatc1 (de la Pompa, Timmerman et al. 1998). A fundamental function of EMT is to make motile cells, and as such migration and invasion into the basal substrate are critical steps made possible

by the transition from the stationary epithelial to the more motile mesenchymal phenotype.

In Vitro Atrioventricular Cushion Assay

Atrioventricular cushion (AVC) transformation has been studied extensively in avian systems using an *in vitro* assay in which the AVC is excised and placed on a collagen gel (reviewed (Barnett and Desgrosellier 2003). In this assay, transformation can be divided into three steps based on cellular morphology. Endocardial cells separate from the epithelial sheet and elongate in a step termed activation. Next, elongate mesenchymal cells enter the matrix, a step termed invasion. Finally, cells migrate through the gel in the migration step. These three steps - activation, invasion, and migration - constitute EMT. As in the developing heart, EMT is tightly restricted such that endocardial cells in AVC explants undergo EMT whereas endocardial cells in the ventricle do not (Bernanke and Markwald 1982; Mjaatvedt, Lepera et al. 1987). Transforming cells alter their pattern of gene expression downregulating molecules such as the endothelial marker PECAM-1 and upregulating SM α A and procollagen type I (Brown, Boyer et al. 1996; Sugi, Yamamura et al. 2004). EMT can be quantitated by counting the number of cells in the gel.

This system has been used to demonstrate that the endocardium of the cushions is functionally different from the endocardium overlaying the ventricle (Mjaatvedt, Lepera et al. 1987). In *in vitro* explants assays, the myocardium adjacent to the endocardial cushions is necessary for the endocardium to

undergo EMT (Bernanke and Markwald 1982). Removal of this myocardium results in a lack of EMT, indicating that inductive signals from the myocardium adjacent to the cushions regulate endocardial EMT (Krug, Mjaatvedt et al. 1987). Ventricular myocardium incubated with cushion endocardium does not result in EMT which implies that the inductive signal is present only in myocardium associated with the cushions. In addition, incubating AV cushion myocardium with ventricular endocardium does not result in endocardial EMT, demonstrating that the endocardium of the cushions is functionally distinct from endocardium overlaying the ventricles. Thus, there is restriction of both the endothelial cell population that transforms and restriction of the myocardial cell population that signals EMT. While the penultimate mechanism underlying this functional heterogeneity in the endocardium is unknown, extensive investigation of this system has defined distinct gene expression profiles and signaling pathway activation in the cushion endocardium as compared to the rest of the endocardium.

The collagen gel assay has been used for several years to study the process of endocardial cell EMT and has led to the identification of several key molecules in EMT (Barnett 2003; Schroeder, Jackson et al. 2003; Butcher and Markwald 2007). A role for members of the TGF β family were identified in this manner and have been shown to be key regulators of endocardial cell EMT (reviewed (Barnett and Desgrosellier 2003)). Three TGF β ligands signal through three receptors: the TGF β Type I (TGF β R1), Type II (TGF β R2), and Type III (TGF β R3) receptors. In the canonical signaling pathway (Shi and Massague

2003) ligand binding to TGF β R2 recruits TGF β R1, activin receptor like kinase (ALK) 5, to the complex. The constitutively active kinase of TGF β R2 phosphorylates and activates the kinase domain of ALK5 which subsequently phosphorylates and activates downstream receptor associated (R-) Smads 2 and 3 (Kretzschmar and Massague 1998). TGF β R3 or betaglycan has a short, highly conserved intracellular domain with no apparent signaling function (Lopez-Casillas, Cheifetz et al. 1991; Wang, Lin et al. 1991; Cheifetz, Bellon et al. 1992). Endoglin is a TGF β co-receptor that shares this highly conserved intracellular domain with TGF β R3 (Lopez-Casillas, Cheifetz et al. 1991). Endoglin regulates endothelial cell migration and proliferation via interactions with ALK1 and ALK5 (Goumans, Valdimarsdottir et al. 2002; Goumans, Valdimarsdottir et al. 2003; Lebrin, Goumans et al. 2004; Lee, Ray et al. 2008). Using the chick *in vitro* model of endothelial cell EMT, and a combination of ligand addition, neutralizing antisera (Potts and Runyan 1989), and antisense oligonucleotides (Potts, Dagle et al. 1991; Mercado-Pimentel, Hubbard et al. 2007), the ligands TGF β 1, TGF β 2, and TGF β 3 as well as TGF β R1 (ALK5), TGF β R2, Endoglin, and TGF β R3 have all been implicated in endocardial cell EMT (reviewed (Barnett 2003; Person, Klewer et al. 2005).

The coupling of experimental embryology with viral gene transfer increased the utility of the AVC transformation assay to test for the role of molecules using both gain and loss of function paradigms (Figure 2). This was first demonstrated by overexpressing TGF β R3 in nontransforming ventricular cells and inducing EMT with ligand addition (Brown, Boyer et al. 1999). This was

compared with antisera to target the receptor in the AVC to inhibit EMT, a result later confirmed by siRNA (Townsend 2011). Therefore, explants from specific regions of the heart tube can be used to determine if molecules are sufficient, required, or both for EMT. This ability to score for gain-of-function and loss-of-function of candidate molecules provides a powerful system in which to assay for molecules that regulate EMT (Desgrosellier, Mundell et al. 2005; Kirkbride, Townsend et al. 2008; Townsend, Wrana et al. 2008). These studies catalyzed an examination of the role of signaling molecules in endocardial cell EMT and the development and characterization of an *in vitro* system in the mouse (Camenisch, Molin et al. 2002). Studies have shown that downstream signaling molecules such as ALK2, Par6, and Smurf1 are both required and sufficient for EMT whereas ALK5, a major downstream effector of TGF β , is only required (Lai, Beason et al. 2000; Desgrosellier, Mundell et al. 2005; Townsend, Wrana et al. 2008). The requirement for ALK5 activity, Par6, and Smurf1 for TGF β R3-dependent endocardial cell EMT is consistent with the documented role of this pathway in the dissolution of tight junctions (Ozdamar, Bose et al. 2005). A modification of these experiments used overexpression of TGF β R3 in normally nontransforming ventricular endocardial cells to identify additional ligands for TGF β R3. These experiments demonstrate that BMP2 not only binds to but can signal via TGF β R3 (Kirkbride, Townsend et al. 2008; Kirkbride, Townsend et al. 2008). Overexpression of TGF β R3 in normally nontransforming ventricular endocardial cells was also used to demonstrate that TGF β R3-dependent

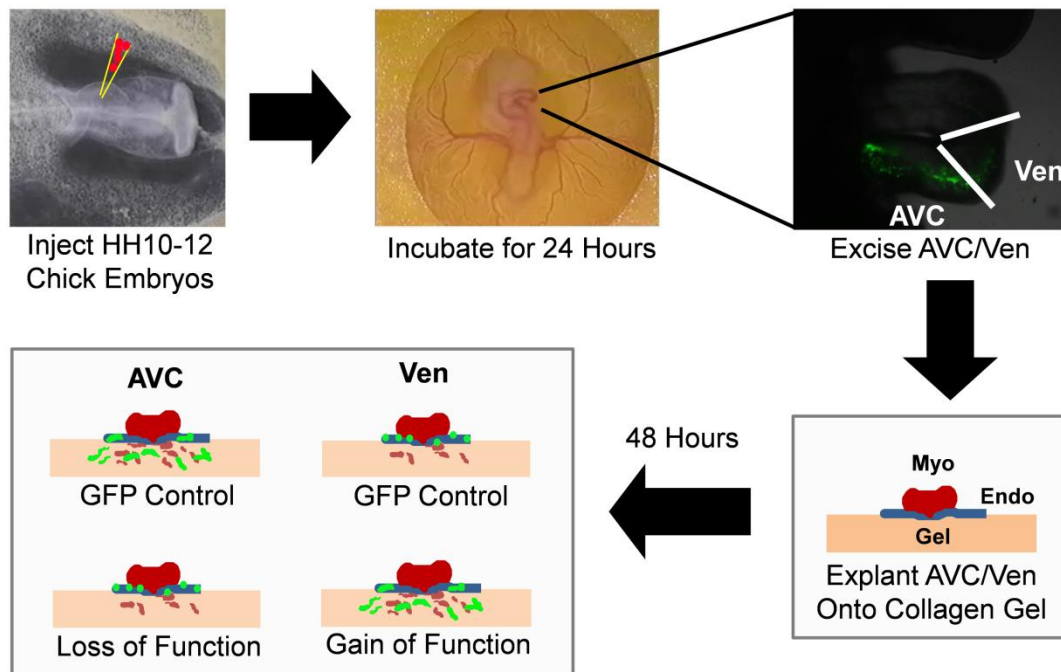


Figure 2: Viral gene transfer into the endocardium of the tubular heart. HH10-12 chicks are dissected into Whatman rings and injected with virus expressing either GFP or a gene of interest. These embryos are incubated for 24 hours on egg agar. The atrioventricular canal (AVC) or ventricle (Ven) are excised, cut lengthwise, and explanted endocardial side down onto a collagen I gel. After 48 hours incubation, the explants are fixed and the total number of GFP positive transformed cells (in green) in the gel are counted. Loss of function can be scored as a reduction in the number of transformed cells in gels incubated with AVC explants. Gain of function scored is scored as the increase in the total number of transformed GFP positive cells in gels incubated with Ven explants. Abbreviations: Endo-Endocardium, Myo-Myocardium, Gel-Rat tail collagen 1.

endocardial cell EMT stimulated by either TGF β 2 or BMP2 requires Smad4 and activation of the Par6/Smurf1/RhoA pathway (Townsend 2011).

These approaches, combined with genetic manipulation experiments in species such as mouse and zebrafish, have established roles for several factors, such as TGF β s, BMP, Notch, Wnt- β catenin, and VEGF, as well as extracellular matrix molecules, in regulating endocardial cell EMT (reviewed (Barnett 2003; Schroeder, Jackson et al. 2003; Person, Klewer et al. 2005; Combs and Yutzey 2009) and Table 1). In particular, studies on BMP and Notch signaling pathways further emphasized the importance of signaling interactions between the endocardium and myocardium during endocardial cell EMT. *In vivo*, BMP2 is expressed specifically in the cushion myocardium and signals to the cushion endocardium to promote EMT (Lyons, Pelton et al. 1990; Sugi, Yamamura et al. 2004; Ma, Lu et al. 2005). BMP type I receptors ALK2 and ALK3, both of which bind BMP2, are required in the endocardium for transformation in the cushion to occur (Wang, Sridurongrit et al. 2005; Song, Fassler et al. 2007). A constitutively active form of ALK2 is sufficient to drive endocardial cell EMT ectopically in ventricular explants *in vitro* (Desgrosellier, Mundell et al. 2005). This myocardial induced BMP signaling drives the endocardial expression of genes important in the progression of EMT, such as Twist1, Msx1, and Msx2, which are expressed in endothelial cells as they transition into mesenchyme (Ma, Lu et al. 2005). Notch signaling in the developing cushions has been shown to interact with BMP2 signaling during tubular heart development. Notch signaling is required for cushion EMT and linked to BMP2 signaling (Timmerman, Grego-Bessa et al.

2004). Notch1 signaling activity is restricted to the endocardium overlaying the cushions and drives Snai1 expression (Luna-Zurita, Prados et al. 2010). While *Notch1* targeted mice have hypoplastic valves, recent work has demonstrated that mice expressing the active form of the Notch receptor throughout the endocardium have expanded regions of EMT marker expression *in vivo*, though BMP2 is required to drive full invasion of ventricular endocardium *in vitro* (Luna-Zurita, Prados et al. 2010). Interestingly, increased Notch signaling in the myocardium reduces BMP2 expression there, while Notch1 deletion in the endocardium expands BMP2 expression, suggesting that the endocardium also signals back to the myocardium during valvulogenesis. Therefore, not only does the myocardium send inductive signals to the endocardium, intact endocardial signaling is required for proper myocardial restriction of BMP signaling. A more robust appreciation of other signal pathways involved in endocardial to myocardial signaling interaction may yield important insights into regulation of endocardial cell EMT during valve development.

A recent example of a concerted approach using mouse and chick model systems to address the role of specific molecules in the endocardium is the identification of the roles of Eph3A and Eph1A in endocardial EMT and valvulogenesis (Frieden 2010). Eph3A is abundantly expressed in the valve mesenchyme as early as e10.5. Targeted deletion of *Eph3A* resulted in hypoplastic cushions associated with decreased EMT and mesenchyme production (Stephen, Fawkes et al. 2007). Eph1A was noted to be expressed in the endocardial cells adjacent to the mesenchyme suggesting that Eph1A

Table 1: Selected genes with valve formation defects *in vivo* in mouse knockout models.

Receptor	Expression in Cushion	KO Phenotype	CHD
<i>Alk2</i>	Endo (Desgrosellier, Mundell et al. 2005)	Endo deletion causes hypoplastic valves (Wang, Sridurongrit et al. 2005)	Primum type ASD, MVP (Smith, Joziasse et al. 2009) ~
<i>Alk3</i>	Endo/Mese/Myo (Dewulf, Verschueren et al. 1995)	Endo deletion causes hypoplastic valves, Myo deletion causes interventricular septum, trabeculae and AV cushion defects (Song, Fassler et al. 2007)	~
<i>Alk5</i>	Endo/Mese/Myo	Endo deletion results in hypoplastic valves (Sridurongrit, Larsson et al. 2008)	~
<i>Bmpr2</i>	Endo/Mese/Myo	Defective septation of conotruncus, atrial septal defect, membranous VSD, and thickened valve leaflets (Beppu, Malhotra et al. 2009)	AVSD, ASD, PDA, PAPVR+PAH (Roberts, McElroy et al. 2004)
<i>Tgfβr2</i>	Endo/Mese/Myo	DILV (Jiao, Langworthy et al. 2006)	~
<i>Tgfβr3</i>	Endo (Brown, Boyer et al. 1999)	Enlarged Valves (ECM) (Unpublished)	~
<i>Notch1</i>	Endo (Loomes, Taichman et al. 2002; Timmerman, Grego-Bessa et al. 2004)	No cushion formation (Timmerman, Grego-Bessa et al. 2004)	VSD, TOF, BAV, MVS (Timmerman, Grego-Bessa et al. 2004; Garg, Muth et al. 2005; Mohamed, Aherrahrou et al. 2006; McKellar, Tester et al. 2007)

Ligands

<i>Bmp2</i>	Myo (Lyons, Pelton et al. 1990)	Cushions do not swell, no EMT, AV Myo patterning defects (Ma, Lu et al. 2005)	~
<i>Tgfβ2</i>	Endo/Mes/Myo (Dickson, Slager et al. 1993)	Conotruncal cardiac malformations (Sanford, Ormsby et al. 1997)	~
<i>Hb-Egf</i>	Endo(Jackson, Qiu et al. 2003)	Enlarged Valves (Iwamoto, Yamazaki et al. 2003)	~

Extracellular Matrix Associated Molecules

<i>Vscn</i>	Myo (Zanin, Bundy et al. 1999)	No cushion formation (Mjaatvedt, Yamamura et al. 1998)	~
<i>Postn</i>	Mese (Kruzynska-Frejtag, Machnicki et al. 2001)	Remodeling defects, AV mesenchyme maturation defects (Norris, Moreno-Rodriguez et al. 2008)	~
<i>Has2</i>	Endo/Mese/Myo (Camenisch, Spicer et al. 2000)	No cushion formation (Camenisch, Spicer et al. 2000)	~

Adapted from (DeLaughter et al. 2011)

functioned as a ligand to stimulate Eph3A (Stephen, Fawkes et al. 2007). Subsequent gene targeting of Eph1A yielded a less severe phenotype characterized by hyperplastic valve leaflets greater in cross sectional area than wildtype mice. Cushion explants studies in chick revealed that the addition of Eph1A-Fc to cushion explants or overexpression of Eph1A in endocardial cells decreased endocardial cell EMT *in vitro* consistent with the loss of Eph1A resulting in enhanced EMT resulting in hyperplasia. These data suggest a relationship between Eph3A and Eph1A that is more than just a unidirectional ligand-receptor interaction. Overexpression of Eph3A was sufficient to induce endocardial cell EMT in normally nontransforming ventricular cells demonstrating that Eph3A is sufficient for EMT while Eph1A is a negative regulator of EMT. Since Eph receptors can signal in both a kinase-dependent and kinase-independent manner the expression of a kinase dead mutant was used to reveal a requirement of Eph3A kinase activity for this gain of function. These complementary approaches reveal a more complex role of this signaling pathway in endocardial cell EMT and valvulogenesis.

What Can In Vitro Results Tell Us About In Vivo Phenotypes?

Studies of the role of the TGF β are perhaps the most conspicuous example of apparently disparate *in vitro* and *in vivo* results. Although the abrogation of the function of the TGF β ligands, and later the Type I, Type II, and Type III TGF β receptors, was shown to inhibit EMT *in vitro*, targeting TGF β 2, TGF β R2, and TGF β R3 *in vivo* revealed that EMT can occur in the more complex

extracellular matrix (ECM) and growth factor environment found in the native cushions. These studies are well exemplified by TGF β R2. This constitutively active, serine threonine kinase receptor is a component of all described TGF β receptor complexes (reviewed (Barnett 2003)). Brown et al (Brown, Boyer et al. 1996) first targeted this receptor *in vitro* and showed that it was required for EMT. Later studies by Jiao et al (Jiao, Langworthy et al. 2006) used Cre-lox technology to selectively delete TGF β R2 from endothelial/endocardial cells. Surprisingly, these cells did undergo EMT *in vivo*. However, when AV cushion explants were placed on collagen gels EMT failed to occur. This suggests that EMT on collagen does require TGF β while EMT on the more complex matrix *in vivo* lacks this requirement. Loss of TGF β R2 does result in abnormal AV cushion remodeling and cardiac looping resulting in double inlet left ventricle (Jiao, Langworthy et al. 2006). Ongoing studies of TGF β R3 yield similar results. In the chick, targeting TGF β R3 *in vitro* inhibits endocardial cell EMT while overexpression of TGF β R3 in nontransforming ventricular endocardial cells causes EMT (Brown, Boyer et al. 1999). Targeted deletion of TGF β R3 in the mouse reveals that EMT does occur in the AV cushion and OFT but the resulting cushions are greatly enlarged (Compton, Potash et al. 2007) (unpublished). When AV cushion explants from TGF β R3 null mice are placed on collagen gels, EMT fails to occur (unpublished). Interestingly, this *in vitro* requirement and *in vivo* phenotype is nearly identical to that seen for TGF β 2, the ligand that requires TGF β R3 for high affinity binding.

These observations suggest two conclusions concerning the role of TGF β in EMT. First, the serendipitous use of collagen as the matrix for *in vitro* studies

revealed that EMT on this substrate is exquisitely sensitive to alterations in TGF β signaling. There is an obligate requirement for intact TGF β signaling for endocardial cells to undergo EMT on collagen. Second, *in vivo*, the more complex ECM and growth factor environment can support EMT in the absence of TGF β signaling as revealed by Jiao (Jiao, Langworthy et al. 2006) and our studies (Compton, Potash et al. 2007). However, in the case of the targeting of TGF β R2 and TGF β R3, although the cells can bypass a requirement for TGF β signaling for EMT, the loss of TGF β signaling via these receptors results in abnormal behavior of the endocardially-derived mesenchyme resulting in double inlet left ventricle in the case of TGF β R2 (Jiao, Langworthy et al. 2006) and Double outlet right ventricle and hyperplastic cushions in the case of TGF β R3 (Compton, Potash et al. 2007) and TGF β 2 (Bartram, Molin et al. 2001).

This requirement for TGF β signaling for EMT on collagen provides an extremely sensitive biological system for studying TGF β signaling in endocardial cells and the role of the extracellular matrix in supporting EMT. First, since EMT on collagen requires TGF β receptor activation, this system can be used to screen for downstream mediators of TGF β signaling. This approach is proving especially useful in identifying the mechanisms by which TGF β R3 signals. In fact, endocardial cell EMT on collagen is the only known assay for TGF β R3 signaling. Second, since EMT on collagen is TGF β dependent while EMT *in vivo* is not, this system provides the opportunity to identify the factors *in vivo* that allow endocardial cells to bypass the requirement for TGF β . Assays using TGF β R3 null endocardial cells can be used as a screen whereby extracellular components or

growth factors can be added back to the matrix in a systematic way in order to identify those that stimulate EMT in the absence of intact TGF β signaling. Therefore, although the *in vitro* collagen gel assay cannot accurately foretell the phenotype *in vivo*, it can uniquely provide essential insight into both the mechanisms of TGF β signaling that regulate EMT and the *in vivo* environment that can support TGF β -independent EMT. In the case of the identification of TGF β signaling mechanisms that regulate EMT, specifically those downstream of TGF β R3 where little is known about the signaling pathway, this data will be essential in selecting molecules that function to control endocardial cell-derived mesenchyme during valve formation and in formulating therapeutic strategies to predictably alter the behavior of this mesenchyme. Therefore, although some significant differences are evident in the results obtained from this *in vitro* assay (Camenisch, Molin et al. 2002) when compared to genetic manipulations *in vivo* (for example, (Jiao, Langworthy et al. 2006)), the AVC transformation assay continues to provide useful insight concerning the molecules that regulate endocardial cell EMT, mesenchymal cell maturation, and valvulogenesis.

Valvular Interstitial Cell Function (VIC) in Valve Remodeling

Finally, after endocardial cell EMT seeds the cardiac jelly of the endocardial cushions, the resultant mesenchyme cells express genes indicative of mesenchyme differentiation, which in VICs include the upregulation of downstream BMP targets *Msx1*, *Msx2* and *Sox9* (Chan-Thomas, Thompson et al. 1993; Akiyama, Chaboissier et al. 2004; Chen, Ishii et al. 2008). These

differentiating mesenchymal cells play multiple roles in the formation and maintenance of valve structure (reviewed (Aikawa, Whittaker et al. 2006; Butcher and Markwald 2007)). One of the roles is the secretion and remodeling of ECM components. Cardiac cushion interstitial cells secrete procollagen-I, hyaluronic acid, and periostin, which are all required for cushion morphogenesis (Camenisch, Spicer et al. 2000; Inai, Norris et al. 2008). Some secreted ECM components, such as periostin and cadherin11, might also regulate the lineage commitment and differentiation of interstitial cells themselves (Butcher, Norris et al. 2007; Shelton and Yutzey 2008). The mesenchyme initiates the remodeling process by secreting ECM components, such as procollagen I, as well as proteins that modify the matrix, such as Mmp2 (Shelton and Yutzey 2008). Specific cleavage of the ECM components in the cardiac jelly continue at this stage, including cleavage of Versican (Kern, Twal et al. 2006). The interstitial cells remodel the cardiac jelly into the highly organized ECM observed in the mature valves whose complexity is still being appreciated(Angel, Nusinow et al.). Compared to the early steps in valvulogenesis, however, the hemodynamic and molecular mechanisms governing remodeling and the subsequent role of endocardium in these processes are relatively unknown (Person, Klewer et al. 2005).

While the processes regulating EMT in the AVC and to a lesser extent, the OFT, have been extensively investigated as described above, our understanding of the mechanisms that regulate post EMT valve remodeling are quite limited. This is due, in part to the fact that unlike EMT, there is no *in vitro* bioassay for

endocardial function in the later stages of valvulogenesis. In addition this period of development has been essentially inaccessible to experimental manipulation because gene perturbation studies in the mouse result in embryonic demise in the midgestation mouse embryo. However, based on studies of normal mouse and human embryos (Maron and Hutchins 1974; Hurle, Colvee et al. 1980; Hurle and Colvee 1983), investigators have demonstrated that following the termination of EMT in the OFT of the mouse at E12.5, the condensed mesenchymal protrusions subsequently “elongate” to provide the true cardiac valve leaflets. The elongation of primitive valves appears to be a result of restricted proliferation of endocardial cells overlying the mesenchymal projections on the vascular side of the valve and selective cell death under the expanding endocardial rim. The growth of the endocardial edge and evacuation of apoptotic cells underneath the proliferating endocardial rim sculpt the swollen mesenchymal primitive valves into a typical excavated shape and results in morphogenesis of the sinuses of Valsalva.

Recently, two studies using histochemistry, immunohistochemistry, and electron microscopy described late gestational and postnatal valve development in chicken and mouse (Hinton, Lincoln et al. 2006) with a remarkably similar progression of developmental events seen in human fetuses (Aikawa, Whittaker et al. 2006). These studies document progression of remodeling and compartmentalization of the valve leaflet from a disorganized matrix of proteoglycans with little detectable elastin, and small amounts of disorganized collagen and relative uniform distribution of vascular interstitial cells (VICs), to a

highly stratified ECM into the 3 organized layers of fibrosa (arterial aspect primarily composed of collagens), spongiosa (central aspect, primarily glycosaminoglycans), and ventricularis (ventricular aspect with elastin fibers) with compartmentalization of VICs resulting in increased cell density in the fibrosa and ventricularis. Notably, this process is not only conserved across species but extends well after birth into postnatal life. Both investigators documented significantly higher VIC density, proliferation, and apoptosis in the fetus which gradually decreased into adult life. This decrease in VIC turnover was accompanied by a greater than 50 fold increase in valve cusp area in the chicken suggesting a major component of valve growth is from the increased production of ECM.

Evaluation of human fetal and adult valve formation resulted in several important observations potentially relevant to this remodeling process (Aikawa, Whittaker et al. 2006). First, valvular endothelial cells express an activated phenotype throughout fetal development as evidenced by accentuated expression of ICAM-1, VCAM-1, MMP-1, MMP13 and MHC-B nonmuscle myosin which is not seen in normal adult endothelium. Second, there is heterogeneity and plasticity of the VIC population with the majority of fetal VICs displaying an activated phenotype with progression to quiescence in the adult. Thus, fetal VIC activation occurs throughout development analogous to the valve changes that occur in pathological conditions and after surgical substitution (Rabkin, Aikawa et al. 2001; Rabkin-Aikawa, Farber et al. 2004) suggesting that analogous molecular mechanisms likely direct both normal developmental and pathological

interstitial cell activation (Rabkin-Aikawa, Farber et al. 2004). A recent *in vitro* study suggests that semilunar VIC plasticity may be the hallmark of a resident subpopulation of valve progenitor cells that maintain the ability to differentiate into either endothelial or interstitial cells in the valve leaflet (Paruchuri, Yang et al. 2006).

There are a few mouse mutants that escape early embryonic demise and are thus informative in unravelling the mechanisms of late gestational and early postnatal semilunar valve pathology and many of these mutants point to a central role for endocardial cell signaling. Most of these mouse models display normal EMT but then evolve a *hyperplastic* valve phenotype that suggests aberrations in valve remodeling. One common feature of many of these defects is perturbations that either enhance or attenuate RAS-MAPK signaling (reviewed (Yutzey, Colbert et al. 2005; Gelb and Tartaglia 2006). Epstein et al showed that hyperplastic aortic valve defects in *Nf1* mutant embryos previously attributed to defects in cardiac NCC, result from a primary defect in OFT and AVC endocardium (Gitler, Zhu et al. 2003). These defects were at least partially due to elevations in endocardial MAPK signaling secondary to the loss of *Nf1* suppression of *Ras-Erk* signaling resulting in increased proliferation and decreased apoptosis (Lakkis and Epstein 1998). Consistent with this, patients with *Nf1* mutations, develop pulmonary stenosis and hypertension but rarely defects in the AVC (Lin, Birch et al. 2000). NF1 loss of function is mimicked by gain of function mutations in the tyrosine phosphatase Shp2/PTPN11 which results in a context and dosage dependent increase in Ras-Erk activation, increased proliferation, and decreased

apoptosis resulting in semilunar valve and AV valve hyperplasia (Araki, Mohi et al. 2004; Gelb and Tartaglia 2006). Autosomal dominant gain of function mutations in *Shp2* have been identified as causative for Noonan's syndrome, the most common non-chromosomal syndrome with cardiac abnormalities characterized by pulmonary stenosis, hypertrophic cardiomyopathy, and occasionally AV valve defects (Tartaglia, Mehler et al. 2001; Tartaglia, Kalidas et al. 2002). Most recently, hypomorphic mutations in SOS1 an essential RAS guanine nucleotide-exchange factor (Ras-Gef), result in enhanced RAS-ERK activation and can account for as high as 20% of the cases of Noonan's syndrome not explained by *Shp2* mutations (Roberts, Araki et al. 2007) (Tartaglia, Pennacchio et al. 2006).

Significant attention has been focused on the potential role of Notch1 signaling in the development of the outflow tract in general and more recently in semilunar valve formation specifically (reviewed (MacGrogan, Nus et al.)). In addition to a prominent role in regulating early events of EMT, as described above, the observation that Notch1 mutations were associated with formation of a bicuspid aortic valve and subsequent calcification of the aortic valve has stimulated significant interest in a role for Notch1 in latter valve remodeling. Garg, and colleagues (Garg, Muth et al. 2005) hypothesized that Notch1 signaling played a role in repressing *Runx2* through activation of the hairy-related family of transcription repressors (*Hrt* or *Hey*). A truncated mutation of *Hrt2* was used to demonstrate a de-repression of calcium deposition in addition to early developmental defects that led to progressive aortic valve disease.

Subsequently, investigators have documented other forms of left ventricular outflow tract obstruction (LVOTO) such as coarctation of the aorta (COA) and hypoplastic left heart syndrome (HLHS) have been linked to polymorphisms of the Notch1 alleles as well as mutations within the ectodomain and extracellular domain of the Notch1 sequence ((McBride, Riley et al. 2008). However, the exact cell populations involved in these defects remains somewhat ambiguous. Del Monte et al. (Del Monte, Grego-Bessa et al. 2007) were able to detect expression of the Notch intracellular domain (NICD), suggesting active Notch signaling, throughout the endocardium adjacent to the myocardium during at E9.0 - E9.5. Subsequently, NICD expression became localized to the endocardial cells of the AVC and OFT. This expression persisted to E14.5 in the endocardium of the semilunar valves and was undetected in the mesenchymal cells of the valve leaflets. NICD was also detected in other endocardial populations such as the atrium and ventricles. This suggested that endocardial specific Notch signaling was the primary sight for Notch activity in latter valve development. However, recently Jain, and colleagues (Jain, Engleka et al.) demonstrated semilunar valve defects utilizing secondary heart field expression of the Notch signaling component mastermind-like (MAML). These data raise the possibility that non-endothelial Notch signaling affects cardiac NCC functions required for valve remodeling.

Recent evidence implicate EGF signaling as an important regulator of later valve remodeling and suggests members of this family may play different roles in OFT and AVC valve morphogenesis. Loss or attenuation of EGFR/ErbB1

signaling results in preferential hypercellularity of semilunar but not AV valves (Sibilia, Wagner et al. 2003) and this hyperplastic semilunar valve phenotype is augmented when crossed to mice heterozygous for a null mutation in Shp2 (Chen, Bronson et al. 2000). Deletion of the EGF ligand, heparin binding (HB)-EGF, results in increased endocardial cushion size and cell proliferation of both semilunar and AV valves (Iwamoto, Yamazaki et al. 2003; Jackson, Qiu et al. 2003). These mice show prolonged Smad 1/5/8 phosphorylation and loss of phospholipase e (Tadano, Edamatsu et al. 2005), a downstream component of EGF and Ras signaling, and similar to mice with a null mutation in inhibitory Smad (Galvin, Donovan et al. 2000), have hyperplastic similunar valves. Interestingly, null mutations in other EGFR ligands (EGF, ampiregulin, TGF- α) have no effect on valve formation. Thus, while abundant evidence suggests that Shp2-enhances signaling through EGF receptors via Ras (Shen, Ouyang et al. 2002) and leads to a transition from proliferation and expansion to remodeling and elongation of the valve leaflet, the exact mechanism of regulation is likely to be context dependent and receptor specific and may involve the intersection of multiple growth factor signaling pathways.

Unique Functions for the Ventricular Endocardium.

While the characteristic ability of the AVC and OFT endocardium to undergo EMT has been appreciated for quite some time, the unique role of the ventricular endocardium was “serendipitously” elucidated by studies of the neuregulin growth factor. Previous studies on neuregulin signaling had primarily

focused on its role in neural development as well as oncogenic transformation. The discovery that mice deficient for neuregulin develop a relatively normal early heart but fail to undergo ventricular trabeculation (Figure 1C) documented an essential role for this receptor and its ligands in cardiac development (Meyer and Birchmeier 1995; Kramer, Bucay et al. 1996). This epidermal growth factor-like molecule signals through a family of protein tyrosine kinases of the EGFR family, Erb2, Erb3, Erb4 (reviewed (Pentassuglia and Sawyer 2009)) that form heterodimers (ErbB2/ErbB3 or ErbB2/ErbB4) at the cell surface. Interestingly, neuregulin is expressed by the endocardium of the heart and the ErbB2/ErbB4 complex is expressed in a reciprocal pattern by the underlying myocardium. In contrast, the ErbB2/ErbB3 complex is expressed by the mesenchymal cells adjacent to the endocardium of the endocardial cushions in the atrioventricular canal and outflow tract. Deletion of either ErbB2 (Shen, Ouyang et al. 2002) or ErbB4 (Gassmann, Casagranda et al. 1995) results in absent trabeculation of the embryonic ventricle, decreased myocyte proliferation, and embryonic lethality at E10.5, similar to that seen in the neuregulin knock-out mice. These data firmly establish the neuregulin signaling pathway between endocardium and myocardium as a very specific and essential step in ventricular morphogenesis. Likewise, targeted null mutations in the ErbB3 receptor (Erickson, O'Shea et al. 1997; Riethmacher, Sonnenberg-Riethmacher et al. 1997) results in abnormal endocardial cushion development and defective valve formation resulting in congestive heart failure at E13.5. Thus, endocardial signaling via neuregulin is critical for several events intrinsic to myocardial development. Similarly,

endocardial expression of Brg1 results in the repressed expression of ADAMTS1, which is required for trabeculation of the ventricle (Stankunas, Hang et al. 2008). These studies confirm unique chamber specific roles for endocardial signaling in the developing heart (reviewed (Brutsaert, De Keulenaer et al. 1996; Sedmera, Pexieder et al. 2000; Smith and Bader 2007)).

Summary of Valve Development

Overwhelming evidence from several lines of investigation supports the importance of endocardial EMT and the subsequently derived mesenchyme in valve development though the gene regulatory networks (GRN) underlying these processes is incompletely understood. Furthermore, there exists a remarkable degree of endocardial heterogeneity that allows endocardial cell populations in the AVC and OFT cushions and in the ventricle to participate in several distinct events during cardiac morphogenesis. The basis for the generation and maintenance of this diversity is only now being revealed. We exploited this endocardial heterogeneity in Chapter II as a powerful tool in delineating the signaling pathways that distinguish between the developmental processes distinct to these endocardial cell populations. This knowledge will contribute to a clearer understanding of cardiac morphogenesis, contribute to our understanding of the molecular basis of congenital heart defects, and may provide novel therapeutic opportunities for the treatment of pediatric and adult cardiovascular disease.

EMT in Coronary Vessel Development

The epicardium is a layer of epithelial cells that covers vertebrate hearts and plays a major role during coronary vessel development (Mikawa and Gourdie 1996; Dettman, Denetclaw et al. 1998; Gittenberger-de Groot, Vrancken Peeters et al. 1998; Cai, Martin et al. 2008; Zhou, Ma et al. 2008). In response to signals from the myocardium, a subpopulation of epicardial cells undergo EMT and invades into the subepicardial space and myocardium. These EPDCs are important for coronary vessel development as disrupting epicardial formation or EMT leads to defects in the myocardium and coronary vessels (Kwee, Baldwin et al. 1995; Yang, Rayburn et al. 1995; Sengbusch, He et al. 2002; Mellgren, Smith et al. 2008; Smith, Baek et al. 2011). Thus, key insights into coronary vessel formation have been derived from studies elucidating the signals that promote epicardial EMT.

Formation of the Epicardium

The epicardium arises from a transient structure composed of mesothelial cells called the proepicardium (Manasek 1969; Viragh and Challice 1981; Manner 1992; Wessels and Perez-Pomares 2004; Serluca 2008). The proepicardium originates from cells adjacent to the septum transversum and the sinus venosus and attaches to heart tube at E10.5 (Viragh and Challice 1981; Rodgers, Lalani et al. 2008). Attachment is dependent of epicardial-myocardial interactions and targeted deletion of genes in the mouse which disrupts this interaction, such as *Vcam1* or *Itga4*, prevents formation of the epicardium and

results in absent coronary vessels as well as myocardial defects (Kwee, Baldwin et al. 1995; Yang, Rayburn et al. 1995; Sengbusch, He et al. 2002). Several signals from the myocardium regulate proepicardial attachment. BMP2 has perhaps the best defined role in direct cells from the proepicardial organ to attach to and migrate over the heart tube (Kruithof, van Wijk et al. 2006; Christiaen, Stolfi et al. 2010; Ishii, Garriock et al. 2010), forming the epicardium. Epicardial cells express *Wt1* and *Tbx18* which are commonly used as markers of embryonic epicardium (Zhou, Honor et al. 2011). The epicardium covers the heart tube and becomes a continuous epithelial layer by E12.5 (Komiyama, Ito et al. 1987).

Between the epicardium and the myocardium a layer of ECM forms in the subepicardial space. The myocardium and proepicardium both contribute to the ECM contained in the subepicardial space (Tidball 1992; Kalman, Viragh et al. 1995). The myocardium secretes laminin, fibronectin, and collagens I and III on the surface of the heart tube (Tidball 1992; Tidball 1992). HA, a major ECM component within the subepicardial space, is produced by the proepicardium and transferred in vesicles to the surface of the heart as the epicardium migrates over the heart tube (Kalman, Viragh et al. 1995). The exact makeup and source of the ECM contained in the subepicardial space is unknown.

The Fate of EPDCs

After epicardial cells begin to migrate over the heart at E10.5, a subset of these cells undergoes EMT and invades into the subepicardial space and myocardium. Cell lineage tracings done principally in avians suggests that these

EPDCs contribute to several cell lineages, including interstitial fibroblasts, perivascular fibroblasts, vascular smooth muscle cells (VSMCs), and coronary endothelial cells (Mikawa and Gourdie 1996; Dettman, Denetclaw et al. 1998; Gittenberger-de Groot, Vrancken Peeters et al. 1998; Manner 1999; Wilting, Buttler et al. 2007). Similar lineage tracing studies in the mouse using cre/loxP systems have supported the epicardial origin of a majority of the VSMCs associated with coronary vessel development when using cre alleles expressing primarily in the epicardium, *WT1*-cre (Wilm, Ipenberg et al. 2005), *Tbx18*-cre (Cai, Martin et al. 2008), or *cGata5*-cre (Merki, Zamora et al. 2005). The EPDC contribution to the fibroblast lineages has also been supported by these same studies and that the absence of EPDCs results in a lack of perivascular and interstitial fibroblasts (Smith, Baek et al. 2011).

The contribution of EPDCs to the coronary endothelial and myocardial cell lineages in mammals has been controversial (reviewed (von Gise and Pu 2012)). Initial lineage tracing studies in mice failed to support an EPDC contribution to coronary endothelial cells using *Wt1*-cre or *Tbx18*-cre (Cai, Martin et al. 2008; Zhou, Ma et al. 2008). A recent lineage tracing study using the *Sema3d*-cre and *Screlaxis*-cre cre alleles labeled populations of proepicardial cells largely distinct from those expressing *WT1* and *Tbx18*, suggesting that, while morphologically homogenous, the proepicardium contains distinct genetic subpopulations (Katz, Singh et al. 2012). *Sema3d*-cre and *Screlaxis*-cre labeled the proepicardium, migrating epicardium cells, and a small fraction (>10%) of either myocardium or coronary endothelial cells (Katz, Singh et al. 2012). Further studies have also

identify other sources of coronary endothelial cells, including major contributions from the sinus venosus to the venous coronary endothelium (Red-Horse, Ueno et al. 2010) and from the ventricular endocardium to the arterial coronary endothelium (Wu, Zhang et al. 2012). These data indicate that there are several lineages that can give rise to coronary endothelial cells. A comprehensive, quantitative examination of the relative contributions of these specific sources may assist in clarifying the mechanisms by which the coronary endothelium arises.

The ability of mammalian proepicardial and epicardial cells to differentiate into cardiomyocytes *in vitro* has been suggested though these studies did not exclude the possible inclusion of non-epicardial cells in culture (Kruithof, van Wijk et al. 2006; del Monte, Casanova et al. 2007). In mice *in vivo*, lineage tracing studies using *WT1*-creERT2 (Wilm, Ipenberg et al. 2005) and *Tbx18*-cre (Cai, Martin et al. 2008) labeled a small fraction of myocardial cells in the ventricular septum cells during cardiogenesis (Cai, Martin et al. 2008; Zhou, Ma et al. 2008). The validity of these results has been placed in doubt (Christoffels, Grieskamp et al. 2009); particularly in the case of *Tbx18*-cre as *Tbx18* expression is seen at low levels in non-epicardial cells in the heart, including a subpopulation of myocardial cells. Overall, these studies indicate the myocardium does not arise from EPDCs. Despite the controversies concerning the contribution of EPDCs to specific lineages, EPDCs are clearly required for coronary vessel development.

Formation of Coronary Vessels

The coronary vessel development is a complex process involving careful coordination between the epicardium, myocardium, coronary endothelial cells and EPDCs (Olivey, Compton et al. 2004; Lavine and Ornitz 2009). At E11.5, the epicardium begins to undergo EMT and seed the subepicardial space with epicardially derived mesenchyme. EPDCs also invade into the myocardium as well. At approximately the same time, coronary vessel formation begins through the process of vasculogenesis. Vasculogenesis is the process in which *de novo* vascular networks are formed. The coronary endothelial cells in the subepicardial space and myocardium coalesce to form interconnected vascular tubes at approximately E11.5. These primitive vessels consist of single layer of endothelium. The formation of a vascular plexus begins at the atrioventricular junction on the inferior surface of the heart and proceeds to cover most of the right and left ventricles by E13.5. The coronary vascular plexus consists of *EphB4*-expressing, venous-fated, subepicardial vessels and *EphrinB2*-expressing, arterial-fated, intramyocardial vessels which can have interconnections (Swift and Weinstein 2009). The coronary vessels attach to the base of the aorta through the right and left coronary ostia which allows the establishment of the coronary circulation (Gonzalez-Iriarte, Carmona et al. 2003). VSMCs and perivascular fibroblasts are then recruited, forming coronary vessels consisting of an inner layer of endothelium, a middle layer of VSMCs, and an outer layer of fibroblasts. The association of VSMCs is required for the stabilization and maturation of the nascent vessels (Poelmann, Gittenberger-de

Groot et al. 1993; Reese, Mikawa et al. 2002). Between E14.5 and E16.5, the process by which new blood vessels arise from existing ones, or angiogenesis, functions to further remodel the coronary vessels to insure adequate blood flow to the entire myocardium. Disruption of the epicardium, EPDCs, or epicardial-myocardial signaling inhibits the formation of mature coronary arteries and veins (Olivey and Svensson 2010).

Signaling Pathways Regulating Epicardial EMT

Significant progress has been made in understanding how epicardial cell EMT is regulated during development in the last decade. Several excellent reviews have recently chronicled the roles of Wnt, TGF β , BMP, PDGF, FGF, and RA signaling pathways and the interactions between the epicardium and myocardium in epicardial EMT (Gittenberger-de Groot, Winter et al. 2010; Olivey and Svensson 2010; von Gise and Pu 2012). Here, we have elected to discuss TGF β signaling in coronary vessel development to provide important details that are pertinent to the research presented in Chapter III.

TGF β Signaling in Coronary Vessel Development

The expression of TGF β ligands in the embryonic epicardium suggested a potential role for TGF β signaling in coronary vessel development. TGF β 2 is expressed in the myocardium while all ligands are expressed in the epicardium at E11.5 (Molin, Bartram et al. 2003; Olivey, Mundell et al. 2006). While it was initially reported that TGF β ligand incubation inhibited epicardial EMT (Morabito,

Dettman et al. 2001), further studies demonstrated that TGF β 1 and TGF β 2 promote loss of epithelial character and smooth muscle differentiation in cultured proepicardial (Olivey, Mundell et al. 2006) and epicardial cells (Compton, Potash et al. 2006; Austin, Compton et al. 2008; Sanchez, Hill et al. 2011) *in vitro*, suggesting a potential role for TGF β in epicardial EMT. TGF β ligand knockout models do not have coronary vessel abnormalities (Shull, Ormsby et al. 1992; Kaartinen, Voncken et al. 1995; Sanford, Ormsby et al. 1997), suggesting the ability of multiple TGF β ligands to engage and signal through the same TGF β receptors allows for compensation of the loss of a single ligand in epicardial cells *in vivo*. Similar to the TGF β ligands, ALK5 is required for epicardial EMT *in vitro* (Austin, Compton et al. 2008; Sridurongrit, Larsson et al. 2008). Disruption of ALK5 signaling in the epicardium using *Alk5:Gata5c-cre* mice revealed a role for TGF β signaling in epicardial development *in vivo*. Targeted deletion of ALK5 in the epicardium in mice *in vivo* results in interrupted epicardial attachment to the myocardium, loss of expression of specific adhesion molecules, thinned myocardium, and a loss of coronary smooth muscle (Sridurongrit, Larsson et al. 2008). *Alk5:Gata5c-cre* embryos survive until birth. This suggests that the coronary vessels were able to support cardiac function to some degree as mice completely lacking coronary vessels die at approximately E14.5-E16.5 (Yang, Rayburn et al. 1995; Moore, McInnes et al. 1999; Tevosian, Deconinck et al. 2000).

Deletion of *Tgfb3* in mice resulted in failed coronary vessel formation associated with embryonic demise at approximately E14.5. (Compton, Potash et

al. 2007). The striking aspect of this phenotype was the specific disruption of coronary vasculature. While vasculature outside of the heart observed using SM22 α transgene labeling appeared grossly normal in *Tgfbr3*^{-/-} embryos, there was reduced staining for the vascular endothelial marker PECAM1 in the coronary vasculature. *Tgfbr3*^{-/-} embryos did form a primitive vascular plexus and ostia. We assume the reduced number of vessels was insufficient to supply the heart with blood, resulting in embryonic death. A thin compact zone myocardium, likely secondary to defects in the epicardium, was also observed in *Tgfbr3*^{-/-} embryos. Compared to *Tgfbr3*^{-/-} littermates, *Tgfbr3*^{-/-} hearts featured a discontinuous epicardium overlying an expanded, hyperplastic supepicardial space containing blood islands. Examination of *Tgfbr3*^{-/-} hearts revealed a significant decrease of proliferation in the epicardium and epicardially-derived mesenchyme. Epicardial cell invasion into the myocardium was decreased in *Tgfbr3*^{-/-} embryos, demonstrating a defect in some component of epicardial EMT (Sanchez, Hill et al. 2011). Overall, the unique phenotype of *Tgfbr3*^{-/-} embryos, when compared to phenotypes of mice with targeted deletions in TGF β 1, TGF β 2, TGF β 3, or ALK5, demonstrated an important and non-redundant role for TGF β R3 in regulating epicardial cell behavior and coronary vessel development.

Further work was undertaken by our laboratory to elucidate the signaling mechanisms by which TGF β R3 regulates epicardial cell behavior in embryonic epicardial cells *in vitro* (Figure 3). *Tgfbr3*^{+/+} epicardial cells undergo loss of epithelial character and invasion into collagen gels *in vitro* in response to TGF β 1, TGF β 2, BMP2, ligands known to bind TGF β R3 (Lopez-Casillas, Cheifetz et al.

1991; Kirkbride, Townsend et al. 2008). While loss of epithelial character was still observed after loss of TGF β R3, *Tgfb3*^{-/-} cells had reduced invasion in response TGF β 1, TGF β 2, and BMP2 that was rescued with TGF β R3 (Sanchez, Hill et al. 2011; Hill, Sanchez et al. 2012; Sanchez and Barnett 2012). TGF β 1 and TGF β 2 also promoted smooth muscle differentiation in *Tgfb3*^{+/+} and *Tgfb3*^{-/-} cells while BMP2 did not (Hill, Sanchez et al. 2012). Surprisingly, other ligands known to be important in epicardial EMT also required TGF β R3 to promote invasion in epicardial cells (FGF2 (Morabito, Dettman et al. 2001; Tomanek, Sandra et al. 2001), High Molecular Weight (HMW)-HA (Craig, Austin et al. 2010; Craig, Parker et al. 2010)). One may hypothesize that this may be explained by binding of these molecules to TGF β R3, and indeed FGF2 has been reported to bind TGF β R3 (Andres, DeFalcis et al. 1992). Additionally, the ability FGF2 to promote repair in porcine VIC cultures required TGF β R3 (Han and Gotlieb 2011). TGF β R3 binding has not been reported for HMW-HA, though. Alternately, signaling directed by FGF2 and HMW-HA may require a common mediator downstream of TGF β R3 signaling. The decrease in invasion in *Tgfb3*^{-/-} epicardial cell invasion was not due to a general inability of these cells invade, as PDGF-AA, PDGF-BB, VEGF, or EGF incubation induced similar levels of invasion in *Tgfb3*^{+/+} and *Tgfb3*^{-/-} epicardial cells (Sanchez, Hill et al. 2011).

The TGF β R3-dependent invasion after incubation with TGF β 1, TGF β 2, BMP2, HMW-HA, or FGF2 *in vitro* was shown to require the cytoplasmic domain of TGF β R3, a domain not required for ligand presentation (Blobe, Schiemann et al. 2001). TGF β R3 rescue invasion in *Tgfb3*^{-/-} epicardial cells *in vitro* in response

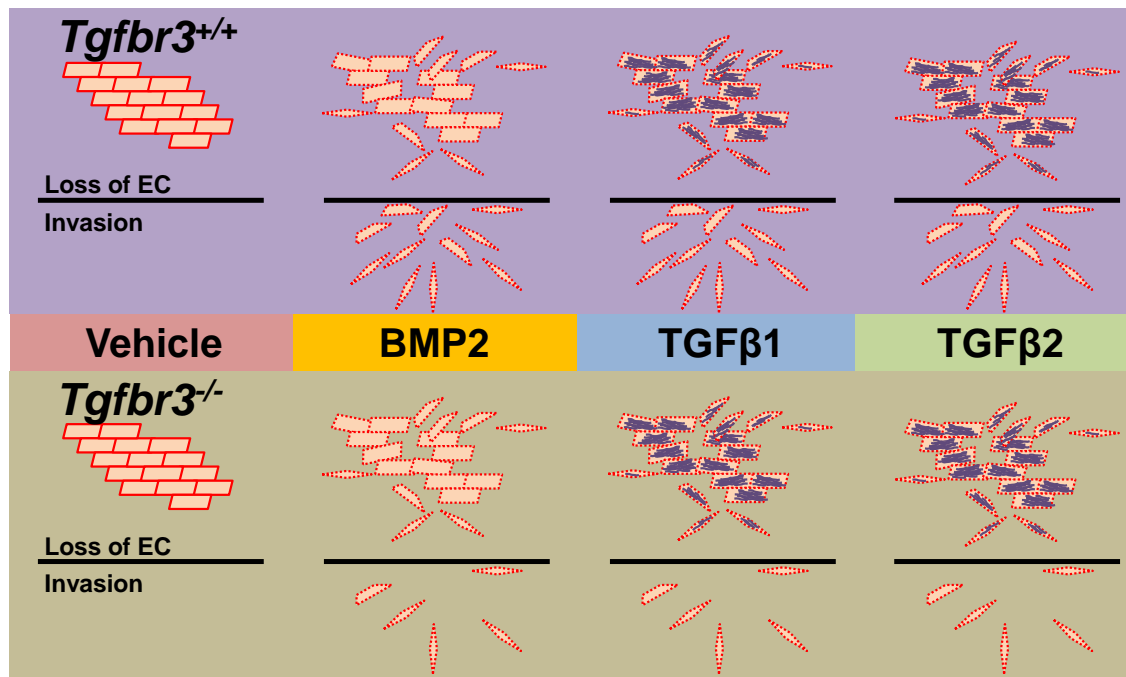


Figure 3: Comparison of *Tgfbr3^{+/+}* and *Tgfbr3^{-/-}* epicardial cell proliferation, apoptosis, and invasion. Depiction of ligand-induced differentiation and invasion in *Tgfbr3^{+/+}* and *Tgfbr3^{-/-}* immortalized epicardial cells *in vitro*. Red line- ZO1. Purple- Smooth muscle actin fibers. EC- Epithelial Character.

to TGF β 1, TGF β 2, BMP2, HMW-HA, or FGF2 whereas constructs expressing a TGF β R3 mutant lacking the last 3 amino acids on the C-terminus fail to rescue invasion (Sanchez, Hill et al. 2011; Hill, Sanchez et al. 2012; Sanchez and Barnett 2012). The C-terminal amino acids of TGF β R3 constitute a class I PDZ binding domain that binds to the scaffolding protein GIPC which in turn stabilizes TGF β R3 on the plasma membrane to promote signaling. The importance of this interaction is supported by the observation that GIPC is not only required for invasion in *Tgfb3^{+/+}* epicardial cells, but GIPC overexpression can promote invasion in the absence of additional ligand. GIPC regulation of epicardial invasion depends on TGF β R3 since *Gipc* expression in *Tgfb3^{-/-}* cells fails to rescue invasion and inhibition of *Gipc* expression blocks the ability of TGF β R3 to rescue invasion in *Tgfb3^{-/-}* cells (Sanchez, Hill et al. 2011). These data support the hypothesis that the interaction of TGF β R3 and GIPC is required for epicardial cell invasion.

Together, these *in vitro* data suggest a model where the ability of the epicardium to respond to FGF, HA, BMP, and TGF β growth factors is compromised after the loss of TGF β R3, contributing to defects in epicardial cell behavior that may lead to failed coronary vessel development. This ability of TGF β R3 to mediate epicardial cell behavior in response to an array of ligands may explain the severity of the *in vivo* phenotype of *Tgfb3^{-/-}* embryos when compared to other mouse models which disrupt TGF β signaling in the epicardium. In particular, the *in vitro* results linking the defects observed in invasion of *Tgfb3^{-/-}* epicardial cells to the cytoplasmic domain of TGF β R3 which

is not required for ligand presentation suggests a unique, non-redundant role for TGF β R3 in regulating epicardial EMT. Intriguingly, these results are similar to those observed in endocardial cushions where the interaction of TGF β R3 with GIPC is required to promote TGF β 2 and BMP2 dependent invasion *in vitro* (Townsend, Robinson et al. 2011). This suggests studies examining the mechanisms by which TGF β R3 regulates invasion may yield insights applicable to both epicardial and endocardial EMT. Together, these results indicate that TGF β R3 may represent a common pathway accessed by several upstream regulators of cell invasion.

Despite the increasing evidence for the unique role of TGFBR3 signaling in important development and disease processes, little is known about the signaling mechanisms downstream of TGF β R3. In Chapter III we undertake the first comprehensive analysis of the signaling pathways dependent on TGF β R3 signaling by coupling the well described epicardial culture system with next generation sequencing.

Summary

EMT is an important process not only in development where it is required for the formation of mature structures in the heart, but in homeostasis and response to injury in the adult hearts as well. A sustained interest in examining EMT during valve and coronary vessel development has yielded many insights into the biology of these systems. In particular, we have shown an important role

for TGF β R3 in endocardial and epicardial EMT. Still, the signaling pathways regulating endocardial and epicardial EMT are incompletely understood and the field often progresses at the pace of a single gene study at a time. Here, we took advantage of known biology of these systems and the power of next-generation sequencing to devise transcriptional profiling strategies which allowed us to identify and validate novel candidate genes and signaling pathways regulating endocardial and epicardial EMT. Further analysis of the gene lists and GRNs identified by these studies may yield important insights into signaling events regulating endocardial and epicardial cell biology, which is essential to the design of novel therapeutic approaches to alter cell behavior in heart disease, and regeneration.

CHAPTER II

SPATIAL TRANSCRIPTIONAL PROFILE OF THE CHICK AND MOUSE ENDOCARDIAL CUSHIONS IDENTIFY NOVEL REGULATORS OF ENDOCARDIAL EMT *IN VITRO*

Introduction

Valvular heart disease comprises a major portion of cardiovascular disease in children and adults. Congenital Heart Disease (CHD), which includes a spectrum of valvular defects, occurs in 1 out of 100 live births and is responsible for ten percent of infant deaths per year (Hoffman 1968; Loffredo 2000). Ninety percent of children with CHD now live to adulthood due to the surgical and medical advances of the past half century (Khairy, Hosn et al. 2008). As a result, adults now represent the largest age group with CHD, but because they are a relatively new class of patient, treatment approaches are as yet unclear. Also, it is now well recognized that there is a developmental basis to adult cardiovascular and valve disease. It is reasonable to assume that the homeostatic and repair functions present in adults would use many of the same mechanisms involved in the original development and remodeling of these tissues (reviewed in (Doetschman T 2012)). Therefore, the careful examination of genes and signaling pathways governing early valve development is likely to provide novel insight into the mechanisms underlying valve disease and suggest potential new therapies.

Valvular interstitial cells (VICs) are a common substrate of both congenital and adult valvular disease (Doetschman T 2012). These cells are derived primarily from specialized endothelium, located in the atrioventricular (AVC) and outflow tract (OFT) cushion regions of the developing heart tube, which undergoes EMT (Barnett and Desgrosellier 2003). VICs direct both the remodeling of the ECM during valvulogenesis in the embryo and the maintenance of the structure of the valve leaflets in the adult. Despite a continued interest in the process of endocardial EMT (reviewed (DeLaughter, Saint-Jean et al. 2011; Lencinas, Tavares et al. 2012; von Gise and Pu 2012)) our understanding remains incomplete and often progresses at the pace of a single gene study at a time. We directed our analysis to an unbiased approach identifying genes and pathways associated with endocardial EMT. Previous studies have used a variety of gene expression analysis approaches to identify cushion-enriched genes in the AVC (Rivera-Feliciano, Lee et al. 2006; Wirrig, Snarr et al. 2007; Chakraborty, Cheek et al. 2008; Vrljicak, Chang et al. 2010). Comparisons of normal and aberrant cushion development, a strategy predicated on the availability of models with known heart defects, yielded only genes associated with the perturbed signaling pathway (Rivera-Feliciano, Lee et al. 2006). While this approach has utility, many of the genes and signaling pathways associated with normal cushion development have yet to be determined. A second approach identified genes temporally regulated in the AVC by comparing different stages of development (Chakraborty, Cheek et al. 2008; Vrljicak, Chang et al. 2010). This strategy identified pathways that change over time in the AVC

but pathways specific to endothelial EMT were not directly queried. Both of these approaches focused on the use of a single spatial region of the heart for analyses.

We recognized that the inherent regional specificity observed in the developing heart tube presents a unique opportunity for analysis of endocardial EMT. EMT occurs specifically in the endothelium of the AVC and OFT but not in the adjacent endothelium of the common ventricle (VEN). Thus, a spatial transcriptional profile of these three regions of the heart tube enables a direct comparison between regions that do and do not undergo EMT. Further, the generation of data from these regions allows for genes expressed in the nontransforming ventricle to be subtracted from those genes expressed in the AVC and OFT in order to enrich for genes associated with endothelial EMT. This approach expands on earlier studies which focused on the AVC by comparisons that allow background subtraction of extraneous, non-target cell populations present during EMT. For example, at E10.5 proepicardial cells attach to the AVC (Viragh and Challice 1981) and subsequently migrate over the myocardium coincident with a population of PAX-3-positive cardiac neural crest cells entering the OFT (Conway, Henderson et al. 1997). The approach here, which identifies genes with enriched expression specific to both the AVC and OFT, excludes genes expressed by either of these non-target cell populations, which are contained in only a single cushion. Therefore, this focuses our analysis on identifying genes directing endocardial EMT and their associated pathways in early valvulogenesis.

In this chapter I collaborated with Jamille Robinson who performed the experiment presented in Figure 13H.

Experimental Methods

Embryo Dissection

HH18 chick (n=200, yielding 8 µg of RNA) and E11.0 ICR (n=100; n=60; yielding 17 µg and 10 µg of RNA, respectively) mouse hearts were dissected into AVC, OFT, and VEN (Figure 4A-B) and the samples were pooled. Standard phenol-chloroform extraction of RNA was performed.

RNA-seq

RNAseq libraries were generated as described without normalizations or RNA/cDNA fragmentation (Christodoulou, Gorham et al. 2011). Libraries were sequenced as 50 bp paired end sequences on a single lane of the Illumina HiSeq2000 producing 7 million reads per chick sample and an average of 10 million reads per mouse sample. HiSeq 2000 reads are aligned by TOPHAT (Trapnell, Pachter et al. 2009) (<http://tophat.ccb.umd.edu/>) to produce bam files. Gene expression profiles were generated as described (Christodoulou, Gorham et al. 2011) using a Bayesian p-value (Audic and Claverie 1997). Reads were normalized to total mRNA (total aligned reads on gene-loci per million). Data files have been deposited in the Gene Expression Omnibus database (<http://www.ncbi.nlm.nih.gov/geo/>) and can be accessed via series record GSE43194. Variability was assessed as described in Figure 5 and 6.

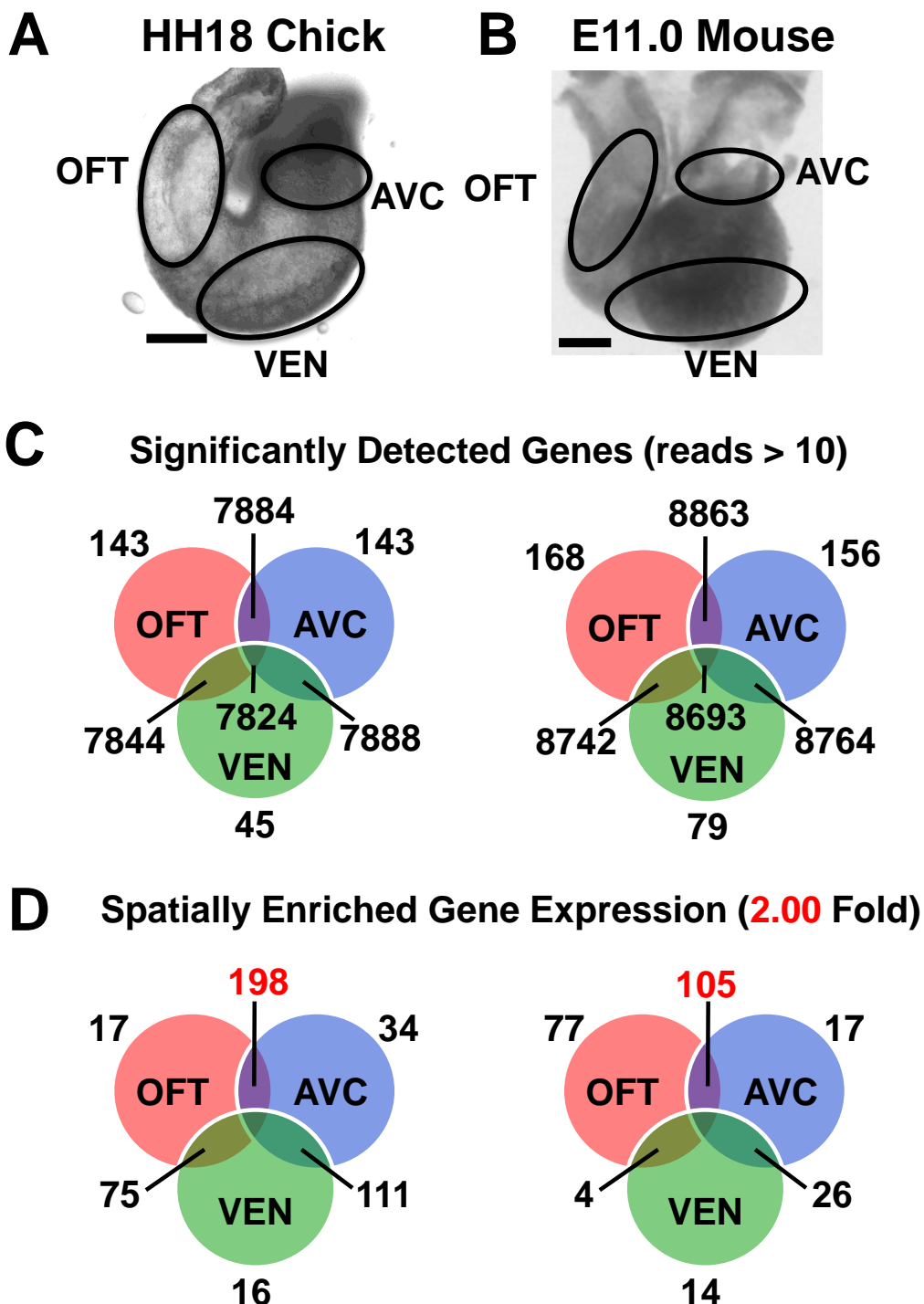


Figure 4: Spatial transcriptional profile of heart identifies cushion-enriched genes. A-B, AVC, OFT and VEN were dissected from equivalent stages of chick HH18 (**A**) and mouse E11.0 (**B**). **C**, RNA-seq analysis identified genes with significantly expressed (>10 reads) in each spatial region of the developing heart tube. **D**, Mapping genes with enriched expression (>2-fold) onto each spatial region identifies those genes with cushion-enriched expression (in red), 198 in the chick and 105 in the mouse. Scale bars - 100 μ m.

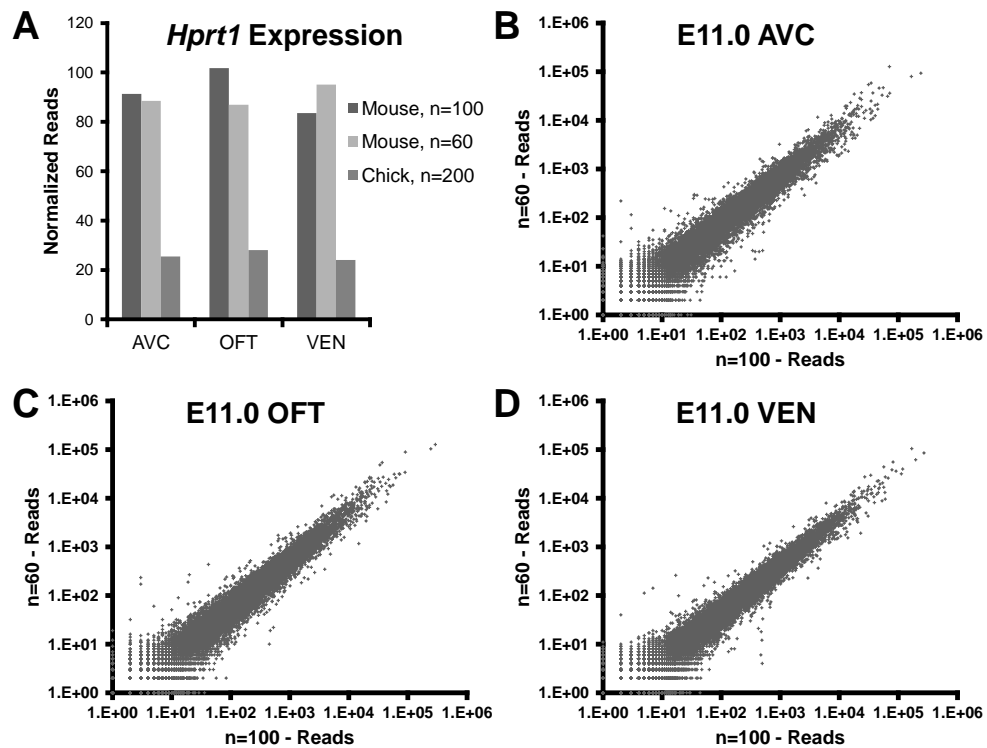


Figure 5: Variability in RNA-seq data sets. **A**, The expression of *Hprt1* (normalized reads) in each region of the heart tube (AVC, OFT, VEN) for HH18 chick and E11.0 mice is depicted. The expression of *Hprt1* is not expected to vary based on the region of the heart tube examined (AVC, OFT, VEN) or biological replicates (n=100, n=6). Little variability in *Hprt1* expression is observed in chick and mice. **B-D**, The two pools (n=100, n=60) of mouse tissue were processed separately as biological replicates for RNA-seq analysis and the reads for each gene in each pool were plotted against each other in (**B**) AVC (R=0.85), (**C**) OFT (R=0.93), and (**D**) VEN (R=0.93). These data support the mouse pools being consistent.

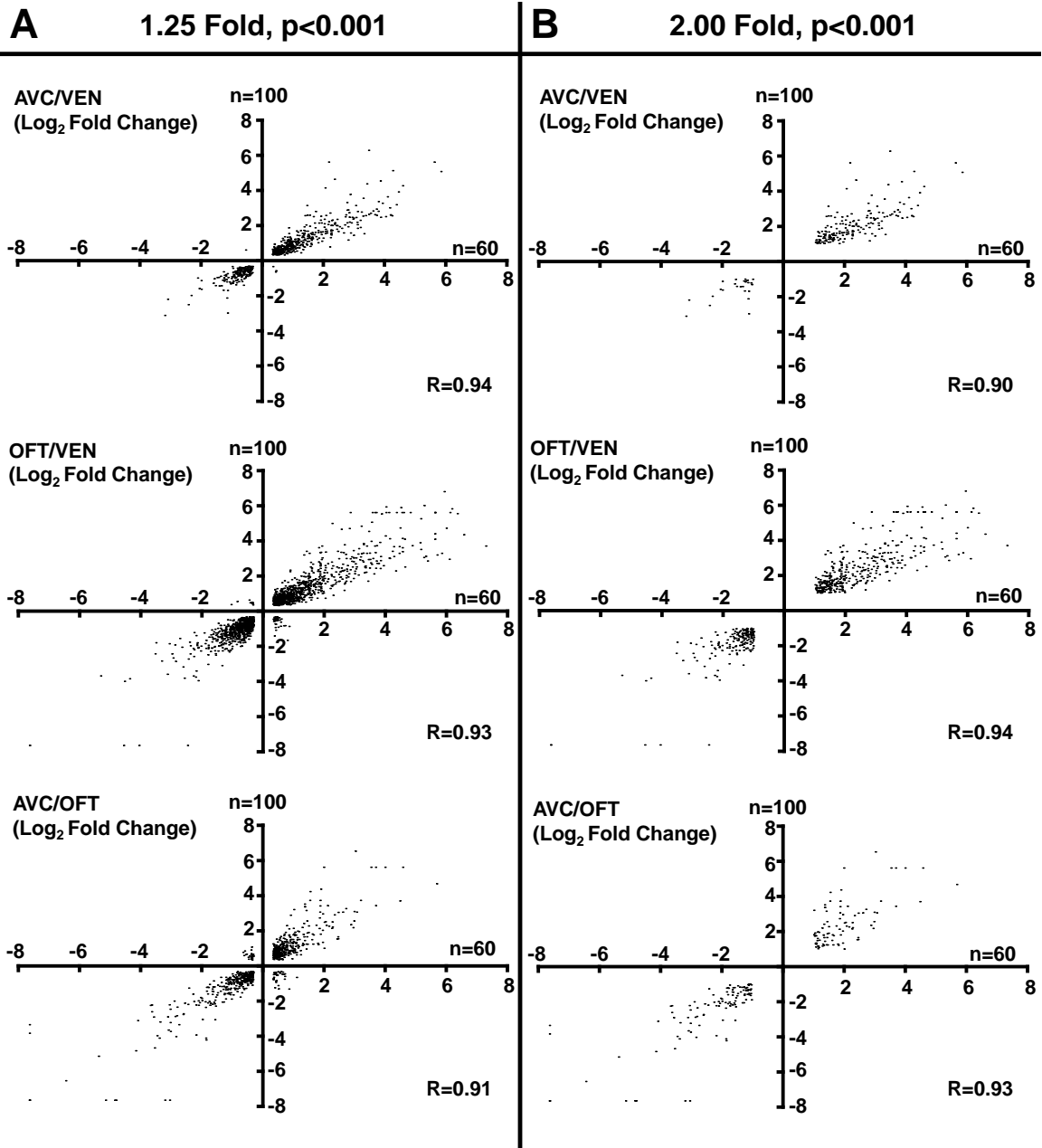


Figure 6: Comparison of differential gene expression between E11.0 biological replicates. Plots mapping the fold (log base 2) difference (either **(A)** >1.25-fold or **(B)** >2.00-fold) in expression between AVC/VEN, OFT/VEN or AVC/OFT in mouse biological replicates (X-axis: n=60, Y-axis: n=100) are shown. Genes that show agreement, defined as having >1.25 or >2.00-fold ($p<0.001$) increased or decreased expression in a specific comparison in both replicates, are mapped to quadrants I (upper right) or III (lower left) of a plot. Genes that show disagreement, defined as having >1.25 or >2.00-fold ($p<0.001$) increased expression in a tissue in one replicate and decreased in another (or vice versa), are mapped to quadrants II (upper left) or IV (lower right). There was a high degree of agreement using either a >1.25-fold ($R>0.91$) or a >2.00-fold ($R>0.90$) across all comparisons.

qRT-PCR

First-strand synthesis was done with SuperScript III kit (Invitrogen). SYBR Green (Biorad) was used for qRT-PCR. Primer sequences are in Table 2.

Table 2: Primers Used to Confirm Gene Knockdown

Gene	Forward Primer	Reverse Primer
FOXP2	5'(GTGCCACAGACAGATGCAACACA)3'	5'(TTTGACGAAGCTCATGCGGAGGAT)3'
MEIS2	5'(AAGGGAGCCTTATGGACAAACCA)3'	5'(AGCTTCAGCTAACACCCGACCT)3'
HAPLN1	5'(AGCACCCAGCTGTGGCTAATTACT)3'	5'(TCTATGTGCAAATGTGCAAGGCCG)3'
ID1	5'(AGACAAACAGGGCTCTCCTCAAAC)3'	5'(ACTGCGAGACCCAAGTCAGCAATA)3'
TGF β R3	5'(ACCAGAGTGGCGTGTAAAGAAGGT)3'	5'(TGCACAGAAAGGACCCAAAGCAAC)3'

Collagen Gel Assay

Collagen gel assays (reviewed (Lencinas, Tavares et al. 2012)) with siRNA or small molecule addition were performed as described (Townsend, Wrana et al. 2008). AVC were excised from stage 16 chick embryos, transected, and explanted endocardial side down onto a collagen I gel and incubated at 37°C with siRNA constructs. Control for siRNA toxicity was a randomized GC matched construct that do not correspond to any sequence. The positive control was siRNA targeting *Tgfb3* (Townsend, Robinson et al. 2011). siRNA sequences are listed in Table 3. EMT was quantified by counting the number cells with mesenchymal morphology that invaded into the collagen gel (Table 4).

Table 3: siRNA Construct Sequences

Target:	siRNA Construct Sequences:
<i>TGFβR3</i>	5'(UUCAGUAGAUUUACUUCtt)3'
<i>FOXP2-A</i>	5'(CGAAUUUUUAUAAAACGCAtt)3'
<i>FOXP2-B</i>	5'(GACAGGCAGUUAACACUUAtt)3'
<i>MEIS2-A</i>	5'(GUACAUUAGUUGUUUGAAAtt)3'
<i>MEIS2-B</i>	5'(GUAAACAACUGGUUUAUUAtt)3'
<i>HAPLN1-A</i>	5'(GGACAAGGAUAAAAGCAGAtt)3'
<i>HAPLN1-B</i>	5'(GCUACAAUUAACUUUCAtt)3'
<i>ID1-A</i>	5'(CCUCGUCUAUUGUUUAAAAtt)3'
<i>ID1-B</i>	5'(GUUAUGCUUUAAUAGACAtt)3'

Table 4: Collagen Gel Assay Counting Data

Experiment	Condition	N	Total Number of Transformed Cells	Normalized Mean Number of Transformed Cells +/- SEM
Foxp2	Control	30	8886	100 +/- 4
	<i>TGFβR3</i>	30	5349	60+/-3
	<i>FOXP2-A</i>	31	5078	55+/-3
	<i>FOXP2-B</i>	30	4785	53+/-2
Meis2	Control	30	8572	100+/-6
	<i>TGFβR3</i>	29	4589	55+/-3
	<i>MEIS2-A</i>	30	3413	39+/-3
	<i>MEIS2-B</i>	30	3209	37+/-3
HAPLN1	Control	28	11592	100+/-7
	<i>TGFβR3</i>	30	6127	49+/-3
	<i>HAPLN1-A</i>	30	5500	44+/-3
	<i>HAPLN1-B</i>	29	4884	40+/-3
ID1	Control	21	6867	100+/-9
	<i>TGFβR3</i>	30	5971	60+/-5
	<i>ID1-A</i>	30	5511	56+/-4
	<i>ID1-B</i>	29	5755	60+/-5

In Situ Hybridization

Dioxygenin labeled probes were generated from cDNA derived from E13.5 whole heart tubes using primers in Table 5. *In situ* hybridization was performed as described (Wei, Manley et al. 2011) and embryos were cryosectioned.

Table 5: Primers Used to Generate ISH Probes

Gene	Forward Primer	Reverse Primer
<i>Foxp2</i>	5'(CGCGAGCCTCCGAGAAAGCG)3'	5'(CATCATGGCCACCGACACGGG)3'
<i>Meis2</i>	5'(TGGCGGACAGGTTATGGACATTCA)3'	5'(TGAAGAAGCCTTCGCTCTGTCTCT)3'
<i>Hapln1</i>	5'(TGGACCAGGACGACGCAGTGATT)3'	5'(GCAGCGGTATAGCCCAGAA)3'
<i>Id1</i>	5'(CCCCCTCCGCTGTTCTCAGGA)3'	5'(TACCCACTGGACCGATCCGC)3'

Results

Defining a spatial transcriptional profile of the developing heart tube

Chick and mouse models were used for their relative strengths as model systems and the ability to use cross species comparison to identify key regulatory genes. Equivalent stages in the chick (HH18) and mouse (E11.0) were chosen when robust EMT occurs in both the OFT and AVC but not the VEN at this time (Camenisch, Molin et al. 2002). Spatial transcriptional profiles of chick and mouse heart tubes were generated as described in methods (Figure 4A-B).

The dynamic nature of gene expression profiles generated by RNA-seq identified approximately 8,000 genes expressed throughout either the chick or mouse heart tube. A smaller number of genes were also localized to specific regions such as the AVC, OFT, & VEN (Figure 4C). As a first step to enrich for

genes mediating EMT, we subtracted genes found in the VEN sample from the AVC & OFT samples. By identifying genes upregulated in both cushions in the comparison we eliminated the influence of the epicardial cells (AVC) and neural crest cells (OFT) which are found only in a single cushion sample and therefore not in the shared gene list we identified (Figure 7A; see *Wt1* (AVC, VEN), *Sox10* (OFT), *BMP10* (VEN)).

This approach yielded a robust list of genes upregulated in the cushions. We mapped genes enriched >2-fold in each spatial region (Figure 4D). Genes associated with distinct regions of the heart tube in chick and mouse cushions, including the T-box family members, had spatial expression patterns consistent with the literature (Figure 7B). We observe a few hundred genes enriched in the cushions, consistent with the hypothesis that the AVC and OFT should share common genes involved in endothelial EMT (Figure 4D). Comparisons of the AVC & VEN or OFT & VEN did not reveal as many enriched genes since they do not share EMT as a common process. Therefore, genes with a significant p-value ($p<.001$) and >2-fold higher expression in the cushions (AVC & OFT) compared to VEN are considered to be enriched in these compartments and were potential candidates for involvement in EMT.

Overall, 198 genes were identified in the chick (Appendix A) and 105 in the mouse (Appendix B) that were >2-fold higher expressed in the cushions. A literature search was used to further characterize these gene lists. In total, 15 of the 198 genes in chick and 18 of the 105 genes in mouse have a previously described role in EMT (Table 6). Genes known to be expressed regionally in the

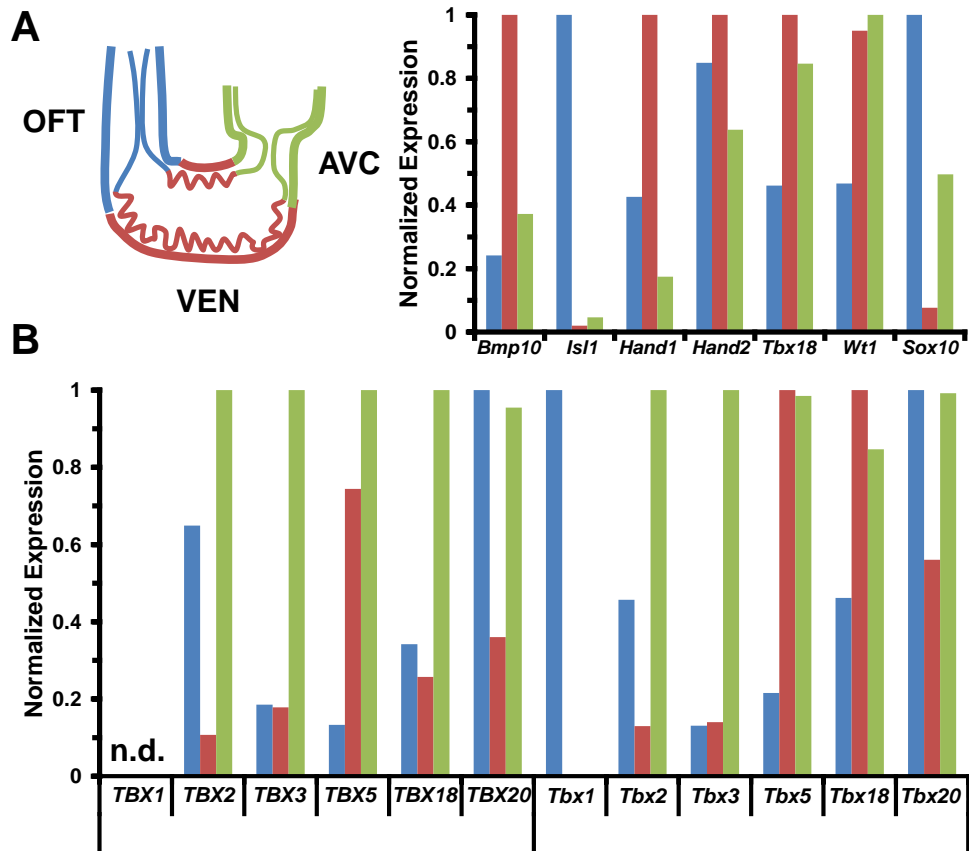


Figure 7: Spatial expression of select genes in the HH18 chick and E11.0 mouse heart tube. For each gene, expression was normalized to the region with the highest read count **A**, Regional expressed patterns in the mouse heart are consistent with previous observations at E10.5-E11.5. *Bmp10* (VEN), *Isl1* (OFT), *Hand1* (VEN), *Hand2* (endocardium throughout heart tube), *Tbx18* and *Wt1* (Epicardium attaching to AVC and migrating towards VEN), and *Sox10* (neural crest in OFT and in OFT and AVC cushions). **B**, Expression of T-box genes in chick and mouse are consistent with previous reports (reviewed (Greulich, Rudat et al.)). n.d.- *TBX1* has not been annotated in the chick genome and is not included in the analysis.

Table 6: Genes >2-fold Enriched in Chick or Mouse Cushions Previously Implicated in Cushion Development

Chick Genes	Mouse Genes
<i>BMP2</i> (Lyons, Pelton et al. 1990; Ma, Lu et al. 2005)	<i>Col2a1</i> (Li, Prockop et al. 1995)
<i>CXCR7</i> (Yu, Crawford et al. 2011)	<i>Eln</i> (Krishnamurthy, Opoka et al. 2012)
<i>FBN1</i> (Ng, Cheng et al. 2004)	<i>Epha3</i> (Stephen, Fawkes et al. 2007)
<i>HAS2</i> (Camenisch, Spicer et al. 2000)	<i>Erbb3</i> (Erickson, O'Shea et al. 1997; Camenisch, Schroeder et al. 2002)
<i>IGF2</i> (Hartnett, Glynn et al. 2010)	<i>Fzd1</i> (Yu, Smallwood et al. 2010)
<i>MSX2</i> (Chen, Ishii et al. 2008)	<i>Gpc1</i> (Niu, Bahl et al. 1998)
<i>SNAI2</i> (Niessen, Fu et al. 2008)	<i>Has2</i> (Camenisch, Spicer et al. 2000)
<i>SOX9</i> (Akiyama, Chaboissier et al. 2004; Lincoln, Kist et al. 2007)	<i>Msx1</i> (Chen, Ishii et al. 2008)
<i>TBX2</i> (Shirai, Imanaka-Yoshida et al. 2009; Singh, Hoogaars et al. 2012)	<i>Msx2</i> (Chen, Ishii et al. 2008)
<i>TBX20</i> (Stennard, Costa et al. 2005)	<i>Pitx2</i> (Kitamura, Miura et al. 1999)
<i>TGFB2</i> (Sanford, Ormsby et al. 1997)	<i>Postn</i> (Norris, Moreno-Rodriguez et al. 2008)
<i>WNT4</i> (Alfieri, Cheek et al. 2010)	<i>Rarg</i> (Mendelsohn, Lohnes et al. 1994)
<i>WNT6</i> (Alfieri, Cheek et al. 2010)	<i>Smad6</i> (Galvin, Donovan et al. 2000)
<i>WT1</i> (Zhou, Ma et al. 2009)	<i>Snai1</i> (Timmerman, Grego-Bessa et al. 2004)
<i>ZFPM2</i> (Ackerman, Herron et al. 2005; Zhou, Ma et al. 2009)	<i>Sox9</i> (Akiyama, Chaboissier et al. 2004; Lincoln, Kist et al. 2007)
	<i>Tbx2</i> (Shirai, Imanaka-Yoshida et al. 2009; Singh, Hoogaars et al. 2012)
	<i>Tgfb2</i> (Sanford, Ormsby et al. 1997)
	<i>Twist1</i> (Chen and Behringer 1995; Shelton and Yutzey 2008; Lee and Yutzey 2011; Vrljicak, Cullum et al. 2012)

myocardium (*Bmp4* (Keyes, Logan et al. 2003), *BMP2* (Keyes, Logan et al. 2003)) were identified as having cushion enriched expression in chick and mouse as expected. Of note, 31 of 105 identified in the mouse were found to be expressed in the endothelium or mesenchyme derived from endothelium. Thus, the RNA-seq methodology was sensitive enough to detect changes in gene expression in the endothelium and mesenchyme when the majority of the sample is derived from the myocardium. Relaxation of the stringency of gene enrichment to a level of >1.25-fold ($p<0.001$) (Figure 8) revealed 574 genes enriched in the chick (Appendix A) and 250 enriched in the mouse (Appendix B). Of these, 54 genes in the chick and 41 genes in the mouse were associated with abnormal heart development and function. Several genes known to play important roles in endocardial EMT were revealed in the >1.25-fold gene lists. Though there is an increased chance of including false positive genes by lowering the stringency, there may also be novel candidate genes in the 1.25 fold gene lists that would otherwise be missed with a 2 fold cutoff. In particular, small changes (<2-fold) in the expression levels of transcription factors may have a significant effect on cell behavior (Niwa, Miyazaki et al. 2000).

Gene Ontology (GO) Analysis of Cushion-Enriched Genes

To gain a better understanding of the genes in the >2-fold cushion enriched gene lists we examined the associated predicted protein location, predicted protein function and biological processes (Figure 9). Enriched genes encoded proteins with various predicted functions and cell locations, including

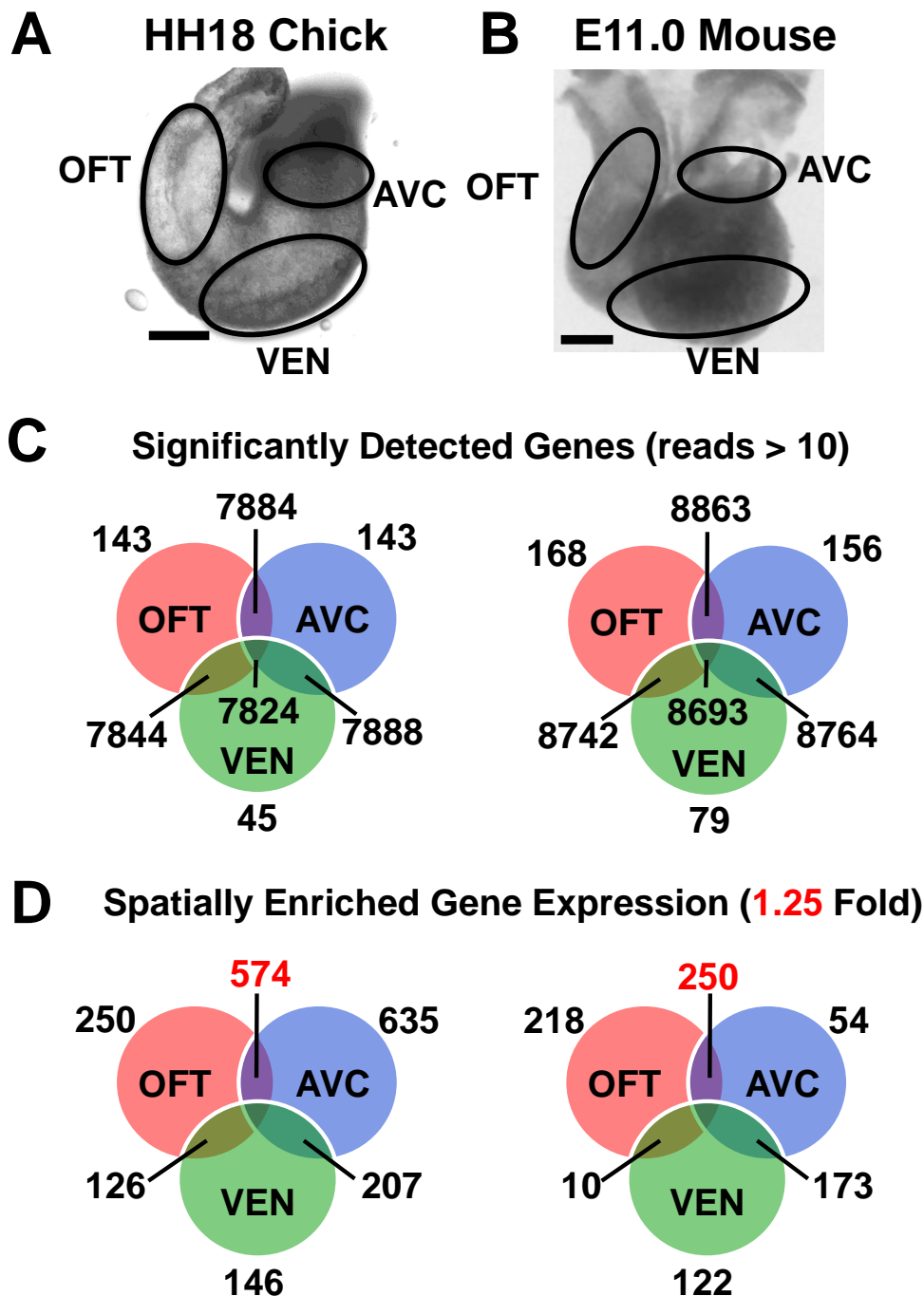


Figure 8: Spatial transcriptional profile of heart identifies cushion-enriched genes. A-B, AVC, OFT and VEN were dissected from equivalent stages of chick HH18 (A) and mouse E11.0 (B). C, RNA-seq analysis identified genes with significantly expressed (>10 reads) in each spatial region of the developing heart tube. D, Mapping genes with enriched expression (>1.25-fold) onto each spatial region identifies those genes with cushion-enriched expression (in red), 547 in the chick and 225 in the mouse.

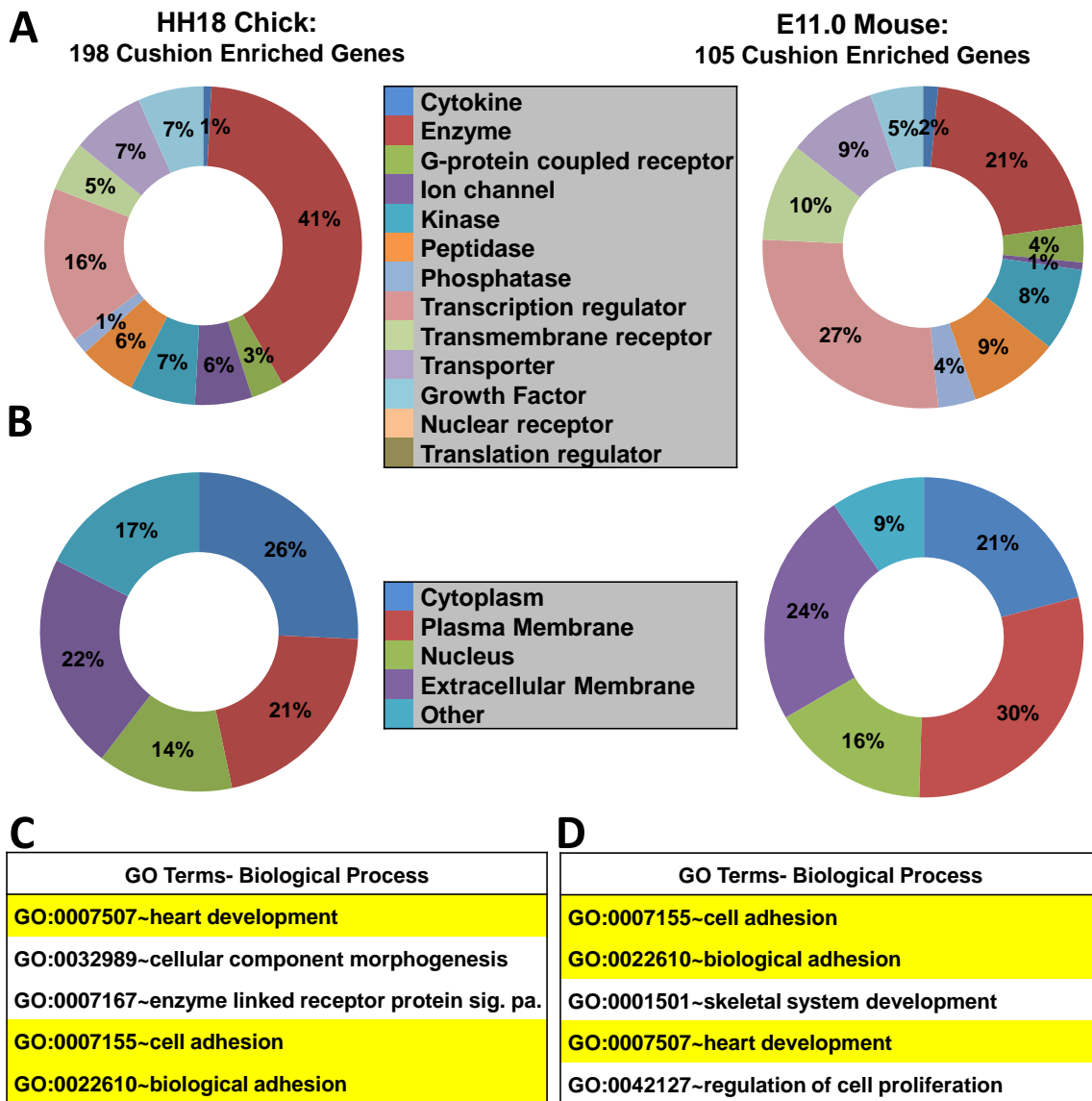


Figure 9: Gene ontology, predicted protein location, and protein function of >2-fold cushion-enriched genes. **A**, Predicted protein function of genes identified in the mouse and chick cushion-enriched gene lists generated using IPA software. Percent of total genes with defined function is depicted. Genes with unknown function in chick (89) and mouse (44) are not shown. **B**, Predicted protein location of genes identified in mouse and chick cushion using IPA software. **C-D**, Analysis of genes found >2-fold enriched in chick and mouse AVC and OFT using DAVID software. Selected significantly enriched biological processes (from DAVID BP-FAT) are depicted for chick and mouse ($p<0.0001$ for all terms). Significance was based on p-values generated by DAVID software(Dennis, Sherman et al. 2003). Biological processes highlighted in yellow are shared between chick and mouse.

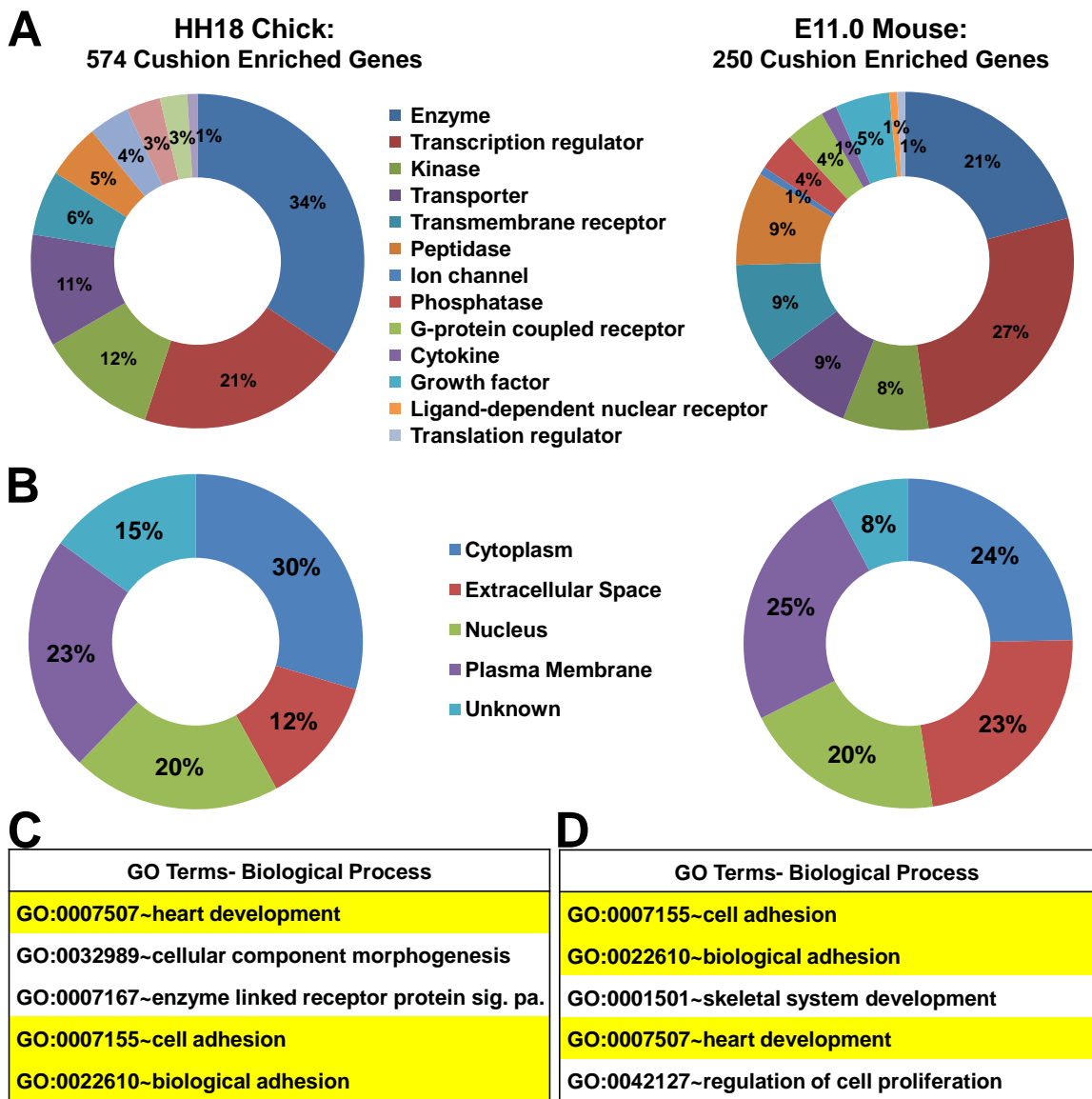


Figure 10: Gene ontology, predicted protein location, and protein function of >1.25 cushion-enriched genes. **A**, Predicted protein function of genes identified in the mouse and chick cushion enriched gene lists generated using IPA software. Percent of total genes with defined function is depicted. Genes with unknown function in mouse (96) and chick (265) are not shown. **B**, Predicted protein location of genes identified in mouse and chick cushion using IPA software. The number of genes predicted to be located to each region is depicted. **C-D**, Analysis of genes found >1.25-fold enriched in chick (**C**) and mouse (**D**) AVC and OFT using DAVID software revealed an enrichment of genes associated with biological processes important in EMT. Significance was based on p-values generated by DAVID software using a modified EASE score. Biological processes highlighted in yellow are shared between chick and mouse.

proteins predicted to be transcriptional regulators (Figure 9A-B). To examine which biological processes were associated with the cushion-enriched gene lists in chick and mouse we performed functional annotation using Database for Annotation, Visualization, & Integrated Discovery (DAVID) software(Dennis, Sherman et al. 2003). Several biological processes were identified in chick (Appendix C) and mouse (Appendix D) genes lists. Consistent with the shared underlying morphological processes occurring in the cushions of each, we identified biological processes enriched in both chick and mouse associated with the process of EMT (Figure 9C-D). Biological processes related to bone development (skeletal system organization) were observed and are consistent with the prior observation that there is a high degree of conservation in signaling pathways which regulate bone and valve development (Chakraborty, Cheek et al. 2008). GO analysis of the >1.25-fold gene lists yielded results similar to those obtained with the >2-fold gene lists (Figure 10). Thus, GO analysis of cushion-enriched gene lists in chick and mouse identified shared processes expected for a population of endothelial cells undergoing EMT.

Gene Regulatory Network (GRN) Analysis of Cushion-Enriched Genes

To gain a better understanding of how the genes enriched in the cushion interact with each other, GRN analysis was undertaken of the chick and mouse >2-fold differentially expressed gene lists using Ingenuity Pathway Analysis software (IPA) (www.ingenuity.com). Figure 11 depicts an example mouse gene network. Consistent with the known importance of endocardial EMT in valve

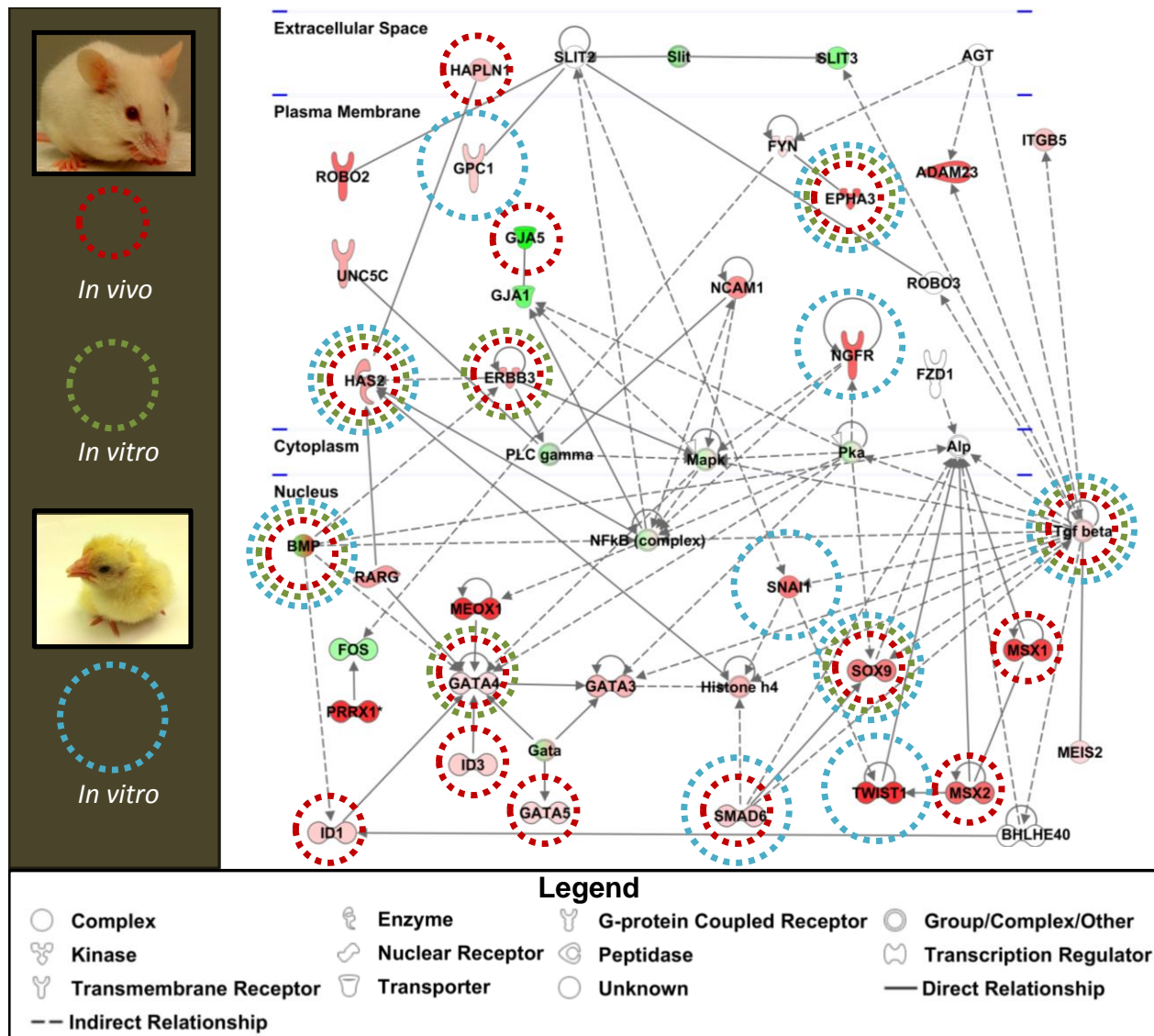


Figure 11: Gene regulatory networks generated from cushion-enriched-gene lists identifies known regulators of endocardial EMT. Gene regulatory networks were generated with IPA software using >2-fold cushion-enriched genes in chick and mouse. An example mouse network is depicted. Lines denote interactions between genes observed in the literature across all systems, with solid lines reflecting a direct interaction and dotted lines denoting an indirect interaction. Gene names over shapes denote nodes. Green nodes have decreased expression and red have increased expression. Additional genes were annotated based on known interactions in the literature (*Bmp*). *Haplh1* and *Meis2* nodes were added to identify potential interactions of novel candidate genes in this network. Genes were marked that are known to regulate EMT in mice *in vivo* (green circles), in mice *in vitro* (red circles), and in chick *in vitro* (blue circles).

development several genes in this network have been previously demonstrated to regulate EMT *in vitro* in mice (green circles) or in chick (blue circles). We observed several genes in the network that when targeted in mice resulted in phenotypes associated with abnormal cushion or valve development (red circles). This high number of genes known to be important in cushion or valve development provides confidence that this gene network reflects the biological processes occurring in the cushions. Our analysis confirms TGF β as a signaling node in regulating endocardial EMT and valvulogenesis (reviewed (DeLaughter, Saint-Jean et al. 2011)). This network also identified NF- κ B as a node and the role of NF- κ B in endocardial EMT is undescribed. Thus, GRN analysis of the cushion-enriched gene lists in chick and mouse provided insight into the relationships between genes known to regulate endocardial EMT and identified candidate signaling pathways for functional analysis.

Identification of Gene Candidates for Functional Analysis

We selected candidate genes for further analysis using our knowledge of the biology of the system to target genes involved in critical signaling pathways. *Hapln1*, *Id1*, *Meis2*, and *Foxp2* comprised our slate of candidate genes which were selected from both the >2-fold (*Hapln1* (chick) and *Foxp2* (mouse)) and >1.25 fold (*Id1* (mouse) and *Meis2* (mouse)) cushion enriched gene lists. For each candidate, whole mount *in situ* hybridization in E11.0 mouse embryos confirmed the expression pattern predicted by RNA-seq analysis (Figure 12). HAPLN1, or CRTL1, interacts with Hyaluronic Acid (HA) and additional ECM

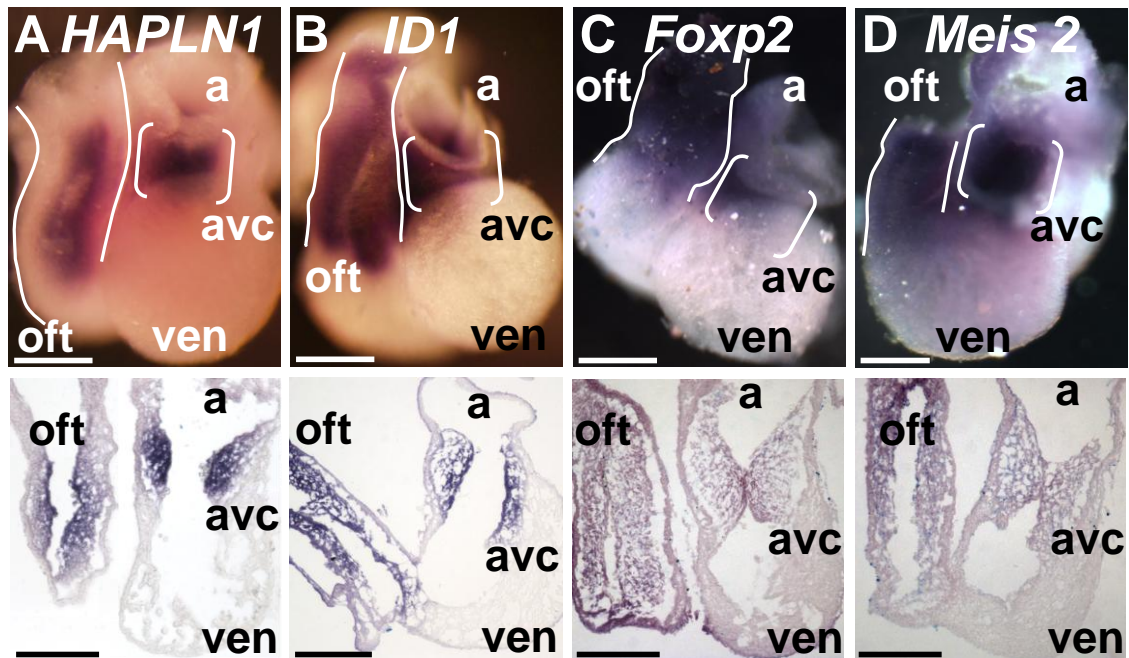


Figure 12: Confirmation of cushion-enriched gene expression in E11.0 hearts. A-D, Whole mount *in situ* hybridization with probes specific for (A) *HaplN1*, (B) *Id1*, (C) *Foxp2*, and (D) *Meis2* in E11.0 embryos in whole hearts (top) and 10 μ M cryosections (bottom) revealed enriched expression in the AVC (brackets) and OFT (outlines) compared to VEN. avc- atrioventricular canal, oft- outflow tract, a- atria, ven- ventricle. Scale bars: 100 μ M.

proteins in the extra-cellular space to affect ECM organization (Morgelin, Paulsson et al. 1995; Matsumoto, Shionyu et al. 2003). The deletion of *Hapln1* in mice results in hypoplastic valves (Wirrig, Snarr et al. 2007). Inhibitor of DNA binding 1, ID1, is a helix-loop-helix (HLH) protein that acts as a dominant negative antagonist of basic HLH transcription factors and can regulate both TGF β and BMP signaling. MEIS2 has recently been reported to be required for cardiac looping in zebra fish but has no described function in valve development (Paige, Thomas et al. 2012). FOXP2 is a forkhead/winged-helix transcription factor that has been extensively studied in the context of neural development. It is required for birds to learn song and mutations in FOXP2 have been linked to human speech pathologies (Enard 2011). Although some candidates have been studied in valvulogenesis, none have a described role in endocardial EMT.

A functional analysis using siRNA to target candidate genes in the well-defined chick AVC explant collagen gel assay *in vitro* was used to assess any role in endocardial EMT (reviewed (DeLaughter, Saint-Jean et al. 2011; Lencinas, Tavares et al. 2012)). Each of two independent siRNA constructs targeting candidates resulted in a decrease of endocardial EMT (Figure 13 A-E). qPCR analysis of explants confirmed both the expression and successful targeting of these genes in the chick AVC explants (Figure 14). These results establish a role for each candidate in the regulation of endocardial EMT *in vitro* and confirm our analysis was successful in identifying genes that regulate endocardial EMT. The lack of effect of control siRNA on EMT and the reported successful targeting of genes and pathways in this model that display no effect

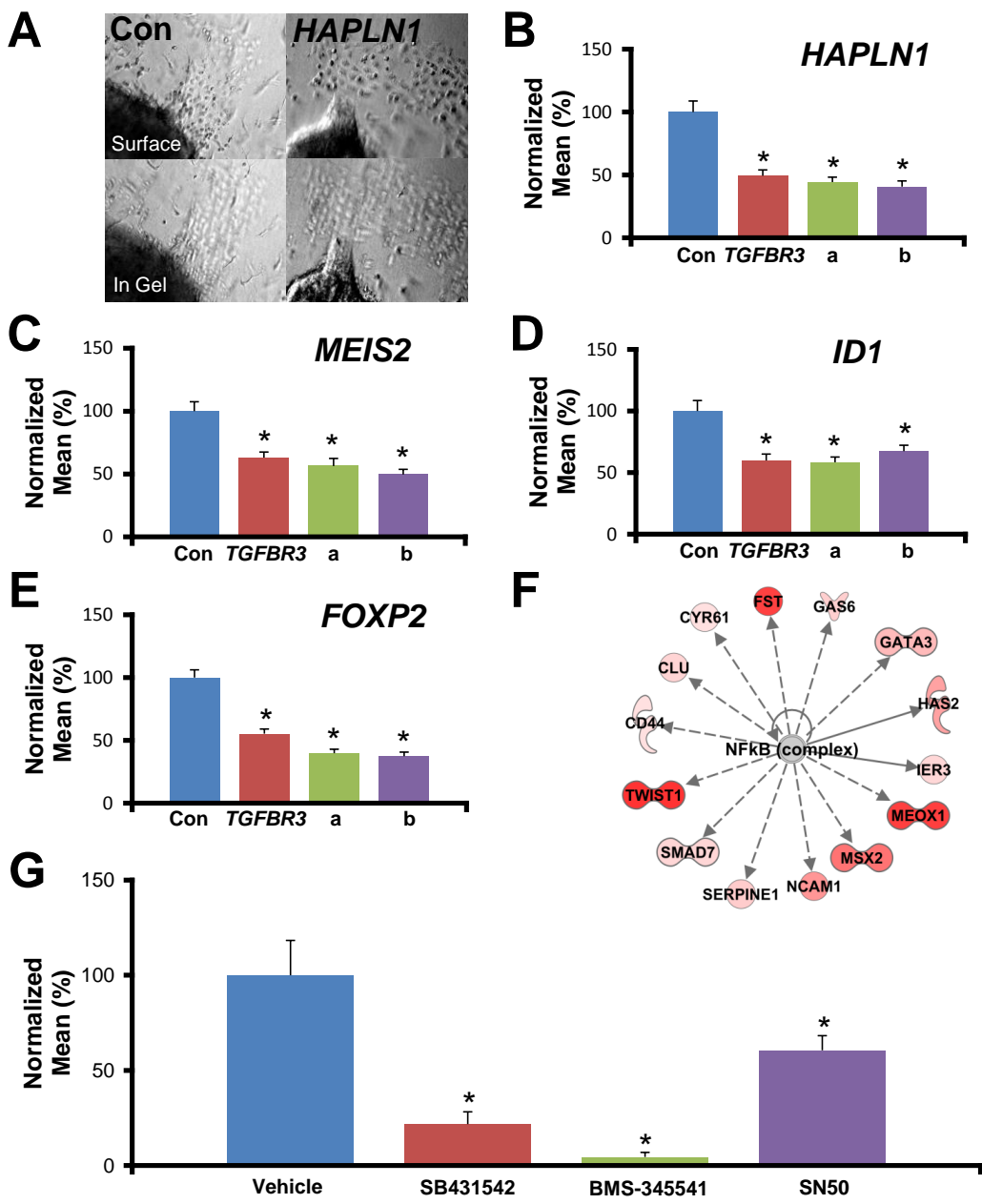


Figure 13: Candidate genes are required for endocardial EMT *in vitro*. **A,** Representative photomicrographs of AVC explants incubated with *HAPLN1*-targeted siRNA. **B-E,** Candidate gene expression in HH16 chick embryos was knocked down with siRNA in an *in vitro* collagen gel assay. The mean number of cells in the collagen gel was determined and normalized to the number of cells in controls (100%). Con - GC-content matched, randomized siRNA constructs with no homology to any known chick gene, *TGF β R3* - siRNA targeting a gene known to be required for EMT *in vitro*. a or b - independent constructs targeting indicated gene. * - p<0.01. **F,** Transcriptional network depicting genes known to be downstream of NF- κ B which had increased expression in the AVC and VEN. See legend in Figure 11. **G,** NF- κ B inhibition by two independent small molecule inhibitors (10 μ M BMS 345541 and 2 μ M SN50) resulted in a loss of function an *in vitro* collagen gel assay. SB431542, an ALK5 kinase inhibitor, was used as a positive control. Vehicle - 0.01% DMSO. * - p<0.01.

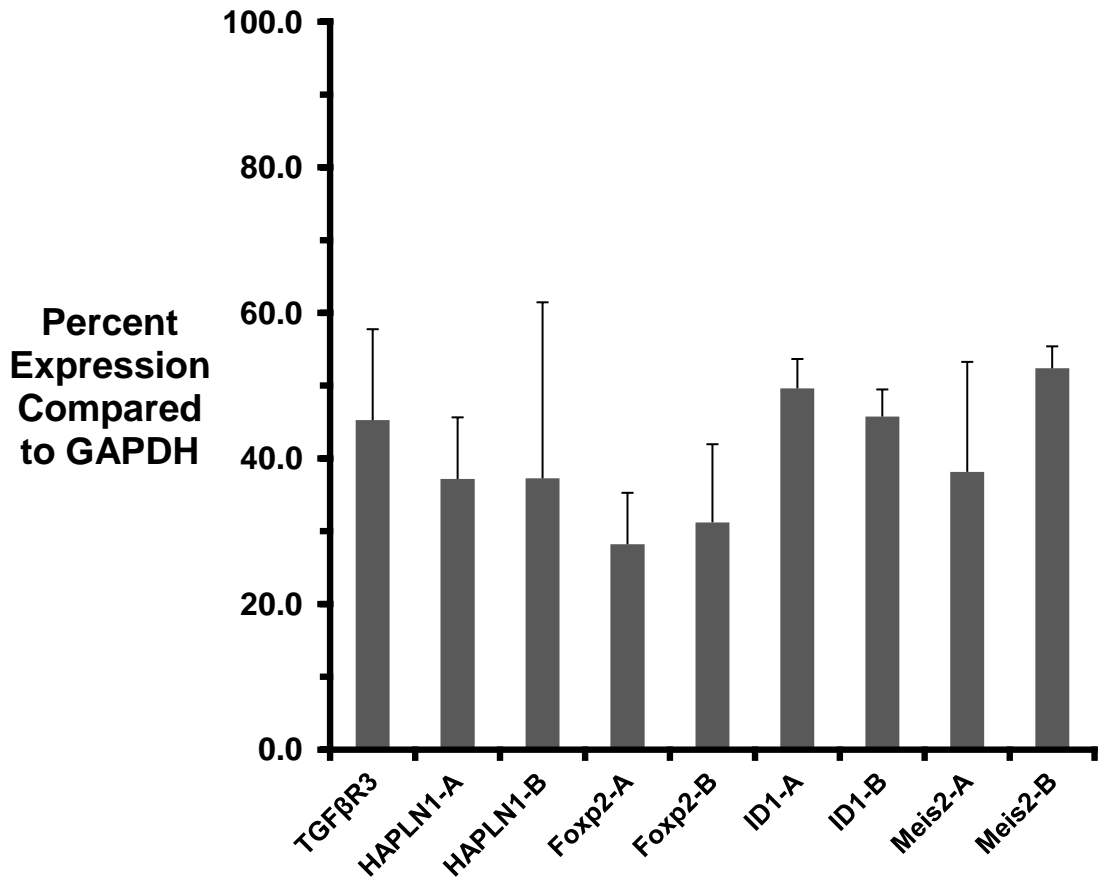


Figure 14: Quantification of siRNA Knockdown. Explants were incubated with siRNA constructs targeting *TGF β R3* (positive control), *HAPLN1*, *Foxp2*, *ID1*, *MEIS2* or a randomized GC-matched construct (negative control) for 48 hours on a collagen gel. To get sufficient RNA, 15 explants were used for each siRNA construct (positive control, negative control, a, b) and repeated in triplicate for each gene targeted (*HAPLN1*, *FOXP2*, *ID1*, *MEIS2*). The expression of these genes was then assayed by quantitative real time (RT)-PCR. Expression was normalized to GAPDH for each experiment. *TGF β R3* siRNA incubation significantly reduced *TGF β R3* mRNA expression level by 53%. *HAPLN1* mRNA expression levels were significantly reduced by 55% and 63% by siRNA treatment with *HAPLN1-A* and *HAPLN1-B* respectively. *FOXP2* mRNA expression levels were significantly reduced by 78% and 76% by siRNA treatment with *FOXP2-A* and *FOXP2-B* respectively. *ID1* mRNA expression levels were significantly reduced by 53% and 57% by siRNA treatment with *ID1-A* and *ID1-B* respectively. *MEIS2* mRNA expression levels were significantly reduced by 67% and 51% by siRNA treatment with *MEIS2-A* and *MEIS2-B* respectively. All genes depicted in the graph were significantly reduced compared to controls ($p < 0.01$).

on EMT (Townsend, Wrana et al. 2008; Townsend, Robinson et al. 2011) supports the validity and specificity of these results.

Selection and Validation of Signaling Pathway Identified by GRN Analysis

An advantage of GRN analysis lies in the ability to generate networks from a list of differentially expressed genes to predict the involvement of genes and signaling pathways where expression is unchanged. This approach can identify potential regulatory nodes that may escape notice if only gene expression is examined. One such example from our GRN analysis is the NF- κ B pathway (Figure 11) where signaling activity is regulated on the protein level (reviewed (Vallabhapurapu and Karin 2009)) making it unlikely to appear in a screen of gene expression. Indeed, NF- κ B pathway signaling components were not found in our cushion-enriched gene lists yet our strategy of using GRN analysis allowed us to identify NF- κ B as a potential regulator of endocardial EMT. Many upstream regulators of NF- κ B were observed and more edges were associated with NF- κ B than other nodes, such as *Pka* (Figure 11). We also examined those genes regulated by NF- κ B in the cushion-enriched gene list. Figure 13F depicts genes enriched in the AVC and OFT which are known to be directly or indirectly regulated by NF- κ B signaling, including several genes known to be important in endocardial EMT (*Has2*, *Msx2*, *Twist1*). NF- κ B signaling has long been associated with adult heart disease (reviewed (Gordon, Shaw et al. 2011)) and has recently been linked to FGF-2 mediated EMT in corneal endothelial cells (Lee and Kay 2012). However, the role of NF- κ B signaling in endocardial EMT

has not been investigated. Together, these data and the known role of NF- κ B in EMT in other systems led us to select NF- κ B for further study.

To test for a role of NF- κ B in endocardial EMT we took advantage of the availability of small molecule inhibitors of NF- κ B signaling. We chose 2 different inhibitors (10 μ M BMS 345541 and 2 μ M SN50) with differing mechanisms of action to block NF- κ B function in the collagen gel assay. BMS 345541 specifically inhibits the phosphorylation of I κ B kinase by inhibition of IKK (Burke, Pattoli et al. 2003) which prevents I κ B targeting for degradation and the subsequent release of NF- κ B into the nucleus. SN50 is a synthetic peptide which blocks the nuclear import of the NF- κ B complex itself (Lin, Yao et al. 1995). Some explants were also incubated with 2.5 μ M SB431542, an ALK5 inhibitor previously characterized in this system (Townsend, Wrana et al. 2008), as a positive control for small molecule inhibition of EMT, or vehicle as a negative control. Incubation with BMS 345541 or SN50 resulted in a 31% or 79% reduction in the number of cells invading into the collagen gel compared to vehicle-incubated explants, respectively (Figure 13G). Together, these data indicate that NF- κ B signaling can regulate endocardial EMT *in vitro*.

Discussion

Spatial transcriptional profile of the heart tube in chick and mice

In this study we used an unbiased approach to identify important regulators of cardiac valvular EMT. Previous studies have used a similar spatial

analysis in E10.5 mouse hearts in an effort to identify genes associated with endocardial EMT and valvulogenesis. Analysis of the AVC and VEN by microarray (Wirrig, Snarr et al. 2007) and, more recently, examination of micro-dissected atria, AVC, OFT, and VEN by TAG-seq (Vrljicak, Cullum et al. 2012), generated lists of genes enriched in the regions of the heart tube undergoing EMT. This information was used to identify and target a single gene, *Hapl1*, *in vivo* in mice. However, our approach was unique in that it coupled the power of spatial analysis with a rapid *in vitro* bioassay to confirm a role for candidate genes and pathways in endocardial EMT. To that end we took advantage of the longstanding collagen gel chick AVC explant assay and expanded our spatial analysis to include equivalent stages of both mouse and chick heart tubes. The inclusion of the chick model allowed for cross species comparison and provided primary data obtained from the species upon which our *in vitro* assay is based.

The genes identified as enriched in these two models were subjected to GO and GRN analysis which revealed biological processes, signaling pathways and gene interactions known to be important in endocardial EMT. Among others, key components of TGF β (*TGF β 2* chick/mouse), BMP (*Bmp2* mouse), retinoic acid (*CYP26B1* chick/mouse), and WNT (*WNT4* chick, *Wnt9b* mouse) signaling pathways were revealed. Several genes common to both lists were known to play a role in valve formation (Table 7). Thus, the cushion-enriched gene lists accurately reflect the biological processes associated with endocardial EMT and suggest candidate genes and networks for functional confirmation.

Table 7: Genes >2-fold Enriched in Both Chick and Mouse Cushions

Chick			Mouse		
Gene	AVC/VEN	OFT/VEN	Gene	AVC/VEN	OFT/VEN
<i>Cyp26b1*</i>	3.799	3.099	<i>Cyp26b1*</i>	2.568	2.918
<i>Doc2b*</i>	49	49	<i>Doc2b*</i>	11.022	16.155
<i>Has2</i>	3.455	4.082	<i>Has2</i>	4.178	6.579
<i>Matn4*</i>	19.256	8.164	<i>Matn4*</i>	23.974	7.754
<i>Msx2</i>	2.991	3.08	<i>Msx2</i>	6.29	6.368
<i>Rspo3*</i>	20.746	19.477	<i>Rspo3*</i>	10.651	15.906
<i>Sox9</i>	3.99	3.549	<i>Sox9</i>	5.433	5.954
<i>Tbx2</i>	6.81	2.826	<i>Tbx2</i>	9.415	4.846
<i>Tgfb2</i>	2.123	3.047	<i>Tgfb2</i>	2.054	3.568

*Denotes genes previously not linked to endocardial EMT.

Mean fold enrichment in the AVC or OFT is indicated.

Validation of candidate genes as regulators of endocardial EMT in vitro

We identified and confirmed the involvement of novel genes and a novel pathway in endocardial EMT *in vitro*. HAPLN1 is expressed throughout the heart tube at E10.0 and becomes restricted to the endocardium and mesenchyme of the AVC and OFT by E11.0 (Figure 12A) (Wirrig, Snarr et al. 2007). Deletion of *Hapl1n1* in mice resulted in hypoplastic valves similar to, but less severe than, the null phenotypes of HA and Versican, both of which HAPLN1 binds (Perkins, Nealis et al. 1989; Matsumoto, Shionyu et al. 2003; Wirrig, Snarr et al. 2007). The authors noted that it was unclear whether the lack of cellularization of the cushions in these animals was due to a defect in post-EMT cell proliferation or in endothelial EMT itself (Wirrig, Snarr et al. 2007). Our data suggests that the hypoplastic valves observed in *Hapl1n1* null mice may be at least partially due to

aberrant endocardial EMT. Similarly, *Id1* is expressed in the endothelium and cushion mesenchyme at E10.5/E11.0 (Figure 12B) (Jen, Manova et al. 1996; Fraidenraich, Stillwell et al. 2004). Deletion of both *Id1* and *Id3* leads to hypoplastic cushions associated with discontinuous endothelium in the context of disrupted heart development (Fraidenraich, Stillwell et al. 2004). Targeting of *Id1* in the endothelium of *Id3* null mice yields a less severe phenotype that displays signs of aberrant cushion mesenchyme development associated with valvular and septal defects (Zhao, Beck et al. 2011). These studies point to a potential role for *Id1* in VIC development, yet *Id1* had not been shown to regulate endothelial EMT. Our results suggest that compromised endothelial EMT may contribute to the phenotypes seen in *Id1* null mice.

Members of the FOXP family of transcription factors have been implicated in heart development including FOXP1 (Wang, Weidenfeld et al. 2004) and FOXP4 (Li, Zhou et al. 2004). At E11.0, *Foxp2* is expressed abundantly in the endocardium and mesenchyme of the OFT and AVC when compared to the VEN as well as in the myocardium of the OFT (Figure 12C). Both FOXP2 and FOXP4 have been shown to promote the delamination of neuroepithelial cells in the mouse (Rousso, Pearson et al. 2012) demonstrating a role for each in regulating EMT *in vivo*. *Foxp4* was also enriched in our RNA-seq data sets and can form heterodimers with FOXP2 (Li, Weidenfeld et al. 2004). The presence of *Foxp4* in the cushions suggests that FOXP4 may compensate for the loss of FOXP2, explaining the lack of a reported cushion or valve phenotype in *Foxp2* null mice (French, Groszer et al. 2007).

A second transcription factor, MEIS2, is expressed in the endocardium and mesenchyme of the AVC and OFT at E11.0 (Figure 12D). Recent studies in zebrafish identified a role for *meis2* in cardiac looping (Paige, Thomas et al. 2012), yet no data concerning the role of MEIS2 in chick or mouse heart development has been reported. MEIS2 induces proximal gene expression while BMP signaling inhibits *MEIS2* expression to promote distal limb gene expression and support proper limb patterning (Capdevila, Tsukui et al. 1999). The well described role of BMP in regulating endocardial EMT (Ma, Lu et al. 2005) provides a potential role for MEIS2 as a modulator of this process and subsequent valve maturation.

NF-κB signaling pathway in endocardial EMT

Although the expression of components of the NF-κB pathway were not enriched in the AVC or OFT, GRN analysis revealed that several genes regulated by NF-κB had enriched expression in the AVC and OFT. Perturbation of the NF-κB signaling pathway with small molecule inhibitors revealed a requirement for NF-κB signaling in endocardial EMT. As the role of NF-κB in driving EMT in cancer cells via regulation of *Snai1/Slug/Twist* is well described (reviewed (Min, Eddy et al. 2008)), the NF-κB pathway may represent a mechanism by which transcription factors that repress the epithelial phenotype in endocardial EMT are regulated. Mouse embryos lacking p50 survive to adulthood with no apparent developmental defects (Sha, Liou et al. 1995) while mice lacking p65 (Beg, Sha et al. 1995) die at E15.5 from liver degeneration by

apoptosis. No valvular phenotypes were reported. Our findings suggest a targeted re-examination of NF- κ B signaling in valve development may reveal previously unappreciated defects. It is also possible that disruption of NF- κ B signaling in VICs may result in adult valvular disease or altered response to injury.

It is clear that the *in vitro* bioassay does not always recapitulate *in vivo* phenotypes (reviewed (Lencinas, Tavares et al. 2012)). The more complex ECM and signaling environment present *in vivo* may allow endocardial cells to compensate in ways cells exposed to the simpler collagen gel system cannot. For example, targeting of *Tgfbr2* *in vivo* does not inhibit endocardial EMT, but AVC explants from these mice fail undergo EMT *in vitro* (Azhar, Runyan et al. 2009). However, later stages of cushion development are abnormal in *Tgfb2* conditionally null mice, suggesting that the mesenchyme resulting from EMT is abnormal. Therefore, this system provides a robust bioassay to identify potential targets for gene perturbation *in vivo*.

Future Studies

Other candidate genes identified by our analysis were left untested, but represent interesting avenues for future work. For example, ECM remodeling is fundamentally important in valve development. We identified several genes encoding ECM related proteins that were enriched in mouse cushions including collagens (*Col2a1*, *Col6a3*, *Col9a1*, *Col9a3*), hyaluronic acid (*Has2*, *Cd44*), and *Eln*. Knowledge of the ECM, which the mesenchymal cells and VICs must

interact with and remodel subsequent to EMT, may provide important clues on how to better design *in vitro* systems that promote VIC differentiation and maintenance. Future studies combining spatial and temporal transcriptional profiles will likely provide further insight into endocardial EMT.

CHAPTER III

TRANSCRIPTIONAL PROFILING OF CULTURED, EMBRYONIC EPICARDIAL CELLS IDENTIFIES NOVEL GENES AND SIGNALING PATHWAYS REGULATED BY TGF β R3 *IN VITRO*

Introduction

The epicardium plays an important role in coronary vessel development (reviewed (Olivey, Compton et al. 2004; Olivey and Svensson 2010)). Formation of the epicardium occurs when a population of mesothelial cells, termed the proepicardium, attach to and migrate over the heart tube myocardium (Viragh and Challice 1981; Manner 1993). A subpopulation of the epithelial, epicardial cells subsequently invade into the subepicardial space with some cells proceeding to invade into the myocardium as well (reviewed (von Gise and Pu 2012)). These EPDCs differentiate into distinct lineages (Poelmann, Gittenberger-de Groot et al. 1993; Gittenberger-de Groot, Vrancken Peeters et al. 1998; Lie-Venema, Eralp et al. 2008; Christoffels, Grieskamp et al. 2009; Grieskamp, Rudat et al. 2011), that include cardiac fibroblasts, pericytes, and vascular smooth muscle cells, and support the formation of coronary vessels. Several lines of evidence are now revealing the importance of these same developmental processes in cardiac repair and that the epicardium makes critical contributions to cardiac response to injury (reviewed (von Gise and Pu 2012)). Despite this, the signaling processes which regulated epicardial EMT are

incompletely understood.

TGF β R3 deletion in mice leads to failed coronary vessel development (Compton, Potash et al. 2007). *Tgfb3*^{-/-} hearts featured a discontinuous epicardium overlying an expanded subepicardial space. Further studies revealed a significant decrease in proliferation and invasion of epicardium and epicardially-derived mesenchyme (Sanchez, Hill et al. 2011). Overall, these studies demonstrated that TGF β R3 plays an important and non-redundant role in epicardial behavior and coronary vessel development *in vivo*.

TGF β R3 binds TGF β 1, TGF β 2 and TGF β 3 and is uniquely required to bind TGF β 2 with high affinity (Lopez-Casillas, Cheifetz et al. 1991; Lopez-Casillas, Wrana et al. 1993). TGF β R3 is also capable of binding and signaling in response to BMP2 (Kirkbride, Townsend et al. 2008) and functions as a receptor for inhibin (Wiater, Harrison et al. 2006). TGF β R3 presents ligand to TGF β R2 to promote both Smad-dependent and -independent signaling (Derynck and Zhang 2003). The highly conserved 43 amino acid intracellular domain of TGF β R3 is not required for ligand presentation (Blobe, Schiemann et al. 2001) but may regulate other signaling events. Phosphorylation of the cytoplasmic domain of TGF β R3 by TGF β R2 at Thr841 is required for β -arrestin2 binding, leading to internalization of TGF β R3 and down-regulation of TGF β signaling. The 3 C-terminal amino acids of TGF β R3, STA, are a Class I PDZ binding domain that binds the scaffolding protein GIPC which in turn stabilizes TGF β R3 on the plasma membrane to promote signaling (Blobe, Liu et al. 2001).

Tgfbr3^{+/+} epicardial cells undergo loss of epithelial character and invasion into collagen gels *in vitro* in response to TGFβ1, TGFβ2, and BMP2, ligands known to bind TGFβR3 (Lopez-Casillas, Cheifetz et al. 1991; Kirkbride, Townsend et al. 2008). While loss of epithelial character was still observed after loss of TGFβR3, *Tgfbr3^{-/-}* cells had reduced invasion in response TGFβ1, TGFβ2, and BMP2, a response that was rescued by the addition of TGFβR3 (Sanchez, Hill et al. 2011; Hill, Sanchez et al. 2012; Sanchez and Barnett 2012). TGFβ1 and TGFβ2 promoted smooth muscle differentiation in *Tgfbr3^{+/+}* and *Tgfbr3^{-/-}* cells while BMP2 did not (Hill, Sanchez et al. 2012). Surprisingly, other ligands known to be important in epicardial EMT also required TGFβR3 to promote invasion in epicardial cells (FGF2 (Morabito, Dettman et al. 2001; Tomanek, Sandra et al. 2001), High Molecular Weight HMW-HA (Craig, Austin et al. 2010; Craig, Parker et al. 2010)). Impaired invasion was not due to a general inability of these cells invade as PDGFAA, PDGFBB and VEGFC still induced invasion in *Tgfbr3^{-/-}* epicardial cells (Sanchez, Hill et al. 2011). This ability of TGFβR3 to regulate epicardial cell behavior in response to an array of ligands may explain the severity of the *in vivo* phenotype of *Tgfbr3^{-/-}* embryos when compared to the absence of a phenotype in mice lacking individual TGFβ ligands (Shull, Ormsby et al. 1992; Sanford, Ormsby et al. 1997; Sridurongrit, Larsson et al. 2008). Targeted deletion of ALK5 in the epicardium in mice *in vivo* results in interrupted epicardial attachment to the myocardium, loss of expression of specific adhesion molecules, thinned myocardium, and a loss of coronary smooth muscle (Sridurongrit, Larsson et al. 2008). These embryos survive until birth, suggesting

that, unlike in embryos lacking TGF β R3, the coronary vessels function to some degree as mice lacking coronary vessels die at approximately E14.5-E16.5 (Yang, Rayburn et al. 1995; Moore, McInnes et al. 1999; Tevosian, Deconinck et al. 2000). These data suggest that TGF β R3 signaling regulates a common pathway accessed by several upstream regulators of cell invasion.

TGF β R3-dependent invasion stimulated by TGF β 1, TGF β 2, BMP2, HMW-HA, or FGF2 was shown to require the cytoplasmic domain of TGF β R3 *in vitro* (Sanchez, Hill et al. 2011). Overexpression of TGF β R3 rescued invasion in *Tgfb3*^{-/-} epicardial cells *in vitro* in response to TGF β 1, TGF β 2, BMP2, HMW-HA, or FGF2, whereas constructs expressing a TGF β R3 mutant lacking the 3 C-terminal amino acids required for GIPC binding fail to rescue invasion (Sanchez, Hill et al. 2011; Hill, Sanchez et al. 2012; Sanchez and Barnett 2012). The importance of this interaction is supported by the observation that GIPC is not only required for invasion in *Tgfb3*^{+/+} epicardial cells, but GIPC overexpression can promote invasion in the absence of additional ligand. GIPC regulation of epicardial invasion depends on TGF β R3 since GIPC expression in *Tgfb3*^{-/-} cells fails to rescue invasion and inhibition of GIPC expression impairs the ability of TGF β R3 to rescue invasion in *Tgfb3*^{-/-} cells (Sanchez, Hill et al. 2011). Similar results were observed in endocardial cushions where the interaction of TGF β R3 with GIPC is required to promote TGF β 2 and BMP2 dependent invasion *in vitro* (Townsend, Robinson et al. 2011). These data linking defects in invasion

A

	Vehicle	TGFβ1	TGFβ2	BMP2	Cell Behavior
<i>Tgfb3^{+/+}</i>	-	+	+	-	SM Diff.
	+	+++	+++	+++	Proliferation
	-	-	-	-	Apoptosis
	-	+	+	+	Loss of EC
	-	+++	+++	+++	Invasion
	Vehicle	TGFβ1	TGFβ2	BMP2	
<i>Tgfb3^{-/-}</i>	-	+	+	-	SM Diff.
	-	+	+	+	Proliferation
	++	++	++	++	Apoptosis
	-	+	+	+	Loss of EC
	-	+	+	+	Invasion

B

<i>Tgfb3^{+/+}</i>	Vehicle	TGFβ1	TGFβ2	BMP2
Reads	49.1×10^6	48.8×10^6	39.9×10^6	24.3×10^6
Genes	15,103	14,806	14,977	14,888
<i>Tgfb3^{-/-}</i>	Vehicle	TGFβ1	TGFβ2	BMP2
Reads	30.6×10^6	42.9×10^6	42.3×10^6	31.5×10^6
Genes	13,966	13,957	14,047	14,088

Figure 15: *Tgfb3^{-/-}* epicardial cells have dysregulated proliferation, apoptosis, and invasion. A, Summary of the phenotypes of *Tgfb3^{+/+}* and *Tgfb3^{-/-}* epicardial cells *in vitro*. EC - epithelial character, SM Diff.- smooth muscle differentiation. B, RNA-seq analysis of *Tgfb3^{+/+}* and *Tgfb3^{-/-}* epicardial cells incubated with ligand for 72 hours. Reads - the total number of mapped sequences for each of the 8 groups (in duplicate). Genes - the total number of genes with a significant number of reads (>10) mapped.

of *Tgfbr3*^{-/-} epicardial cells to the cytoplasmic domain of TGF β R3 which is not required for ligand presentation suggests a unique, non-redundant role for TGF β R3 in regulating epicardial and endocardial EMT.

Here, we use a well defined *in vitro* system based on immortalized epicardial cells coupled with RNA-seq analysis to generate a transcriptional profile of *Tgfbr3*^{+/+} and *Tgfbr3*^{-/-} cells incubated with ligands that stimulate TGF β R3-dependent invasion. The resulting transcriptional profiles has identified regulators of epicardial cell behavior downstream of TGF β R3 and provided the first description of genes downstream of TGF β R3.

Experiments in this chapter were performed in collaboration with Cyndi Hill, who performed the NF- κ B reporter and invasion assays in Figure 24, and Anita Austin, who performed the immunohistochemistry in Figure 16.

Methods

Generation of cell lines

Tgfbr3^{+/-}:Immorto mice were generated as described (Austin, Compton et al. 2008) and maintained on a C57BL/6 SV129 mixed background. *Tgfbr3*^{+/+}:Immorto and *Tgfbr3*^{-/-}:Immorto immortalized epicardial cell lines were generated from littermates as described (Austin, Compton et al. 2008) from E11.5 embryos (Figure 16).

Cell culture

To maintain the immortalized state, cells were grown at 33°C in DMEM containing 10% fetal bovine serum, 100 U/ml penicillin/streptomycin, Insulin–Transferrin–Selenium (ITS: 1 µg/ml insulin, 5.5×10^{-4} µg/ml transferrin, 0.677 µg/ml selenium), and 10 U/ml interferon γ (INFγ). For experiments, the T-antigen was inactivated by culturing at 37°C in the absence of ITS or INFγ. Cells were seeded at 200,000 cells per well of a 6-well tissue culture plate and allowed to adhere overnight at 37°C. The medium was replaced with medium containing either VEH, 250 pM TGFβ1, 250 pM TGFβ2, or 5 nM BMP2. After a 72 hour incubation period at 37°C, total RNA was isolated via standard phenol-chloroform extraction (TRIzol Invitrogen). RNA was purified (Qiagen mini-prep kit) following the manufacturer's protocol. Quantity and quality of RNA was determined by an Agilent Bioanalyzer. One well of a 6-well plate yielded 10-20 µg of RNA.

RNA-seq

The generation of RNAseq libraries without normalizations or RNA/cDNA fragmentation were performed as described (Christodoulou, Gorham et al.). Libraries were sequenced as 50bp paired end sequences on a single lane of the Illumina HiSeq2000. TOPHAT (Trapnell, Pachter et al. 2009) (<http://tophat.cbcb.umd.edu/>) was used to align HiSeq 2000 reads to produce bam files. Reads were normalized to total mRNA (total aligned reads per gene-loci per million). Gene expression profiles were generated as described (Christodoulou, Gorham et al. 2011) using a Bayesian p-value

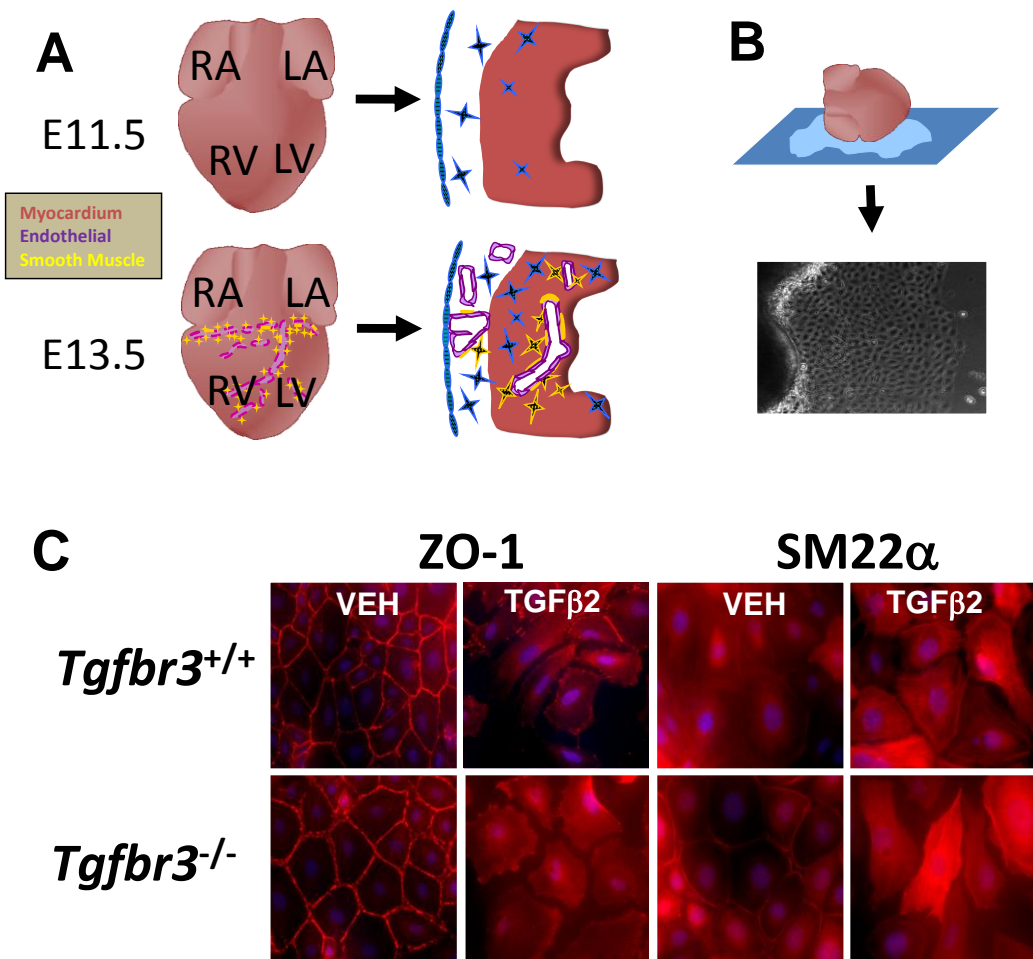


Figure 16: Immortalized epicardial cells undergo loss of epithelial character. **A**, The epicardium undergoes EMT at E11.5-13.5. Subsequently, transforming epicardial cells invade the subepicardial space and myocardium towards forming coronary vessels. Blue- epicardium. Purple- endothelium. Yellow- smooth muscle cells. Red- myocardium. **B**, Immortalized epicardial cells were derived from E11.5 *Tgfb3*^{+/+} and *Tgfb3*^{-/-} embryos which expressed a temperature-sensitive large T-antigen. **C**, Immunohistochemistry of *Tgfb3*^{+/+} or *Tgfb3*^{-/-} immortalized epicardial cells after 72 hours incubation with TGF β 2 or vehicle. TGF β 2 increased expression of SM22 α and form stress fibers in the enlarged, elongated cells. ZO1 becomes redistributed to the cytoplasm.

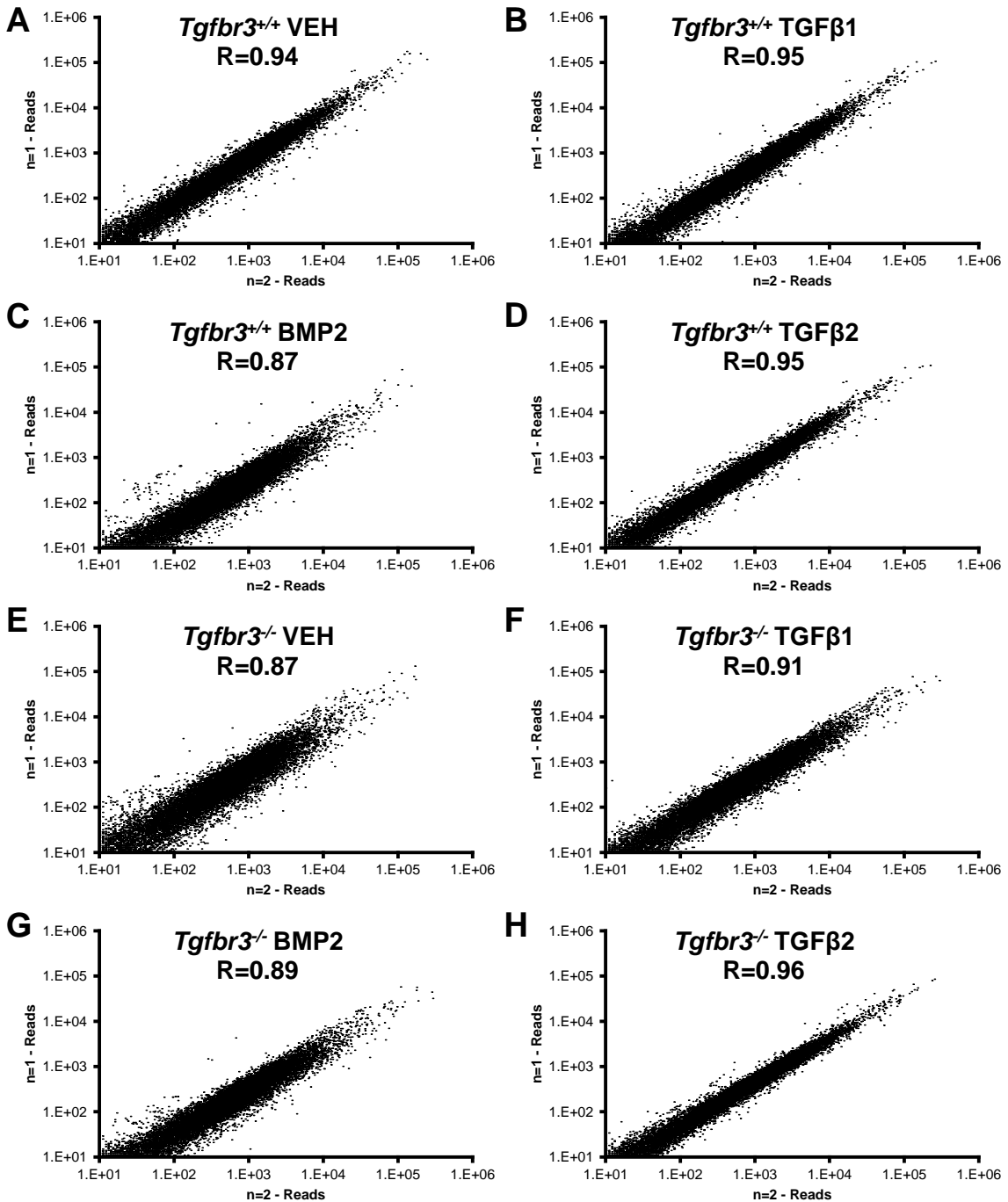


Figure 17: Variability of RNA-seq data sets. The reads for the two biological replicates ($n=1$, $n=2$) for each group (VEH, TGF β 1, TGF β 2, BMP2) in *Tgfb3^{+/+}* (A-D) or *Tgfb3^{-/-}* (E-H) were plotted against each other. There was a high degree of agreement in *Tgfb3^{+/+}* (A-D) ($R>0.87$) or *Tgfb3^{-/-}* (E-H) ($R>0.89$) datasets. These comparisons support a high degree of agreement between biological replicates.

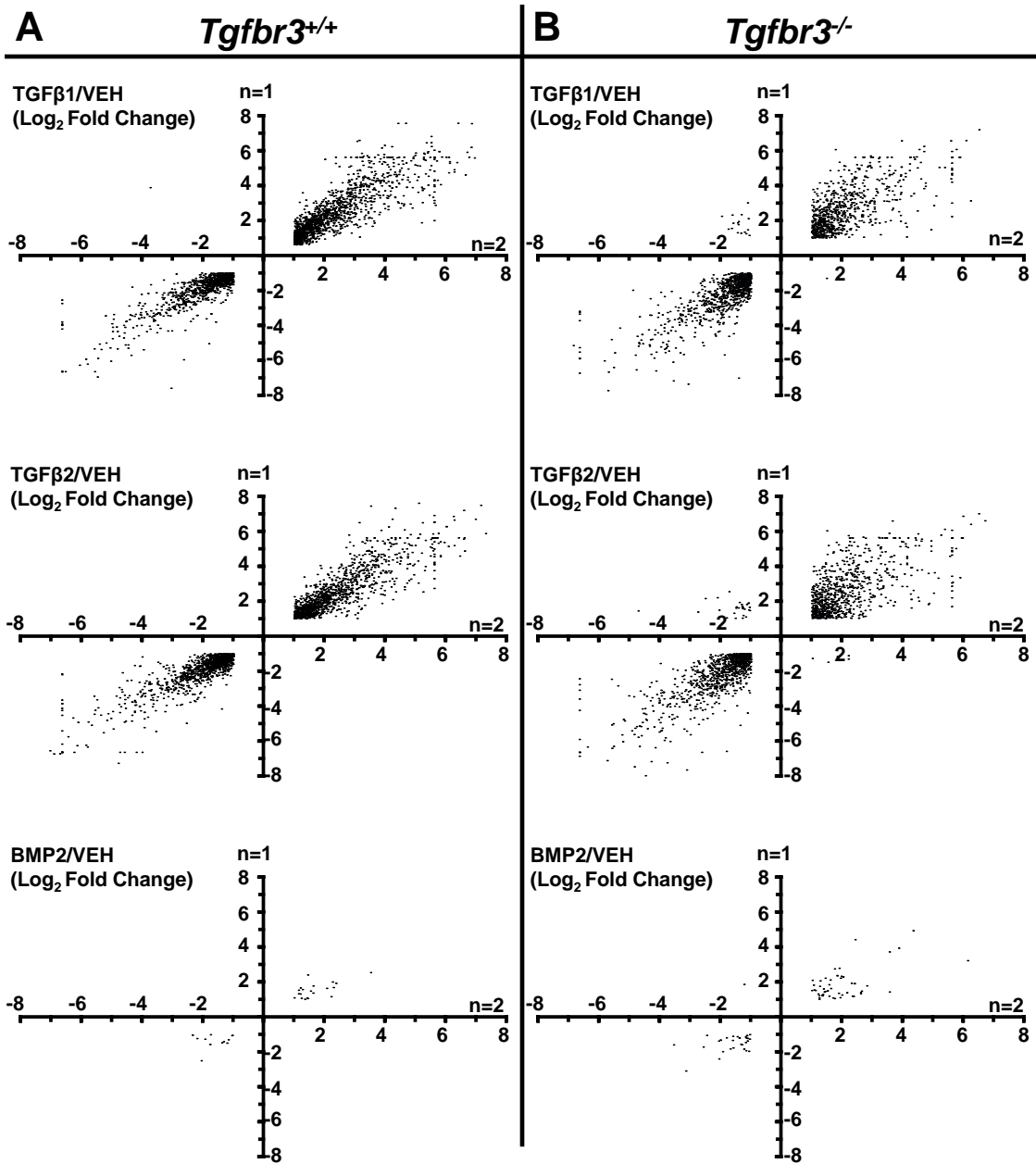


Figure 18: Comparison of differential gene expression between biological replicates. Plots mapping the fold (log base 2) difference >2-fold in expression between VEH and ligand incubated groups in *Tgfb3^{+/+}* (A) or *Tgfb3^{-/-}* (B) in biological replicates (X-axis: n=1, Y-axis: n=2) shown. Genes that have agreement, defined as having >2-fold ($p<0.001$) increased or decreased expression in a specific comparison in both replicates, are mapped to quadrants I (upper right) or III (lower left) of a plot. Genes that show disagreement, defined as having >2-fold ($p<0.001$) increased expression in a tissue in one replicate and decreased in another (or vis versa), are mapped to quadrants II (upper left) or IV (lower right). There was a high degree of agreement in *Tgfb3^{+/+}* (A) ($R>0.85$) or *Tgfb3^{-/-}* (B) ($R>0.89$) datasets across all comparisons.

(Audic and Claverie 1997). Variability between biological replicates was determined (Figure 17-18).

SEAP Reporter System

The pNF- κ B-SEAP (Clonetech) reporter was used to determine NF- κ B activity in cells as described (Craig, Parker et al. 2009; Craig, Parker et al. 2010). Briefly, cells were co-transfected with pNF- κ B-SEAP and β -galactosidase expression vector (p-CMV β) and after 24 hours incubated with ligand (250pM TGF β 1, 250 pM TGF β 2, or 5nM BMP2). 24 hours after ligand addition the supernatant was assayed for alkaline phosphatase. β -galactosidase activity was used to normalize alkaline phosphatase activity.

Transwell Invasion Assay

Invasion assay performed as described in (Sanchez, Hill et al. 2011).

Results

Transcriptional profiles of $Tgfb3^{+/+}$ and $Tgfb3^{-/-}$ cells confirm epicardial cell identity and ligand response

We undertook a transcriptional profiling approach to examine the genes downstream of TGF β R3 in epicardial cells *in vitro*. This system was chosen since it provides defined phenotypic endpoints to contrast between genotypes and different ligand incubation groups (Figure 15A). $Tgfb3^{+/+}$ and $Tgfb3^{-/-}$ epicardial

cells were incubated for 72 hours with VEH or ligands known to drive TGF β R3-dependent invasion (TGF β 1, TGF β 2, BMP2) (Sanchez and Barnett 2012). After incubation RNA was harvested and analyzed by RNA-seq as described. More than 24 million reads were obtained for each group (VEH, TGF β 1, TGF β 2, BMP2) in each genotype (Figure 15B – Genes). Over 13,900 genes were significantly expressed (Reads >10) in each dataset (Figure 15B – Reads). Of these genes, we observed that markers of embryonic epicardial cells (*Wt1* (Moore, Schedl et al. 1998), *Tbx18* (Kraus, Haenig et al. 2001), *Sema3d* (Katz, Singh et al. 2012), *Scx* (Katz, Singh et al. 2012)) were markedly expressed in all data sets (Figure 19A) but markers of endothelial (*Cdh5* (*Lampugnani*, Resnati et al. 1992), *Pecam1* (Newman, Berndt et al. 1990), *Tie1* (Partanen, Armstrong et al. 1992)) or myocardial (*Tnni2* (Saggin, Gorza et al. 1989; Wang, Reiter et al. 2001), *Tnni3* (Saggin, Ausoni et al. 1988; Wang, Reiter et al. 2001)) lineages were not (Figure 19C). The expression profile observed confirms the epicardial identity of these cells.

We have previously reported that TGF β 1 and TGF β 2 promote loss of epithelial character, invasion, and smooth muscle differentiation defined as the increased expression of the smooth muscle markers α -Sma, *Sm22 α* , and *Cnn1* (reviewed (Rensen, Doevedans et al. 2007)) in *Tgfb3 $^{+/+}$* and *Tgfb3 $^{-/-}$* epicardial cells (TGF β 2 depicted in Figure 16C). BMP2 promotes loss of epithelial character and invasion but not smooth muscle differentiation (Hill, Sanchez et al. 2012). RNA-seq data sets demonstrated that the level of expression of α -Sma, *Sm22 α* , and *Cnn1* were >2-fold higher in TGF β 1- and TGF β 2-incubated cells of each

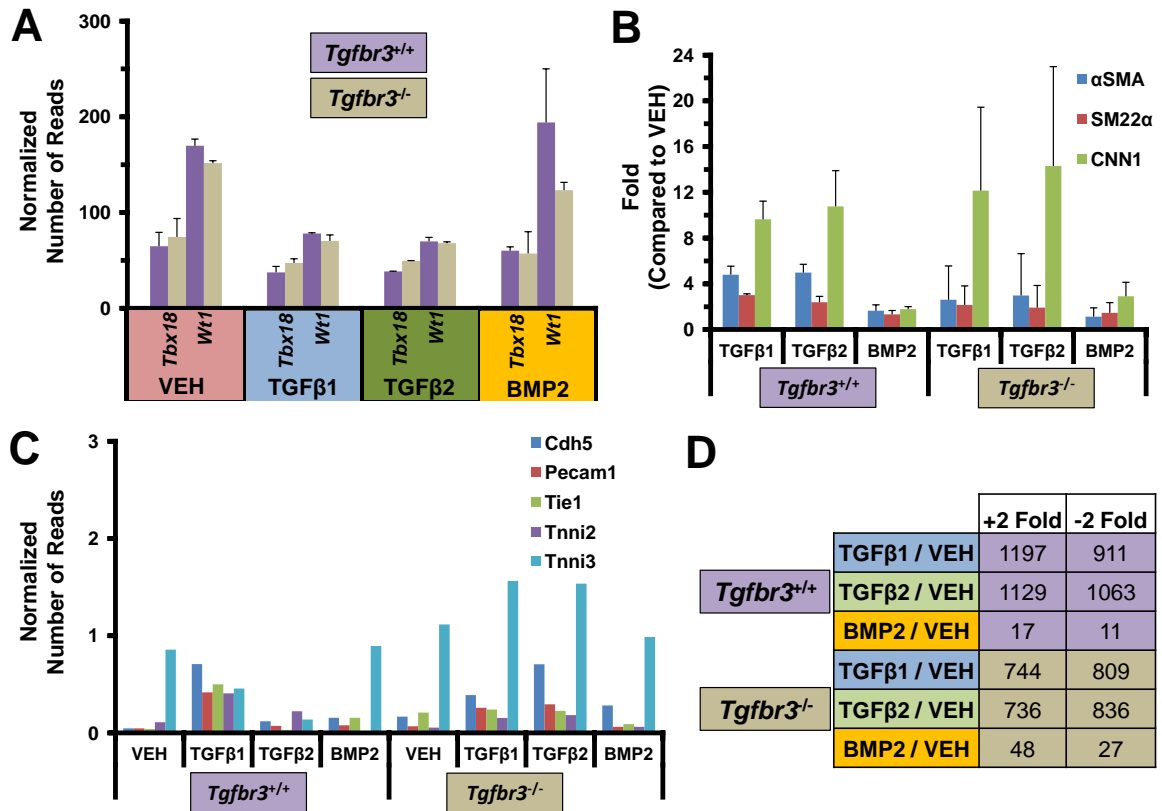


Figure 19: *Tgfbr3^{+/+}* and *Tgfbr3^{-/-}* epicardial RNA-seq datasets confirm cell identity and differential ligand response. **A**, Cells express epicardial markers. Mean normalized reads between replicates and standard error are depicted. **B**, Smooth muscle markers are markedly induced with TGFβ1 and TGFβ2 compared to BMP2 incubation. Fold is relative to VEH for each genotype. **C**, Endothelial or myocardial markers are not notably expressed. Mean normalized reads between replicates and standard error are depicted. **D**, Genes >2-fold differentially expressed after ligand treatment compared to vehicle are depicted. Fewer genes are induced by incubation with TGFβ1-2 treatment in *Tgfbr3^{-/-}* epicardial cells compared to *Tgfbr3^{+/+}*, while the opposite is true with BMP incubation.

genotype (Figure 19B). BMP2 incubation resulted in a considerably lower induction of smooth muscle markers (Figure 2B). Hundreds of genes had >2-fold increased or decreased expression after TGF β 1 or TGF β 2 incubation (Figure 2B). Far fewer genes were >2-fold differentially expressed after BMP2 incubation (Figure 19B) which is likely due to the inability of BMP2 to induce smooth muscle differentiation. Of note, fewer genes were induced with TGF β 1 or TGF β 2 incubation in *Tgfb3*^{-/-} cells when compared to *Tgfb3*^{+/+} cells, while the opposite was found with BMP2 incubation. This transcriptional profile of *Tgfb3*^{+/+} and *Tgfb3*^{-/-} epicardial cells confirms both the epicardial identity and the known response of these cells to ligand. Therefore we used these data sets for further analysis towards delineating the downstream signaling pathways of TGF β R3 in the epicardium.

Dysregulation of gene expression in epicardial cells lacking TGF β R3

To ascertain the genes differentially regulated after the loss of *Tgfb3*, we compared the expression profiles of *Tgfb3*^{+/+} and *Tgfb3*^{-/-} epicardial cells incubated with VEH, TGF β 1, TGF β 2, or BMP2. We observed hundreds of genes >2-fold ($p<0.001$) differentially regulated between genotypes in cells incubated with VEH (604), TGF β 1 (515), TGF β 2 (553), or BMP2 (632) (Figure 20A; Appendices E-H). The overlap between these >2-fold differentially expressed gene lists were plotted (Figure 20B) identifying 129 genes similarly dysregulated across all groups. This list of genes is defined as those that are differentially expressed after the loss of *Tgfb3* regardless of ligand incubation. To gain a

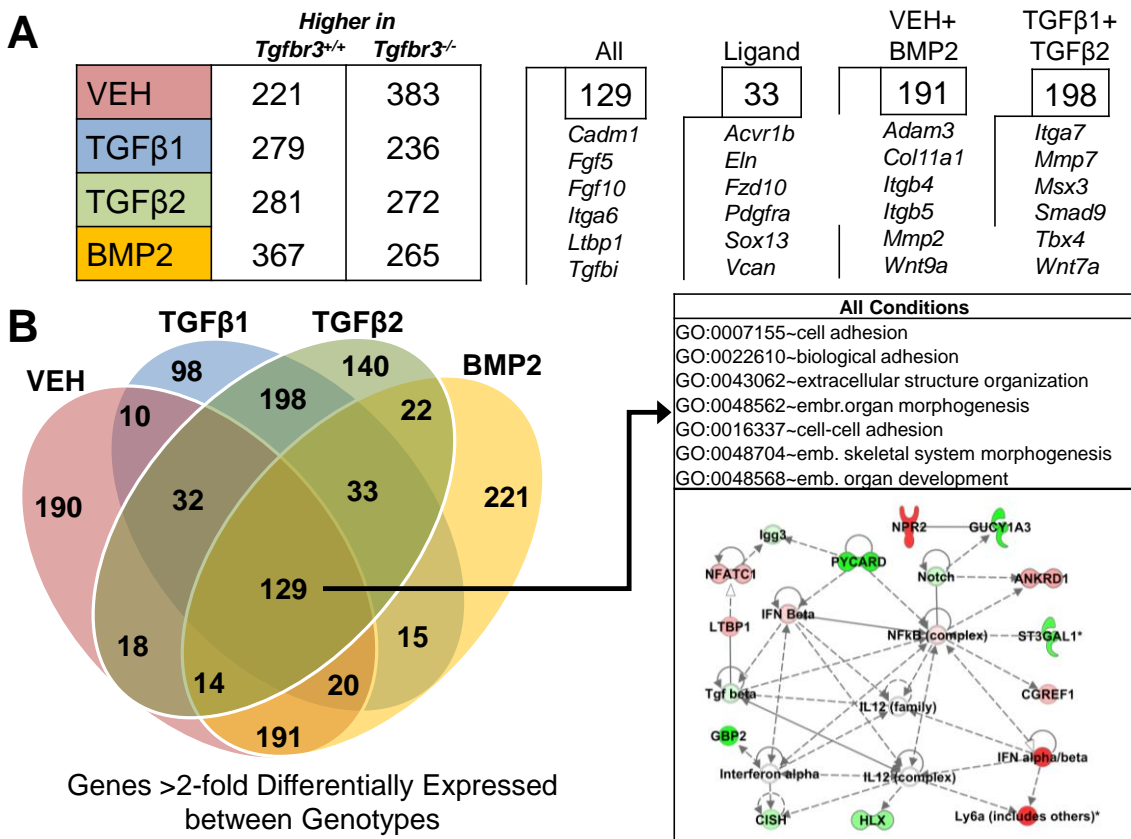


Figure 20: RNA-seq analysis identifies genes dysregulated in *Tgfb3^{-/-}* epicardial cells: **A**, (Left) The number of genes >2-fold ($p<0.001$) differentially expressed between *Tgfb3^{+/+}* and *Tgfb3^{-/-}* epicardial cells for each group. (Right) The number genes similarly dysregulated within selected groups are shown with genes found in each. **B**, The number of overlapping genes >2-fold differentially regulated ($p<0.001$) was determined and mapped. 129 genes were similarly dysregulated across all groups. **C**, (Top) Gene ontology analysis of these 129 genes by DAVID revealed a significant ($p<0.0001$) enrichment of genes associated with specific biological processes. emb.- embryonic. (Bottom) A representative network generated by gene regulatory network analysis of the 129 genes using Ingenuity Pathway Analysis software is depicted. Green- expressed higher in *Tgfb3^{+/+}*, Red- expressed higher in *Tgfb3^{-/-}*.

better understanding of the biological processes these genes may be associated with, Gene Ontology (GO) analysis was undertaken using Database for Annotation, Visualization, & Integrated Discovery (DAVID) software (Dennis, Sherman et al. 2003). GO analysis identified enriched biological processes ($p<0.0001$) associated with cell adhesion and extracellular structure organization indicating a potential defect in cell interaction with the ECM, a vital component of cell invasion (Figure 20C – Top). In order to understand how these genes may interact, Ingenuity Pathway Analysis (IPA) software (www.ingenuity.com) was used to perform Gene Regulatory Network (GRN) analysis. An example network is depicted (Figure 20C – Bottom) which revealed TGF β and Notch signaling pathways (del Monte, Casanova et al. 2007), both known important regulators of epicardial cell behavior and subsequent coronary vessel development. We also identified signaling pathways previously unexamined in epicardial development. For example, NF- κ B signaling emerged as a central node in this analysis providing a candidate for further evaluation.

To gain a more detailed understanding of the genes dysregulated after loss of TGF β R3, we examined genes with dysregulated expression in specific ligand incubation groups. When considering the overlap between genes in at least any two groups (VEH, TGF β 1, TGF β 2, or BMP2) that are similarly >2-fold differentially expressed between genotypes (Figure 20B), we observed that there are many more genes shared between TGF β 1-TGF β 2 (198) and VEH-BMP2 (191) than any other comparison (for example; VEH-TGF β 1 (10), BMP2-TGF β 2 (22)). This may reflect the fact that both TGF β 1 and TGF β 2 induce smooth

muscle differentiation. GO analysis of the 198 genes uniquely dysregulated in *Tgfbr3*^{-/-} cells after TGFβ1 and TGFβ2 incubation identified vasculature development as the most enriched biological process ($p<0.001$) (Table 8). This analysis is consistent with altered vascular development in epicardial cells after loss of *Tgfbr3*. However, processes associated with vascular development were not found to be significantly enriched by GO analysis in the 191 genes uniquely >2-fold dysregulated between genotypes with VEH and BMP2 incubation or in the 221 genes uniquely dysregulated with BMP2 incubation (Table 8).

Although we have reported that TGFβ2 promotes loss of epithelial character and smooth muscle differentiation via ALK5 signaling and BMP2 promotes only the loss of epithelial character via ALK3 signaling, both ligands require TGFβR3 to mediate invasion (Hill, Sanchez et al. 2012). To gain a better understanding of how TGFβ and BMP signaling are impacted by the loss of *Tgfbr3*, we examined genes >2-fold differentially expressed between *Tgfbr3*^{+/+} and *Tgfbr3*^{-/-} epicardial cells incubated with TGFβ2 or BMP2. GO analysis identified that biological processes associated with blood vessel development and angiogenesis were enriched ($p<0.0001$) in TGFβ2 but not BMP2 gene lists (genes including *Fgf2* and *Vegfc*) (Figure 21A). Thus, while TGFβ induces smooth muscle differentiation in *Tgfbr3*^{-/-} cells, there remain defects in the signaling networks associated with formation of the vasculature. Biological processes enriched in both of these TGFβ2 and BMP2 gene lists include processes associated with cell adhesion, extracellular matrix (ECM) organization, and proliferation (Figure 21A-B). These results are consistent with the known

Table 8: GO Analysis of Genes >2-fold Differentially Expressed Between Genotypes Unique to Specific Ligand Incubation Groups.

GO Term	p-value
TGFβ1 + TGFβ2	
GO:0001944~vasculature development	3.71E-04
GO:0000122~negative regulation of transcription from RNA polymerase II promoter	0.001014
GO:0032963~collagen metabolic process	0.001046
GO:0006357~regulation of transcription from RNA polymerase II promoter	0.001059
GO:0001525~angiogenesis	0.001153
VEH + BMP2	
GO:0022037~metencephalon development	0.017354
GO:0050900~leukocyte migration	0.018991
GO:0030902~hindbrain development	0.043128
GO:0042127~regulation of cell proliferation	0.048931
GO:0008284~positive regulation of cell proliferation	0.051412
BMP2	
GO:0007242~intracellular signaling cascade	1.63E-04
GO:0009069~serine family amino acid metabolic process	0.001428
GO:0006534~cysteine metabolic process	0.002140
GO:0007188~G-protein signaling, coupled to cAMP nucleotide second messenger	0.002451
GO:0030534~adult behavior	0.002719

TGFβ2	
Adhesion	
GO:0007155-cell adhesion GO:0022610-biological adhesion GO:0016337-cell-cell adhesion	<i>Kira18, Cxadr, Icam5, Pcdh9, Itgb1</i>
Bone and Cartilage Development	
GO:0048705-skeletal system morphogenesis GO:0001501-skeletal system development	<i>Col2a1, Uncx, Wnt7b, Bmpr1b</i>
ECM	
GO:0043062-extracellular structure organization GO:0030198-extracellular matrix organization	<i>Adamts14, Col5a3, Acan</i>
Blood Vessel and Vasculature Development	
GO:0001944-vasculature development GO:0048514-blood vessel morphogenesis GO:0001525-angiogenesis	<i>Mmp19, Fgf10, Vegfc, Itga7, Tbx4, Fgf2</i>
Proliferation	
GO:0008284-positive regulation of cell proliferation GO:0042127-regulation of cell proliferation	<i>Cd24a, Tlr4, Cntrr, Mdm4</i>
Wound Healing	
GO:0009611-response to wounding	<i>I16, Id3, Igfbp4</i>

BMP2	
Adhesion	
GO:0007155-cell adhesion GO:0022610-biological adhesion GO:0016337-cell-cell adhesion	<i>Kira18, Itgb5, Itgb1, Cdh13, Cdh26, Cdh23</i>
Bone and Cartilage Development	
GO:0048705-skeletal system morphogenesis GO:0048704-emb. skeletal system morphogenesis	<i>Bmp4, Wnt9a, Mmp2</i>
ECM	
GO:0043062-extracellular structure organization	<i>Col5a3, Postn</i>
Proliferation	
GO:0050678-regulation of epithelial cell proliferation	<i>Cdkn2a, Foxp2</i>
Metabolic Processes	
GO:0006790-sulfur metabolic process GO:0009069-serine family amino acid meta. process GO:0006534-cysteine metabolic process	<i>Gstt1, Ggt5 Cth, Sardh Gclm, Cdo1</i>

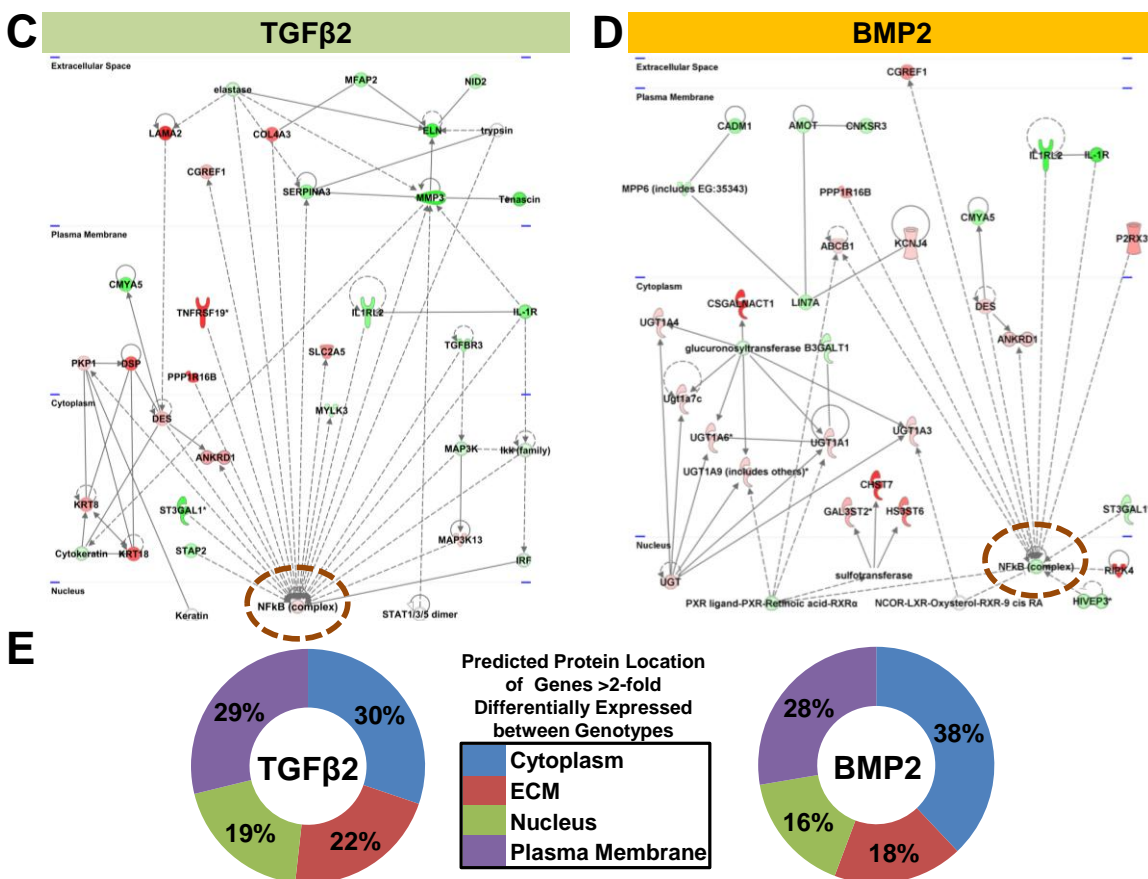


Figure 21: Gene regulatory network analysis identifies NF- κ B signaling as a central node. Genes >2-fold ($p<0.001$) differentially expressed between $Tgfb3^{+/+}$ and $Tgfb3^{-/-}$ epicardial cells incubated with either TGF β 2 (**A**) or BMP2 (**B**) were subjected to gene ontology analysis (using DAVID software, $p<0.0001$). (**C-D**) NF- κ B signaling (orange circle) is a central node in representative networks generated by gene regulatory network analysis (using Ingenuity Pathway Analysis software). Green- expressed higher in $Tgfb3^{+/+}$, Red-expressed higher in $Tgfb3^{-/-}$. (**E**) The distribution of the predicted protein location in the cell is depicted (proteins with unknown location are not shown).

epicardial phenotype of *Tgfbr3*^{-/-} embryos (Compton, Potash et al. 2007; Sanchez, Hill et al. 2011).

To reveal interactions, genes >2-fold differentially expressed between genotypes after TGF β 2 or BMP2 incubation were used to generated GRNs using IPA software. Example networks are depicted in Figure 21C-D. The TGF β 2 network features predicted proteins known to be located in the ECM that regulate cell-ECM interactions. Several of these genes have lower levels of expression in *Tgfbr3*^{-/-} cells compared to *Tgfbr3*^{+/+} cells (green nodes). Also present are several genes encoding cytoplasm and plasma membrane proteins that are expressed at higher levels in *Tgfbr3*^{-/-} epicardial cells compared to *Tgfbr3*^{+/+} cells (red nodes). These genes are associated with epithelial sheet stability and adhesion, for example (*Krt18*, *Krt8*). The BMP2 network also features genes that are expressed at higher levels in *Tgfbr3*^{+/+} cells whose proteins are known to associate with the plasma membrane to regulate cell adhesion and cell migration (*Lin7a* (Monzani, Bazzotti et al. 2009), *Amot* (Troyanovsky, Levchenko et al. 2001)). Nodes associated with ECM protein synthesis (*Csgalnact1* (Sato, Gotoh et al. 2003)) or post translation modification of receptors that interact with ECM (*Chst7* (Ruffell, Poon et al. 2011)) were also observed in the BMP2 network. These networks indicate a deficit in the ability of cells to interact with the ECM and a potential defect in cell motility. NF- κ B was a central node in not only the TGF β 2 and BMP2 networks (Figure 21C-D – Orange circle), but also in GRNs derived from genes differentially expressed between genotypes with VEH or TGF β 1 incubation (Figure 22). We identified several genes known to be

TGFβ1		VEH
Adhesion		Adhesion
GO:0007155-cell adhesion		<i>Itgb1l1, Klr4, Faf2, Pkp1</i>
GO:0022610-biological adhesion		
Bone and Cartilage Development		Bone and Cartilage Development
GO:0048705-skeletal system morphogenesis		<i>Gast, Dlx2, Tbx15, Tbx4, Wnt7a, Hoxa5</i>
GO:0048704-emb. skeletal system morphogenesis		
Blood Vessel and Vasculature Development		Blood Vessel and Vasculature Development
GO:0001944-vasculature development		<i>Fgf2, Fgf10, Scg2, Sema5a</i>
GO:0048514-blood vessel morphogenesis		
Proliferation		Proliferation
GO:0008284-positive regulation of cell proliferation		<i>Cd80, Gli1, Ereg, Sp6, Clu</i>
Lung Development		Lung Development
GO:0030324-lung development		<i>Tcf21, Id1, Hsd1b1, Foxp2, Mgp</i>
GO:0060541-respiratory system development		
ECM		ECM
GO:0043062-extracellular structure organization		<i>Adamts14, Adamts20</i>
Epithelial Development		Epithelial Development
GO:0060429-epithelium development		<i>Irf6, Nkx2-3, Sfrp1, Id3</i>
GO:0030855-epithelial cell differentiation		
Brain Development		Brain Development
GO:0030902-hindbrain development		<i>Phox2a, Smad9, Lhx5, Cacna1a</i>
GO:0022037-metencephalon development		

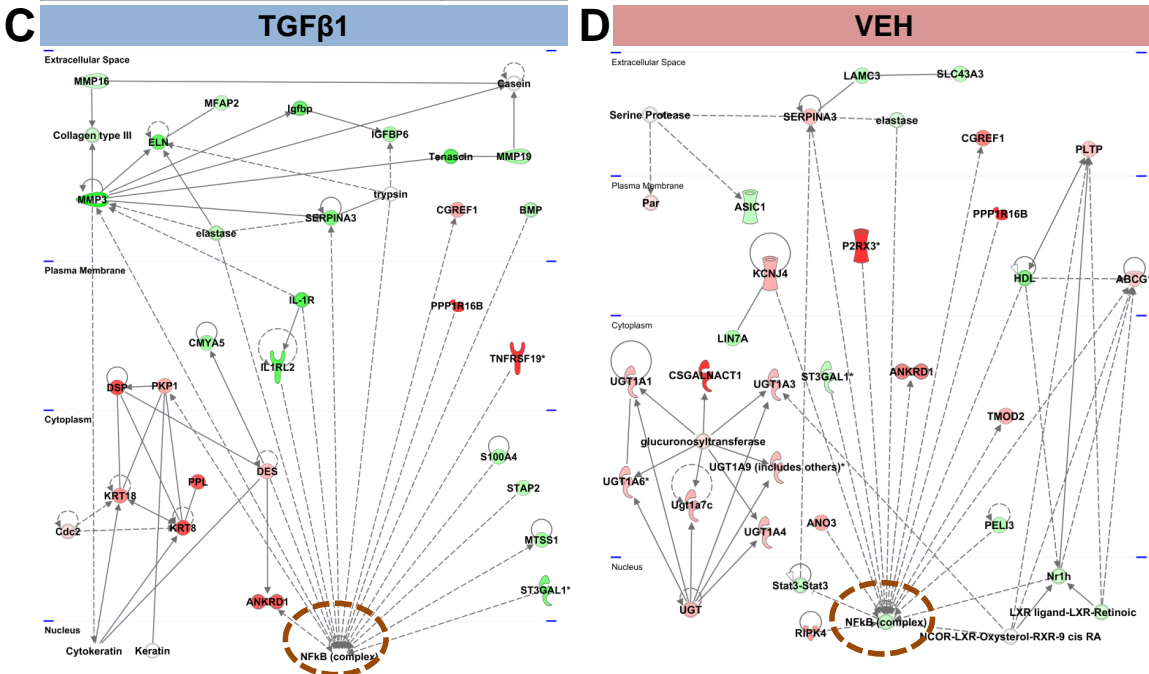


Figure 22: Gene regulatory network analysis identifies NF-κB signaling as a central node. Genes >2-fold ($p<0.001$) differentially expressed between *Tgfb3^{+/+}* and *Tgfb3^{-/-}* epicardial cells incubated with either TGFβ1 (A) or VEH (B) were subjected (A) to gene ontology analysis (using DAVID software, $p<0.0001$). C-D, NF-κB signaling (orange circle) is a central node in representative networks generated by gene regulatory network analysis (using Ingenuity Pathway Analysis software). Green- expressed higher in *Tgfb3^{+/+}*, Red- expressed higher in *Tgfb3^{-/-}*.

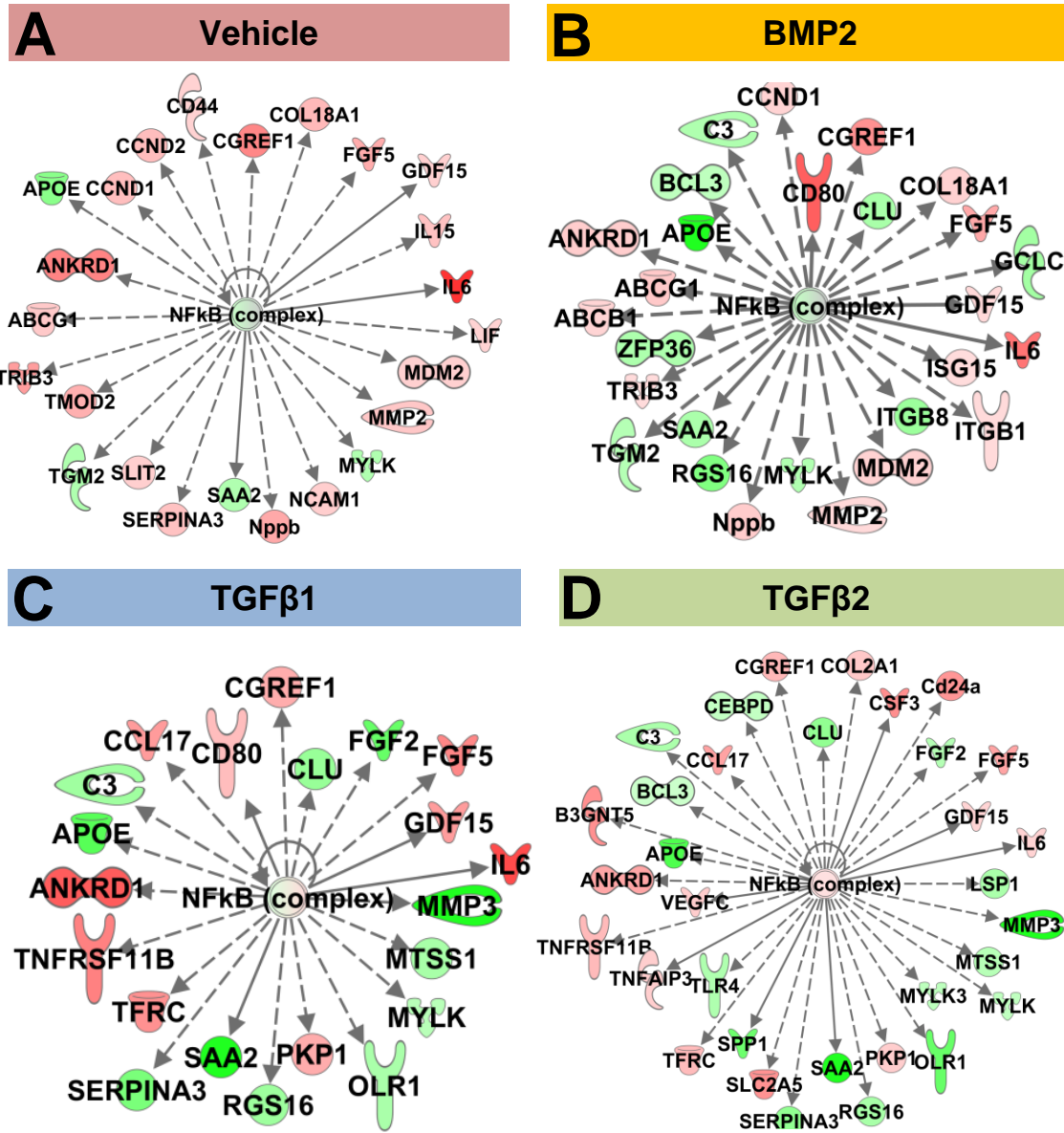


Figure 23: Genes downstream of NF- κ B signaling dysregulated with loss of *Tgfb3* in epicardial cells *in vitro*. Genes identified as being >2-fold differentially regulated between *Tgfb3*^{+/+} or *Tgfb3*^{-/-} epicardial cells incubated with (A) VEH, (B) BMP2, (C) TGF β 1, or (D) TGF β 2. Solid lines denote a direct interaction while dotted lines denote indirect interaction between proteins. Green- higher expression in *Tgfb3*^{+/+}. Red- higher expression in *Tgfb3*^{-/-}.

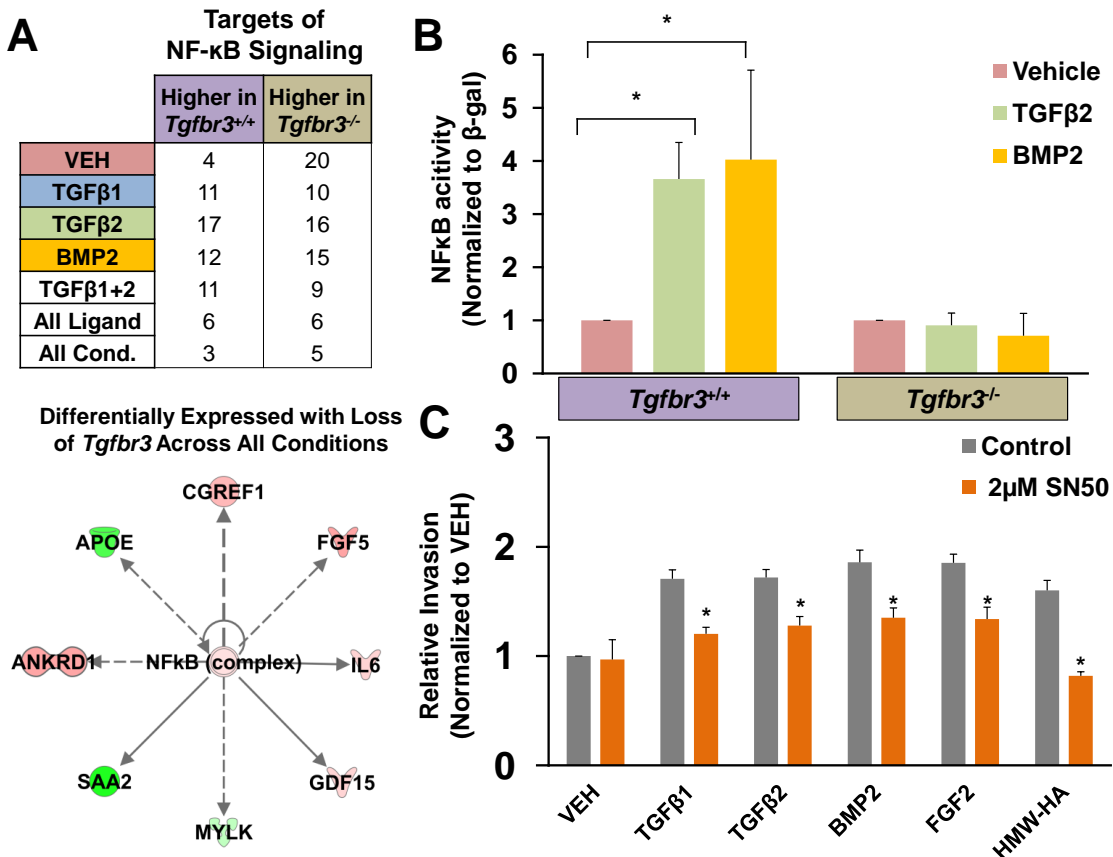


Figure 24: *Tgfb3^{-/-}* epicardial cells fail to activate the NF-κB signaling pathway. A, (TOP) Genes dysregulated in each group (>2-fold, p<0.001) were counted. (BOTTOM) Shared targets of NF-κB signaling dysregulated in all groups are shown. Red - expressed higher in *Tgfb3^{+/+}*, Green - expressed higher in *Tgfb3^{-/-}*. B, Cells transfected with an NF-κB responsive SEAP reporter construct and incubated with VEH, TGFβ2, or BMP2 revealed the inability of *Tgfb3^{-/-}* cells to induce NF-κB signaling. C, Incubation of *Tgfb3^{+/+}* epicardial cells in a transwell invasion assay with an NF-κB inhibitor (SN50) significantly reduced invasion (*=p<.01) in response to ligands known to promote *Tgfb3*-dependent invasion.

downstream of NF-κB signaling that were differentially regulated in each ligand incubation group (Figure 23A-D) when compared between genotypes. A table depicting the overlap between these genes is shown (Figure 24A – Top). GRN analysis indicates that NF-κB signaling may be dysregulated with loss of TGFβR3 in epicardial cells. The dysregulated NF-κB signaling in both TGFβ2 and BMP2 gene lists, where a common phenotype is loss of invasion, suggests that NF-κB signaling may regulate cell invasion in response to these ligands.

*NF-κB signaling is dysregulated in *Tgfbr3*^{-/-} epicardial cells in vitro*

To test the hypothesis that TGFβR3 promotes NF-κB signaling to regulate epicardial cell invasion we examined if NF-κB activity was induced by TGFβ2 or BMP2 ligand incubation in epicardial cells *in vitro* (Figure 24B). Immortalized epicardial cells incubated with TGFβ2 or BMP2 increased NF-κB activity compared to VEH in *Tgfbr3*^{+/+} epicardial cells as described (Craig, Parker et al. 2010). TGFβ2 or BMP2 ligand incubation failed to induce NF-κB activity in *Tgfbr3*^{-/-} cells (Figure 24B). To determine if NF-κB signaling was required for epicardial cell invasion *in vitro*, we performed a transwell invasion assay with TGFβ1, TGFβ2, and BMP2 in the presence or absence of the NF-κB inhibitor, SN50. SN50 (2 μm) significantly decreased TGFβ1-, TGFβ2-, or BMP2-induced invasion in *Tgfbr3*^{+/+} cells when compared to VEH (Figure 24C). Together these data demonstrate that NF-κB signaling is dysregulated in *Tgfbr3*^{-/-} epicardial cells and that NF-κB is required for epicardial cell invasion *in vitro*. These data support the hypothesis that TGFβR3 promotes NF-κB activity to regulate epicardial cell

invasion.

Discussion

Transcriptional profiling of epicardial cells

We developed a transcriptional profiling strategy using immortalized, embryonic epicardial cells *in vitro* to identify genes and signaling pathways downstream of TGF β R3 that regulate cell invasion. Previous studies have profiled gene expression in adult epicardial cells (Rosati, Grau et al. 2006; Bochmann, Sarathchandra et al. 2010), the proepicardium (Buermans, van Wijk et al. 2010), and primary epicardial cells (E12.5) (Smith, Baek et al. 2011) using microarrays, but a comprehensive transcriptional profiling of embryonic epicardial cells has been lacking. Additionally, our choice of this system allows for a first systematic examination of the genes and signaling pathways regulated by TGF β R3.

Tgfb3^{-/-} epicardial cells have altered expression of ECM associated genes

GO and GRN analysis of genes whose expression was >2-fold dysregulated between *Tgfb3^{+/+}* and *Tgfb3^{-/-}* cells for each ligand incubation group revealed biological processes associated with ECM production, ECM binding, cell adhesion, and invasion. The dysregulation of gene expression associated with these processes is consistent with the known defects identified after loss of *Tgfb3* *in vivo* and *in vitro*. Epicardial cell abnormalities in *Tgfb3^{-/-}* embryos

include expansion of the subepicardial space and a hyperplastic, irregular epicardium, both of which suggest defects in epicardial cell interactions with the ECM (Compton, Potash et al. 2007). Invasion of epicardial cells is also defective *in vivo* and *in vitro* in cells lacking TGF β R3 (Sanchez, Hill et al. 2011). Consistent with a defect in cell interaction with the ECM, we observe that epicardial cells *in vitro* fail to invade in response to high molecular weight HA (Sanchez, Hill et al. 2011), a major ECM component of the subepicardial space (Kalman, Viragh et al. 1995). CD44 is the cell surface receptor which binds HA and this interaction is important for epicardial invasion (Craig, Parker et al. 2010). Upregulated expression of the chondroitin sulfotransferase, *Chst7*, is associated with increased chondroitin sulfation of CD44 and decreased CD44-HA binding in multiple cell types (Ruffell and Johnson 2005; Tjew, Brown et al. 2005; Ruffell, Poon et al. 2011). *Chst7* had markedly increased expression (>4-fold) in *Tgfb3*^{-/-} cells when compared to *Tgfb3*^{+/+} cells across all ligand incubation groups. These data suggest that the inability of *Tgfb3*^{-/-} cells to undergo invasion in respond to HA may result from increased chondroitin sulfation of CD44.

The myocardium and proepicardium both contribute to the ECM contained in the subepicardial space (Tidball 1992; Kalman, Viragh et al. 1995), yet the exact makeup and source is unknown. *Tgfb3*^{-/-} epicardial cells show dysregulated expression of genes encoding proteins found in the ECM, suggesting that epicardial contributions to the ECM are altered after loss of TGF β R3. *Mgp*, *Eln*, and *Tnc* have decreased expression in *Tgfb3*^{-/-} cells when compared to *Tgfb3*^{+/+} cells, while *Matn4* and *Emilin1* have increased expression

irrespective of ligand. Alterations in the expression of specific genes were also found to be ligand-specific. *Versican* is an ECM component contained in the supepicardial space (Zanin, Bundy et al. 1999) that promotes cell invasion in some cancer cells (reviewed (Ricciardelli, Sacco et al. 2009)) and is required for endocardial cushion formation and subsequent EMT (Mjaatvedt, Yamamura et al. 1998; Kern, Twal et al. 2006). *Versican* has >2-fold higher expression after ligand (TGF β 1, TGF β 2, BMP2) incubation when compared to VEH in *Tgfbr3*^{+/+} cells. Ligand induction of *Versican* expression is lost in *Tgfbr3*^{-/-} cells, demonstrating that *Versican* expression is dependent on *Tgfbr3*-ligand interaction. Together, these data suggest the defects in coronary vessel development are due to both the altered response to, and expression of, ECM components by epicardial cells following the loss of *Tgfbr3*.

*TGF β - and BMP-mediated gene expression programs are dysregulated in *Tgfbr3*^{-/-} epicardial cells*

Distinct differences were observed in dysregulated gene expression between epicardial cells incubated with BMP and TGF β ligands after loss of TGF β R3. Analysis of the genes dysregulated between *Tgfbr3*^{+/+} and *Tgfbr3*^{-/-} epicardial cells revealed potentially different mechanisms between BMP2 and TGF β 1 or TGF β 2 mediated-GRNs that may underlay a defect in cell invasion. BMP2 is important in the specification and maintenance of proepicardial cell identity (Schlueter, Manner et al. 2006), directed proepicardial cell migration (Ishii, Garriock et al. 2010), and epicardial cell loss of epithelial character and

invasion (Sanchez and Barnett 2012). GRNs generated from the genes dysregulated between genotypes after BMP2 incubation revealed a grouping of genes encoding PDZ domain-containing proteins that had decreased expression in *Tgfbr3*^{-/-} epicardial cells when compared to *Tgfbr3*^{+/+} cells (*Amot*, *Cadm1*, *Cnksr3*, *Lin7a*, *Mpp6*). Several of these genes (*Amot* (Troyanovsky, Levchenko et al. 2001; Ernvist, Luna Persson et al. 2009; Zheng, Vertuani et al. 2009), *Cadm1* (Masuda, Maruyama et al. 2010), *Cnksr3* (Attar, Salem et al. 2012), *Lin7a* (Perego, Vanoni et al. 2002; Monzani, Bazzotti et al. 2009)) have been previously reported to promote cell migration but a role in the epicardium has not been described. These observations are consistent with the known role in BMP2 in directing epicardial migration and the decrease of invasion observed in *Tgfbr3*^{-/-} epicardial cells. These data also provide an intriguing set of candidate genes as the PDZ domain of TGF β R3 and a protein that interacts with this domain, GIPC, are required for TGF β R3-mediated invasion *in vitro* (Sanchez, Hill et al. 2011). GRNs generated from the genes dysregulated between genotypes after TGF β 1 or TGF β 2 incubation had different features from the BMP2 network. A large grouping of genes whose expression was reduced after loss of TGF β R3 was localized to the extracellular space in the TGF β 1 and TGF β 2 networks. These genes were involved in the production of ECM components (*Eln*), matrix degradation (*Mmp3*, *Elastase*), and ECM organization (*Mfap2*). A different grouping of genes expressed at higher levels after loss of TGF β R3 localized to the cytoplasm were associated with epithelial sheet stability and non-motile cells (*Krt8*, *Krt18*). The GRNs are consistent with a population of cells with

dysregulated ECM interaction and reduced motility. In addition, genes in signaling pathways associated with vascular development and angiogenesis were dysregulated between genotypes with TGF β 1 and TGF β 2 but not BMP2 incubation. This finding is particularly interesting as factors secreted by the epicardium after injury to the heart are hypothesized to promote the formation of new vessels in the impacted area (Zhou, Honor et al. 2011). To support proper coronary vessel development signaling events must be tightly regulated in the epicardium *in vivo*. Our data demonstrates TGF β R3 is an important component of the regulatory machinery that integrates TGF β and BMP signaling in epicardial cells.

Loss of TGF β R3 disrupts NF- κ B signaling in embryonic epicardium

TGF β R3 is required for invasion promoted by TGF β 1, TGF β 2 and BMP2, suggesting that a TGF β R3-dependent signaling mechanism that regulates invasion is shared between these ligands. Our data predicts NF- κ B signaling is dysregulated in *Tgfb3*^{-/-} epicardial cells. GRN's generated from genes >2-fold differentially expressed between *Tgfb3*^{+/+} and *Tgfb3*^{-/-} epicardial cells across each ligand incubation group (VEH, TGF β 1, TGF β 2, BMP2) identified NF- κ B signaling as a central node. In support of a role for NF- κ B signaling, genes known to be regulated directly or indirectly downstream of NF- κ B were also dysregulated. Incubation of epicardial cells with TGF β 2 or BMP2 increased NF- κ B activity in *Tgfb3*^{+/+} but not in *Tgfb3*^{-/-} cells, demonstrating that TGF β R3 is required for NF- κ B activity in epicardial cells. Several mechanisms may account

for the ability of TGF β R3 to regulate NF- κ B signaling. Previous studies have found that TGF β R3 can suppress NF- κ B signaling via interaction with β -arrestin2 (You, How et al. 2009). IL-1 β , an upstream regulator of NF- κ B signaling, can suppress TGF β R3 signaling by binding to TRAF6 which subsequently sequesters TGF β R3 from TGF β R2 (Lim, Bae et al. 2012). Here, reduced NF- κ B activity may result from a >2-fold reduction in the expression of an important upstream regulator of NF- κ B signaling, *IIL1r* (reviewed (Verstrepen, Bekaert et al. 2008)), in *Tgfb3^{-/-}* cells when compared to *Tgfb3^{+/+}* cells. Reduced NF- κ B activity may also result from decreased expression in *Tgfb3^{-/-}* cells of Myosin Light Chain Kinase (*Mylk*), which has recently been shown to promote activation of NF- κ B signaling (Tauseef, Knezevic et al. 2012). MYLK kinase activity is required for MyD88 and IRAK4 complex formation, which in turn is required to activate NF- κ B downstream of lipopolysaccharide (Medvedev, Lentschat et al. 2002; Kawagoe, Sato et al. 2008), in lung endothelial cells (Tauseef, Knezevic et al. 2012). Given the known roles of *Mylk* in regulating smooth muscle behavior (Cole and Welsh 2011), cell migration (Kamm and Stull 2001), and a link to coronary artery disease (Wang, Hauser et al. 2007), the elucidation of the regulatory interactions between MYLK, TGF β R3, and NF- κ B in epicardial cells may provide key insights into coronary vessel development.

While TGF β R3 signaling has been previously reported to both inhibit (Criswell and Arteaga 2007; You, How et al. 2009) and promote (Criswell, Dumont et al. 2008) NF- κ B signaling, a consistent fact in all of these studies is that a decrease in NF- κ B activity was coincident with decreased invasion. We

showed that NF-κB activity was required for epicardial cell invasion. These data suggest that NF-κB is a shared signaling pathway downstream of ligand and that TGFβR3 interaction is required for cell invasion. Therefore, we propose that the disruption of TGFβR3 regulated NF-κB signaling is a mechanism responsible for the loss of invasion in epicardial cells and ultimately failed coronary vessel development in *Tgfb3*^{-/-} embryos.

Summary

Together, our data confirms the epicardial identity and ligand responses of embryonic epicardial cells *in vitro*. GO and GRN analysis identified novel genes and signaling pathways dysregulated after the loss of TGFβR3, which led us to the identification and validation of NF-κB as a potential regulator of epicardial cell invasion. Finally, the genes and signaling pathways identified through our analysis yield the first comprehensive list of candidate genes whose expression is dependent on TGFβR3 signaling. Further analyses of these data will likely yield insights into epicardial cell biology and TGFβR3 signaling. Our findings have broad applicability to development and disease given the importance of EMT and TGFβR3 not only in cardiogenesis but in pathological processes such as fibrosis and cancer.

CHAPTER IV

SUMMARY AND CONCLUSIONS

Heart disease and EMT

Cardiovascular disease remains a leading cause of death in the world. The understanding the signaling mechanisms that can give rise to or modulate cardiovascular disease remains a key goal of scientists. Coronary and valvular heart disease both contribute a significant portion to the global disease burden represented by cardiovascular disease and it has become increasingly appreciated that signaling pathways that promotes these complaints share many similarities with the signaling processes regulating the development of coronary arteries and the valves. In development, distinct cell populations undergo tightly regulated EMT events that are critical in the development of both coronary arteries and valves. In the adult, EMT in the epicardium has been implicated in cardiac regeneration following injury, making epicardial behavior an attractive target for therapeutic intervention. The goal of generating a stable population of functioning VICs to seed next-generation, prosthetic valves requires an understanding of the signaling pathways that regulate EMT to give rise to VICs in development. Given the shared pathways regulating EMT in the endocardium and epicardium, a careful examination of the GRNs that promote EMT is critical to the future design of therapeutic strategies to modulate coronary and valvular heart disease. In addition, EMT in endocardial cells has been linked to fibrosis in

adult hearts and a dysregulation of cell invasion outside of the heart has long been linked to cancer progression which broadens the impact of this study.

Transcriptional profiling using next-generation sequencing

Despite the importance of EMT, our knowledge often progresses at the pace of a single gene study at time. In an effort to overcome this single gene focus we examined the GRNs regulating endocardial and epicardial EMT using transcription profiling strategies. We used next-generation sequencing, in the form of RNA-seq analysis, to analyze global gene expression. The use of RNA-seq analysis can allow us to identify transcripts with low levels of or changes in expression on a global level that would have otherwise been missed. Transcription factors, in particular, can dramatically alter cell behavior with small changes in expression (Niwa, Miyazaki et al. 2000). Though not leveraged in the presented studies, the generated RNA-seq datasets may also allow for an examination of alternate splicing and alternate 5' start sites during EMT in cardiogenesis (Shapiro, Cheng et al. 2011). Despite the sensitivity of RNA-seq methodology, in order to generate useful datasets for analysis careful consideration must be given to account for technical and biological variability. In our studies in the epicardium and endocardium we the observed low levels of biological and technical variability. Overall, the use of RNA-seq analysis enabled us to generate transcriptional profiles of cells undergoing EMT during cardiogenesis.

Spatial transcriptional profiling of the developing heart tube

In Chapter II we present an unbiased strategy to identify genes important in endocardial EMT using a spatial transcriptional profile. Endocardial cells overlaying the cushions of the AVC and OFT undergo an EMT to yield VICs. RNA-seq analysis of gene expression between AVC, OFT, and VEN isolated from chick and mouse embryos at comparable stages of development (chick HH18; mouse E11.0) was performed. EMT occurs in the AVC and OFT cushions, but not VEN at this time. We exploited this well described heterogeneity of the developing heart tube to identify genes with enriched expression in the valve forming regions of the heart. We found 198 genes in the chick and 105 genes in the mouse were enriched 2-fold in the cushions. GRN generated from cushion-enriched gene lists confirmed TGF β as a nodal point and identified NF- κ B as a potential node. To reveal previously unrecognized regulators of EMT four candidate genes, *Hapln1*, *Id1*, *Foxp2*, and *Meis2*, and a candidate pathway, NF- κ B, were selected. *In vivo* spatial expression of each gene was confirmed by *in situ* hybridization and a functional role for each in endocardial EMT was determined by siRNA knockdown in a collagen gel assay. Our spatial-transcriptional profiling strategy yielded gene lists which reflected the known biology of the system. Further analysis accurately identified and validated previously unrecognized novel candidate genes and the NF- κ B pathway as regulators of endocardial cell EMT *in vitro*.

These data validate our approach and suggest further examination of the cushion-enriched gene lists in chick and mouse may yield useful insights into VIC

behavior. It is important to note that the cushion-enriched genes could potentially regulate other aspects of VIC behavior aside from EMT. For example, after VICs invade into the endocardial cushions, they secrete proteins that interacting with, bind, cleave, or constitute ECM components found in the cardiac jelly. The signaling pathways which regulate valve remodeling are poorly understood yet this process is important for proper valve maturation (Lockhart, Wirrig et al. 2011). In the cushion-enriched gene lists in chick and mice we identified several genes that play a role in ECM remodeling or organization. *Adamts15* was identified as enriched in both chick and mouse cushions and is an intriguing candidate for involvement in valve remodeling because it is known to cleave Versican (Cross, Chandrasekharan et al. 2005). Versican cleavage is an important feature of valve remodeling (Kern, Twal et al. 2006; Dupuis, McCulloch et al. 2011). *Matn4* is also enriched in chick and mouse cushions and is associated with ECM organization during cartilage formation, a process involving many of the same signaling pathways as valve development.

Thus, further analysis of the cushion-enriched candidate genes may reveal novel regulators of VIC behavior. To expand on this idea, broadening the spatial transcriptional profile to include different time points in valve development, such as before EMT (E9.0) or during remodeling (E13.5), may identify genes important in different aspects of valve development. Comparing the spatial expression observed before EMT occurs in the heart tube (E9.0) to the profile observed during EMT (E11.0) could identify the GRNs which initiate endocardial EMT. Comparing the expression of ECM components when the cardiac jelly

initially forms (E9.0), during EMT (E11.0) and during remodeling may identify ECM components associated specifically with EMT initiation and remodeling. Also, a spatial-temporal profile comparing AVC and OFT development may identify the signaling pathways that serve to remodel these tissues into distinctly different structures. Our understanding of endocardial EMT during valve formation is still incomplete, but comprehensive studies using transcription profiling approaches coupled with efficient functional assays may allow us to more rapidly delineate the GRNs regulating this EMT process.

Transcriptional profile of epicardial cells identifies genes downstream of TGF β R3

Signaling mediated by TGF β R3 plays important roles in heart development and cancer progression. However, the signaling mechanisms and genes specifically activated by TGF β R3 are not well described. Therefore, we undertook a transcriptional profiling approach to identify the genes downstream of TGF β R3 in a well characterized epicardial cell culture system. The epicardium plays an important role in coronary vessel formation and *Tgfb3*^{-/-} mice exhibit failed coronary vessel development associated with decreased epicardial cell invasion and proliferation. Immortalized *Tgfb3*^{-/-} epicardial cells display the same defects. *Tgfb3*^{+/+} and *Tgfb3*^{-/-} cells incubated with VEH or ligands known to promote invasion via TGF β R3, TGF β 1, TGF β 2, or BMP2, for 72 hours and harvested for RNA-seq analysis. We selected for genes >2-fold differentially expressed between *Tgfb3*^{+/+} and *Tgfb3*^{-/-} cells when incubated with VEH, TGF β 1, TGF β 2, or BMP2. GO analysis of the genes >2-fold differentially

expressed between *Tgfbr3*^{+/+} and *Tgfbr3*^{-/-} cells identified dysregulated biological processes consistent with the defects observed in *Tgfbr3*^{-/-} cells, including those associated with the ECM interaction. GO and GRN analysis identified distinct expression profiles between TGF β 1 or TGF β 2 and VEH or BMP2 incubated cells, consistent with the differential ligand response of epicardial cells to these ligands *in vitro*. Despite the differences observed between *Tgfbr3*^{+/+} and *Tgfbr3*^{-/-} cells after TGF β and BMP ligand addition, GRNs constructed from these gene lists identified NF- κ B as a key nodal point for all ligands examined. *Tgfbr3*^{-/-} cells exhibited decreased expression genes known to be activated by NF- κ B signaling. NF- κ B activity was stimulated in *Tgfbr3*^{+/+} epicardial cells after TGF β 2 or BMP2 incubation, while *Tgfbr3*^{-/-} cells failed to activate NF- κ B in response to these ligands. *Tgfbr3*^{+/+} epicardial cells incubated with an inhibitor of NF- κ B signaling no longer invaded into a collagen gel in response to TGF β 2 or BMP2. These data suggest that NF- κ B signaling is dysregulated in *Tgfbr3*^{-/-} epicardial cells and that NF- κ B signaling is required for epicardial cell invasion *in vitro*. Thus, our approach was successful in identifying signaling pathways important in epicardial cell behavior downstream of TGF β R3. Overall, the genes and signaling pathways identified through our analysis yield the first comprehensive list of candidate genes whose expression is dependent on TGF β R3 signaling.

To further elucidate the role of TGF β R3-dependent in regulating epicardial cell behavior the transcriptional profiling strategy used in chapter III can be expanded temporally. The epicardial cells harvested for RNA-seq analysis in chapter III were collected after 72 hours of incubation with ligand. We know,

however, that EMT occurs within the first 24 hours after ligand addition. Also, defects in invasion after the loss of TGF β R3 are observed after 24 hours in the transwell invasion assay. Consistent with these observations, it has previously been described that there are distinct phases of gene expression that occur within the first 24 hours after ligand addition that are important in regulating different aspects of EMT (Vetter, Le Bechec et al. 2009; Tran, Corsa et al. 2011). RNA-seq analysis of time points before 72 hours after ligand incubation would allow for the definition of a temporal map of gene expression dependent on TGF β R3. This would allow us to ask more precise questions about the nature of the dysregulated expression observed in *Tgfbr3*^{-/-} cells. Do *Tgfbr3*^{-/-} cells have different phases of gene expression compared to *Tgfbr3*^{+/+} cells? Are the distinct phases of Snai1-regulated (early) and Twist1-regulated (late) gene expression altered in *Tgfbr3*^{-/-} cells? Is the temporal expression pattern of cells incubated with TGF β 1 or TGF β 2 different from that of BMP2? Does this change in *Tgfbr3*^{-/-} cells? When does the dysregulation of NF- κ B signaling regulated genes occur? We predict that the temporal expression pattern of genes regulating loss of epithelial character and smooth differentiation will not be altered between genotypes while the temporal expression pattern of genes regulating cell motility may be disrupted. Whether the expression of these genes is completely lost from an early time point or whether their expression is delayed is unknown.

TGF β R3 signaling in epicardial and endocardial EMT

Despite considerable effort by our laboratory and others, many questions

remain regarding the role of TGF β R3 in epicardial and endocardial EMT. Our laboratory has shown that TGF β R3 plays a unique role in both valve and coronary vessel development. TGF β R3 is required for invasion for embryonic endocardial and epicardial cells *in vitro*. *In vivo*, absence of the TGF β R3 results in a dysregulated EMT process, leading to hyperplasia in the endocardial cushion and the subepicardial space. These mesenchymal cells display defects in remodeling the cushion and in the epicardium there is a decrease in the ability of EPDCs to invade the myocardium. Despite these similarities, the regulation of EMT by TGF β signaling is not identical in all cell types. ALK5 is required in endocardial and epicardial EMT *in vitro*, but it is sufficient for EMT only in the epicardium (Desgrosellier, Mundell et al. 2005; Hill, Sanchez et al. 2012). In addition, the Par6c/Smurf1/RhoA pathway was shown to be required and sufficient for EMT in endocardial and epicardial cells *in vitro*, but this pathway required the presence of TGF β R3 only in the epicardium (Townsend, Wrana et al. 2008; Sanchez and Barnett 2012). These differences underscore the importance of delineating the mechanisms by which TGF β R3 signaling regulates the common process of EMT in both the endocardium and the epicardium to yield distinct mesenchymal cell populations.

A major advantage of developing transcriptional profiles of both endocardial and epicardial EMT is the ability to compare these data sets. As previously mentioned, there is significant overlap between the signaling mechanisms which regulate endocardial and epicardial EMT, including Wnt, Notch, TGF β , and BMP signaling pathways. In Chapter I and Chapter II we

demonstrated the requirement for NF- κ B signaling for epicardial and endocardial EMT *in vitro*. This ability of TGF β 2 and BMP2 to stimulate NF- κ B signaling was shown to be TGF β R3 dependent in the epicardium. These data suggest that NF- κ B may be a common downstream mediator of TGF β R3 promoted invasion in the epicardium. This begs the question; do endocardial cells require TGF β R3 to stimulate NF- κ B signaling as well? Is NF- κ B activity required for TGF β 2 or BMP2 induced invasion in the endocardium? Is NF- κ B signaling sufficient to induce EMT in either the epicardium or endocardium? The ability of TGF β R3 to both inhibit (Criswell and Arteaga 2007; You, How et al. 2009) and promote (Criswell, Dumont et al. 2008) NF- κ B signaling in different cancer cell lines suggests the nature of TGF β R3 and NF- κ B signaling crosstalk may be cell specific. Understanding the mechanisms that underlie the ability of TGF β R3 signaling to modulate NF- κ B signaling in specific cells will be crucial in addressing the ability of TGF β R3 to promote invasion in different therapeutic contexts. Additional comparisons between the endocardially- and epicardially-derived gene lists may identify other common regulators EMT. For example, we observed a significant dysregulation in the expression of genes associated with ECM proteins, degradation, and organization after loss of TGF β R3 in epicardial cells, which may also underlay the valve phenotype of *Tgfb3*^{-/-} embryos. The AVC explants culture system is particularly amenable to study the importance of cell-ECM interaction and could be used to investigate how the loss of TGFB3 affects and is affected by the ECM. In an iterative process, we may be able to use the findings from one system in the other to take advantage of the unique strengths

of each, furthering our ability to understand the regulatory mechanism that govern EMT in the developing valves and coronary vessels.

APPENDIX

APPENDIX A

HH18 Chick Genes with >1.25-fold Higher Expression in AVC and OFT Compared to VEN

Red= >2-fold Enriched in both AVC and OFT compared to VEN

Orange= >1.25-fold Enriched in both AVC and OFT compared to VEN

Gene Name	AVC/VEN (Fold)	p-value	OFT/VEN (Fold)	p-value
FAM26E	49.00	2.06E-04	49.00	7.92E-04
KCTD8	49.00	2.06E-04	49.00	7.92E-04
ATOH8	28.72	6.87E-08	15.58	2.06E-04
GAL3ST1	26.42	2.95E-07	25.96	2.58E-07
MOXD1	25.53	2.79E-107	22.73	9.64E-97
SOX9	21.49	8.83E-83	22.12	1.61E-88
PENK	21.44	1.27E-15	10.73	2.39E-07
BMP2	18.38	5.41E-37	3.46	4.39E-04
PTX3	17.23	3.39E-45	19.47	4.15E-54
CNTN2	14.93	3.79E-04	39.47	3.61E-11
RSPO3	14.29	2.68E-113	5.22	6.64E-28
MATN4	13.79	1.66E-09	6.23	6.26E-04
CA10	13.02	6.55E-09	12.12	1.91E-08
BCMO1	13.02	6.55E-09	8.31	1.79E-05
SOX8	11.49	1.65E-05	19.73	3.86E-10
TMEM132C	11.49	4.18E-25	6.89	3.83E-13
APCDD1L	10.91	3.26E-05	14.02	5.27E-07
AASS	10.80	3.11E-11	10.59	2.60E-11
SLC6A15	10.34	6.39E-05	7.79	9.99E-04
ADCYAP1R1	9.70	9.60E-17	6.12	2.56E-09
KCNJ5	9.57	1.85E-16	3.46	4.39E-04
CD3E	9.38	4.14E-11	20.25	5.19E-29
TBX2	9.36	7.50E-34	6.08	6.34E-19
FGF13	9.08	5.11E-34	9.25	4.07E-36
PDE1C	8.94	1.09E-22	5.42	1.60E-11
SLIT1	8.81	2.92E-10	11.77	3.48E-15
PCDH15	8.62	4.69E-04	19.73	3.86E-10
Angptl1	8.62	4.81E-07	17.14	2.61E-16
ARSI	8.04	3.84E-09	4.50	2.15E-04
RELN	7.67	9.90E-32	2.99	4.98E-07
DMRT1	7.47	1.11E-10	6.23	1.23E-08
GAD1	7.24	1.73E-12	5.09	7.44E-08
SOD3	7.18	3.89E-10	11.04	2.77E-18
TMEM132D	7.12	1.02E-06	6.44	4.40E-06

Appendix A: Continued

Gene Name	AVC/VEN (Fold)	p-value	OFT/VEN (Fold)	p-value
SMAD9	7.08	9.02E-08	4.33	3.61E-04
DIXDC1	6.89	1.91E-06	6.23	7.80E-06
CD9	6.80	1.60E-14	4.63	1.56E-08
HAPLN1	6.80	1.11E-39	3.61	2.35E-14
CSGALNACT1	6.77	2.26E-10	4.15	2.34E-05
TCF21	6.35	9.80E-36	3.80	8.75E-16
WNT4	6.15	1.89E-13	5.27	4.71E-11
SCTR	6.13	4.74E-09	14.19	5.95E-28
TWIST2	6.13	1.95E-06	7.96	2.63E-09
GEM	5.97	2.22E-05	10.18	9.00E-11
MSX2	5.92	4.90E-28	3.97	5.37E-15
PRMT8	5.91	5.80E-07	3.86	5.53E-04
SAMD11	5.90	1.75E-25	3.32	5.38E-10
IL1RL2	5.74	2.57E-04	5.19	6.52E-04
COL20A1	5.74	4.70E-09	4.99	1.27E-07
METRNL	5.74	4.69E-29	2.86	1.06E-08
DBC1	5.49	9.21E-08	3.46	4.39E-04
WNT6	5.32	5.06E-25	6.88	1.02E-38
ANGPTL4	5.27	2.41E-09	3.38	7.34E-05
CHODL	5.17	7.51E-17	3.20	1.02E-07
GREB1	5.16	1.16E-67	4.43	4.71E-54
AKR1B10	5.14	8.51E-15	2.52	2.00E-04
EMID2	5.11	5.63E-21	4.52	9.07E-18
SOX6	5.03	3.18E-06	7.27	1.23E-10
CNTN4	4.83	4.23E-04	4.78	3.76E-04
CHN2	4.79	1.11E-31	6.83	3.76E-58
APCDD1	4.74	1.51E-18	2.78	2.83E-07
ZNF608	4.68	1.52E-24	2.42	4.72E-07
NID1	4.65	6.09E-36	2.54	3.11E-11
SLC8A3	4.60	4.29E-07	6.04	6.39E-11
TGFB2	4.56	4.61E-51	4.34	1.52E-48
RERG	4.45	3.02E-05	6.88	7.04E-10
COL24A1	4.44	9.71E-09	2.98	1.15E-04
PXDNL	4.33	1.91E-07	3.12	1.57E-04
PCDH17	4.33	1.91E-07	2.96	3.77E-04
GRID1	4.31	6.50E-07	4.33	3.49E-07
MMP24	4.16	2.48E-08	3.44	2.78E-06
SMOX	4.11	9.88E-46	5.32	8.18E-75
KIAA1324L	4.08	9.58E-10	2.54	2.41E-04
ABCG4	3.97	1.10E-05	10.01	1.02E-21
EPHA4	3.95	2.64E-18	2.39	6.79E-07
SCD	3.94	4.58E-15	3.18	1.78E-10
DPP10	3.91	4.03E-07	4.09	6.61E-08
MXRA8	3.91	3.75E-05	3.84	3.56E-05
TMEM86A	3.88	2.62E-04	3.64	4.97E-04
IDNK	3.82	5.47E-15	4.66	5.21E-22
RASD1	3.79	6.32E-05	3.32	3.84E-04
HAS2	3.75	1.52E-55	3.12	1.24E-39

Appendix A: Continued

Gene Name	AVC/VEN (Fold)	p-value	OFT/VEN (Fold)	p-value
TSHZ2	3.73	4.42E-04	3.64	4.97E-04
NEDD9	3.73	6.28E-13	3.53	4.02E-12
BMP5	3.69	5.96E-112	2.45	7.18E-46
SMTNL2	3.65	8.95E-17	3.30	2.33E-14
GFPT2	3.64	1.96E-80	3.00	9.05E-56
SESN3	3.62	2.82E-10	2.65	6.30E-06
VSTM5	3.60	3.11E-06	4.92	1.41E-10
WT1	3.60	3.11E-06	3.19	3.07E-05
PRELP	3.60	7.30E-09	4.79	7.50E-15
ANXA2	3.58	6.37E-55	4.14	4.46E-76
CXCR7	3.41	7.29E-43	2.92	4.37E-32
CADM1	3.40	1.98E-66	3.95	1.04E-93
SYNPO2	3.38	3.38E-06	8.19	5.69E-25
CERS1	3.32	1.23E-39	2.77	8.90E-28
CTNNAL1	3.31	4.91E-19	2.72	4.49E-13
IFNGR1	3.30	1.39E-16	2.04	8.31E-06
GRIN3A	3.29	3.48E-09	2.22	2.56E-04
C1R	3.26	2.81E-09	2.74	7.53E-07
SYK	3.23	8.77E-07	9.79	4.96E-39
BNC2	3.22	7.80E-04	3.32	3.84E-04
CBLN1	3.18	7.17E-09	5.95	7.97E-27
MYO16	3.16	2.09E-32	2.27	2.41E-15
KRT222	3.14	5.81E-05	4.22	2.44E-08
GDF3	3.14	2.62E-35	2.74	3.66E-27
CADPS	3.08	1.78E-06	3.07	1.21E-06
GPM6B	3.06	4.84E-04	4.41	2.10E-07
MSANTD3	3.06	1.81E-05	3.52	3.44E-07
GULP1	3.03	9.12E-09	2.58	1.44E-06
CD109	3.01	8.95E-08	2.54	9.53E-06
COLQ	3.00	3.58E-08	6.16	3.49E-29
PIK3IP1	3.00	1.78E-07	2.34	1.08E-04
LARGE	2.99	2.23E-14	5.16	2.80E-41
SNAI2	2.98	1.30E-12	2.56	2.15E-09
CACNA1H	2.97	3.73E-10	3.09	2.08E-11
RAI14	2.96	4.89E-24	3.63	3.69E-38
DISP1	2.96	8.13E-25	2.32	1.78E-14
BMF	2.94	4.52E-05	3.35	1.37E-06
CRMP1	2.93	2.99E-34	2.00	2.92E-13
SLTRK4	2.92	6.03E-04	3.52	1.61E-05
CAMKK1	2.90	5.49E-06	4.65	3.55E-14
MAP1B	2.83	3.10E-52	2.59	6.23E-44
ROBO1	2.82	5.46E-51	2.53	8.58E-41
RGS9	2.82	4.32E-05	3.17	1.63E-06
VDAC1	2.80	3.66E-19	2.07	2.41E-09
CSRP2	2.79	1.11E-23	9.73	4.33E-217
PRKCD	2.78	4.10E-06	2.28	3.29E-04
LRP4	2.73	3.82E-10	2.62	1.43E-09
ADORA2A	2.72	1.52E-06	2.98	4.20E-08

Appendix A: Continued

Gene Name	AVC/VEN (Fold)	p-value	OFT/VEN (Fold)	p-value
FUT8	2.70	6.23E-16	2.05	2.30E-08
CCDC149	2.70	3.15E-05	3.43	1.92E-08
IGF2	2.70	9.68E-06	3.08	1.18E-07
HMGCLL1	2.66	3.32E-11	2.67	1.11E-11
LECT1	2.65	4.70E-144	3.48	1.47E-280
CPE	2.65	5.68E-62	3.65	1.94E-132
TBX20	2.65	9.84E-152	2.77	5.64E-178
PLCB4	2.65	8.25E-09	2.17	8.68E-06
COL22A1	2.64	5.25E-04	5.07	2.15E-12
ARSJ	2.63	3.73E-05	2.38	2.37E-04
FOXO3	2.62	2.14E-06	2.14	2.77E-04
ATRNL1	2.62	1.22E-21	3.52	3.86E-43
Nrg1	2.61	9.85E-08	2.23	1.19E-05
SNCB	2.60	5.37E-06	3.29	8.41E-10
COL11A1	2.60	5.37E-06	2.56	5.39E-06
DOCK5	2.59	6.94E-11	4.76	3.70E-37
HMBOX1	2.59	1.38E-25	2.40	7.07E-22
ST6GAL1	2.53	2.93E-06	2.08	3.57E-04
ASTN2	2.53	1.04E-07	5.29	5.94E-32
ADCY2	2.50	8.24E-07	2.02	2.47E-04
ST8SIA6	2.49	9.32E-04	4.33	3.83E-10
HINT3	2.49	9.32E-04	2.83	6.93E-05
CD59	2.49	6.55E-09	3.21	5.16E-16
SH3D19	2.48	7.15E-04	2.51	4.31E-04
ZNF518A	2.47	6.54E-06	2.11	2.58E-04
MSH2	2.46	6.92E-21	4.17	1.39E-67
RPS6KA6	2.43	7.51E-06	2.40	6.48E-06
ABTB2	2.42	1.81E-14	2.76	1.20E-20
NKD1	2.39	2.09E-07	2.40	1.05E-07
AMY2A	2.38	1.81E-11	2.74	1.27E-16
CITED4	2.37	8.06E-16	2.28	9.10E-15
DOC2B	2.35	5.51E-04	2.98	1.60E-06
GDPD1	2.35	7.47E-07	2.59	7.75E-09
LAMA4	2.33	1.98E-20	2.69	1.38E-30
LPIN1	2.33	3.10E-05	2.63	5.52E-07
FBN1	2.31	4.49E-72	3.57	4.32E-212
ATP13A3	2.30	2.47E-84	2.14	3.09E-71
BDH2	2.30	2.04E-06	2.21	4.43E-06
LDHA	2.29	7.53E-251	2.33	5.62E-273
OPTN	2.27	2.15E-29	2.00	6.50E-21
COL27A1	2.27	2.33E-05	2.98	6.37E-10
CYP27A1	2.26	3.28E-12	3.23	5.58E-29
BOK	2.26	1.36E-34	4.19	2.09E-146
GLIPR2	2.25	6.32E-09	4.85	5.92E-45
PNPLA8	2.24	7.03E-09	2.01	6.06E-07
CYP26B1	2.21	2.51E-15	2.81	3.35E-29
MMP16	2.20	3.51E-07	2.18	2.85E-07
KATNAL1	2.19	1.78E-04	2.01	8.32E-04

Appendix A: Continued

Gene Name	AVC/VEN (Fold)	p-value	OFT/VEN (Fold)	p-value
IGFBP5	2.18	4.51E-06	3.34	6.29E-16
ZFPM2	2.17	1.58E-12	2.03	7.89E-11
PPARGC1A	2.17	2.51E-10	2.51	1.58E-15
MYOZ1	2.17	1.51E-04	5.04	7.76E-24
SLC35F1	2.16	1.96E-04	2.69	2.52E-07
PDZRN4	2.15	8.77E-08	2.12	8.87E-08
ME3	2.14	4.01E-07	3.45	1.43E-21
MRVI1	2.11	7.97E-04	4.36	3.21E-16
ADAMTSL3	2.10	3.98E-04	2.96	6.36E-09
SCUBE1	2.09	1.12E-06	4.38	1.25E-33
SORBS1	2.08	2.04E-45	2.10	6.62E-49
TPCN1	2.08	6.03E-06	2.50	1.26E-09
WFIKKN1	2.06	8.44E-06	4.10	2.15E-26
PLA2R1	2.05	4.41E-07	2.51	2.88E-12
TOX2	2.03	1.57E-11	2.95	8.98E-31
FADS2	2.02	4.08E-13	2.06	2.31E-14
PARP8	2.02	2.54E-04	2.13	4.55E-05
GRAMD1C	2.01	1.73E-09	2.09	5.78E-11
TOM1	2.00	2.68E-08	2.29	2.00E-12
NKAIN4	2.00	3.49E-05	2.08	6.56E-06
SFRP1	3.54	1.52E-39	1.75	7.51E-07
ITGA4	3.48	2.65E-50	1.59	3.66E-06
C7	3.35	1.77E-11	1.96	8.43E-04
SULF2	3.05	8.43E-35	1.66	8.67E-07
HCN4	2.96	1.82E-36	1.56	6.70E-06
PTPN13	2.91	1.43E-15	1.93	5.92E-06
ANKH	2.85	5.02E-27	1.96	1.28E-10
BAMBI	2.73	1.82E-80	1.91	2.52E-30
GPX3	2.65	4.81E-62	1.49	2.16E-09
ADSSL1	2.65	2.04E-11	1.99	6.41E-06
HDAC10	2.61	3.09E-08	1.87	7.46E-04
TRIM2	2.58	2.36E-22	1.96	4.45E-11
LMO4	2.47	4.37E-44	1.99	7.30E-25
LMBR1	2.43	1.34E-22	1.40	9.28E-04
CNOT6L	2.43	2.45E-09	1.78	2.65E-04
BRWD3	2.41	2.65E-14	1.85	3.96E-07
KCTD15	2.39	2.47E-09	1.68	9.06E-04
PXDN	2.36	3.11E-92	1.87	2.10E-46
MICAL2	2.30	9.47E-73	1.64	6.88E-24
FAM135A	2.29	5.23E-16	1.99	3.59E-11
TLK1	2.29	7.82E-14	1.54	3.43E-04
SOX5	2.28	3.82E-07	1.90	1.03E-04
ATG13	2.27	5.92E-14	1.80	2.14E-07
CNOT6	2.27	4.75E-26	1.67	3.76E-10
SLC12A2	2.25	1.20E-61	1.33	1.94E-07
PIK3C2A	2.24	3.48E-25	1.99	9.15E-19
ALDH18A1	2.23	5.87E-16	1.69	4.80E-07
RHOU	2.19	1.47E-05	1.94	3.09E-04

Appendix A: Continued

Gene Name	AVC/VEN (Fold)	p-value	OFT/VEN (Fold)	p-value
ADCK3	2.19	2.29E-49	1.76	4.48E-25
REV3L	2.18	1.18E-27	1.77	1.31E-14
ITFG1	2.18	6.44E-12	1.61	6.87E-05
MAPK11	2.16	6.81E-17	1.92	1.91E-12
LOX	2.15	1.97E-06	1.84	2.17E-04
NAA16	2.15	1.89E-14	1.44	6.59E-04
DPY19L4	2.14	2.41E-07	1.69	6.23E-04
RASSF7	2.13	6.65E-07	1.78	2.18E-04
SDC2	2.12	3.48E-15	1.99	3.24E-13
ZNF217	2.12	5.30E-19	1.64	1.96E-08
STXBP3	2.12	1.33E-20	1.47	7.58E-06
DKK3	2.09	5.44E-121	1.28	7.04E-13
CEP170	2.09	1.80E-28	1.66	2.27E-13
TRPS1	2.08	1.16E-07	1.76	6.06E-05
CLSTN3	2.08	4.62E-08	1.75	3.96E-05
ING3	2.07	3.75E-07	1.95	2.98E-06
CERK	2.07	6.10E-10	1.64	5.04E-05
PARP4	2.06	1.67E-05	1.90	1.25E-04
AFF1	2.05	2.29E-09	1.66	4.04E-05
VCAN	2.04	4.09E-148	1.47	9.17E-39
RECK	2.04	9.71E-08	1.62	4.89E-04
EPCAM	2.03	1.01E-06	1.70	3.13E-04
PLCB1	2.03	1.78E-14	1.68	3.19E-08
ASB2	2.03	8.82E-34	1.48	1.87E-10
EPHA5	2.02	6.45E-06	1.94	1.58E-05
EML1	2.02	6.41E-05	1.87	3.68E-04
PAPSS1	2.01	3.38E-20	1.96	1.76E-19
SLCO5A1	2.01	8.39E-09	1.64	6.48E-05
UBL3	2.00	2.01E-16	1.43	6.40E-05
LPHN3	1.98	1.05E-16	1.86	4.13E-14
CREB3L2	1.98	3.02E-11	2.39	9.55E-20
GPC1	1.98	6.81E-21	1.40	1.17E-05
PLXNA2	1.97	1.45E-10	3.01	3.24E-32
FBXO7	1.97	2.13E-17	1.39	1.02E-04
PRKD1	1.97	2.78E-08	1.65	6.13E-05
MAN2B2	1.97	6.14E-09	2.02	5.04E-10
LRRC73	1.96	4.90E-04	2.15	3.27E-05
LSP1	1.96	2.06E-39	1.46	1.72E-12
RNF130	1.95	1.01E-07	2.22	1.77E-11
TMEM8A	1.95	1.01E-07	1.79	3.01E-06
ADAMTS7	1.94	5.01E-10	2.87	5.38E-29
BCAS3	1.94	1.99E-08	1.82	3.35E-07
HEG1	1.93	1.80E-12	2.14	1.48E-17
NETO2	1.93	2.80E-04	2.50	3.52E-08
SACS	1.93	1.64E-28	1.62	1.61E-15
SEC24D	1.92	4.39E-07	2.31	3.66E-12
WNT11	1.91	3.60E-13	1.85	3.00E-12
AKT1	1.91	2.48E-21	1.40	3.36E-06

Appendix A: Continued

Gene Name	AVC/VEN (Fold)	p-value	OFT/VEN (Fold)	p-value
SEMA5B	1.90	4.13E-07	1.68	5.53E-05
PMP22	1.90	1.52E-10	1.88	1.03E-10
NPC1	1.90	3.47E-09	1.49	4.27E-04
SMARCAD1	1.89	2.01E-09	1.57	3.77E-05
PKNOX1	1.89	1.31E-06	1.57	8.17E-04
RAB11FIP4	1.88	5.92E-07	1.62	1.90E-04
BPGM	1.88	3.44E-17	1.37	5.84E-05
SYNE2	1.87	3.23E-58	2.14	1.46E-95
ITPR1	1.87	7.53E-10	1.75	2.85E-08
ANKRD50	1.85	5.71E-18	1.91	6.47E-21
OSBPL5	1.84	1.60E-18	1.86	6.67E-20
FUT10	1.84	7.50E-04	1.93	1.87E-04
ROR2	1.84	3.36E-06	1.91	4.23E-07
EP400	1.84	4.97E-20	1.39	2.11E-06
PHF16	1.84	9.75E-11	1.56	3.15E-06
SH3BGRL	1.83	1.52E-42	2.18	2.55E-79
INPP4B	1.83	7.01E-09	1.88	3.96E-10
NIPBL	1.83	3.56E-34	1.30	5.67E-07
IGF2R	1.82	4.71E-16	1.69	7.80E-13
SIPA1L1	1.82	2.45E-14	1.49	8.66E-07
SEMA6A	1.82	4.96E-06	1.78	7.76E-06
TBC1D14	1.82	1.49E-08	1.67	1.05E-06
TBC1D1	1.81	8.57E-12	1.55	7.60E-07
ROR1	1.81	1.16E-23	1.57	5.12E-14
FBN2	1.81	8.74E-188	2.08	4.63E-319
SNTB1	1.81	4.21E-21	1.27	3.12E-04
FNDC3B	1.81	4.51E-15	1.64	5.51E-11
OSBPL8	1.80	4.10E-14	1.44	5.24E-06
INPP5A	1.80	1.04E-10	1.37	9.97E-04
DOPEY2	1.80	3.07E-09	1.85	8.14E-04
YPEL5	1.79	1.07E-21	2.35	1.07E-52
PAM	1.79	7.92E-07	1.49	9.13E-04
P4HA1	1.79	3.24E-19	1.35	9.62E-06
DSC2	1.79	9.15E-04	2.48	9.63E-09
ZBED4	1.79	4.29E-15	1.41	7.82E-06
XRN1	1.79	2.51E-17	1.27	9.12E-04
DAGLB	1.78	6.75E-05	1.87	7.73E-06
LNPEP	1.78	5.47E-08	1.50	2.18E-04
ADAMTS15	1.78	1.85E-04	2.02	1.76E-06
KIAA1551	1.78	1.98E-10	1.42	1.98E-04
AHNAK2	1.78	6.13E-13	2.00	9.24E-20
LRRN4	1.78	1.20E-09	1.45	1.32E-04
PPM1L	1.77	4.81E-05	2.09	2.38E-08
ICK	1.77	1.46E-05	1.58	5.76E-04
THBS1	1.77	1.94E-08	2.03	1.69E-13
PIK3R1	1.77	1.31E-04	2.02	6.61E-07
UTRN	1.77	1.21E-28	2.08	1.04E-52
TTC28	1.77	5.79E-17	1.87	1.28E-21

Appendix A: Continued

Gene Name	AVC/VEN (Fold)	p-value	OFT/VEN (Fold)	p-value
EXOC6B	1.77	5.37E-10	1.38	7.23E-04
RB1CC1	1.76	9.88E-08	1.87	1.22E-09
GATA5	1.76	1.11E-141	1.72	5.73E-137
GATA4	1.76	5.50E-39	1.62	8.50E-29
SLC16A10	1.76	1.58E-08	1.84	2.67E-10
MYO1C	1.76	1.31E-08	1.38	8.03E-08
DSG2	1.75	4.83E-14	2.10	1.07E-26
MRC2	1.75	2.49E-14	2.15	2.60E-29
HECW1	1.74	1.04E-09	2.91	1.31E-42
FILIP1L	1.74	2.04E-16	1.95	1.93E-25
TRANK1	1.74	2.77E-04	1.74	2.13E-04
FAM171B	1.74	1.23E-05	1.71	1.73E-05
App	1.74	1.69E-89	1.81	1.05E-109
CCNT2	1.74	1.05E-04	1.83	1.09E-05
RALGAPA1	1.73	1.22E-15	1.44	2.16E-07
FGFR3	1.73	4.22E-11	1.68	2.35E-10
KIF13B	1.73	9.03E-05	2.09	1.61E-08
STAT1	1.73	1.51E-09	1.46	3.69E-05
MEF2A	1.72	1.78E-55	1.42	1.49E-22
SSFA2	1.72	6.90E-08	1.72	3.77E-08
TP53INP1	1.72	5.19E-09	1.99	3.67E-15
NCALD	1.72	6.63E-05	2.05	1.28E-08
NBR1	1.72	1.32E-16	1.47	7.41E-09
FAT1	1.72	2.61E-62	1.30	2.15E-14
PI4KA	1.72	4.76E-18	1.26	4.14E-04
CAPRIN2	1.71	2.78E-06	1.59	5.00E-05
DPYSL3	1.71	2.13E-23	1.94	6.96E-39
KIF5B	1.70	5.39E-35	1.36	1.08E-11
CHGB	1.70	2.93E-05	2.03	2.13E-09
SMAD6	1.70	1.49E-45	1.70	8.23E-48
RHOB	1.69	1.29E-20	2.75	4.81E-95
GNB5	1.69	1.71E-05	1.50	9.68E-04
FBXO8	1.68	9.50E-04	1.80	1.01E-04
IDH1	1.68	1.60E-15	1.40	5.48E-07
SHROOM3	1.68	4.45E-19	1.70	7.61E-21
DST	1.68	4.12E-10	1.38	1.34E-04
HEPH	1.67	8.07E-04	3.40	2.09E-22
ALDH7A1	1.67	4.57E-18	1.49	2.01E-11
GALNT1	1.67	6.69E-30	1.28	1.06E-07
TACC2	1.67	6.47E-26	1.33	1.18E-08
KIAA0232	1.67	2.28E-12	1.38	1.53E-05
GNS	1.66	2.72E-13	1.53	1.02E-09
MCAM	1.66	4.78E-12	1.88	1.68E-19
ATP11C	1.66	1.92E-15	1.52	7.58E-11
VPS13B	1.66	6.33E-08	1.39	6.63E-04
MYH11	1.66	5.41E-08	2.46	7.44E-28
LPGAT1	1.66	5.11E-17	1.35	1.22E-06
USP46	1.65	5.70E-09	1.49	4.03E-06

Appendix A: Continued

Gene Name	AVC/VEN (Fold)	p-value	OFT/VEN (Fold)	p-value
USP3	1.65	1.28E-12	1.34	4.94E-05
MLLT4	1.64	2.31E-39	1.42	9.90E-20
LIMD2	1.64	3.89E-10	2.07	1.86E-23
ADC	1.64	2.29E-10	2.03	1.89E-22
TYRO3	1.64	6.64E-11	1.58	9.07E-10
NRIP1	1.64	1.47E-05	1.68	2.61E-06
ITGB5	1.64	3.07E-10	1.59	1.40E-09
FNIP2	1.64	2.07E-06	1.53	3.42E-05
LIMA1	1.63	4.79E-09	1.74	4.96E-12
ZFYVE20	1.63	1.13E-07	1.43	9.65E-05
ID2	1.62	2.71E-26	1.84	6.56E-45
SLC19A1	1.62	5.77E-33	1.25	1.12E-07
C16orf62	1.62	1.95E-14	1.36	2.48E-06
MSANTD4	1.62	9.82E-05	1.90	3.39E-08
NCAPG2	1.62	2.81E-05	1.60	2.83E-05
Syng	1.62	1.08E-08	1.39	1.23E-04
STAU1	1.61	1.04E-29	1.27	4.26E-08
ARHGAP32	1.61	1.31E-07	1.51	4.01E-06
MAPK8	1.61	2.94E-09	1.35	3.06E-04
C6orf62	1.61	2.19E-09	1.49	4.82E-07
TCP11L2	1.61	6.32E-04	1.71	5.53E-05
TM9SF3	1.60	1.48E-28	1.49	9.81E-21
ERC1	1.60	3.75E-05	1.82	3.25E-08
PUM2	1.60	8.80E-19	1.32	4.42E-07
TIMP3	1.60	1.59E-17	2.08	8.78E-48
HIF1A	1.60	1.37E-26	1.25	9.79E-07
SMAD3	1.59	1.19E-05	1.67	6.06E-07
SCD5	1.59	2.28E-07	2.03	1.09E-17
TTC9	1.59	2.51E-05	1.65	2.00E-06
ABCA5	1.59	1.35E-06	1.57	1.25E-06
TGFBR1	1.59	1.36E-11	1.37	4.18E-06
SMARCD3	1.58	1.53E-05	1.47	2.50E-04
TPD52	1.58	7.11E-27	1.69	1.04E-37
SLC25A6	1.58	3.05E-280	1.32	8.61E-102
KDM3A	1.58	2.98E-17	1.26	4.03E-05
RCBTB2	1.58	2.53E-04	1.68	1.44E-05
LRRC10	1.57	3.32E-07	1.60	4.26E-08
TIAM1	1.57	2.79E-05	1.58	1.24E-05
CRB2	1.57	2.09E-11	1.75	3.30E-18
PPFIBP2	1.57	2.26E-06	1.44	1.25E-04
RASA3	1.56	1.17E-06	1.46	3.46E-05
ADAM9	1.56	1.82E-08	1.36	1.11E-04
LTBP1	1.56	1.01E-37	1.71	2.40E-58
SERINC1	1.56	1.26E-28	1.28	3.13E-09
TOP2B	1.56	6.20E-37	1.28	5.58E-12
RNF19A	1.56	1.96E-04	1.52	3.39E-04
TTL	1.56	1.79E-12	1.31	2.87E-05
CTNNA3	1.55	2.91E-25	1.54	1.18E-25

Appendix A: Continued

Gene Name	AVC/VEN (Fold)	p-value	OFT/VEN (Fold)	p-value
VAT1	1.55	5.36E-12	1.38	3.14E-07
FZD1	1.54	2.73E-15	1.29	5.00E-06
DCLK2	1.54	2.05E-05	1.85	1.16E-10
FGD3	1.54	1.80E-05	1.48	8.59E-05
DBX2	1.54	3.01E-05	2.23	1.84E-18
PRKACB	1.53	5.14E-08	1.53	3.54E-08
EFR3A	1.53	8.06E-10	1.37	6.39E-06
MAP4K4	1.53	1.05E-26	1.74	1.68E-49
CFC1/CFC1B	1.52	9.09E-07	1.42	3.72E-05
GJC2	1.52	6.55E-05	2.10	3.16E-15
EAF2	1.52	2.96E-04	1.69	1.71E-06
UFSP2	1.52	2.11E-05	1.39	6.70E-04
GLI3	1.52	1.52E-05	1.36	2.99E-08
SPECC1	1.52	4.32E-07	1.61	1.50E-09
RFTN2	1.51	5.99E-04	2.09	1.01E-11
RAP1GDS1	1.51	2.50E-10	1.32	2.16E-05
SASH1	1.51	3.94E-07	1.71	2.85E-12
ROCK2	1.51	4.79E-13	1.43	2.69E-10
FKBP15	1.50	3.79E-05	1.59	1.28E-06
NNT	1.50	2.86E-22	1.28	6.24E-09
ASAP1	1.50	2.73E-07	1.35	1.17E-04
DNM1L	1.49	1.14E-23	1.25	2.80E-08
PATZ1	1.49	7.81E-04	1.50	4.97E-04
IGSF3	1.49	8.66E-08	2.55	1.85E-49
MKL1	1.49	8.60E-06	1.51	2.11E-06
PNPLA7	1.49	7.45E-08	1.49	2.61E-08
SLC12A4	1.49	6.14E-13	1.26	4.32E-05
GPI	1.48	1.09E-78	1.27	1.77E-29
KIDINS220	1.48	1.39E-17	1.32	1.60E-09
MYLK3	1.48	9.23E-16	1.40	5.15E-12
CLSTN1	1.48	2.06E-13	1.35	2.48E-08
KBTBD10	1.48	9.99E-05	1.68	4.31E-08
TTYH3	1.48	3.96E-07	1.42	3.89E-06
NOTCH2	1.48	8.67E-15	1.46	2.35E-14
PLCD1	1.48	4.91E-21	1.88	2.37E-62
NDST2	1.47	1.07E-06	1.44	2.56E-06
UGDH	1.47	1.18E-09	1.45	3.13E-09
FBXO34	1.47	1.12E-06	1.72	2.06E-13
RCBTB1	1.46	4.98E-05	1.55	1.48E-06
PROS1	1.46	2.07E-04	1.40	8.21E-04
TBC1D9	1.46	1.10E-04	1.38	9.73E-04
VASH1	1.46	6.36E-11	1.36	7.02E-08
LRP12	1.46	8.95E-04	1.77	7.70E-08
COL4A6	1.46	6.64E-39	1.94	8.72E-141
LIFR	1.46	9.51E-13	1.66	2.68E-24
COL5A1	1.46	4.57E-21	2.13	1.98E-101
PTPN21	1.46	1.34E-04	1.50	2.27E-05
RAVER2	1.45	6.17E-05	1.45	5.13E-05

Appendix A: Continued

Gene Name	AVC/VEN (Fold)	p-value	OFT/VEN (Fold)	p-value
ADCY5	1.45	1.10E-06	1.51	2.84E-08
CD151	1.45	8.48E-21	1.34	2.43E-13
RBFOX2	1.45	6.76E-19	1.30	4.84E-10
HIVEP1	1.45	1.15E-08	1.42	4.19E-08
PLXNA1	1.45	3.94E-19	1.38	1.77E-15
RSU1	1.45	3.07E-14	1.27	1.14E-06
TMTC3	1.45	5.63E-10	1.39	3.02E-08
TBC1D16	1.45	3.68E-04	1.52	2.31E-05
NCOA4	1.44	5.03E-24	1.33	6.33E-15
PTGFRN	1.44	2.69E-05	1.71	4.16E-11
UBE4B	1.44	2.33E-05	1.48	2.49E-06
SNAP29	1.44	1.29E-07	1.34	1.76E-05
COL4A5	1.43	4.30E-65	1.88	8.48E-234
TES	1.43	1.56E-06	1.43	1.12E-06
WAPAL	1.43	7.69E-11	1.26	3.93E-05
KALRN	1.43	9.82E-06	1.42	8.78E-06
EHMT1	1.43	9.65E-12	1.28	2.51E-06
PLEKHA7	1.43	3.07E-16	1.28	1.49E-08
UNC5B	1.42	2.59E-06	1.62	1.26E-11
LRRN1	1.42	1.27E-07	1.31	6.49E-05
ACTA1	1.42	1.34E-23	2.59	1.39E-226
EGFL7	1.42	7.66E-05	1.38	2.32E-04
SETX	1.42	5.78E-06	1.36	5.00E-05
ALDH6A1	1.41	3.36E-06	1.28	7.10E-04
MYOZ2	1.41	3.28E-05	3.24	4.06E-73
PBX1	1.41	2.70E-07	1.38	9.58E-07
RBMS1	1.41	8.91E-09	1.27	7.38E-05
MEX3B	1.41	1.76E-04	2.07	1.68E-19
HTATSF1	1.40	5.58E-06	1.33	1.02E-04
LAMP1	1.40	1.23E-18	1.33	9.34E-14
STAM	1.40	5.24E-04	1.44	1.08E-04
FAS	1.40	2.58E-20	2.02	6.79E-04
CDH5	1.40	1.74E-19	1.52	5.14E-32
BNIP3L	1.40	5.94E-15	1.30	8.60E-10
MLL5	1.40	5.98E-10	1.25	3.39E-05
ARRDC1	1.40	3.46E-05	1.77	2.11E-14
LDB3	1.40	2.05E-12	1.31	6.98E-09
PPFIBP1	1.40	3.45E-14	1.28	3.65E-08
SDK1	1.40	2.12E-08	1.50	1.55E-12
BMPR2	1.40	2.34E-09	1.38	3.92E-09
ARID1B	1.39	6.62E-09	1.36	3.97E-08
KSR1	1.39	5.43E-04	1.53	2.97E-06
CLTC1	1.39	2.82E-19	1.31	7.89E-14
CSRP3	1.39	1.03E-47	1.27	1.32E-25
JAM3	1.39	1.18E-06	1.27	5.28E-04
AMBRA1	1.39	9.51E-06	1.47	7.08E-08
TMEM131	1.39	2.11E-11	1.27	7.15E-07
PPM1E	1.38	5.87E-05	1.83	1.90E-16

Appendix A: Continued

Gene Name	AVC/VEN (Fold)	p-value	OFT/VEN (Fold)	p-value
LAMB2	1.38	9.26E-05	2.00	4.00E-21
PTGR1	1.38	4.87E-04	1.37	4.99E-04
EP300	1.38	5.39E-13	1.29	1.04E-08
CPPED1	1.38	2.27E-06	1.30	9.82E-05
ZFHX3	1.38	1.73E-06	1.43	4.24E-08
MECOM	1.38	9.50E-05	1.97	1.11E-20
MFGE8	1.37	3.57E-16	1.44	1.20E-22
IWS1	1.37	2.24E-10	1.25	6.01E-06
ACLY	1.37	4.08E-12	1.27	9.67E-08
WFS1	1.37	1.54E-04	1.64	1.34E-10
SNAP23	1.37	1.60E-06	1.53	4.68E-12
SLC25A17	1.36	8.23E-04	1.38	3.11E-04
CCDC88A	1.36	9.45E-07	1.34	1.88E-06
FKBP9	1.35	3.95E-09	1.29	6.33E-07
CPM	1.35	2.50E-04	1.53	5.00E-08
TOM1L2	1.35	6.16E-04	1.63	2.21E-09
ZMZ1	1.35	1.29E-06	1.35	7.79E-07
UBE2H	1.35	1.11E-07	1.29	5.75E-06
IRS2	1.35	2.08E-05	1.65	7.67E-15
CDC42BPB	1.35	2.10E-15	1.43	4.24E-23
PDCD6IP	1.34	1.41E-11	1.27	4.08E-08
LY6E	1.34	4.20E-17	1.81	1.86E-79
TPRG1L	1.33	2.15E-05	1.84	9.10E-24
DCHS1	1.33	7.41E-04	1.65	1.64E-10
SMYD1	1.33	1.89E-26	1.49	4.86E-56
SRP68	1.33	1.03E-07	1.26	9.24E-06
CALD1	1.32	5.07E-06	1.27	7.98E-05
OLFML2B	1.32	4.10E-04	2.46	6.96E-43
RNF11	1.32	7.80E-08	1.52	1.18E-17
B4GALNT4	1.32	9.36E-05	1.57	6.64E-12
HIPK2	1.32	6.49E-12	1.58	7.13E-35
FARP1	1.31	4.35E-07	1.52	1.38E-16
SLC25A12	1.31	8.06E-05	1.32	4.37E-05
AKAP13	1.31	2.62E-04	1.51	4.54E-09
SEPSECS	1.31	1.68E-04	1.28	3.79E-04
TMTC4	1.30	1.43E-04	1.39	1.12E-06
PHF21A	1.30	1.92E-04	1.26	9.69E-04
CACNA2D1	1.30	7.86E-05	1.41	7.76E-08
PTPRA	1.30	2.79E-05	1.55	4.39E-14
ANXA11	1.30	4.63E-04	1.45	1.25E-07
CAND2	1.30	7.25E-04	1.42	1.86E-06
LAMB1	1.30	3.87E-17	1.39	2.43E-28
KIF26B	1.29	3.48E-09	1.33	1.95E-11
NFIB	1.29	6.16E-04	1.30	3.36E-04
SEC63	1.29	1.52E-11	1.38	1.54E-18
COL18A1	1.29	1.11E-41	1.66	1.62E-186
UNC5C	1.29	3.31E-04	1.78	9.97E-20
PAC SIN3	1.29	1.35E-04	1.37	9.64E-07

Appendix A: Continued

Gene Name	AVC/VEN (Fold)	p-value	OFT/VEN (Fold)	p-value
LBH	1.28	3.83E-20	1.95	7.04E-173
TNRC6C	1.28	6.12E-05	1.27	6.53E-05
MAP7D3	1.28	7.81E-04	1.36	1.51E-05
CMTM7	1.28	4.24E-04	2.53	5.07E-59
AHCYL1	1.28	3.13E-04	1.38	6.11E-07
PLS3	1.28	3.79E-09	1.29	5.25E-10
BMP7	1.27	5.74E-05	1.35	2.05E-07
NFRKB	1.27	6.27E-17	1.48	2.49E-49
PAPPA	1.27	6.10E-04	1.29	1.64E-04
ALDH2	1.27	1.46E-08	1.29	3.59E-10
DOCK7	1.26	3.40E-06	1.38	2.20E-11
NFATC1	1.26	2.77E-05	1.47	1.42E-13

APPENDIX B

E11.0 MOUSE GENES WITH >1.25-FOLD HIGHER EXPRESSION IN AVC AND OFT COMPARED TO VEN

Red= >2-fold Enriched in both AVC and OFT compared to VEN

Orange= >1.25-fold Enriched in both AVC and OFT compared to VEN

Gene Name	n=100		n=60			
	AVC / VEN (Fold)	p-value	OFT / VEN (Fold)	p-value	AVC / VEN (Fold)	p-value
MATN4	23.97	5.58E-27	7.75	1.30E-07	19.26	1.55E-10
CTHRC1	20.78	6.54E-109	34.98	6.97E-218	9.11	1.14E-50
WNT9B	19.14	1.94E-36	9.21	5.40E-16	34.90	5.00E-20
BAALC	17.91	1.09E-15	51.43	9.93E-55	8.02	4.68E-13
CA3	16.31	3.03E-198	17.56	1.11E-237	5.69	9.12E-30
PRRX1	14.58	9.00E-54	49.00	1.49E-04	5.55	2.96E-11
TWIST1	13.83	1.26E-211	13.17	1.39E-217	10.29	1.34E-159
COL9A3	13.25	4.41E-96	17.31	1.56E-147	5.99	2.47E-31
PAPSS2	13.22	6.77E-120	29.28	0.00E+00	7.66	4.27E-56
CHST3	12.75	1.38E-10	21.81	3.00E-21	6.15	4.35E-04
PDE1A	11.60	7.37E-26	14.18	2.41E-36	6.50	5.43E-12
DOC2B	11.02	5.01E-05	16.16	4.34E-08	49.00	1.61E-04
RSPO3	10.65	1.78E-48	15.91	5.07E-89	20.75	3.04E-37
COL9A1	10.34	2.72E-162	23.40	0.00E+00	5.93	6.86E-30
BMPER	9.80	6.80E-45	11.53	3.80E-61	11.74	8.00E-29
CLMP	9.73	2.04E-52	14.30	1.68E-95	5.81	1.70E-16
TBX2	9.42	2.66E-74	4.85	1.20E-29	6.81	5.25E-46
NDUFA4L2	9.19	3.42E-10	20.10	1.91E-28	3.71	2.02E-04
MEOX1	8.61	3.35E-28	63.38	0.00E+00	3.59	1.21E-07
PCDHAC2	8.61	1.14E-06	9.96	1.54E-08	6.95	1.01E-04
PI16	8.57	2.25E-25	12.68	1.08E-46	4.15	3.12E-07
FST	8.54	5.85E-08	12.28	2.22E-13	4.55	9.70E-05
KIAA1755	8.27	2.37E-06	6.46	4.61E-05	8.83	1.72E-04
TNC	7.89	3.45E-40	94.42	0.00E+00	2.73	1.95E-12
MSX1	7.88	2.18E-63	5.16	3.38E-36	5.36	7.30E-21
SCARA3	7.62	3.46E-18	11.99	1.97E-36	5.54	1.50E-09
IGFBP7	7.50	2.19E-38	23.41	1.41E-185	4.45	3.77E-22
ELN	7.36	1.42E-41	81.48	0.00E+00	2.98	2.48E-09
ADAMTS8	7.17	6.46E-31	7.95	2.37E-39	4.59	1.17E-09
POSTN	7.14	0.00E+00	12.97	0.00E+00	5.58	3.15E-178
ADAM23	7.12	1.73E-13	11.22	5.08E-27	6.65	5.06E-09
NT5E	6.97	6.20E-19	10.71	1.81E-37	2.26	6.07E-04
TUBB3	6.95	3.24E-63	9.63	1.39E-111	3.82	5.99E-22

Appendix B: Continued

Gene Name	n=100				n=60			
	AVC / VEN (Fold)	p-value	OFT / VEN (Fold)	p-value	AVC / VEN (Fold)	p-value	OFT / VEN (Fold)	p-value
DLG2	6.80	1.82E-15	24.56	1.67E-87	7.36	5.17E-09	17.15	1.44E-25
EPHA3	6.79	1.12E-38	3.64	4.76E-15	9.92	3.44E-23	5.42	5.15E-10
NGFR	6.61	8.48E-06	23.48	1.45E-28	6.10	4.70E-06	10.45	6.92E-12
LUM	6.53	4.18E-18	6.97	8.10E-22	5.65	3.63E-25	4.37	1.49E-16
ROBO2	6.44	9.97E-36	13.65	4.73E-112	4.10	2.00E-14	6.56	2.04E-30
MSX2	6.29	1.88E-20	6.37	7.69E-23	2.99	7.72E-07	3.08	3.43E-07
PITX2	6.03	4.14E-36	6.25	5.53E-42	3.59	3.04E-13	2.27	3.13E-05
SNAI1	5.73	1.29E-46	3.65	2.12E-23	3.82	7.31E-33	2.58	2.19E-14
PDGFRA	5.57	2.28E-270	7.23	0.00E+00	3.16	2.87E-60	3.22	2.41E-62
SOX9	5.43	1.63E-205	5.95	6.62E-265	3.99	2.56E-102	3.55	8.29E-81
COL2A1	5.38	0.00E+00	8.94	0.00E+00	3.46	6.59E-94	7.57	0.00E+00
COL6A3	5.14	1.40E-25	3.49	2.75E-14	4.47	2.76E-13	2.92	3.00E-06
PCSK6	5.12	2.35E-86	4.02	7.65E-62	4.21	7.83E-45	3.64	7.01E-34
TMEM26	5.12	1.99E-05	14.62	1.44E-22	24.87	1.98E-07	46.54	5.00E-14
CLSTN2	4.86	1.65E-10	8.62	1.80E-26	4.98	3.57E-08	4.16	3.09E-06
AQP1	4.79	4.15E-89	2.99	4.88E-39	4.87	6.51E-41	5.33	2.24E-47
FRZB	4.73	2.78E-21	11.43	1.17E-86	2.95	2.03E-07	6.73	2.48E-29
NCAM1	4.73	3.13E-261	4.66	1.06E-282	3.19	8.40E-50	2.75	1.44E-35
C1QB	4.72	4.36E-12	8.15	5.71E-30	3.37	1.63E-04	5.31	6.10E-09
NFATC4	4.71	3.58E-49	6.66	7.95E-96	2.84	3.44E-14	4.84	4.92E-39
CRABP1	4.67	8.07E-17	19.28	3.56E-134	2.48	9.31E-05	8.65	3.84E-37
STMN4	4.62	1.06E-09	22.24	4.59E-88	6.55	9.51E-08	26.67	1.33E-42
PPP1R14A	4.48	1.79E-12	4.71	7.35E-15	4.65	2.96E-04	5.39	3.90E-05
PDLIM3	4.30	0	7.44	0	2.99	4.14E-128	7.15	0
FAM167A	4.20	5.55E-10	5.54	5.46E-17	5.96	8.75E-08	7.93	2.40E-11
HAS2	4.18	2.17E-38	6.58	3.17E-91	3.46	3.36E-18	4.08	1.09E-24
RGMA	4.16	1.82E-19	5.77	4.71E-37	3.17	2.45E-07	3.85	2.76E-10
RARG	4.15	2.11E-41	6.73	1.61E-103	2.91	8.38E-15	6.06	2.81E-55
C12orf68	4.13	4.10E-06	4.76	3.35E-08	17.65	2.93E-05	31.84	1.62E-09
LPPR3	4.06	1.48E-15	5.53	9.24E-29	4.30	2.58E-10	4.27	3.50E-10
PRSS35	4.06	2.19E-22	3.27	2.14E-16	5.13	2.24E-14	3.58	5.75E-08
ERBB3	4.04	6.10E-29	8.57	8.16E-108	3.76	1.51E-11	9.54	4.63E-48
SERINC2	3.90	1.33E-05	11.13	9.64E-27	3.13	5.17E-04	9.88	5.54E-21
HTRA1	3.79	9.83E-26	7.42	2.54E-87	4.43	1.97E-16	8.53	2.20E-44
UNC5C	3.72	5.85E-47	3.46	2.97E-45	3.12	4.17E-26	2.09	7.03E-10
COX4I2	3.58	8.02E-06	9.62	2.67E-27	4.41	7.71E-07	9.88	5.54E-21
NFIX	3.58	8.26E-17	4.56	8.71E-29	2.44	6.42E-05	2.45	6.22E-05
ZNF503	3.53	3.00E-15	3.88	4.48E-20	3.29	2.42E-14	2.18	7.23E-06
ADAMTS15	3.53	4.70E-36	3.88	3.35E-48	3.03	6.45E-18	3.32	2.19E-21
DPYSL4	3.34	3.15E-06	2.83	4.66E-05	6.95	1.01E-04	9.80	5.08E-07
THBS1	3.30	5.24E-152	6.53	0.00E+00	3.05	1.69E-86	3.72	7.24E-131
ADA	3.23	5.10E-09	2.73	4.36E-07	2.79	6.98E-05	2.59	2.91E-04
FOXP2	3.17	1.56E-10	7.75	8.24E-52	5.69	8.37E-11	8.24	4.91E-18
GATA3	3.08	2.46E-13	10.83	5.59E-115	2.54	1.73E-05	7.67	1.64E-35
TPBG	3.03	4.71E-20	2.68	7.29E-17	2.23	1.14E-05	2.74	8.21E-09
DNM1	2.96	1.68E-18	3.04	1.17E-21	2.39	2.28E-09	2.25	5.45E-08

Appendix B: Continued

Gene Name	n=100				n=60			
	AVC / VEN (Fold)	p-value	OFT / VEN (Fold)	p-value	AVC / VEN (Fold)	p-value	OFT / VEN (Fold)	p-value
CRISPLD1	2.91	1.05E-04	3.11	9.78E-06	2.52	9.52E-05	2.68	2.48E-05
MFAP4	2.86	3.62E-44	3.87	9.14E-94	2.45	3.84E-27	3.85	1.17E-73
FZD1	2.86	6.90E-67	6.05	7.79E-317	2.15	1.91E-21	3.65	2.04E-74
WNT2	2.85	1.50E-06	3.12	1.64E-08	2.69	1.39E-04	2.88	3.57E-05
EDIL3	2.82	5.10E-23	2.78	8.74E-25	2.82	9.53E-13	2.04	6.45E-06
PRRT4	2.79	2.50E-08	3.55	1.08E-14	2.41	5.63E-06	3.11	4.38E-10
PHLDA1	2.78	1.48E-21	2.46	7.76E-18	2.61	1.98E-11	3.27	2.54E-18
EEF1A2	2.77	5.57E-93	2.26	1.01E-60	3.21	1.27E-53	3.10	1.57E-49
BMP6	2.76	8.82E-09	2.37	6.40E-07	2.41	5.03E-04	3.09	1.98E-06
ADAMTSL2	2.62	9.59E-13	2.51	8.93E-13	5.92	1.21E-08	9.19	1.64E-15
GARNL3	2.61	3.78E-11	2.14	1.45E-07	2.23	9.75E-07	2.13	5.61E-06
CYP26B1	2.57	2.06E-16	2.92	1.81E-24	3.80	8.94E-22	3.10	1.36E-14
INHBA	2.55	6.40E-07	14.05	3.52E-119	3.30	4.89E-04	15.06	2.99E-32
BOC	2.55	5.70E-12	3.01	2.71E-19	2.74	1.13E-07	3.27	9.31E-11
STX1A	2.50	1.01E-11	4.04	2.11E-35	2.05	4.81E-04	2.98	5.49E-09
ITGB5	2.44	1.64E-64	2.46	1.04E-73	2.50	1.48E-41	2.53	6.91E-43
SERPINE1	2.30	2.40E-04	9.26	2.01E-50	2.69	5.55E-04	9.68	4.36E-28
BCAT1	2.28	8.60E-07	3.13	4.86E-15	2.06	4.97E-05	2.07	4.21E-05
HSD17B11	2.24	8.94E-26	2.39	1.44E-34	2.24	4.46E-14	2.47	4.33E-18
GPC1	2.22	2.57E-92	2.07	8.49E-84	2.37	5.34E-52	2.22	4.54E-43
PXDC1	2.21	4.10E-14	4.84	9.56E-85	2.07	3.79E-06	5.97	2.31E-49
RNF130	2.18	1.75E-08	2.78	8.36E-17	2.72	5.47E-10	2.92	1.59E-11
LRP3	2.16	7.89E-07	2.25	2.55E-08	3.24	1.92E-09	3.39	3.33E-10
ENC1	2.14	1.29E-41	2.88	1.36E-102	2.15	8.00E-28	2.42	1.48E-38
SMAD6	2.12	6.43E-42	2.55	1.72E-78	2.04	5.19E-30	2.97	3.44E-80
TGFB2	2.05	7.51E-53	3.57	1.34E-239	2.12	1.05E-32	3.05	4.67E-82
APCDD1	6.20	3.49E-06	2.25	3.76E-23	6.02	5.66E-05	1.75	5.39E-07
SNAI2	4.59	3.88E-33	4.86	2.08E-40	1.72	6.82E-04	1.87	6.75E-05
ENO2	3.52	1.86E-21	1.92	7.82E-06	2.03	4.51E-04	2.22	5.70E-05
FGFR2	3.12	9.22E-30	2.55	6.30E-21	2.38	2.84E-11	1.88	5.78E-06
ROBO1	3.07	8.57E-89	2.61	2.49E-67	2.49	9.70E-36	1.43	2.14E-05
GPC6	2.95	7.68E-33	3.18	4.13E-43	1.76	1.04E-06	1.96	2.96E-09
HAPLN1	2.75	2.50E-198	2.07	1.50E-100	2.14	2.71E-72	1.51	2.63E-19
PKNOX2	2.73	1.58E-11	3.92	2.74E-26	1.86	1.33E-05	2.05	2.57E-07
CDH6	2.73	1.58E-11	1.83	1.11E-04	8.83	2.15E-11	4.76	4.98E-05
SERPINF1	2.72	3.40E-21	7.18	5.67E-141	1.89	5.95E-07	5.12	1.52E-60
ITGA4	2.69	3.59E-30	4.07	6.75E-81	1.96	7.78E-11	1.67	2.17E-06
PCDH18	2.60	3.10E-31	2.97	4.02E-48	2.35	3.98E-16	1.96	8.78E-10
SEMA3C	2.59	4.01E-25	5.49	7.82E-125	1.71	3.63E-05	3.23	8.68E-26
HMGCS2	2.51	8.97E-09	2.48	2.56E-09	2.24	6.96E-07	1.93	1.01E-04
KCNE1	2.48	9.43E-35	2.25	9.71E-30	2.05	1.06E-12	1.55	5.46E-05
SPINT2	2.47	1.84E-27	2.15	3.32E-21	1.80	9.90E-06	2.18	9.15E-10
HIST2H3C	2.34	7.70E-05	2.45	8.36E-06	1.37	6.82E-42	3.12	2.93E-04
COL9A2	2.31	1.18E-14	2.41	3.64E-18	1.81	1.01E-04	1.97	6.50E-06
SSBP2	2.29	1.02E-10	2.20	1.01E-10	1.39	3.74E-04	1.39	3.72E-04
IGF1	2.28	4.14E-17	3.00	5.57E-37	2.28	9.86E-12	1.71	3.82E-05

Appendix B: Continued

Gene Name	n=100				n=60			
	AVC / VEN (Fold)	p-value	OFT / VEN (Fold)	p-value	AVC / VEN (Fold)	p-value	OFT / VEN (Fold)	p-value
TNFRSF19	2.24	3.72E-23	2.08	9.43E-21	1.99	3.25E-10	4.08	4.52E-04
UCHL1	2.24	7.87E-22	2.33	2.46E-27	1.60	5.64E-09	2.49	3.38E-36
MFAP2	2.22	5.73E-83	2.44	9.91E-122	1.68	1.61E-30	1.56	2.16E-22
ANTXR1	2.19	1.81E-12	5.11	7.26E-83	1.87	2.42E-06	2.93	1.46E-19
BNIP3	2.17	6.07E-85	1.86	1.77E-57	1.46	5.80E-10	1.33	6.99E-06
PRRX2	2.17	2.74E-34	2.41	4.94E-52	1.66	1.13E-08	2.30	2.97E-24
LIMCH1	2.14	2.58E-34	2.19	1.13E-40	1.91	1.11E-14	1.58	2.51E-07
GAS6	2.14	3.20E-23	2.00	5.95E-21	2.12	1.99E-10	2.50	5.97E-16
ID1	2.08	1.08E-60	2.33	1.20E-95	1.75	5.71E-18	2.01	5.90E-29
LMCD1	2.08	1.02E-14	1.71	8.53E-09	2.30	9.58E-09	2.53	5.60E-11
UNC5B	2.04	9.39E-150	2.62	0.00E+00	1.77	6.43E-51	2.59	1.22E-165
SYT11	2.01	1.89E-17	3.64	3.52E-84	1.54	1.94E-05	2.93	1.13E-35
LGALS1	1.99	3.15E-170	3.60	0.00E+00	1.73	6.99E-67	4.76	0.00E+00
RASL11B	1.99	1.22E-23	3.39	8.85E-104	1.74	5.69E-09	2.91	7.95E-37
ID3	1.99	3.65E-69	2.06	9.37E-88	1.46	9.87E-19	1.74	7.44E-41
SORCS2	1.97	3.98E-16	1.42	4.76E-05	1.89	1.12E-08	1.78	3.09E-07
FBLN2	1.97	4.34E-76	3.66	0.00E+00	1.73	3.14E-32	2.87	1.17E-146
TAGLN2	1.97	9.06E-178	2.63	0.00E+00	1.64	2.89E-54	3.09	0.00E+00
SYNPO	1.97	1.59E-37	3.85	3.39E-226	1.73	1.03E-14	3.55	1.76E-99
CLIP3	1.95	8.97E-20	3.13	1.47E-77	2.06	8.91E-23	2.73	6.68E-48
LTBP4	1.92	2.03E-38	4.27	0.00E+00	1.58	4.55E-13	3.20	9.79E-107
EFS	1.91	7.70E-09	2.03	1.29E-11	1.67	2.01E-04	2.36	1.21E-11
VASH1	1.91	2.45E-27	2.78	1.47E-89	1.79	7.04E-15	2.40	5.29E-36
CLU	1.91	2.99E-39	3.43	9.72E-210	1.97	6.86E-22	4.87	7.67E-173
NKD1	1.88	2.86E-09	1.75	5.33E-08	2.44	9.04E-10	1.98	8.18E-06
PDGFC	1.88	1.22E-04	5.69	3.63E-50	2.05	1.54E-04	4.69	1.51E-23
SOX11	1.88	2.13E-39	1.94	4.55E-49	1.39	9.20E-05	1.45	6.04E-06
BMF	1.87	5.48E-10	2.80	4.30E-33	2.01	6.84E-08	3.83	4.08E-34
TSPAN7	1.87	3.73E-22	1.52	6.15E-11	1.39	2.05E-05	1.44	1.86E-06
TGIF1	1.86	1.45E-10	2.09	6.70E-17	1.61	2.67E-05	1.90	3.42E-09
LTBP1	1.85	2.36E-65	2.81	2.46E-251	2.05	1.28E-56	1.99	8.73E-51
CHST11	1.85	7.72E-14	1.52	3.50E-07	2.54	1.33E-13	1.68	2.18E-04
SMAD7	1.84	3.35E-21	2.31	5.42E-48	2.19	1.92E-15	2.53	3.56E-22
ATP1B1	1.84	2.90E-156	1.36	9.69E-39	2.06	4.38E-105	1.38	2.66E-18
LOXL2	1.82	1.53E-95	3.70	0.00E+00	1.43	3.09E-20	2.45	1.96E-152
PTPRB	1.81	1.33E-14	3.62	1.46E-98	2.92	1.06E-21	4.37	1.16E-47
BAMBI	1.81	3.31E-50	2.12	1.06E-96	1.52	1.29E-15	1.63	4.52E-21
ADAMTS17	1.81	2.94E-05	1.72	5.76E-05	3.65	4.80E-09	2.49	1.91E-04
LTBP3	1.80	2.42E-14	2.29	8.83E-34	1.77	2.42E-09	2.01	5.45E-14
SERF1A	1.80	8.89E-15	1.82	2.53E-17	1.96	6.06E-11	1.99	2.40E-11
KLHDC8B	1.80	5.15E-38	1.47	1.86E-17	1.40	2.61E-06	1.72	2.81E-15
ATOH8	1.79	3.21E-10	1.46	4.21E-05	2.31	3.83E-13	1.59	2.69E-04
MMP11	1.79	2.64E-06	1.65	2.51E-05	2.13	6.15E-07	2.70	4.19E-12
IER3	1.78	2.01E-05	2.82	7.82E-20	1.91	4.76E-05	2.08	2.66E-06
NLGN2	1.78	7.95E-15	2.50	4.59E-46	1.46	2.26E-05	1.57	3.29E-07
LOC728392	1.77	2.01E-13	2.39	1.35E-37	1.79	4.19E-11	1.62	8.02E-08

Appendix B: Continued

Gene Name	n=100				n=60			
	AVC / VEN (Fold)	p-value	OFT / VEN (Fold)	p-value	AVC / VEN (Fold)	p-value	OFT / VEN (Fold)	p-value
SBK1	1.77	4.92E-20	2.12	4.37E-41	1.65	2.77E-11	2.11	4.79E-26
FLRT3	1.76	1.29E-13	2.47	3.89E-43	1.42	2.96E-04	1.54	4.96E-06
NNAT	1.76	7.82E-49	1.69	3.30E-47	1.63	1.14E-20	1.70	1.53E-24
PCDH1	1.75	6.53E-06	3.23	8.42E-32	1.64	6.84E-05	2.91	5.91E-23
COL1A1	1.75	1.27E-79	2.95	0.00E+00	1.32	8.51E-19	1.56	1.44E-49
VCAN	1.75	4.89E-236	2.47	0.00E+00	2.24	2.32E-239	2.12	1.33E-201
CRIP1	1.74	6.02E-40	1.95	3.78E-69	1.80	2.76E-21	2.57	4.48E-62
FURIN	1.73	3.75E-84	1.60	1.35E-66	1.80	2.02E-50	1.57	9.52E-29
GLI3	1.72	6.60E-13	3.39	2.35E-92	1.41	3.72E-04	1.67	4.47E-08
CD248	1.72	3.49E-11	2.84	5.50E-54	2.07	2.89E-12	2.76	1.46E-25
HIST2H2AB	1.70	1.21E-10	1.34	3.45E-04	1.62	2.32E-05	1.93	2.06E-09
TGFBI	1.70	2.80E-26	5.98	0.00E+00	1.33	2.86E-06	4.97	6.60E-281
RGS12	1.70	6.04E-19	1.40	1.68E-08	1.99	3.33E-20	1.76	2.82E-13
GPR153	1.67	3.10E-10	1.54	2.90E-08	1.63	1.76E-05	2.12	1.60E-12
LHFPL2	1.67	4.35E-10	1.85	4.84E-16	2.03	6.91E-13	2.10	3.52E-14
DBI	1.66	7.09E-32	1.31	6.06E-10	1.69	1.57E-13	2.05	4.60E-26
CACHD1	1.66	6.89E-08	3.80	8.09E-79	1.61	1.92E-05	2.00	4.48E-11
GATA5	1.64	1.34E-22	1.54	1.93E-19	1.67	4.36E-18	1.30	3.83E-05
MEIS2	1.64	5.94E-21	1.69	5.48E-27	1.58	9.62E-12	1.39	2.50E-06
DCHS1	1.62	1.70E-10	1.69	8.51E-14	1.45	8.20E-06	1.46	7.86E-06
PTMS	1.62	8.24E-109	1.62	1.47E-120	1.37	4.20E-19	1.45	5.33E-27
SLC12A2	1.62	3.33E-13	3.46	1.76E-128	1.47	1.38E-04	2.31	3.08E-20
TRIM32	1.62	6.61E-13	1.63	1.06E-14	1.43	7.21E-05	1.39	2.57E-04
FGFRL1	1.61	1.73E-09	2.79	2.19E-56	1.75	5.70E-08	3.34	5.06E-42
NREP	1.59	4.33E-44	1.68	2.20E-63	1.51	2.11E-17	1.46	3.20E-14
PLEKHA6	1.58	3.13E-12	2.04	1.77E-34	1.78	1.00E-11	1.65	6.52E-09
COL6A1	1.57	3.54E-14	1.51	5.53E-13	2.41	8.77E-26	1.69	1.04E-08
PPP2R5B	1.53	4.40E-08	1.89	7.86E-20	1.48	3.31E-05	1.76	3.50E-10
MAP1B	1.52	2.58E-06	2.24	3.62E-26	1.55	3.32E-26	1.45	4.32E-05
RHOB	1.52	2.86E-30	1.83	9.59E-76	1.42	4.91E-14	1.83	8.11E-43
CHSY1	1.52	8.21E-18	2.07	1.73E-66	2.13	5.01E-28	2.47	8.78E-42
TEAD3	1.51	6.08E-06	1.55	2.71E-07	1.59	1.77E-05	1.52	1.12E-04
APBB1	1.51	1.29E-14	1.59	7.41E-21	1.30	3.14E-04	1.68	7.44E-14
ERF	1.50	1.08E-29	1.91	5.14E-94	1.42	3.82E-15	1.85	4.69E-49
FOXP4	1.50	2.04E-14	1.87	8.55E-41	1.29	1.05E-05	1.32	1.20E-06
ANGPTL2	1.49	6.14E-19	1.72	2.07E-40	2.20	2.10E-07	2.12	1.08E-06
RCOR2	1.49	9.56E-08	1.53	1.08E-09	1.40	6.28E-04	1.84	3.31E-11
SKIL	1.49	1.44E-08	2.26	3.80E-43	1.50	2.72E-05	1.64	1.59E-07
DPYSL3	1.48	4.89E-49	1.66	1.52E-94	1.37	1.08E-14	1.44	1.07E-19
H2afv	1.47	1.36E-11	1.54	6.55E-16	1.46	3.76E-06	1.51	5.64E-07
CDC42EP4	1.47	3.55E-09	1.41	3.07E-08	1.56	3.29E-07	1.67	2.66E-09
ADAM19	1.47	4.18E-17	2.36	1.57E-112	1.50	1.77E-11	2.26	1.97E-50
DDAH2	1.46	3.35E-19	1.57	3.06E-30	1.29	1.24E-05	1.72	2.29E-23
NDUFA1	1.46	1.65E-45	1.33	2.90E-28	1.33	1.09E-07	1.28	8.17E-06
ITGB3	1.46	9.68E-04	2.65	1.63E-25	1.78	4.99E-05	1.90	5.31E-06
DBN1	1.46	3.14E-24	1.45	7.17E-27	1.26	3.94E-06	1.57	7.98E-21

Appendix B: Continued

Gene Name	n=100				n=60			
	AVC / VEN (Fold)	p-value	OFT / VEN (Fold)	p-value	AVC / VEN (Fold)	p-value	OFT / VEN (Fold)	p-value
P4HA1	1.45	8.39E-14	1.54	3.77E-21	1.30	5.00E-04	1.35	7.43E-05
PRAF2	1.44	1.43E-10	2.00	7.07E-46	1.36	1.57E-05	1.47	4.21E-08
IRF2BPL	1.43	2.25E-21	1.30	8.38E-13	1.43	1.62E-10	1.28	1.51E-05
WNT11	1.43	9.47E-05	2.58	3.13E-37	1.51	1.95E-04	2.72	1.03E-25
DACT3	1.43	2.36E-13	1.99	3.10E-60	1.32	5.93E-06	1.90	5.64E-30
PPM1L	1.42	9.72E-05	1.42	6.16E-04	1.78	4.61E-05	1.97	1.06E-05
PCBP4	1.41	3.71E-19	1.51	2.62E-32	1.34	1.58E-10	1.42	4.60E-15
MPP2	1.41	3.60E-07	1.43	1.59E-08	1.69	8.21E-11	1.79	2.91E-13
NES	1.40	1.24E-15	2.78	5.99E-207	1.41	4.86E-08	2.47	1.00E-59
Cd24a	1.40	1.39E-12	1.75	2.22E-40	1.40	1.76E-08	1.66	1.03E-18
LRFN4	1.39	5.43E-08	1.85	9.58E-31	1.45	2.02E-06	2.01	2.63E-22
ASB4	1.38	1.51E-06	2.25	4.66E-47	1.51	8.10E-06	2.01	7.91E-16
GPC3	1.38	1.36E-43	1.41	4.51E-56	1.28	4.78E-14	1.30	9.44E-16
WNK4	1.38	1.71E-05	1.52	1.15E-09	1.73	5.41E-06	2.01	2.29E-09
PLOD1	1.38	2.28E-10	1.53	4.39E-20	1.25	4.56E-04	1.57	2.34E-13
PLOD2	1.37	1.41E-05	2.10	2.52E-34	1.41	2.30E-04	1.97	4.13E-15
LPHN1	1.37	2.51E-08	1.82	2.50E-34	1.46	1.56E-09	1.52	2.58E-11
CTSB	1.37	1.13E-37	1.33	1.19E-35	1.43	2.14E-25	1.60	6.08E-45
SSSCA1	1.35	1.39E-13	1.62	5.69E-39	1.27	3.19E-05	1.79	1.02E-27
MESDC1	1.35	2.83E-10	1.50	1.01E-20	1.34	5.34E-05	1.49	1.26E-08
GATA4	1.35	1.33E-34	1.47	6.76E-66	1.45	1.99E-39	1.61	3.55E-66
S100A10	1.34	3.43E-08	1.69	1.45E-28	1.29	7.25E-06	1.61	1.91E-18
ZNF516	1.33	2.91E-11	1.42	1.45E-18	1.37	5.79E-07	1.25	5.89E-04
CD44	1.33	4.90E-06	1.81	2.51E-27	1.43	2.40E-05	1.42	3.70E-05
PDGFRB	1.33	2.61E-07	1.44	6.25E-13	1.47	3.62E-08	1.58	1.83E-11
HNRNPA0	1.31	2.86E-35	1.32	4.46E-42	1.29	3.10E-09	1.42	1.16E-16
H1FX	1.31	1.53E-04	1.47	1.93E-09	1.90	3.11E-14	1.92	1.23E-14
LMNA	1.30	6.42E-09	1.92	2.25E-64	1.46	3.12E-08	2.62	9.94E-59
TNS3	1.29	7.01E-06	1.67	5.45E-25	1.29	3.80E-04	1.35	2.89E-05
CYR61	1.27	6.22E-05	1.97	2.72E-41	1.33	1.52E-05	1.54	5.38E-12
HIST1H2AB	1.27	5.52E-20	1.44	2.96E-110	1.50	2.16E-51	1.98	7.74E-196
NDRG2	1.27	1.26E-07	1.27	1.82E-08	1.27	6.01E-04	1.35	1.10E-05
GLIPR2	1.26	2.60E-06	1.98	7.90E-62	1.28	1.56E-06	1.78	7.07E-34

APPENDIX C

CHICK GO ANALYSIS OF HH18 CHICK GENES WITH >2-FOLD HIGHER EXPRESSION IN AVC AND OFT COMPARED TO VEN

GO Term	p-value	Genes
GO:0007507~heart development	2.90E-05	MSX2, BMP2, TBX2, SCUBE1, FBN1, TBX20, ZFPM2, SOX6, SOX9, NRG1, COL11A1, TGFB2
GO:0007167~enzyme linked receptor protein signaling pathway	1.19E-04	BMP2, SMAD9, FUT8, ADORA2A, CD3E, ADCYAP1R1, IGF2, TGFB2, MSX2, EPHA4, SORBS1, ANGPTL1, NRG1, SYK
GO:0032989~cellular component morphogenesis	1.43E-04	BMP2, ADORA2A, MAP1B, MYOZ1, SOX6, SOX9, SLIT1, TGFB2, CD9, EPHA4, SLTRK4, ROBO1, CNTN2, RELN, CNTN4
GO:0009891~positive regulation of biosynthetic process	2.68E-04	BMP2, SMAD9, ADORA2A, CD3E, TBX20, IGF2, FOXO3, SOX6, SOX9, ABCG4, PPARGC1A, CITED4, SOX8, WT1, TGFB2, TCF21, SORBS1, ZFPM2, PTX3, SYK
GO:0007155~cell adhesion	2.93E-04	CTNNAL1, CADM1, COL22A1, NEDD9, PCDH15, NID1, PCDH17, SOX9, CD9, LAMA4, SORBS1, ROBO1, COL27A1, CNTN2, RELN, CNTN4, COL24A1, COL11A1, COL20A1, SYK
GO:0022610~biological adhesion	2.99E-04	CTNNAL1, CADM1, COL22A1, NEDD9, PCDH15, NID1, PCDH17, SOX9, CD9, LAMA4, SORBS1, ROBO1, COL27A1, CNTN2, RELN, CNTN4, COL24A1, COL11A1, COL20A1, SYK
GO:0000904~cell morphogenesis involved in differentiation	4.11E-04	EPHA4, SLTRK4, BMP2, ROBO1, MAP1B, CNTN2, CNTN4, RELN, SOX9, SLIT1, TGFB2
GO:0007517~muscle organ development	6.01E-04	TBX2, CACNA1H, CHODL, ZFPM2, SOX6, NRG1, CSRP2, COL11A1, IGFBP5, TGFB2
GO:0000902~cell morphogenesis	6.47E-04	BMP2, ADORA2A, MAP1B, SOX6, SOX9, SLIT1, TGFB2, EPHA4, SLTRK4, ROBO1, CNTN2, RELN, CNTN4
GO:0001501~skeletal system development	9.03E-04	MSX2, BMP2, LECT1, FBN1, IGF2, SOX6, SOX9, COL11A1, BMP5, PRELP, IGFBP5, ANXA2

APPENDIX D

MOUSE GO ANALYSIS OF E11.0 MOUSE GENES WITH >2-FOLD HIGHER EXPRESSION IN AVC AND OFT COMPARED TO VEN

GO Term	p-value	Genes
GO:0001501~skeletal system development	5.20E-07	PRRX1, POSTN, COL2A1, SOX9, FRZB, MSX2, COL9A1, INHBA, MSX1, PDGFRA, PAPSS2, TWIST1, BMP6
GO:0007155~cell adhesion	9.26E-07	CLSTN2, ADAM23, TNC, IGFBP7, ITGB5, POSTN, COL2A1, EDIL3, SOX9, TPBG, PCDHAC2, NCAM1, COL9A1, COL6A3, ROBO2, MFAP4, THBS1, BOC
GO:0022610~biological adhesion	9.45E-07	CLSTN2, ADAM23, TNC, IGFBP7, ITGB5, POSTN, COL2A1, EDIL3, SOX9, TPBG, PCDHAC2, NCAM1, COL9A1, COL6A3, ROBO2, MFAP4, THBS1, BOC
GO:0042127~regulation of cell proliferation	1.94E-05	RARG, TBX2, ERBB3, IGFBP7, PRRX1, SOX9, ADA, TGFB2, FOXP2, MSX2, WNT2, MSX1, ADAMTS8, SERPINE1, PDGFRA, NGFR, THBS1
GO:0030510~regulation of BMP signaling pathway	3.20E-05	BMPER, HTRA1, SMAD6, PCSK6
GO:0007507~heart development	5.07E-05	MSX2, MSX1, TBX2, ERBB3, PDLIM3, NFATC4, COL2A1, SOX9, TGFB2
GO:0009968~negative regulation of signal transduction	6.15E-05	BMPER, ERBB3, HTRA1, SMAD6, CYP26B1, NGFR, FRZB, THBS1, ADA
GO:0009611~response to wounding	8.84E-05	ERBB3, TNC, CHST3, EPHA3, TGFB2, C1QB, SERPINE1, PDGFRA, NFATC4, NGFR, THBS1, PAPSS2, BMP6
GO:0051216~cartilage development	8.90E-05	COL9A1, MSX1, PRRX1, COL2A1, SOX9, BMP6
GO:0022404~molting cycle process	1.23E-04	FST, NGFR, SOX9, SNAI1, TGFB2
GO:0042303~molting cycle	1.36E-04	FST, NGFR, SOX9, SNAI1, TGFB2
GO:0010648~negative regulation of cell communication	1.37E-04	BMPER, ERBB3, HTRA1, SMAD6, CYP26B1, NGFR, FRZB, THBS1, ADA
GO:0030509~BMP signaling pathway	1.48E-04	MSX2, MSX1, SMAD6, FST, BMP6
GO:0048545~response to steroid hormone stimulus	1.74E-04	WNT2, C1QB, IGFBP7, GATA3, PDGFRA, AQP1, THBS1, TGFB2
GO:0035113~embryonic appendage morphogenesis	1.92E-04	MSX2, MSX1, RARG, CYP26B1, PRRX1, TWIST1
GO:0030326~embryonic limb morphogenesis	1.92E-04	MSX2, MSX1, RARG, CYP26B1, PRRX1, TWIST1
GO:0051094~positive regulation of developmental process	2.99E-04	INHBA, FST, ROBO2, NGFR, THBS1, BOC, ADA, BMP6, TGFB2

Appendix D: Continued

GO:0007517~muscle organ development	3.09E-04	MSX1, TBX2, ERBB3, TNC, COL6A3, ELN, FOXP2, TGFB2
GO:0043066~negative regulation of apoptosis	3.10E-04	MSX2, MSX1, ERBB3, EEF1A2, SMAD6, COL2A1, NGFR, PCSK6, THBS1, ADA
GO:0045682~regulation of epidermis development	3.15E-04	INHBA, FST, NGFR, TGFB2
GO:0043069~negative regulation of programmed cell death	3.44E-04	MSX2, MSX1, ERBB3, EEF1A2, SMAD6, COL2A1, NGFR, PCSK6, THBS1, ADA
GO:0042981~regulation of apoptosis	3.50E-04	RARG, ERBB3, SMAD6, EEF1A2, COL2A1, SOX9, ADA, TGFB2, MSX2, INHBA, MSX1, NGFR, THBS1, PCSK6, PHLDA1
GO:0060548~negative regulation of cell death	3.51E-04	MSX2, MSX1, ERBB3, EEF1A2, SMAD6, COL2A1, NGFR, PCSK6, THBS1, ADA
GO:0043067~regulation of programmed cell death	3.87E-04	RARG, ERBB3, SMAD6, EEF1A2, COL2A1, SOX9, ADA, TGFB2, MSX2, INHBA, MSX1, NGFR, THBS1, PCSK6, PHLDA1
GO:0010941~regulation of cell death	4.02E-04	RARG, ERBB3, SMAD6, EEF1A2, COL2A1, SOX9, ADA, TGFB2, MSX2, INHBA, MSX1, NGFR, THBS1, PCSK6, PHLDA1
GO:0007178~transmembrane receptor protein serine/threonine kinase signaling pathway	4.21E-04	MSX2, MSX1, SMAD6, FST, BMP6, TGFB2
GO:0030198~extracellular matrix organization	4.40E-04	LUM, ELN, PDGFRA, POSTN, COL2A1, TGFB2
GO:0048730~epidermis morphogenesis	4.65E-04	FST, NGFR, SNAI1, TGFB2
GO:0043062~extracellular structure organization	4.90E-04	TNC, LUM, ELN, PDGFRA, POSTN, COL2A1, TGFB2
GO:0014706~striated muscle tissue development	8.14E-04	TBX2, ERBB3, TNC, ELN, FOXP2, TGFB2

APPENDIX E

GENES >2-FOLD DYSREGULATED BETWEEN *TGFBR3^{+/+}* AND *TGFBR3^{-/-}* EPICARDIAL CELLS AFTER VEH INCUBATION

Gene Symbol	n=1		n=2	
	Fold Change (<i>Tgfbr3^{-/-}</i> / <i>Tgfbr3^{+/+}</i>)	p-value	Fold Change (<i>Tgfbr3^{-/-}</i> / <i>Tgfbr3^{+/+}</i>)	p-value
XIST	999.00	0.00E+00	4515.39	0.00E+00
1700125H03Rik	999.00	7.82E-06	999.00	9.82E-05
9030619P08Rik	999.00	2.69E-15	999.00	2.55E-24
RIMS2	999.00	7.67E-47	999.00	3.65E-41
Rprl2	999.00	1.17E-57	999.00	2.66E-06
Rprl3	999.00	5.16E-132	999.00	1.06E-15
TSIX	999.00	0.00E+00	999.00	0.00E+00
ALX4	999.00	5.76E-64	142.05	5.65E-73
Ly6a	999.00	4.68E-22	111.30	6.43E-29
ITIH5	999.00	9.82E-07	14.65	7.40E-04
Gm8378	999.00	2.77E-06	6.83	5.19E-04
CTNND2	102.98	2.38E-48	26.85	1.64E-18
ANGPTL4	84.10	7.52E-134	9.08	1.39E-22
CPNE7	70.17	1.89E-32	999.00	3.98E-05
FZD10	45.56	1.22E-20	27.83	3.77E-07
PPP1R16B	43.01	1.22E-46	17.99	4.71E-26
BAI1	35.69	4.14E-89	9.37	3.50E-16
FGF10	35.54	6.95E-16	21.97	7.73E-15
DSP	33.87	5.77E-84	23.43	1.00E-25
PVRL4	32.08	9.93E-34	6.96	5.96E-09
NFATC2	30.98	3.14E-26	4.94	1.24E-05
FAM134B	29.16	6.89E-13	14.65	1.93E-09
DSCAML1	28.86	1.11E-35	68.83	9.30E-18
KCNK1	25.52	3.72E-06	17.57	1.41E-04
TACSTD2	25.52	3.72E-06	7.81	1.18E-04
BCAT1	23.97	7.10E-184	30.98	1.02E-217
ANKRD1	23.87	0.00E+00	5.62	1.57E-126
PPP2R2C	23.51	3.93E-46	6.10	6.11E-06
LIMCH1	22.61	0.00E+00	7.22	7.21E-98
SH2D4A	21.48	4.52E-169	5.83	1.29E-87
Usp44	19.44	5.43E-12	10.98	1.88E-12

Appendix E: Continued

Gene Symbol	n=1		n=2	
	Fold Change (<i>Tgfbr3</i> ^{-/-} / <i>Tgfbr3</i> ^{+/+})	p-value	Fold Change (<i>Tgfbr3</i> ^{-/-} / <i>Tgfbr3</i> ^{+/+})	p-value
FLT1	17.92	1.27E-20	3.09	3.98E-05
RYR3	17.73	3.89E-36	20.50	6.41E-18
PLD5	17.42	3.33E-29	60.78	3.27E-30
Pbp2	17.13	1.60E-16	7.69	3.23E-10
CSGALNACT1	16.58	1.16E-214	17.78	2.86E-274
IL6	15.49	1.30E-06	11.42	4.23E-11
ST14	15.49	2.91E-165	7.32	3.53E-37
KCNC3	15.37	8.61E-62	7.20	2.15E-13
LMO7	15.37	2.24E-278	9.44	4.89E-262
GRM8	15.04	1.30E-11	5.57	1.37E-04
GALNTL4	14.65	6.12E-68	9.90	2.92E-41
AASS	14.58	1.02E-08	3.05	9.66E-04
GNA15	14.19	1.37E-34	3.99	7.38E-08
HMHA1	14.08	3.17E-69	6.85	5.36E-30
B4GALNT2	13.81	1.36E-76	18.89	3.92E-184
RIPK4	13.77	6.16E-22	4.69	3.10E-06
CASQ2	13.67	8.38E-06	999.00	1.62E-05
CUBN	13.67	8.38E-06	4.88	1.89E-04
RBM20	13.65	7.80E-89	7.85	1.15E-45
NFATC1	13.47	3.47E-41	6.02	6.18E-15
WNT3	13.46	3.76E-30	5.02	4.03E-09
RNF152	13.37	6.48E-08	4.39	6.99E-04
CTSC	13.12	4.36E-12	999.00	1.91E-18
IRF6	12.99	2.73E-18	20.50	2.64E-05
CGREF1	12.89	1.29E-57	5.49	7.18E-17
CKMT1A/CKMT1B	12.76	5.17E-22	11.72	2.12E-09
SYCE1	12.76	5.17E-22	6.65	7.28E-13
NKX2-8	12.69	1.77E-58	8.37	1.06E-27
PARM1	12.53	3.80E-127	8.46	3.93E-52
LRRC3	12.10	1.69E-22	4.03	3.07E-04
LHX5	11.85	5.28E-05	8.79	6.61E-04
MAB21L2	11.85	1.75E-27	8.42	1.65E-11
Xlr3c	11.43	6.14E-21	10.49	1.33E-44
LTBP1	11.40	3.07E-145	5.36	3.93E-85
PPL	11.32	2.14E-140	5.41	1.45E-52
PTPRB	11.24	8.38E-12	4.88	1.89E-04
SPOCK2	11.10	4.70E-59	12.27	1.72E-63
P2RX7	11.08	2.95E-126	3.53	1.17E-28

Appendix E: Continued

Gene Symbol	n=1		n=2	
	Fold Change (<i>Tgfb3</i> ^{-/-} / <i>Tgfb3</i> ^{+/+})	p-value	Fold Change (<i>Tgfb3</i> ^{-/-} / <i>Tgfb3</i> ^{+/+})	p-value
Klra18	10.94	2.47E-06	20.99	4.14E-14
5930403L14Rik	10.94	1.31E-04	12.45	4.32E-10
BC067074	10.94	9.06E-15	7.81	3.85E-08
ANK2	10.94	4.29E-13	3.73	8.68E-05
ATG9B	10.78	9.69E-188	4.13	1.78E-46
SP9	10.68	1.93E-46	5.27	2.21E-07
MATN4	10.61	5.18E-73	3.05	6.61E-09
Klra4	10.33	6.05E-06	20.50	9.56E-14
PDK4	10.21	3.93E-24	3.45	6.75E-06
HS3ST6	10.17	5.22E-30	8.54	4.10E-09
SLC37A2	9.78	2.26E-55	2.49	5.03E-05
SERPINE2	9.73	0.00E+00	5.49	3.55E-121
ODZ4	9.46	5.92E-65	6.41	4.12E-32
MMP15	9.39	1.85E-255	3.51	3.18E-44
NDUFA4L2	9.23	4.13E-21	9.00	3.93E-11
MS4A10	9.11	2.67E-46	15.93	8.98E-77
RAB39B	9.11	1.67E-06	13.67	9.74E-09
GAL3ST2	9.11	2.01E-10	6.56	1.65E-19
NT5E	8.91	1.22E-12	10.67	3.11E-26
ANXA8L2	8.91	1.01E-317	6.16	9.29E-175
CA12	8.83	2.93E-72	5.76	5.98E-41
REM1	8.63	3.00E-19	2.76	1.57E-16
PEX5L	8.40	2.65E-59	5.40	4.14E-25
Ces2f	8.39	1.39E-44	4.06	9.14E-18
PCOLCE2	8.20	9.44E-06	6.07	1.12E-06
COL18A1	7.99	0.00E+00	3.18	6.09E-176
GRHL3	7.97	5.07E-58	5.47	1.43E-20
NPR2	7.96	8.55E-186	7.43	1.06E-83
FAM159B	7.75	2.21E-05	10.25	4.89E-08
NALCN	7.75	2.21E-05	8.49	9.55E-08
RASGRP3	7.66	4.76E-36	4.25	1.26E-17
DAPK2	7.63	4.94E-28	4.09	5.01E-18
CTHRC1	7.62	2.01E-50	12.23	7.56E-74
VAX2	7.59	2.86E-07	5.57	1.37E-04
ZNF750	7.38	3.39E-20	3.24	1.33E-04
Fhod3	7.31	6.79E-114	2.98	6.02E-24
TLR5	7.29	8.89E-09	8.91	6.84E-18
COL15A1	7.29	5.15E-05	8.79	6.61E-04
COLQ	7.29	1.04E-09	4.03	3.07E-04
FAM65B	7.29	7.62E-08	3.45	4.31E-05

Appendix E: Continued

Gene Symbol	n=1		n=2	
	Fold Change (<i>Tgfb3</i> ^{-/-} / <i>Tgfb3</i> ^{+/+})	p-value	Fold Change (<i>Tgfb3</i> ^{-/-} / <i>Tgfb3</i> ^{+/+})	p-value
B230344G16Rik	7.29	6.06E-50	2.21	1.12E-06
APOL2	7.20	1.75E-19	4.39	2.46E-04
WISP1	7.18	1.92E-229	7.93	8.93E-312
FAM26E	7.13	3.33E-11	2.50	1.15E-04
NIPAL4	7.06	2.14E-29	3.00	1.83E-05
NKX2-3	6.99	1.51E-06	3.11	1.73E-06
Mei4	6.93	1.33E-05	5.95	3.37E-13
Cbr2	6.93	1.33E-05	3.60	1.57E-04
PERP	6.90	0.00E+00	4.85	1.83E-166
MAP2	6.90	9.83E-52	6.14	4.09E-46
WASF3	6.88	6.63E-20	5.49	1.02E-11
TMEM117	6.79	1.70E-10	6.96	9.11E-13
D730039F16Rik	6.75	1.99E-23	9.15	2.97E-24
ESR1	6.68	3.43E-06	6.87	1.75E-13
INHBA	6.59	3.74E-107	3.06	4.05E-30
FAXC	6.56	3.91E-13	7.54	7.59E-23
COL5A3	6.52	3.74E-32	3.10	2.77E-10
PAK6	6.46	9.32E-35	3.31	6.28E-10
C1orf106	6.38	2.32E-07	4.21	1.64E-04
MMRN1	6.38	2.32E-07	2.93	5.42E-06
CRABP2	6.28	7.02E-42	18.58	2.37E-129
CYFIP2	6.24	4.23E-25	5.58	5.18E-12
FGF21	6.23	1.27E-23	6.22	9.60E-34
CORO2A	6.21	3.26E-48	3.01	1.46E-15
ZDHHC2	6.20	6.79E-05	999.00	1.62E-05
LIN28B	6.20	1.60E-08	9.41	8.57E-12
SOGA2	6.18	3.68E-14	2.93	4.32E-04
KLRG2	5.95	6.59E-49	5.49	1.15E-29
Apol10a	5.94	3.12E-42	2.74	7.02E-20
PIANP	5.93	1.37E-37	8.45	1.50E-93
VNN1	5.93	2.55E-183	3.73	2.68E-96
GDF15	5.91	1.09E-36	2.12	1.84E-05
FGF18	5.86	1.16E-40	3.25	2.71E-18
P2RX3	5.83	5.63E-91	9.56	6.17E-62
ROBO3	5.82	1.13E-92	2.97	4.37E-39
A730035I17Rik	5.81	1.18E-11	16.11	1.66E-10
COL4A3	5.80	2.02E-08	2.70	3.40E-04
KCNJ4	5.79	1.46E-40	3.61	5.06E-09
IL17RE	5.77	1.32E-31	9.75	1.42E-74
KIAA1467	5.77	2.37E-20	3.91	1.21E-08

Appendix E: Continued

Gene Symbol	n=1		n=2	
	Fold Change (<i>Tgfb3</i> ^{-/-} / <i>Tgfb3</i> ^{+/+})	p-value	Fold Change (<i>Tgfb3</i> ^{-/-} / <i>Tgfb3</i> ^{+/+})	p-value
ANKS1B	5.77	2.27E-66	4.49	5.58E-43
STRA6	5.62	1.15E-08	4.52	7.70E-07
STOX2	5.56	3.40E-46	3.55	1.06E-18
ADRB2	5.54	1.38E-15	4.39	1.45E-06
SNAI3	5.42	3.17E-21	3.85	1.84E-10
PRDM6	5.34	3.56E-49	3.75	3.60E-40
FRAS1	5.32	1.84E-123	4.87	8.57E-96
VSTM5	5.30	2.03E-07	2.75	3.81E-05
CTH	5.27	8.61E-36	3.58	1.29E-28
CUX2	5.27	3.77E-11	2.81	2.31E-05
AVIL	5.26	2.01E-15	2.79	1.84E-06
NOTCH3	5.21	0.00E+00	2.20	2.01E-35
SLC7A5	5.17	0.00E+00	3.09	9.36E-248
ITGB4	5.17	2.52E-313	2.90	5.58E-108
ELL3	5.16	1.13E-07	2.60	2.42E-04
MOXD1	5.14	1.16E-24	3.29	2.71E-10
CCND1	5.12	0.00E+00	2.97	0.00E+00
PLCXD2	5.07	8.25E-70	2.09	7.88E-15
PTPRVP	5.01	7.12E-196	3.33	3.99E-55
KRT8	4.99	5.18E-39	4.15	1.97E-20
FAM132B	4.99	1.06E-121	3.55	8.51E-54
MAMDC2	4.93	1.33E-09	8.22	2.33E-23
KRT18	4.93	9.40E-18	4.49	3.71E-08
SLC7A3	4.91	1.08E-49	4.38	6.89E-54
MREG	4.91	3.21E-55	2.47	1.19E-15
GJB3	4.91	1.31E-07	2.78	1.33E-04
KCNT1	4.86	7.33E-10	4.27	2.72E-06
LOC100129924	4.86	1.36E-05	3.02	1.64E-04
FGFBP3	4.84	1.59E-41	3.64	2.91E-19
PID1	4.81	4.63E-37	4.84	1.52E-23
MAP1B	4.79	1.09E-209	2.57	6.15E-55
ST6GALNAC2	4.77	2.74E-07	5.75	1.93E-10
SCUBE3	4.73	1.46E-35	2.58	7.08E-10
ABCG1	4.71	1.42E-22	2.44	3.49E-05
SPACA3	4.69	2.07E-04	7.69	1.02E-05
SNRPN	4.66	2.85E-05	35.15	5.11E-09
ST6GAL1	4.66	3.14E-09	2.56	1.64E-04
TMEM125	4.58	2.63E-15	4.95	5.87E-24
TNFRSF18	4.58	1.35E-101	2.24	1.50E-17
SLC4A4	4.49	2.67E-322	4.04	0.00E+00

Appendix E: Continued

Gene Symbol	n=1		n=2	
	Fold Change (<i>Tgfb3</i> ^{-/-} / <i>Tgfb3</i> ^{+/+})	p-value	Fold Change (<i>Tgfb3</i> ^{-/-} / <i>Tgfb3</i> ^{+/+})	p-value
DGKA	4.48	9.00E-219	2.47	9.25E-55
PLTP	4.48	0.00E+00	2.67	6.96E-155
AIF1L	4.44	3.00E-150	2.00	8.60E-27
EPB41L3	4.43	5.97E-18	7.18	2.84E-21
PRDM8	4.42	3.99E-17	6.80	3.37E-14
ICA1L	4.37	3.15E-05	3.84	5.68E-04
SEC16B	4.34	4.97E-29	3.73	2.87E-24
AMN	4.31	1.14E-09	4.66	1.12E-06
PROS1	4.27	4.79E-44	3.29	1.57E-27
Ces2e	4.25	0.00E+00	2.80	5.10E-187
COL8A1	4.24	0.00E+00	2.14	0.00E+00
Nppb	4.23	1.83E-10	3.95	3.90E-23
SP6	4.20	3.16E-20	2.13	6.17E-05
RFTN2	4.17	2.58E-06	2.56	5.81E-04
MFAP5	4.15	1.07E-07	10.54	7.46E-19
ABLIM1	4.14	3.41E-05	2.63	5.37E-106
CHD5	4.12	2.21E-30	2.08	7.49E-07
CD109	4.09	3.40E-118	2.98	1.05E-142
FAM196A	4.07	1.43E-45	2.60	1.52E-12
Abcb1b	4.05	1.40E-119	2.09	4.22E-37
SSC5D	3.98	8.07E-28	2.45	5.89E-11
SHANK2	3.96	8.53E-40	2.96	3.95E-17
ITGA6	3.96	2.02E-54	3.08	3.87E-23
LRP2	3.95	0.00E+00	2.10	2.47E-95
SVOP	3.94	6.40E-55	3.40	8.98E-36
PSAT1	3.90	0.00E+00	2.11	1.65E-85
LTK	3.88	1.88E-08	3.20	8.72E-04
PGF	3.87	9.37E-04	6.15	3.37E-05
P2RY6	3.87	4.61E-21	2.74	1.60E-07
LTB4R	3.82	1.47E-75	3.35	2.44E-53
MAP7D2	3.79	3.78E-05	5.86	3.82E-04
KLK10	3.79	3.78E-05	5.13	9.65E-05
CD44	3.78	1.83E-138	2.03	7.48E-57
C9orf116	3.76	2.25E-84	2.86	2.69E-68
STON2	3.72	4.16E-37	3.48	1.27E-31
ACPP	3.72	1.10E-08	2.69	9.35E-07
Tnfrsf26	3.71	1.01E-34	5.88	4.61E-122
IGSF9B	3.70	3.09E-192	2.01	8.59E-29
HLA-DRB1	3.70	0.00E+00	2.65	1.58E-235
ARHGAP24	3.68	5.77E-17	3.66	1.74E-10

Appendix E: Continued

Gene Symbol	n=1		n=2	
	Fold Change (<i>Tgfb3</i> ^{-/-} / <i>Tgfb3</i> ^{+/+})	p-value	Fold Change (<i>Tgfb3</i> ^{-/-} / <i>Tgfb3</i> ^{+/+})	p-value
SNURF	3.65	2.65E-04	11.23	5.29E-07
COL11A1	3.65	1.30E-33	7.69	1.02E-05
BGLAP	3.65	1.40E-04	3.91	1.72E-05
KRT80	3.65	5.05E-04	3.84	5.68E-04
FGF5	3.65	8.03E-11	3.80	3.31E-22
5830418P13Rik	3.65	5.46E-22	3.66	1.03E-17
CELF5	3.64	2.98E-108	4.06	1.67E-69
EXTL1	3.61	5.14E-14	2.63	6.76E-07
PPFIBP2	3.60	5.99E-13	3.52	9.77E-12
PLEK2	3.60	5.75E-22	2.07	4.99E-07
EPHA1	3.54	1.28E-110	2.45	2.30E-48
COX6A2	3.53	3.42E-09	4.45	4.26E-23
REEP2	3.53	1.19E-51	2.79	9.65E-29
ANGPTL2	3.51	5.80E-48	2.20	3.84E-13
CPE	3.50	9.66E-310	3.85	1.92E-189
LRRK2	3.50	1.42E-07	2.84	2.99E-04
SAMD12	3.49	4.93E-07	2.21	2.74E-05
CNKS2R2	3.46	9.80E-04	9.76	5.54E-06
BFSP2	3.46	8.64E-11	4.74	7.14E-12
NEURL	3.45	1.60E-10	2.45	3.94E-07
F2R	3.44	2.75E-287	2.34	4.47E-149
LTB4R2	3.37	1.06E-117	3.57	4.46E-87
E430014L09Rik	3.37	3.00E-10	3.25	4.65E-10
SLC2A3	3.35	1.15E-76	2.53	1.10E-60
PRRG4	3.33	3.35E-33	2.73	1.01E-34
1700003M07Rik	3.33	1.39E-11	2.42	1.67E-08
ARHGAP8	3.31	3.08E-14	2.37	1.03E-10
Fndc3c1	3.28	1.42E-04	3.53	3.82E-06
PITPNM1	3.25	3.26E-33	3.00	6.21E-25
SULF2	3.24	0.00E+00	2.07	0.00E+00
CEND1	3.23	6.00E-06	5.37	7.83E-09
UGT1A3	3.22	9.41E-112	3.13	1.84E-145
PVRL1	3.22	6.91E-42	2.32	1.29E-16
SYN2	3.22	7.47E-05	4.52	7.70E-07
UGT1A4	3.21	1.00E-110	3.12	1.80E-144
UGT1A1	3.21	9.94E-111	3.14	2.30E-146
UGT1A9	3.20	3.26E-110	3.13	5.19E-145
DPP6	3.20	3.60E-53	2.31	1.22E-18
PCSK6	3.18	0.00E+00	2.22	2.86E-216
FAM115C	3.18	1.46E-34	2.06	3.18E-18

Appendix E: Continued

Gene Symbol	n=1		n=2	
	Fold Change (<i>Tgfb3</i> ^{-/-} / <i>Tgfb3</i> ^{+/+})	p-value	Fold Change (<i>Tgfb3</i> ^{-/-} / <i>Tgfb3</i> ^{+/+})	p-value
HMCN2	3.18	6.57E-17	2.08	5.48E-06
EVPL	3.15	1.65E-48	2.12	5.96E-12
PRKAA2	3.14	1.88E-17	2.32	1.21E-09
UGT1A6	3.13	3.27E-117	3.14	3.83E-179
TEX15	3.10	4.71E-07	3.42	7.01E-07
NETO1	3.08	1.24E-24	3.71	5.04E-36
ENG	3.08	6.51E-30	2.39	2.20E-16
WNT9A	3.07	6.66E-235	3.01	9.03E-193
ADM2	3.07	2.29E-15	3.10	1.42E-28
SH3YL1	3.07	6.67E-12	2.44	1.34E-06
GPX3	3.07	1.70E-17	2.81	9.15E-08
SLC17A9	3.05	6.51E-12	3.33	4.63E-13
SYTL1	3.04	2.24E-57	2.66	3.42E-33
BMPR1B	3.04	3.75E-05	5.77	1.33E-12
Ugt1a7c	3.02	6.44E-127	3.53	5.98E-256
STC2	3.01	1.80E-12	2.78	2.00E-14
B230206H07Rik	3.00	7.29E-11	2.39	1.25E-04
NHSL2	2.99	2.72E-21	2.20	1.64E-16
DCLK3	2.98	7.08E-11	3.83	1.13E-11
CYP1B1	2.98	4.39E-129	2.66	1.48E-190
SLC9A9	2.95	4.21E-07	2.16	3.12E-04
GRIA4	2.95	2.43E-78	2.11	3.19E-61
SNTG1	2.93	3.51E-05	2.70	3.98E-07
CDH26	2.92	4.16E-10	3.20	2.43E-11
RPRM	2.90	1.49E-72	3.04	2.36E-58
PDGFRL	2.89	3.38E-05	3.47	1.04E-08
FYN	2.86	9.37E-29	2.02	7.42E-12
NOG	2.85	2.08E-89	5.22	8.03E-160
TRIB3	2.85	2.82E-87	4.50	0.00E+00
CAMK4	2.83	8.61E-25	3.04	8.84E-26
PCDH19	2.83	1.03E-56	2.64	1.29E-64
GLCE	2.83	2.95E-42	2.79	3.37E-18
Gm11149	2.80	9.44E-30	2.11	2.93E-10
PMEPA1	2.79	5.74E-180	2.73	1.13E-140
POU3F1	2.79	3.19E-19	2.57	3.81E-24
BMP3	2.78	6.45E-65	3.56	7.44E-127
BHLHA15	2.76	1.14E-06	3.04	8.07E-07
CRISPLD2	2.75	5.89E-15	3.52	5.55E-22
APOL6	2.73	3.94E-04	5.19	8.11E-08
NRN1	2.73	5.42E-05	2.38	2.64E-08

Appendix E: Continued

Gene Symbol	n=1		n=2	
	Fold Change (<i>Tgfb3</i> ^{-/-} / <i>Tgfb3</i> ^{+/+})	p-value	Fold Change (<i>Tgfb3</i> ^{-/-} / <i>Tgfb3</i> ^{+/+})	p-value
MGLL	2.72	1.51E-144	2.65	8.27E-234
NUPR1	2.72	7.62E-101	2.87	5.61E-179
WNT11	2.70	8.49E-69	2.21	6.15E-41
LRP4	2.69	3.73E-04	3.10	6.17E-05
GPC4	2.69	7.87E-123	2.68	2.03E-33
BST1	2.66	9.38E-05	2.90	2.89E-18
FBLN5	2.66	0.00E+00	2.83	0.00E+00
9530053A07Rik	2.66	2.81E-11	2.56	2.49E-09
SERPINA3	2.63	3.34E-19	2.76	4.95E-14
DUSP8	2.63	2.64E-22	2.13	3.84E-14
THPO	2.62	1.71E-04	2.70	3.40E-04
CDKL2	2.62	1.14E-09	2.98	3.96E-24
MMP2	2.61	0.00E+00	2.53	0.00E+00
LHFPL2	2.61	1.19E-22	2.01	1.34E-14
SRPX	2.61	5.04E-88	3.51	1.29E-282
FOXC2	2.59	4.98E-08	2.15	1.70E-06
C15orf59	2.58	4.71E-14	2.12	2.83E-11
ANO3	2.58	9.42E-33	3.85	3.64E-99
ITGB5	2.57	2.01E-108	2.32	5.97E-72
KIF21B	2.56	1.15E-08	2.38	2.45E-09
MDM2	2.55	0.00E+00	2.13	0.00E+00
GATSL3	2.54	4.63E-15	2.22	8.83E-11
FAM129A	2.54	1.81E-104	2.61	9.73E-154
ACOT2	2.54	1.01E-37	3.27	9.34E-147
SLIT2	2.53	0.00E+00	2.16	8.30E-237
CTSH	2.53	8.70E-11	2.73	1.83E-27
MEIS3	2.52	1.80E-08	4.50	8.54E-21
COL12A1	2.51	0.00E+00	2.58	3.50E-273
Pmaip1	2.50	1.05E-91	2.22	2.38E-133
VAT1L	2.50	1.18E-21	2.12	5.96E-12
AXIN2	2.50	2.01E-32	2.58	7.07E-48
TMOD2	2.49	1.53E-05	3.62	7.67E-11
CCND2	2.49	0.00E+00	3.02	0.00E+00
KIF26B	2.49	1.67E-30	2.74	5.03E-34
SIGLEC10	2.48	1.56E-11	3.52	9.32E-23
FAM212B	2.45	2.30E-93	2.36	6.85E-77
NPAS3	2.43	2.00E-32	2.21	1.34E-35
CNTN2	2.42	2.30E-28	2.15	3.68E-16
LRRTM1	2.41	2.39E-10	4.20	9.46E-34
COL4A6	2.39	0.00E+00	2.09	0.00E+00

Appendix E: Continued

Gene Symbol	n=1		n=2	
	Fold Change (<i>Tgfb3</i> ^{-/-} / <i>Tgfb3</i> ^{+/+})	p-value	Fold Change (<i>Tgfb3</i> ^{-/-} / <i>Tgfb3</i> ^{+/+})	p-value
Peg12	2.39	1.90E-05	3.08	1.90E-13
Trim12a	2.38	1.45E-25	2.00	2.53E-29
FGF9	2.38	2.08E-06	3.20	8.97E-15
ALDH1L2	2.38	1.38E-71	3.40	7.50E-238
WNT2B	2.34	2.84E-14	3.27	9.45E-26
GPC1	2.31	1.35E-11	2.85	1.52E-14
GARS	2.31	0.00E+00	2.04	1.42E-268
NELL2	2.29	1.82E-71	2.05	1.49E-38
FBXW7	2.29	1.07E-35	2.03	9.63E-35
LIF	2.28	4.78E-55	2.01	1.16E-35
GPR126	2.27	4.94E-18	2.10	7.33E-19
DHRS9	2.26	7.68E-16	2.60	5.58E-38
GLDC	2.24	1.20E-14	2.45	7.94E-12
SEMA3C	2.22	5.81E-107	2.59	0.00E+00
SEMA3B	2.21	3.12E-17	2.08	1.62E-15
Rasl2-9	2.21	3.84E-10	2.30	2.77E-09
LRFN3	2.20	2.04E-05	2.48	1.76E-04
PAPPA2	2.19	3.79E-23	3.62	1.46E-87
FAM131B	2.19	4.13E-05	2.78	2.84E-06
C11orf88	2.18	2.77E-06	2.09	1.38E-09
TMEM37	2.17	4.74E-09	2.95	4.74E-30
DLX2	2.16	2.94E-05	2.64	3.93E-13
RUNX1T1	2.15	2.42E-09	3.58	2.76E-47
SERPINF1	2.12	6.84E-32	3.61	2.62E-95
C13orf33	2.12	4.11E-12	3.33	9.79E-76
AKR1B1	2.12	1.41E-64	2.06	3.22E-63
Gm6644	2.11	2.14E-64	2.06	3.22E-63
MORN4	2.07	1.31E-04	2.87	1.83E-09
TTC9	2.03	7.43E-13	3.01	9.98E-41
IL15	2.02	5.31E-04	2.76	2.43E-11
NCAM1	2.02	1.81E-156	2.24	3.66E-264
Bmyc	2.02	1.06E-21	3.37	7.67E-67
PLXDC2	2.01	2.28E-91	2.25	5.58E-193
PDIA5	2.01	6.34E-46	2.42	4.68E-80
ASIC1	-2.00	6.60E-22	-2.40	1.63E-21
BC026600	-2.00	9.28E-17	-3.61	1.59E-19
HSPB7	-2.01	2.54E-26	-3.58	2.32E-25
ZNF845	-2.01	8.35E-05	-3.57	1.68E-04
PCDHA1	-2.01	6.66E-05	-3.76	3.18E-07
PCDHA3	-2.01	6.66E-05	-3.76	3.18E-07

Appendix E: Continued

Gene Symbol	n=1		n=2	
	Fold Change (<i>Tgfb3</i> ^{-/-} / <i>Tgfb3</i> ^{+/+})	p-value	Fold Change (<i>Tgfb3</i> ^{-/-} / <i>Tgfb3</i> ^{+/+})	p-value
PCDHA4	-2.01	6.66E-05	-3.76	3.18E-07
PCDHA5	-2.01	6.66E-05	-3.76	3.18E-07
PCDHA6	-2.01	6.66E-05	-3.76	3.18E-07
PCDHA7	-2.01	6.66E-05	-3.76	3.18E-07
PCDHA9	-2.01	6.66E-05	-3.76	3.18E-07
Pcdha10	-2.01	6.66E-05	-3.76	3.18E-07
PCDHA12	-2.01	6.66E-05	-3.76	3.18E-07
PCDHAC1	-2.01	6.66E-05	-3.76	3.18E-07
FAM84B	-2.02	4.80E-269	-3.06	7.34E-239
BNIP3	-2.02	1.05E-11	-3.58	3.27E-09
NOS1AP	-2.03	3.09E-11	-2.64	2.88E-19
RAB20	-2.03	2.25E-12	-2.32	3.26E-09
2310015A10Rik	-2.03	1.77E-08	-2.45	2.08E-08
CABLES1	-2.03	1.42E-08	-2.77	1.36E-14
PCDHA11	-2.03	5.24E-05	-3.76	3.18E-07
PCDHA13	-2.03	5.24E-05	-3.76	3.18E-07
RASSF4	-2.04	1.43E-17	-2.57	9.66E-13
NKX6-2	-2.04	6.53E-08	-2.61	1.09E-09
CAPN6	-2.05	8.91E-13	-3.54	3.16E-19
ZFP36L2	-2.05	1.61E-131	-2.02	1.56E-71
H3f3a/H3f3b	-2.06	0.00E+00	-2.48	0.00E+00
PM20D2	-2.06	1.33E-12	-4.32	3.95E-28
GMPR	-2.06	1.10E-108	-3.20	5.32E-128
SLC43A3	-2.07	1.06E-168	-2.48	1.24E-164
CD1D	-2.08	3.89E-08	-4.01	3.31E-11
FAM19A2	-2.08	2.85E-07	-7.46	6.43E-16
ALCAM	-2.09	0.00E+00	-3.42	0.00E+00
ST3GAL1	-2.10	9.23E-273	-4.56	1.14E-109
FAM110C	-2.11	4.60E-165	-2.31	1.09E-149
MGAT3	-2.11	3.41E-49	-2.62	7.36E-46
MATN2	-2.14	6.97E-28	-2.29	8.37E-18
1010001N08Rik	-2.14	8.33E-80	-3.03	4.47E-84
ROM1	-2.15	2.80E-09	-2.00	5.67E-06
IFI27L2	-2.18	3.28E-22	-2.37	0.00E+00
BDH1	-2.18	5.06E-09	-3.19	1.13E-14
SMPDL3A	-2.19	3.64E-07	-9.64	4.84E-16
LAMC3	-2.19	2.29E-14	-2.74	2.06E-12
ID2	-2.19	1.13E-271	-2.81	6.07E-168
IGSF3	-2.20	3.18E-96	-2.10	1.27E-41
9930014A18Rik	-2.20	1.02E-156	-3.03	1.39E-135

Appendix E: Continued

Gene Symbol	n=1		n=2	
	Fold Change (<i>Tgfb3</i> ^{-/-} / <i>Tgfb3</i> ^{+/+})	p-value	Fold Change (<i>Tgfb3</i> ^{-/-} / <i>Tgfb3</i> ^{+/+})	p-value
GSTM5	-2.21	2.55E-100	-2.39	5.94E-74
TMEM44	-2.22	2.80E-08	-2.63	1.65E-06
VSTM4	-2.22	1.31E-05	-3.29	1.64E-06
PDGFRA	-2.23	6.44E-268	-2.50	6.67E-108
HEXIM2	-2.24	2.04E-05	-4.72	2.92E-08
IGFBP5	-2.24	5.80E-62	-5.32	3.21E-62
CPQ	-2.26	2.44E-39	-2.24	5.55E-23
Mocs1	-2.26	1.85E-90	-3.28	5.84E-99
IDUA	-2.26	4.75E-13	-2.67	2.78E-11
G630016G05Rik	-2.27	4.11E-04	-3.16	9.98E-07
SPSB1	-2.30	1.87E-112	-2.15	7.22E-57
LGI4	-2.30	2.37E-11	-6.67	2.36E-17
Gm16793	-2.30	1.79E-06	-2.17	1.37E-04
ABCC10	-2.30	2.99E-35	-2.22	2.21E-25
KCNA7	-2.31	1.39E-08	-5.63	2.92E-19
MAOA	-2.32	4.92E-228	-4.10	3.83E-265
PELI3	-2.33	8.72E-06	-2.38	4.46E-06
TLE2	-2.34	1.87E-18	-3.94	6.85E-27
PRRX2	-2.34	4.28E-15	-2.97	3.06E-17
GPSM3	-2.34	1.23E-20	-2.82	6.77E-14
CYP39A1	-2.37	2.86E-14	-2.24	2.10E-07
C1orf226	-2.40	5.85E-32	-2.78	1.84E-29
TMEM176A	-2.40	8.51E-149	-2.04	7.06E-60
CACNA1A	-2.42	1.69E-14	-4.70	3.57E-22
PLS1	-2.43	9.08E-04	-4.50	2.25E-04
FDXR	-2.45	2.77E-54	-2.34	3.73E-33
PTPN18	-2.45	2.77E-09	-2.77	5.25E-06
ME3	-2.46	6.41E-31	-2.36	4.42E-21
CNRIP1	-2.46	1.07E-24	-4.02	2.09E-26
TMEM138	-2.47	3.70E-18	-2.24	3.78E-06
NRGN	-2.52	1.29E-07	-3.17	4.29E-04
TBX20	-2.53	7.72E-197	-2.59	1.66E-126
NDRG2	-2.54	2.80E-27	-2.47	4.99E-18
MYLK	-2.60	0.00E+00	-2.96	1.36E-190
SLC16A2	-2.61	8.07E-08	-4.01	1.97E-06
SAA2	-2.61	4.53E-102	-5.22	3.47E-117
NOVA1	-2.62	3.97E-06	-2.59	5.23E-04
CPXM1	-2.63	7.45E-241	-3.19	2.18E-189
TGM2	-2.65	0.00E+00	-4.23	0.00E+00
CLDN15	-2.65	1.00E-156	-4.64	5.82E-147

Appendix E: Continued

Gene Symbol	n=1		n=2	
	Fold Change (<i>Tgfb3</i> ^{-/-} / <i>Tgfb3</i> ^{+/+})	p-value	Fold Change (<i>Tgfb3</i> ^{-/-} / <i>Tgfb3</i> ^{+/+})	p-value
FMO5	-2.67	7.27E-17	-2.57	8.93E-09
MERTK	-2.69	1.75E-97	-2.01	3.91E-32
FAM84A	-2.74	0.00E+00	-5.59	0.00E+00
LIN7A	-2.74	8.45E-13	-2.49	4.61E-07
HIST1H2AB	-2.75	1.16E-125	-2.74	1.23E-144
ARHGEF3	-2.75	9.28E-17	-2.74	5.26E-08
FMO2	-2.75	1.24E-14	-21.76	4.51E-19
CXCL14	-2.77	1.97E-08	-3.67	2.76E-08
HDDC3	-2.79	2.18E-41	-4.33	2.18E-47
GSTA3	-2.81	4.14E-89	-3.55	4.19E-58
FAM40B	-2.81	2.40E-09	-2.39	5.72E-04
RHOBTB1	-2.85	2.12E-42	-5.01	2.66E-46
HOXB4	-2.85	8.05E-11	-3.45	1.38E-10
EMILIN1	-2.89	1.23E-82	-2.67	1.38E-61
SLFN13	-2.90	2.39E-52	-3.07	2.40E-19
SEPP1	-2.93	1.45E-108	-2.47	6.66E-30
RTN1	-2.96	6.56E-157	-3.78	6.86E-144
DAAM2	-2.98	5.28E-71	-2.27	1.47E-21
A930033H14Rik	-3.03	1.38E-07	-5.71	5.22E-06
SLC2A13	-3.04	5.44E-11	-2.48	1.80E-06
ALDH1A2	-3.07	6.03E-38	-3.05	2.11E-21
FADS6	-3.08	3.36E-31	-3.33	1.86E-23
CPLX2	-3.09	7.16E-77	-2.64	1.40E-29
MDK	-3.09	1.73E-36	-2.73	6.03E-26
ACVR1B	-3.13	3.70E-68	-3.05	1.59E-41
TBC1D10C	-3.17	6.10E-08	-4.31	2.27E-05
TGM1	-3.18	1.82E-17	-5.95	3.69E-28
TUBA4A	-3.20	6.51E-105	-3.44	1.10E-68
LBP	-3.21	2.50E-04	-5.67	5.75E-04
H19	-3.23	0.00E+00	-10.68	0.00E+00
RASL11A	-3.23	0.00E+00	-6.02	0.00E+00
PLEKHA6	-3.28	3.74E-06	-2.92	1.72E-64
GUCY1A3	-3.28	0.00E+00	-6.19	0.00E+00
CADM1	-3.29	4.01E-169	-9.72	7.44E-246
FXYD1	-3.29	2.92E-41	-8.71	1.30E-30
DLK2	-3.31	6.93E-16	-2.14	6.46E-09
GBX2	-3.33	6.91E-04	-4.66	2.64E-05
TNNT1	-3.33	6.91E-04	-7.41	5.94E-04
MGP	-3.33	0.00E+00	-11.79	0.00E+00
IGLON5	-3.34	1.49E-19	-4.58	1.39E-18

Appendix E: Continued

Gene Symbol	n=1		n=2	
	Fold Change (<i>Tgfb3</i> ^{-/-} / <i>Tgfb3</i> ^{+/+})	p-value	Fold Change (<i>Tgfb3</i> ^{-/-} / <i>Tgfb3</i> ^{+/+})	p-value
ADAM33	-3.37	2.30E-67	-2.69	8.01E-37
TMEM178A	-3.41	2.83E-40	-14.46	7.47E-52
CISH	-3.44	3.66E-37	-2.75	3.44E-19
AVPR1A	-3.54	3.58E-130	-5.81	7.52E-115
LGALS2	-3.54	1.18E-61	-7.64	3.37E-42
E130310I04Rik	-3.55	2.67E-37	-2.74	8.52E-14
PLEK	-3.62	7.25E-19	-4.51	6.03E-13
EHD3	-3.65	0.00E+00	-4.41	0.00E+00
MT1H	-3.65	0.00E+00	-3.14	2.85E-44
SCARB2	-3.69	0.00E+00	-2.35	2.53E-192
GATA2	-3.72	3.85E-41	-6.69	6.66E-51
TGFB1	-3.74	6.39E-75	-4.28	1.03E-27
ITIH4	-3.79	3.45E-05	-8.50	1.31E-04
LRP3	-3.86	5.14E-09	-2.85	2.74E-05
APOE	-3.86	0.00E+00	-4.95	0.00E+00
NRXN2	-3.90	8.15E-32	-11.86	1.28E-37
FAM189A2	-4.00	2.38E-18	-5.61	1.05E-09
STBD1	-4.06	2.30E-111	-3.36	3.40E-59
BMF	-4.09	6.67E-70	-7.83	4.29E-53
Dcaf12l1	-4.15	1.48E-07	-4.71	1.18E-09
TPBGL	-4.17	9.80E-31	-12.96	4.49E-42
KIAA1324L	-4.19	6.88E-60	-2.80	4.31E-24
1010001B22Rik	-4.21	2.06E-04	-13.72	2.35E-04
NXPH1	-4.35	3.88E-12	-3.37	8.46E-18
ELN	-4.35	0.00E+00	-7.79	0.00E+00
SLC16A5	-4.35	3.63E-33	-2.18	3.52E-07
HCN4	-4.37	4.25E-23	-6.75	7.39E-14
EEF1A2	-4.40	4.36E-131	-3.04	7.27E-30
PGAM2	-4.43	1.31E-26	-4.81	8.66E-24
NPL	-4.48	1.83E-32	-3.11	1.22E-14
PRPH	-4.58	3.35E-210	-11.43	0.00E+00
RBKS	-4.59	3.70E-15	-3.06	8.19E-05
PYCARD	-4.66	9.27E-28	-3.66	9.51E-12
DOCK10	-4.67	7.66E-17	-3.09	5.19E-08
PADI3	-4.78	2.17E-09	-3.13	2.47E-04
NAP1L3	-4.95	5.45E-07	-5.41	2.06E-07
SYNPO2	-5.05	1.59E-37	-4.11	2.87E-19
SOSTDC1	-5.07	1.65E-15	-19.75	9.94E-12
TEK	-5.14	3.81E-56	-3.99	4.03E-29
PCDH17	-5.23	2.25E-161	-10.53	3.61E-229

Appendix E: Continued

Gene Symbol	n=1		n=2	
	Fold Change (<i>Tgfb3</i> ^{-/-} / <i>Tgfb3</i> ^{+/+})	p-value	Fold Change (<i>Tgfb3</i> ^{-/-} / <i>Tgfb3</i> ^{+/+})	p-value
Cyp2d22	-5.60	2.10E-37	-13.25	1.75E-46
PRR15	-5.83	4.25E-221	-19.79	4.77E-182
TGFBR3	-5.84	4.03E-318	-4.93	3.99E-133
C10orf10	-5.93	2.40E-79	-14.68	1.02E-30
Serpib6b	-5.95	2.20E-92	-12.10	4.50E-50
FGF8	-6.08	2.25E-11	-31.28	4.14E-10
2410017I17Rik	-6.12	2.50E-64	-14.66	1.16E-140
NPAS4	-6.24	1.27E-08	-10.15	1.30E-05
CYP7B1	-6.32	1.82E-05	-12.62	5.25E-04
PDE3A	-6.37	9.28E-08	-11.34	4.78E-09
TNC	-6.44	0.00E+00	-4.39	0.00E+00
SUSD2	-6.49	1.88E-61	-4.65	9.16E-20
TMEM196	-6.58	5.20E-23	-7.86	1.66E-15
WDR86	-6.66	1.39E-10	-7.79	5.28E-09
ADAMTSL2	-6.73	3.26E-33	-25.97	3.22E-23
HOXB3	-6.73	2.03E-34	-4.54	1.07E-15
GALNT14	-6.83	9.92E-10	-13.72	7.61E-08
ALDOC	-7.20	0.00E+00	-19.03	0.00E+00
CFI	-7.26	6.40E-16	-8.23	2.29E-11
H2-Q10	-7.40	0.00E+00	-2.26	1.12E-106
SLC39A4	-7.60	4.75E-24	-10.15	1.68E-28
STC1	-7.63	0.00E+00	-23.59	2.53E-106
PNLDC1	-7.65	7.66E-23	-23.04	2.49E-20
HOXB2	-7.72	3.10E-49	-22.03	1.23E-43
FGL2	-7.89	8.18E-63	-11.93	4.24E-35
AQP1	-8.05	4.16E-66	-14.86	2.00E-42
ACSS3	-8.48	5.17E-33	-7.53	1.30E-17
UCP2	-8.52	0.00E+00	-4.93	0.00E+00
ACTN3	-8.78	8.75E-61	-5.98	1.25E-34
2610507I01Rik	-9.13	1.11E-21	-44.99	1.04E-14
H2-M2	-9.31	2.88E-22	-4.80	5.25E-07
GGT5	-9.95	3.68E-45	-2.96	1.24E-12
LINGO1	-10.24	1.37E-215	-9.36	2.07E-102
CCDC68	-10.93	7.41E-06	-7.68	4.08E-04
1700008P20Rik	-10.93	7.41E-06	-13.72	2.35E-04
IL16	-11.10	4.40E-40	-2.81	2.06E-07
9530082P21Rik	-11.42	5.04E-29	-61.45	2.81E-20
8030451A03Rik	-12.29	8.83E-04	-4.48	9.56E-65
BC023719	-12.36	2.81E-29	-4.39	1.17E-08
AARD	-13.66	3.41E-04	-16.46	3.10E-05

Appendix E: Continued

Gene Symbol	n=1		n=2	
	Fold Change (<i>Tgfb3</i> ^{-/-} / <i>Tgfb3</i> ^{+/+})	p-value	Fold Change (<i>Tgfb3</i> ^{-/-} / <i>Tgfb3</i> ^{+/+})	p-value
CDH13	-13.96	8.66E-31	-4.85	4.37E-10
HLX	-14.65	6.16E-71	-75.53	2.46E-73
DLX3	-15.36	4.95E-16	-5.67	5.75E-04
GBP2	-15.66	5.87E-62	-25.57	2.56E-37
SDK1	-17.75	1.89E-05	-6.31	1.09E-05
PADI1	-19.12	7.11E-06	-7.13	3.17E-05
PDE2A	-19.39	6.07E-26	-2.74	9.81E-04
VSTM2A	-20.36	6.59E-59	-19.31	4.41E-27
USH1G	-23.90	3.20E-20	-11.11	1.94E-11
HLA-B	-23.97	0.00E+00	-12.78	0.00E+00
SORBS2	-28.58	1.75E-157	-17.90	5.63E-39
TMEM215	-29.64	5.27E-42	-15.03	3.38E-20
PKD1L2	-30.73	1.57E-09	-13.72	2.35E-04
ADAM23	-32.78	3.50E-10	-14.81	1.05E-04
CYP4F22	-41.84	9.67E-134	-43.68	1.60E-67

APPENDIX F

GENES >2-FOLD DYSREGULATED BETWEEN $TGFBR3^{+/+}$ AND $TGFBR3^{-/-}$ EPICARDIAL CELLS AFTER TGF β 1 INCUBATION

Gene Symbol	n=1		n=2	
	Fold Change ($Tgfb3^{-/-}$ / $Tgfb3^{+/+}$)	p-value	Fold Change ($Tgfb3^{-/-}$ / $Tgfb3^{+/+}$)	p-value
Rprl2	999.00	4.83E-15	999.00	1.41E-29
TSIX	999.00	0.00E+00	999.00	2.65E-73
XIST	999.00	0.00E+00	999.00	0.00E+00
Rprl3	999.00	9.59E-35	164.74	3.99E-45
Ly6a	999.00	4.33E-14	36.75	7.69E-10
TMEM117	999.00	1.65E-05	11.41	2.50E-05
Klra4	999.00	3.07E-04	5.07	1.55E-17
CTNND2	49.70	2.14E-168	27.03	6.68E-111
RIMS2	49.40	3.59E-65	45.20	3.20E-34
ALX4	34.52	6.97E-27	38.65	1.18E-19
9030619P08Rik	31.28	9.71E-09	27.88	1.85E-07
LCE1B	30.20	1.95E-08	41.82	3.28E-11
Lce1f	28.58	8.96E-29	3.66	3.34E-04
FGF10	26.61	3.24E-20	10.14	1.63E-06
FRMPD1	17.62	8.94E-13	12.67	3.34E-13
FAM134B	14.56	3.16E-07	3.55	2.48E-04
KCNK1	13.58	2.37E-89	3.59	5.38E-20
BCAT1	12.26	2.15E-152	7.29	8.76E-63
EPB41L3	12.19	2.98E-25	8.11	4.37E-14
Lce1h	11.94	6.67E-34	5.97	1.92E-12
NECAB1	11.87	1.67E-10	999.00	1.81E-06
MEIG1	11.87	6.37E-36	4.37	1.98E-05
Xlr3c	11.66	8.82E-60	7.48	1.27E-12
9330179D12Rik	11.43	0.00E+00	27.76	1.76E-70
IL17RE	10.07	2.26E-12	7.60	2.97E-08
TLL1	9.71	1.75E-06	5.39	6.77E-04
Lce1g	9.27	1.50E-45	5.88	2.71E-18
SYCE1	8.56	2.72E-23	8.76	5.06E-17
BMPR1B	8.27	4.72E-18	6.62	9.64E-10
TBX4	8.22	2.23E-12	30.41	3.88E-08
Klra18	7.99	5.63E-79	5.30	1.91E-19

Appendix F: Continued

Gene Symbol	n=1		n=2	
	Fold Change (<i>Tgfb3</i> ^{-/-} / <i>Tgfb3</i> ^{+/+})	p-value	Fold Change (<i>Tgfb3</i> ^{-/-} / <i>Tgfb3</i> ^{+/+})	p-value
TMEM132C	7.55	2.33E-07	4.53	1.04E-04
FAXC	7.38	1.16E-23	6.80	7.33E-20
WNT7A	7.21	6.95E-23	5.15	1.25E-21
LIMCH1	6.79	6.36E-302	6.19	8.48E-126
NKX2-3	6.74	1.68E-09	16.47	6.77E-08
TNFRSF19	6.74	2.50E-05	5.83	4.49E-05
Apol10a	6.74	2.50E-05	3.23	5.22E-04
PPP1R16B	6.49	2.81E-68	5.16	2.03E-28
B4GALNT2	6.46	4.11E-133	4.98	6.49E-43
NPR2	6.38	2.13E-274	6.09	9.62E-217
PIANP	6.37	1.65E-39	8.62	3.20E-22
HMHA1	6.34	6.80E-55	8.72	7.17E-48
PTPRB	6.20	1.17E-185	4.76	3.62E-110
SNRPN	6.11	3.34E-09	3.69	6.28E-05
FAM89A	6.09	3.80E-16	4.85	8.86E-11
IL6	5.96	3.59E-82	2.85	1.10E-17
DSP	5.88	1.21E-177	4.41	5.46E-94
KRT8	5.85	7.55E-34	2.84	1.73E-17
WASF3	5.81	8.13E-12	6.52	1.07E-07
SEMA3G	5.53	3.19E-13	2.45	2.94E-05
PPL	5.52	6.10E-131	7.00	1.71E-145
PRDM6	5.49	3.24E-79	4.19	6.87E-41
ANKRD1	5.40	0.00E+00	4.42	0.00E+00
C6orf132	5.39	5.02E-12	5.76	1.50E-09
SNURF	5.29	3.35E-08	4.12	2.98E-06
MANSC1	5.29	3.35E-08	3.96	2.55E-04
Msx3	5.20	1.11E-08	5.45	3.92E-08
BTBD11	5.16	1.36E-10	6.59	6.41E-06
MAB21L2	5.14	1.74E-129	3.72	3.73E-49
Masp1	5.13	6.97E-23	4.24	6.40E-14
ANGPTL4	5.12	3.63E-262	5.78	1.67E-173
CDKN1C	5.11	0.00E+00	2.78	9.41E-170
RUNX1T1	5.10	3.59E-18	19.26	1.33E-21
Snhg9	5.08	3.31E-66	3.19	2.22E-38
SEMA7A	4.97	1.70E-12	3.33	7.52E-10
DUOXA1	4.78	2.06E-09	4.22	7.77E-04
FAM43B	4.75	2.93E-21	7.18	2.98E-17
CTSC	4.74	1.07E-52	2.72	9.01E-13

Appendix F: Continued

Gene Symbol	n=1		n=2	
	Fold Change (<i>Tgfb3</i> ^{-/-} / <i>Tgfb3</i> ^{+/+})	p-value	Fold Change (<i>Tgfb3</i> ^{-/-} / <i>Tgfb3</i> ^{+/+})	p-value
FSTL3	4.56	1.70E-116	3.60	5.13E-51
GAP43	4.51	2.11E-15	2.48	2.63E-04
RPH3A	4.49	2.41E-04	6.34	8.00E-04
SOX21	4.47	1.72E-08	10.56	7.97E-07
CHST7	4.47	7.65E-05	8.87	4.36E-04
COL4A3	4.43	7.27E-38	3.27	7.25E-16
GALNT9	4.31	4.15E-05	8.87	4.36E-04
RNF152	4.24	3.60E-22	2.23	7.09E-05
CKMT1A/CKMT1B	4.24	1.16E-99	3.96	3.80E-43
GATM	4.23	3.84E-195	2.55	4.20E-32
GALNTL4	4.22	6.32E-41	2.63	2.07E-11
C1orf115	4.21	5.95E-45	2.19	1.29E-07
TLR5	4.20	5.29E-10	4.35	1.87E-04
IL28RA	4.20	2.24E-05	7.60	6.80E-06
BCL11B	4.18	6.99E-05	8.24	8.78E-04
TNFRSF11B	4.18	3.65E-150	2.06	1.18E-22
PARVB	4.16	2.19E-04	8.24	8.78E-04
AASS	4.12	3.93E-06	6.59	6.41E-06
NPR3	4.12	2.26E-25	3.14	3.37E-10
PP2D1	4.10	1.21E-05	4.53	1.04E-04
CSGALNACT1	4.01	2.18E-70	5.18	3.54E-45
FGF5	3.98	1.80E-38	2.79	8.45E-12
PCOLCE2	3.96	4.80E-26	3.49	6.61E-12
ZDHHC2	3.92	7.26E-68	3.62	6.46E-48
FZD10	3.77	1.10E-81	5.66	4.07E-95
SLC4A4	3.77	7.61E-144	3.87	1.21E-94
DKKL1	3.76	1.05E-58	2.21	2.62E-11
PM20D1	3.75	9.41E-10	5.65	4.01E-20
TUBA8	3.74	3.09E-12	3.08	1.33E-07
ST8SIA2	3.73	5.11E-10	2.20	4.58E-04
KRT18	3.73	2.82E-09	3.30	1.45E-12
CXXC4	3.71	1.05E-16	2.05	4.23E-07
2410124H12Rik	3.71	1.97E-18	2.46	2.77E-08
AMN	3.71	4.45E-182	2.85	2.76E-51
CPNE7	3.70	1.14E-53	5.09	2.92E-61
TFRC	3.63	2.73E-39	3.55	1.54E-28
TSPAN12	3.54	5.32E-24	2.00	9.58E-05
C4orf32	3.51	1.60E-11	2.11	9.52E-05
KCNS3	3.48	3.10E-08	3.34	3.04E-07
PLD5	3.44	1.05E-56	2.66	1.55E-18

Appendix F: Continued

Gene Symbol	n=1		n=2	
	Fold Change (<i>Tgfb3</i> ^{-/-} / <i>Tgfb3</i> ^{+/+})	p-value	Fold Change (<i>Tgfb3</i> ^{-/-} / <i>Tgfb3</i> ^{+/+})	p-value
SOX13	3.43	7.47E-43	3.33	1.09E-33
KIAA1467	3.42	3.86E-85	3.75	1.27E-53
DUOX1	3.41	1.65E-14	3.25	3.74E-07
RBM20	3.41	1.32E-31	4.30	5.94E-24
HECW2	3.40	4.29E-17	4.37	1.17E-14
BAI1	3.32	1.05E-162	3.18	5.41E-68
CCL17	3.31	5.40E-21	2.49	2.71E-09
ACSBG1	3.29	1.02E-37	3.42	1.86E-21
POU4F3	3.29	3.71E-07	3.56	2.98E-06
LTBP1	3.28	3.16E-222	2.55	6.00E-73
GDF15	3.28	7.24E-27	2.02	9.74E-06
Usp44	3.28	3.09E-08	4.35	1.87E-04
Pde4d	3.28	1.66E-08	3.36	2.02E-08
AGPAT9	3.27	7.55E-10	5.07	9.38E-10
AMPD3	3.24	6.18E-04	16.47	1.86E-04
PEX5L	3.24	4.87E-08	5.42	3.44E-18
Fndc3c1	3.17	1.14E-05	5.23	2.23E-06
MEIS3	3.16	1.41E-19	3.01	2.79E-14
GJB3	3.10	3.35E-05	3.06	4.73E-05
ST6GAL1	3.09	2.45E-37	3.32	6.04E-26
Rasl2-9	3.08	3.06E-14	2.38	6.46E-09
CMAHP	3.07	4.24E-06	4.28	8.11E-05
DSCAML1	3.03	2.64E-51	3.00	2.67E-22
FERMT1	2.99	1.93E-45	2.16	8.09E-15
Gm3230	2.95	7.55E-08	3.80	3.63E-05
KIF1A	2.92	2.01E-06	4.05	1.16E-11
NDUFA4L2	2.91	6.34E-88	4.69	1.02E-59
KRT80	2.90	4.03E-10	3.80	1.05E-15
RASGEF1A	2.88	8.16E-11	2.88	2.71E-06
CORO2A	2.88	7.33E-145	2.51	2.70E-85
ITGA2	2.88	3.09E-06	5.91	2.40E-08
POU3F3	2.88	7.38E-07	4.25	1.87E-07
B4GALNT1	2.87	1.68E-22	2.13	9.35E-07
DGKI	2.85	4.48E-04	7.29	1.34E-05
MAP2	2.85	4.17E-40	2.06	9.90E-11
GRM8	2.84	5.17E-43	2.02	3.14E-08
TMEFF2	2.84	2.65E-63	2.51	2.96E-30
FOXL1	2.80	3.71E-05	7.42	3.93E-09
ALOX12	2.80	4.43E-08	5.28	4.47E-09
DLX2	2.80	1.71E-06	4.58	7.40E-08

Appendix F: Continued

Gene Symbol	n=1		n=2	
	Fold Change (<i>Tgfb3</i> ^{-/-} / <i>Tgfb3</i> ^{+/+})	p-value	Fold Change (<i>Tgfb3</i> ^{-/-} / <i>Tgfb3</i> ^{+/+})	p-value
NFATC1	2.79	2.76E-63	3.59	1.52E-64
EGFL8	2.78	4.10E-279	2.22	3.13E-42
ETNK2	2.78	6.96E-18	3.38	4.66E-12
SLC7A5	2.77	0.00E+00	2.48	9.95E-321
MAP7	2.76	2.93E-10	2.84	2.41E-08
NRIP3	2.75	5.65E-05	2.99	3.29E-04
PKP1	2.74	8.99E-09	3.17	4.55E-07
KCNC3	2.72	1.45E-144	3.42	1.18E-159
CGREF1	2.72	2.78E-224	2.31	1.20E-85
C10orf47	2.71	3.03E-08	2.57	4.50E-07
PRKAA2	2.71	1.89E-97	2.01	1.18E-20
D730039F16Rik	2.70	8.25E-58	2.34	4.25E-20
PLCXD2	2.69	1.36E-85	3.52	1.75E-71
OLFM2	2.68	5.14E-07	2.83	1.76E-08
Serpina3h	2.66	2.71E-09	2.14	2.88E-04
FAM159B	2.66	4.67E-88	3.16	1.31E-34
BC106179	2.65	3.42E-07	3.57	1.08E-04
SORCS2	2.63	1.29E-20	2.47	4.83E-23
LHX5	2.62	4.47E-34	3.36	1.87E-20
Tnfrsf26	2.61	4.03E-176	2.09	1.03E-32
LOXL4	2.58	6.16E-07	2.68	8.12E-10
LMO7	2.55	4.73E-20	3.17	2.26E-19
CPE	2.50	6.62E-300	2.21	1.66E-224
MAP3K13	2.50	8.08E-11	2.00	3.17E-05
GLIS3	2.49	8.42E-34	2.00	6.94E-11
TEX15	2.48	4.19E-35	2.28	1.06E-14
C21orf7	2.48	8.90E-30	2.02	1.72E-05
ADRA1B	2.47	1.81E-08	5.15	7.60E-20
MATN4	2.47	1.20E-230	2.34	1.79E-99
WSCD1	2.45	7.85E-05	3.88	3.44E-07
RAB37	2.44	5.11E-09	3.80	2.62E-07
VCAN	2.42	6.91E-95	2.20	4.48E-57
Foxl2os	2.42	2.35E-07	4.48	1.48E-08
IRF6	2.40	1.23E-15	2.81	2.95E-11
DPF1	2.40	7.03E-09	4.97	2.02E-16
NFATC2	2.39	2.45E-27	3.83	1.08E-30
SH2D4A	2.39	2.45E-27	3.20	4.17E-17
FOSB	2.38	1.59E-14	2.88	9.47E-21
CNTFR	2.36	1.34E-04	2.04	2.68E-04
IGF2BP3	2.35	1.20E-27	2.18	4.23E-10

Appendix F: Continued

Gene Symbol	n=1		n=2	
	Fold Change (<i>Tgfb3</i> ^{-/-} / <i>Tgfb3</i> ^{+/+})	p-value	Fold Change (<i>Tgfb3</i> ^{-/-} / <i>Tgfb3</i> ^{+/+})	p-value
NPAS1	2.33	3.04E-04	3.72	2.32E-06
SDC3	2.33	1.17E-58	2.29	2.85E-43
LPL	2.32	8.99E-57	3.05	4.07E-21
C16orf74	2.32	9.33E-11	3.02	2.17E-11
SLC22A15	2.31	1.86E-05	2.53	1.23E-04
SLC7A3	2.29	8.74E-27	2.50	1.03E-22
Rps19-ps3	2.28	2.74E-109	2.67	8.23E-138
ARTN	2.25	2.54E-13	3.11	6.66E-09
ARHGAP8	2.25	2.38E-07	2.32	1.94E-04
KDM6A	2.25	5.82E-48	2.14	3.85E-21
DES	2.25	1.54E-34	2.86	8.41E-43
UBA6	2.25	3.05E-05	4.89	3.12E-05
PRDM16	2.24	1.81E-09	3.34	2.25E-09
REM1	2.23	9.58E-15	2.81	2.88E-12
PPP2R2C	2.23	3.00E-55	2.77	4.83E-62
ITGA6	2.22	1.61E-48	2.20	4.36E-18
COX7A1	2.22	3.23E-18	3.32	1.86E-17
RANGRF	2.21	3.44E-13	2.05	2.05E-08
PTP4A1	2.20	1.85E-172	3.36	9.21E-07
FOXL2	2.20	1.43E-10	3.26	3.08E-14
CCDC73	2.20	4.62E-14	2.60	4.12E-04
CD80	2.19	9.58E-17	4.65	1.09E-13
PRSS56	2.19	1.06E-10	3.31	8.45E-11
FAT2	2.19	1.50E-04	4.97	6.88E-09
RNF11	2.19	9.48E-15	2.09	3.51E-07
DUS2L	2.19	9.60E-05	2.25	5.55E-04
TMEM37	2.18	1.26E-56	2.04	9.22E-17
HCK	2.17	4.54E-08	2.38	4.65E-07
CYCS	2.16	4.04E-35	2.10	4.76E-26
BCAP29	2.16	4.09E-16	4.06	3.46E-21
TBX15	2.16	2.67E-08	2.26	1.43E-05
SP6	2.14	5.79E-64	3.09	3.36E-82
ARHGAP22	2.14	1.86E-06	2.26	3.90E-08
THBD	2.13	9.64E-28	2.74	2.07E-21
FLT1	2.12	2.82E-19	2.79	2.72E-15
BOK	2.12	1.85E-23	2.31	1.08E-19
EREG	2.11	4.59E-36	2.12	2.49E-20
TM4SF1	2.10	5.56E-15	2.82	9.80E-13
MFAP3L	2.10	2.83E-11	2.71	1.35E-09
HOXA5	2.10	2.14E-04	2.66	1.36E-04

Appendix F: Continued

Gene Symbol	n=1		n=2	
	Fold Change (<i>Tgfb3</i> ^{-/-} / <i>Tgfb3</i> ^{+/+})	p-value	Fold Change (<i>Tgfb3</i> ^{-/-} / <i>Tgfb3</i> ^{+/+})	p-value
Gm15645	2.09	1.35E-05	3.88	3.44E-07
RAP1GAP2	2.08	2.75E-17	2.62	1.09E-22
APOO	2.08	2.70E-12	2.39	2.11E-08
FRMD4B	2.07	1.73E-18	2.43	4.05E-21
4833438C02Rik	2.05	8.19E-52	2.80	2.54E-51
CILP2	2.04	3.93E-18	2.98	1.28E-27
4921504A21Rik	2.01	2.35E-08	2.78	6.87E-06
IGFBP6	-2.01	9.16E-12	-3.33	8.60E-79
CTSW	-2.01	5.45E-19	-2.29	3.85E-54
GPSM3	-2.01	2.72E-06	-2.06	9.79E-16
LTBP4	-2.01	5.08E-84	-2.34	2.56E-194
NUP210	-2.01	4.93E-12	-2.67	3.99E-27
SERPING1	-2.02	3.17E-105	-3.50	0.00E+00
SNX32	-2.02	2.22E-09	-2.18	3.83E-21
MAF	-2.03	1.63E-29	-2.27	6.93E-121
SYNE2	-2.03	1.54E-234	-2.00	0.00E+00
AHR	-2.03	6.14E-96	-2.80	0.00E+00
MGAT3	-2.03	6.42E-06	-2.92	4.16E-19
ENTPD4	-2.03	5.60E-35	-3.02	4.99E-45
GPR68	-2.03	3.45E-04	-3.08	9.44E-12
BPHL	-2.04	5.05E-04	-2.18	5.28E-11
Gbp4	-2.04	3.22E-06	-2.40	2.27E-27
1010001N08Rik	-2.05	1.70E-06	-2.55	1.19E-38
PHACTR2	-2.05	1.08E-09	-2.60	7.06E-33
MMP19	-2.06	9.21E-09	-3.66	8.11E-75
CCDC125	-2.06	7.85E-04	-2.34	3.27E-13
PAQR8	-2.07	6.56E-07	-2.04	1.74E-20
E130310I04Rik	-2.07	5.65E-04	-3.25	1.26E-15
RGL3	-2.07	4.77E-07	-2.19	3.00E-11
PLEKHF1	-2.08	7.47E-17	-3.24	9.69E-78
ADAM12	-2.08	7.13E-28	-3.04	4.64E-125
BTBD6	-2.09	1.05E-06	-2.44	4.45E-11
ADAMTS20	-2.09	2.93E-04	-2.21	2.04E-08
SLIT3	-2.10	1.07E-76	-2.89	1.74E-197
NKD2	-2.10	2.11E-04	-3.71	4.33E-16
MYO10	-2.10	5.18E-81	-2.36	1.35E-220
C1S	-2.11	1.75E-111	-4.21	1.55E-288
SNCAIP	-2.11	4.32E-11	-2.02	9.43E-23
GAS1	-2.11	2.19E-144	-2.96	0.00E+00
TMEM176B	-2.11	1.04E-90	-2.19	5.23E-198

Appendix F: Continued

Gene Symbol	n=1		n=2	
	Fold Change (<i>Tgfb3</i> ^{-/-} / <i>Tgfb3</i> ^{+/+})	p-value	Fold Change (<i>Tgfb3</i> ^{-/-} / <i>Tgfb3</i> ^{+/+})	p-value
CPXM1	-2.11	1.47E-42	-3.55	1.64E-269
SMTNL2	-2.12	5.70E-14	-3.12	2.33E-33
ELN	-2.12	9.92E-27	-6.24	1.29E-290
WBSCR17	-2.12	1.62E-07	-2.85	4.19E-19
DCN	-2.12	4.72E-55	-3.66	0.00E+00
FOLR1	-2.14	1.06E-42	-2.25	1.44E-119
CLU	-2.15	3.47E-18	-4.05	7.35E-134
BICD1	-2.15	3.43E-08	-2.23	2.30E-17
EML6	-2.16	4.05E-06	-2.05	3.55E-08
FUOM	-2.17	1.69E-19	-2.01	2.30E-50
GSTM5	-2.17	6.72E-29	-2.35	7.69E-74
PODXL	-2.17	7.29E-04	-2.75	5.55E-07
RBM47	-2.17	7.29E-04	-3.92	1.69E-16
OLFML3	-2.17	3.41E-14	-3.37	2.17E-61
KLHL29	-2.18	5.82E-07	-2.57	3.26E-16
NOS1AP	-2.18	4.73E-05	-2.73	1.95E-08
RAI14	-2.20	1.61E-138	-2.11	1.93E-275
Sprr3	-2.21	6.30E-17	-3.72	4.61E-45
NDRG1	-2.21	1.55E-78	-3.41	0.00E+00
SEMA3D	-2.23	1.06E-96	-2.26	6.35E-277
Mir546	-2.24	1.38E-05	-4.93	1.56E-15
BC039771	-2.24	2.91E-04	-2.73	2.47E-20
PHOX2A	-2.25	5.17E-06	-2.80	1.44E-25
CCDC8	-2.25	2.09E-04	-4.33	4.77E-12
COLEC12	-2.25	2.16E-57	-2.54	7.33E-134
EZR	-2.26	0.00E+00	-2.45	0.00E+00
SFRP2	-2.26	3.39E-50	-3.41	7.01E-252
IGFBP5	-2.26	5.54E-05	-4.64	1.05E-04
ZBTB8B	-2.29	8.88E-29	-2.88	1.72E-80
CNKS3R	-2.29	2.97E-27	-3.34	6.04E-104
GNAI1	-2.30	3.22E-11	-2.98	2.57E-30
RAB6B	-2.30	5.97E-10	-5.40	1.62E-51
Speer4a	-2.30	3.13E-04	-2.74	3.61E-06
GPNMB	-2.31	1.23E-22	-3.00	2.32E-72
A730049H05Rik	-2.31	8.48E-10	-2.19	1.25E-14
MYLK	-2.32	2.93E-37	-2.77	3.76E-144
SRRM4	-2.33	1.84E-11	-3.67	1.59E-57
FGF2	-2.33	1.71E-09	-6.00	2.09E-81
SMAD9	-2.33	4.53E-04	-4.45	4.12E-20
PPP1R9A	-2.33	1.66E-04	-2.36	2.50E-07

Appendix F: Continued

Gene Symbol	n=1		n=2	
	Fold Change (<i>Tgfb3</i> ^{-/-} / <i>Tgfb3</i> ^{+/+})	p-value	Fold Change (<i>Tgfb3</i> ^{-/-} / <i>Tgfb3</i> ^{+/+})	p-value
HEG1	-2.33	1.23E-91	-2.69	3.47E-138
ADAMTS14	-2.34	1.63E-05	-3.73	1.56E-18
CCDC141	-2.35	2.83E-12	-3.16	1.65E-42
CCDC19	-2.37	8.75E-05	-2.61	1.73E-08
Neat1	-2.39	2.77E-10	-3.88	1.89E-46
Sprr1a	-2.40	1.25E-17	-2.14	1.38E-48
AIG1	-2.40	2.38E-05	-2.95	2.70E-11
SCARB2	-2.40	0.00E+00	-3.08	0.00E+00
MTSS1	-2.40	2.67E-26	-3.42	1.67E-141
H6PD	-2.40	4.52E-80	-4.47	0.00E+00
SELENBP1	-2.40	1.75E-04	-2.78	2.83E-04
ME3	-2.40	4.11E-11	-2.91	6.01E-31
MMP16	-2.41	3.00E-27	-2.18	4.06E-56
C3	-2.42	4.51E-60	-3.73	5.47E-175
DPEP1	-2.42	4.68E-06	-2.03	1.08E-05
FAM180A	-2.43	1.53E-42	-2.49	7.67E-197
FOXP2	-2.44	3.43E-06	-3.21	9.73E-18
HLA-DQB1	-2.45	4.47E-49	-4.05	2.11E-246
NLRC3	-2.45	5.85E-26	-2.62	1.78E-82
PCDH9	-2.45	9.40E-17	-3.27	1.00E-50
FAM184A	-2.46	5.85E-15	-2.59	2.01E-34
KALRN	-2.46	8.13E-81	-3.02	7.66E-173
PEG3	-2.46	7.99E-54	-2.81	2.23E-108
STAP2	-2.46	3.90E-09	-2.69	6.74E-20
ZNF467	-2.47	3.48E-06	-3.43	6.20E-22
CFH	-2.47	6.15E-42	-2.70	6.41E-167
E130102H24Rik	-2.49	1.81E-04	-3.41	4.57E-20
KCNT1	-2.49	1.61E-10	-2.31	9.01E-19
Cfh2/Cfh3	-2.51	4.95E-04	-2.76	3.40E-08
KANK4	-2.52	1.33E-06	-3.01	5.73E-13
HOXB4	-2.57	4.60E-11	-3.97	1.32E-33
SERPINA3	-2.57	1.27E-15	-5.22	2.96E-140
EPS8	-2.58	5.49E-72	-2.94	4.52E-201
SLC43A3	-2.58	1.36E-218	-2.64	0.00E+00
LDOC1L	-2.59	1.17E-14	-2.61	6.70E-25
SEMA5A	-2.61	2.66E-07	-3.73	1.17E-22
ART3	-2.62	2.54E-05	-3.75	5.66E-18
N4BP2L1	-2.63	5.28E-08	-2.24	3.07E-23
CNRIP1	-2.63	9.50E-06	-2.82	1.08E-11
Gm2895	-2.64	2.17E-14	-4.10	7.78E-114

Appendix F: Continued

Gene Symbol	n=1		n=2	
	Fold Change (<i>Tgfb3</i> ^{-/-} / <i>Tgfb3</i> ^{+/+})	p-value	Fold Change (<i>Tgfb3</i> ^{-/-} / <i>Tgfb3</i> ^{+/+})	p-value
ACVR1B	-2.64	2.54E-16	-3.51	3.63E-57
BACE2	-2.66	6.80E-05	-2.86	5.04E-11
LPAR1	-2.67	1.86E-85	-2.10	6.97E-147
IL1RL2	-2.68	9.94E-08	-6.72	6.04E-58
FMOD	-2.68	4.94E-182	-2.55	0.00E+00
ITGA7	-2.69	4.67E-65	-3.28	5.05E-147
MT1H	-2.74	1.42E-18	-2.92	8.68E-121
TNIK	-2.74	8.12E-20	-2.35	2.68E-34
NEU3	-2.75	1.21E-31	-3.01	2.24E-85
NID2	-2.75	0.00E+00	-3.18	0.00E+00
XDH	-2.77	2.90E-81	-4.61	0.00E+00
SLC39A4	-2.80	3.74E-15	-3.09	6.09E-35
NPR1	-2.81	2.07E-43	-2.88	5.61E-91
NXPH1	-2.81	3.76E-24	-2.80	8.39E-90
TF	-2.83	2.07E-73	-2.48	2.32E-132
SLFN13	-2.85	8.10E-13	-5.49	2.64E-58
TMEM221	-2.86	6.47E-05	-2.17	4.01E-06
SPRR2G	-2.87	2.36E-06	-4.59	1.39E-74
FAM110C	-2.88	4.87E-65	-2.58	1.61E-121
ID2	-2.88	2.38E-33	-4.56	4.02E-292
PRPH	-2.91	1.74E-16	-7.27	1.25E-61
RGS3	-2.92	1.93E-46	-3.44	1.85E-133
PCDHB16	-2.94	1.19E-05	-3.49	5.27E-11
AUTS2	-2.99	1.20E-30	-5.67	1.01E-155
IGFBP4	-3.00	1.16E-83	-5.52	0.00E+00
ALCAM	-3.01	2.56E-225	-2.34	0.00E+00
CISH	-3.05	2.05E-27	-2.53	5.75E-42
FIGF	-3.05	1.36E-55	-2.74	1.62E-120
THR8	-3.05	2.06E-07	-3.60	3.49E-32
MTUS2	-3.06	3.34E-16	-6.21	7.41E-105
ATP1B1	-3.10	0.00E+00	-5.53	0.00E+00
SEPP1	-3.11	1.53E-16	-10.42	8.84E-123
IDUA	-3.13	2.60E-10	-2.55	2.65E-16
GJB4	-3.16	1.11E-04	-2.48	1.63E-05
TCF21	-3.17	1.63E-151	-3.62	0.00E+00
DPP4	-3.21	1.72E-63	-4.38	2.00E-172
RIMS1	-3.21	1.01E-05	-2.13	3.53E-05
Gm19557	-3.21	1.01E-05	-2.46	5.11E-06
GAS7	-3.23	3.32E-08	-4.29	6.79E-19
ECSCR	-3.23	1.82E-26	-2.50	2.39E-35

Appendix F: Continued

Gene Symbol	n=1		n=2	
	Fold Change (<i>Tgfb3</i> ^{-/-} / <i>Tgfb3</i> ^{+/+})	p-value	Fold Change (<i>Tgfb3</i> ^{-/-} / <i>Tgfb3</i> ^{+/+})	p-value
TGFBR3	-3.27	2.12E-44	-4.99	1.98E-227
RGS16	-3.28	1.60E-31	-3.80	6.84E-59
RASL11A	-3.31	2.96E-64	-3.14	2.09E-250
KLHL30	-3.33	2.08E-51	-4.81	4.76E-175
LRRN4	-3.34	1.61E-162	-7.63	0.00E+00
5430435G22Rik	-3.37	3.25E-06	-2.42	6.58E-09
Nup62cl	-3.38	1.30E-10	-3.26	7.28E-15
ISLR	-3.39	1.40E-04	-5.10	1.58E-09
PCDH10	-3.40	1.54E-46	-4.10	1.19E-107
SYNPO2	-3.41	7.64E-15	-3.87	2.76E-40
BMF	-3.42	2.77E-04	-6.18	1.87E-15
AVPR1A	-3.43	1.29E-41	-3.10	3.37E-84
EMILIN1	-3.43	8.23E-57	-7.37	1.08E-186
HMCN1	-3.44	4.81E-05	-3.32	3.88E-09
MFAP2	-3.49	2.80E-31	-2.52	6.33E-40
MSRB2	-3.52	3.13E-09	-2.59	7.31E-11
ST3GAL1	-3.57	5.45E-21	-5.51	0.00E+00
APOE	-3.57	7.70E-131	-6.60	0.00E+00
UCP2	-3.58	0.00E+00	-5.23	0.00E+00
Gsta4	-3.63	2.51E-32	-2.27	1.96E-23
SVEP1	-3.64	2.27E-55	-4.20	7.96E-136
IL4R	-3.73	4.15E-127	-4.41	1.24E-290
BC023719	-3.74	2.12E-07	-6.12	1.82E-24
CMYA5	-3.75	3.42E-06	-3.84	3.04E-10
RAB27B	-3.76	3.01E-13	-4.02	2.54E-38
CPQ	-3.76	1.82E-23	-2.79	1.17E-35
SLC2A13	-3.79	1.93E-05	-2.82	4.32E-06
GLI1	-3.84	9.51E-08	-2.86	5.05E-12
SMOC2	-3.87	3.22E-31	-7.51	8.96E-99
IVL	-3.88	5.12E-60	-4.72	2.37E-171
FADS6	-4.07	1.55E-07	-4.92	4.14E-16
PGAM2	-4.08	5.29E-10	-3.58	4.31E-22
Gm10389	-4.08	7.66E-27	-3.71	2.41E-49
RORC	-4.10	1.24E-08	-6.15	4.23E-32
DAAM2	-4.15	4.42E-34	-5.47	1.66E-120
PRR15	-4.21	3.72E-15	-7.87	4.42E-107
PPP2R2B	-4.24	1.51E-38	-5.11	7.14E-121
H2-Q10	-4.28	3.72E-311	-9.19	0.00E+00
A930024E05Rik	-4.34	1.83E-04	-2.91	8.21E-08
KIAA1244	-4.38	2.42E-07	-2.39	8.29E-05

Appendix F: Continued

Gene Symbol	n=1		n=2	
	Fold Change (<i>Tgfb3</i> ^{-/-} / <i>Tgfb3</i> ^{+/+})	p-value	Fold Change (<i>Tgfb3</i> ^{-/-} / <i>Tgfb3</i> ^{+/+})	p-value
ID3	-4.44	0.00E+00	-3.55	0.00E+00
TNC	-4.50	0.00E+00	-6.88	0.00E+00
HLX	-4.56	1.31E-06	-7.99	1.84E-19
SFRP1	-4.56	7.48E-112	-6.44	4.51E-308
CACNA1A	-4.59	3.93E-21	-4.22	1.45E-40
UNC5A	-4.60	1.53E-08	-4.68	1.55E-12
DOCK10	-4.60	7.73E-05	-16.50	7.24E-20
MMP3	-4.62	7.98E-39	-10.92	0.00E+00
OTUD7A	-4.62	1.71E-05	-3.11	1.01E-05
ANKRD65	-4.74	2.28E-04	-2.70	2.54E-09
8030451A03Rik	-4.76	5.25E-44	-12.98	8.75E-04
STAC	-4.77	7.64E-15	-3.60	2.81E-22
GGT5	-4.83	6.52E-55	-5.86	6.24E-122
TNNT2	-4.89	0.00E+00	-3.82	0.00E+00
EHD3	-4.91	4.60E-203	-7.37	0.00E+00
PDZD2	-4.93	9.88E-143	-30.60	7.14E-09
OLR1	-4.96	5.89E-11	-3.33	3.99E-13
ID1	-4.99	0.00E+00	-3.42	0.00E+00
PLEK	-5.07	2.93E-06	-4.17	6.58E-10
HDDC3	-5.21	1.80E-33	-5.70	8.96E-77
HOXB3	-5.24	3.13E-20	-6.00	1.13E-48
AMDHD1	-5.38	5.79E-14	-9.35	2.96E-43
SEMA6D	-5.60	9.27E-10	-7.68	5.54E-25
HAL	-5.63	2.50E-46	-5.78	1.26E-122
ATOH8	-5.63	1.65E-45	-8.59	9.15E-154
IGLON5	-5.71	1.15E-19	-7.08	3.97E-43
CNTNAP3	-5.72	2.78E-08	-2.09	7.46E-05
Clca1/Clca2	-5.76	0.00E+00	-5.78	0.00E+00
CFI	-5.79	2.55E-09	-9.52	3.05E-28
PRSS12	-5.85	8.58E-26	-5.03	1.63E-46
PDE2A	-5.88	1.61E-09	-6.54	2.80E-36
LRTM2	-6.12	4.30E-05	-4.37	6.95E-05
Gbp6	-6.12	4.30E-05	-4.85	1.80E-09
TGFB1	-6.23	2.17E-19	-30.21	5.45E-147
CADM1	-6.28	2.15E-126	-6.29	0.00E+00
Lipo1	-6.31	3.15E-04	-3.83	2.23E-07
PDGFRA	-6.47	1.93E-53	-15.73	0.00E+00
SOD3	-6.51	5.28E-40	-4.83	1.67E-79
Serpina3k	-7.10	3.95E-06	-9.40	1.18E-13
STEAP4	-7.22	4.17E-10	-35.65	2.42E-103

Appendix F: Continued

Gene Symbol	n=1		n=2	
	Fold Change (<i>Tgfb3</i> ^{-/-} / <i>Tgfb3</i> ^{+/+})	p-value	Fold Change (<i>Tgfb3</i> ^{-/-} / <i>Tgfb3</i> ^{+/+})	p-value
MEGF6	-7.25	4.85E-227	-10.21	0.00E+00
C2orf40	-7.28	8.40E-13	-4.38	1.86E-31
PNMAL2	-7.30	2.43E-06	-36.16	4.79E-20
SAA2	-7.37	4.57E-05	-50.76	2.33E-56
Cyp2d22	-7.38	1.31E-19	-9.55	6.97E-50
SCG2	-7.50	8.98E-04	-5.56	1.25E-07
mir-101	-7.50	8.98E-04	-7.11	1.08E-04
SEZ6L	-7.50	8.98E-04	-7.42	3.19E-06
CCDC68	-7.65	4.30E-15	-5.42	1.23E-31
Clca4	-7.74	4.30E-46	-5.22	8.73E-177
HLA-B	-7.76	1.30E-224	-20.49	0.00E+00
SYT8	-7.89	5.46E-04	-3.64	5.00E-06
PLAC8	-7.89	5.46E-04	-6.80	1.86E-04
TEK	-7.94	1.34E-24	-11.24	1.31E-57
ITGBL1	-7.96	1.94E-33	-5.26	8.11E-41
ANGPTL7	-8.08	6.36E-52	-22.50	0.00E+00
SMPDL3A	-8.21	7.04E-09	-4.00	4.64E-14
S100A4	-8.38	0.00E+00	-3.29	0.00E+00
SLC13A4	-8.42	6.32E-06	-3.48	6.99E-04
2410137M14Rik	-8.68	2.01E-04	-67.68	6.04E-20
HOXB2	-9.13	3.13E-26	-5.68	4.84E-34
WDR86	-9.47	7.27E-05	-5.72	3.11E-06
SDK1	-9.67	6.18E-09	-5.47	5.12E-09
GPR88	-10.00	3.04E-07	-12.61	1.27E-27
STBD1	-10.05	7.61E-234	-10.25	0.00E+00
TMEM215	-10.06	1.33E-17	-20.61	8.29E-65
ADAMTSL2	-10.06	0.00E+00	-4.65	0.00E+00
A630023A22Rik	-10.10	1.69E-11	-3.35	2.63E-13
KIAA1324L	-10.44	1.30E-67	-14.70	1.19E-183
PCDH17	-11.05	2.85E-98	-16.87	5.25E-298
ADAM23	-11.44	5.52E-06	-4.97	1.62E-08
2610507I01Rik	-12.10	4.87E-09	-10.51	7.54E-20
GUCY1A3	-12.17	1.02E-69	-26.14	9.06E-241
PYCARD	-12.31	1.23E-14	-7.53	1.58E-53
REC8	-12.63	1.71E-09	-24.85	7.71E-32
GBP2	-16.97	2.25E-17	-55.32	1.19E-46
AIF1	-17.36	1.90E-09	-11.44	3.85E-08
SLC16A2	-18.15	2.00E-05	-10.43	2.12E-09
HSD11B1	-18.15	2.00E-05	-26.89	1.36E-14
ZFHX4	-18.94	1.16E-05	-65.83	2.19E-19

Appendix F: Continued

Gene Symbol	n=1		n=2	
	Fold Change (<i>Tgfb3</i> ^{-/-} / <i>Tgfb3</i> ^{+/+})	p-value	Fold Change (<i>Tgfb3</i> ^{-/-} / <i>Tgfb3</i> ^{+/+})	p-value
INPP5D	-20.04	5.18E-26	-12.13	3.43E-61
PNLDC1	-21.50	8.57E-23	-11.40	2.13E-56
CLDN15	-21.62	2.22E-28	-9.83	1.86E-85
2410017I17Rik	-22.10	2.35E-212	-6.69	2.77E-127
Serpinb6b	-26.30	2.58E-42	-40.24	7.39E-214
MGP	-57.85	0.00E+00	-26.77	0.00E+00

APPENDIX G

GENES >2-FOLD DYSREGULATED BETWEEN $TGFBR3^{+/+}$ AND $TGFBR3^{-/-}$ EPICARDIAL CELLS AFTER TGF β 2 INCUBATION

Gene Symbol	n=1		n=2	
	Fold Change ($Tgfb3^{-/-}$ / $Tgfb3^{+/+}$)	p-value	Fold Change ($Tgfb3^{-/-}$ / $Tgfb3^{+/+}$)	p-value
3300005D01Rik	2.05	2.96E-06	2.50	2.11E-06
4833438C02Rik	2.13	2.24E-46	2.14	2.22E-35
5730588L14Rik	2.07	6.11E-15	2.08	2.47E-07
9330179D12Rik	71.64	0.00E+00	2.31	2.82E-20
A330033J07Rik	3.39	2.70E-07	3.26	1.37E-04
AASS	15.85	2.65E-12	18.00	1.21E-08
ABCB11	5.15	1.37E-11	2.42	1.78E-04
ACAN	84.79	4.14E-26	10.28	1.35E-06
ACSBG1	2.85	2.06E-28	2.04	1.41E-10
AGPAT9	2.85	5.77E-07	4.67	5.14E-07
AKAP12	2.03	5.50E-155	2.03	2.62E-149
ALOX12	3.11	4.54E-09	4.46	1.89E-08
ALX4	86.38	1.31E-26	71.98	2.29E-19
AMN	3.43	1.31E-121	2.23	1.56E-31
ANGEL1	2.68	1.77E-09	2.38	1.20E-06
ANGPTL4	7.55	5.20E-298	6.32	1.00E-142
ANKRD1	4.34	0.00E+00	5.30	0.00E+00
ANKRD33B	4.04	5.28E-06	10.28	1.35E-06
Apol10a	13.63	1.59E-16	3.42	1.27E-21
ARHGAP20	3.96	2.72E-06	4.04	7.70E-07
ARHGAP22	2.70	4.51E-08	2.50	2.94E-06
ARHGAP8	2.12	4.91E-05	3.59	3.18E-07
ARTN	2.28	4.39E-11	2.47	1.30E-07
ATP2A3	2.16	4.62E-04	2.39	9.75E-04
B3GNT5	5.42	5.00E-06	4.79	2.82E-07
B4GALNT1	2.16	1.68E-11	2.06	1.49E-07
B4GALNT2	10.80	2.66E-155	5.91	9.36E-53
BAI1	3.69	1.78E-135	3.67	3.49E-74
BC067074	17.43	3.31E-05	8.36	7.94E-04
BCAP29	2.25	5.60E-16	2.23	5.25E-12
BCAT1	11.71	7.23E-136	5.91	1.43E-56
BMPR1B	6.02	8.28E-11	5.66	1.56E-08

Appendix G: Continued

Gene Symbol	n=1		n=2	
	Fold Change (<i>Tgfb3</i> ^{-/-} / <i>Tgfb3</i> ^{+/+})	p-value	Fold Change (<i>Tgfb3</i> ^{-/-} / <i>Tgfb3</i> ^{+/+})	p-value
BTBD11	8.88	8.75E-10	10.71	6.59E-07
C10orf47	5.90	7.08E-18	3.18	6.49E-11
C1orf115	2.55	4.10E-13	3.21	1.29E-11
C21orf7	2.75	1.23E-26	2.36	4.14E-08
C6orf132	4.88	5.46E-10	4.67	5.14E-07
CAMK2N1	2.34	5.93E-04	2.19	1.14E-04
CCDC36	7.92	1.62E-05	28.28	1.54E-07
CCDC153	3.32	1.29E-09	2.52	2.09E-04
CCL17	4.50	3.54E-30	2.21	2.35E-08
CCRN4L	2.27	3.89E-24	2.25	1.75E-20
Cd24a	5.14	5.95E-24	3.72	1.08E-07
CDKN1C	7.25	0.00E+00	3.25	7.14E-220
CGNL1	2.03	3.26E-45	2.31	7.57E-38
CGREF1	3.45	1.48E-270	2.79	3.64E-98
CHD5	2.59	5.33E-38	2.51	1.60E-19
CILP2	3.05	6.42E-35	3.72	3.49E-30
CKMT1A/CKMT1B	4.40	2.57E-84	4.32	3.65E-37
CMAHP	7.92	5.87E-10	3.86	3.83E-04
CNTFR	2.02	2.81E-04	3.50	1.08E-08
COL2A1	2.68	1.03E-17	2.52	1.08E-07
COL4A3	7.06	1.51E-53	4.34	2.01E-26
COL5A3	2.10	6.69E-28	2.45	1.77E-25
COL7A1	2.80	5.73E-27	2.65	5.66E-22
COL9A2	2.58	3.21E-06	3.03	1.04E-06
CORO2A	3.96	4.14E-213	2.35	3.43E-68
COX7A1	2.01	7.23E-14	2.28	5.33E-14
CPE	4.37	0.00E+00	2.21	8.20E-181
CPNE7	4.22	5.11E-57	5.88	3.52E-62
CSF3	5.55	4.46E-07	5.36	3.20E-05
CSGALNACT1	6.44	7.90E-97	4.29	1.77E-31
CTNNND2	121.88	5.51E-185	32.69	3.86E-107
CTSC	3.30	6.83E-27	2.25	2.62E-11
CYP46A1	2.74	1.19E-07	2.17	2.19E-04
DENND5B	2.03	3.02E-15	2.58	7.07E-17
DES	3.39	2.81E-57	2.87	1.01E-29
DGKI	7.33	2.29E-06	5.78	3.15E-04
DKKL1	3.75	1.29E-49	3.80	3.13E-25
DLX2	5.28	1.68E-10	4.76	1.18E-06

Appendix G: Continued

Gene Symbol	n=1		n=2	
	Fold Change (<i>Tgfb3</i> ^{-/-} / <i>Tgfb3</i> ^{+/+})	p-value	Fold Change (<i>Tgfb3</i> ^{-/-} / <i>Tgfb3</i> ^{+/+})	p-value
DPF1	2.12	1.20E-05	2.47	2.32E-06
DSCAML1	3.15	1.63E-39	3.00	1.59E-20
DSP	8.03	7.27E-195	5.56	1.14E-109
Dux (includes others)	20.60	3.71E-06	3.39	2.61E-04
E230032D23Rik	3.43	2.63E-04	16.71	1.67E-04
ENG	2.11	5.41E-29	3.28	1.19E-49
EPB41L1	2.05	1.29E-22	2.06	1.30E-17
EPB41L3	19.49	3.66E-25	11.39	1.13E-15
EREG	2.01	8.65E-28	2.22	5.28E-25
ETNK2	4.74	3.68E-29	2.88	1.53E-08
EXOC3L2	2.34	3.31E-16	2.72	1.42E-12
FAM123A	2.12	2.61E-10	2.14	1.50E-06
FAM134B	6.08	4.88E-04	3.86	3.83E-04
FAM159B	2.59	3.56E-70	3.11	3.57E-53
FAM20A	3.22	1.82E-16	2.05	8.69E-05
FAM43B	5.65	7.37E-22	4.39	3.64E-09
FAM71F1	2.54	3.19E-06	2.44	8.96E-04
FAM81A	3.17	4.00E-21	2.43	5.77E-08
FAM89A	7.44	1.84E-18	2.97	1.40E-04
FAT2	3.09	1.88E-06	10.03	6.64E-10
FAXC	12.48	5.86E-34	8.21	1.51E-24
FCHO1	2.18	1.34E-06	2.79	1.64E-07
FERMT1	2.87	1.01E-33	2.57	2.44E-20
FEV	5.07	8.92E-05	999.00	2.25E-04
FGF5	4.47	8.13E-39	2.82	2.59E-14
FGF10	54.68	1.16E-16	10.28	1.35E-06
Fhod3	2.42	2.11E-39	2.40	3.69E-37
FLT1	2.54	5.33E-22	2.93	9.16E-13
FOSB	2.62	4.62E-15	2.18	1.33E-10
FOXL2	4.03	4.65E-22	2.92	2.21E-11
Foxl2os	3.96	8.13E-12	2.71	6.53E-06
FRMD4B	2.55	6.22E-24	2.91	1.88E-22
FRMPD1	14.66	1.20E-14	20.14	4.57E-14
FSTL3	4.44	5.82E-92	4.90	7.65E-72
FZD10	6.32	1.09E-128	4.54	2.25E-72
GALNT9	8.72	3.62E-06	20.57	1.67E-05
GALNTL4	5.35	1.81E-36	3.18	6.49E-11
GAP43	4.43	7.11E-11	3.36	2.26E-08
GATM	3.24	9.61E-111	2.86	7.13E-48
GDF15	2.10	3.54E-09	2.94	1.48E-07

Appendix G: Continued

Gene Symbol	n=1		n=2	
	Fold Change (<i>Tgfb3</i> ^{-/-} / <i>Tgfb3</i> ^{+/+})	p-value	Fold Change (<i>Tgfb3</i> ^{-/-} / <i>Tgfb3</i> ^{+/+})	p-value
GLIS3	3.42	2.62E-46	2.49	7.71E-19
Gm3230	2.41	5.89E-05	3.47	3.58E-04
Gm11549	2.35	1.09E-04	3.05	8.54E-05
GNAL	2.46	3.42E-47	2.69	1.35E-39
GRID2	4.29	2.52E-10	3.16	1.71E-07
GRM8	3.32	1.03E-43	3.30	5.96E-20
HCK	2.56	9.34E-10	2.54	2.63E-07
HECW2	3.49	1.16E-18	5.14	1.16E-19
HIST1H1D	2.35	1.09E-04	2.97	1.22E-06
HIST1H2BL	2.10	4.76E-07	2.17	1.69E-07
Hist3h2ba	3.60	2.05E-05	3.09	1.19E-04
HMHA1	16.35	2.54E-74	7.16	6.22E-38
IGDCC4	2.46	6.78E-27	2.03	4.08E-12
IGHA1	15.06	1.68E-04	14.14	7.63E-04
IL6	2.13	9.65E-17	2.23	2.96E-11
INSL3	2.58	4.03E-89	2.42	8.09E-53
IRF6	2.44	5.13E-13	2.67	8.00E-10
ITGA6	2.82	3.65E-75	2.49	1.54E-29
JAK3	2.48	8.60E-133	2.39	3.28E-74
KCNC3	3.70	1.92E-180	3.01	8.55E-146
KCNK1	11.15	1.04E-73	3.97	1.37E-23
KCNQ5	2.15	1.33E-21	2.13	1.84E-14
KCNS3	6.67	1.01E-14	5.49	7.08E-09
KDM6A	2.14	5.57E-30	2.34	1.08E-30
KIAA1467	4.34	1.57E-99	3.16	3.75E-44
KIF1A	5.75	7.00E-12	5.57	7.13E-12
Klra18	4.76	2.62E-36	4.46	1.55E-15
Klra4	4.82	3.68E-35	3.99	7.92E-13
KRT8	4.90	1.69E-27	3.31	6.55E-15
KRT18	7.68	2.63E-19	3.99	1.80E-12
KRT80	2.75	6.13E-08	2.87	3.26E-10
LAMA2	11.49	5.24E-06	3.31	5.92E-05
LAMC2	2.08	7.46E-19	2.58	3.04E-20
LCE1B	18.23	1.92E-05	47.56	1.02E-12
LCE1E	10.30	1.71E-07	4.93	1.11E-04
Lce1f	8.88	8.75E-10	3.26	1.37E-04
Lce1g	8.89	4.03E-32	6.63	5.00E-19
Lce1h	9.29	2.34E-21	7.07	1.06E-13
LIMCH1	7.74	7.57E-243	5.52	1.60E-93
LIN28B	11.89	7.58E-09	4.63	8.88E-04

Appendix G: Continued

Gene Symbol	n=1		n=2	
	Fold Change (<i>Tgfb3</i> ^{-/-} / <i>Tgfb3</i> ^{+/+})	p-value	Fold Change (<i>Tgfb3</i> ^{-/-} / <i>Tgfb3</i> ^{+/+})	p-value
LMO7	4.05	4.54E-32	3.37	1.10E-18
LOC100503496	2.59	3.43E-09	2.30	3.15E-04
LOXL4	3.33	2.51E-09	3.67	1.01E-12
LRCH2	4.36	1.29E-05	4.96	2.19E-09
LRRK2	3.21	8.30E-08	4.42	8.30E-09
LTBP1	3.73	2.22E-214	3.29	2.21E-106
LURAP1L	3.29	9.50E-39	2.75	2.73E-20
Ly6a	999.00	5.66E-04	4.21	5.38E-06
MAB21L2	6.02	1.41E-125	4.29	2.75E-61
MANSC1	6.82	5.26E-07	21.21	2.60E-10
MAP2	3.22	2.81E-41	2.36	5.03E-16
MAP7	5.38	2.45E-16	2.35	8.71E-06
MAP3K13	2.81	6.37E-11	3.40	6.21E-13
MAP7D2	3.74	1.19E-08	3.24	1.42E-07
Masp1	8.44	8.05E-38	5.53	4.58E-22
MATN4	3.13	4.70E-307	2.51	8.38E-96
MDGA1	2.04	1.59E-12	2.07	1.57E-11
MECOM	4.16	3.02E-05	6.43	7.16E-04
MEIG1	4.37	3.75E-16	3.78	7.66E-07
MEIS3	4.25	4.07E-23	2.43	6.36E-09
MFAP3L	2.49	1.51E-13	2.42	8.82E-09
MME	3.17	2.19E-09	3.86	3.63E-08
MMP15	2.41	0.00E+00	2.21	4.19E-215
Msx3	8.88	8.75E-10	5.86	3.42E-08
MYH14	3.23	3.62E-05	4.44	1.68E-06
NAT8L	2.46	3.63E-12	2.49	3.57E-10
NDUFA4L2	2.99	8.56E-67	4.52	1.03E-63
NECAB1	28.53	1.46E-08	6.86	3.66E-04
NFATC1	3.45	3.21E-71	3.12	2.05E-48
NFATC2	3.19	8.21E-34	3.80	4.16E-33
NPAS1	2.84	4.34E-05	2.79	1.86E-04
NPR2	9.75	4.88E-286	6.12	2.60E-181
NPR3	4.79	6.90E-33	2.45	1.76E-10
OAS3	4.90	1.07E-08	7.86	3.24E-12
ODZ3	2.56	7.32E-161	2.30	7.23E-91
OLFM2	2.16	3.90E-05	2.63	2.66E-08
Olfr212/Olfr213	7.70	5.36E-11	16.71	1.67E-04
OTUD1	2.61	1.67E-14	2.08	1.05E-06
PAK6	2.64	4.35E-55	4.17	2.17E-88
PARM1	3.72	7.58E-211	2.42	1.52E-79

Appendix G: Continued

Gene Symbol	n=1		n=2	
	Fold Change (<i>Tgfb3</i> ^{-/-} / <i>Tgfb3</i> ^{+/+})	p-value	Fold Change (<i>Tgfb3</i> ^{-/-} / <i>Tgfb3</i> ^{+/+})	p-value
PAX3	999.00	9.83E-05	15.43	3.58E-04
PCOLCE2	4.92	8.92E-30	3.52	1.90E-11
Pde4d	5.22	4.32E-14	3.86	6.91E-09
Peg12	2.15	5.43E-05	2.57	4.89E-05
PEX5L	4.51	7.36E-09	7.83	1.43E-14
PIANP	5.31	1.38E-27	6.79	1.21E-21
PKP1	2.44	3.08E-05	2.95	1.00E-04
PLCG2	2.73	6.77E-11	3.86	9.40E-12
PLCL2	4.45	2.44E-14	3.39	2.05E-10
PLCXD2	2.88	2.04E-79	3.46	1.02E-83
PLD5	3.29	1.86E-41	2.18	5.37E-12
PM20D1	2.98	1.44E-06	4.88	1.74E-17
POU3F3	6.54	6.02E-10	3.75	2.21E-05
POU4F3	8.22	1.58E-13	3.86	2.36E-06
PPL	12.29	5.69E-182	7.94	5.62E-112
PPP1R16B	8.76	3.82E-63	9.64	4.86E-37
PPP2R2C	3.93	4.57E-130	3.13	4.12E-62
PRDM6	6.64	3.12E-97	3.80	3.65E-34
PRDM16	2.77	6.18E-09	2.87	6.48E-08
PRSS56	2.63	4.11E-13	2.67	1.71E-07
PTPRB	5.76	9.99E-174	5.20	2.31E-132
RAB37	4.36	8.83E-19	2.95	8.79E-07
RAB39B	20.21	3.88E-11	7.71	9.33E-05
RADIL	4.70	1.04E-10	3.74	5.15E-05
RAP1GAP2	3.03	4.83E-33	3.76	1.60E-34
RAP1GAP	2.06	3.35E-04	2.67	1.43E-05
RASD1	3.34	1.89E-16	2.13	8.85E-06
RASGEF1A	4.42	4.59E-13	4.00	2.75E-08
RBM20	4.63	6.41E-33	6.32	3.74E-33
RHBDL2	2.13	2.99E-04	3.07	2.70E-05
RHOV	2.52	1.20E-07	2.30	2.52E-05
RIMS2	59.96	5.84E-53	44.99	6.80E-34
RMRP	2.55	7.73E-31	2.13	3.40E-08
RNF152	3.72	8.56E-12	2.79	1.18E-07
Rprl2	999.00	2.16E-16	999.00	1.25E-12
Rprl3	999.00	3.24E-40	999.00	1.18E-17
RUNX1T1	10.30	2.45E-22	6.03	3.93E-14
SCT	2.08	8.16E-07	2.40	4.93E-04
SDC3	3.22	5.62E-101	2.52	9.48E-53
SEMA3G	4.88	5.46E-10	3.94	2.54E-07

Appendix G: Continued

Gene Symbol	n=1		n=2	
	Fold Change (<i>Tgfb3</i> ^{-/-} / <i>Tgfb3</i> ^{+/+})	p-value	Fold Change (<i>Tgfb3</i> ^{-/-} / <i>Tgfb3</i> ^{+/+})	p-value
SEMA7A	4.23	1.33E-10	2.57	6.55E-06
SH2D4A	3.56	1.03E-43	3.75	7.34E-17
SH3BGR	6.08	4.88E-04	6.11	1.64E-04
SHC3	12.28	1.84E-06	20.57	1.67E-05
SLC2A5	5.32	1.11E-06	2.85	7.25E-04
SLC38A4	3.57	1.04E-05	3.57	4.91E-04
SLC4A4	4.33	7.81E-128	4.22	3.50E-108
SLC7A5	3.96	0.00E+00	2.09	1.13E-192
Snhg9	3.14	6.89E-28	4.36	3.18E-88
SNRPN	6.34	1.55E-09	3.54	6.55E-05
SNTG1	4.96	1.29E-22	6.31	8.13E-11
SNURF	6.24	2.48E-09	3.54	6.55E-05
SORCS2	2.88	1.15E-25	2.88	4.16E-24
SOX11	13.08	1.24E-18	3.11	8.76E-07
SOX13	4.82	1.86E-58	3.19	1.42E-27
SP6	3.34	1.59E-135	2.40	1.08E-48
ST6GAL1	4.13	1.50E-44	3.30	5.63E-25
ST8SIA2	7.61	5.98E-15	2.38	1.20E-06
STOX2	2.19	2.51E-34	2.00	1.61E-15
SYCE1	6.58	1.50E-15	13.71	4.53E-17
SYT13	999.00	4.83E-09	13.50	2.37E-06
TACSTD2	9.77	6.66E-19	3.18	7.17E-06
TBX1	13.47	3.76E-07	5.46	5.99E-04
TBX4	9.19	3.20E-10	5.66	7.26E-05
TEX15	2.12	1.35E-18	2.52	3.74E-26
TFRC	3.32	8.56E-29	3.28	2.98E-30
THBD	3.02	2.50E-39	2.83	2.50E-21
TLL1	17.43	1.76E-09	7.71	5.70E-06
TLR5	7.47	1.42E-10	4.24	1.25E-05
TMEFF2	2.92	6.96E-54	2.39	1.11E-26
TMEM132C	12.15	4.49E-09	5.14	5.98E-05
TNFAIP3	2.39	1.20E-65	2.24	1.90E-46
TNFRSF19	13.08	6.39E-07	3.86	9.09E-04
TNFRSF11B	3.36	5.69E-98	2.06	3.76E-28
TRANK1	39.62	5.59E-12	11.57	1.54E-07
TSIX	999.00	0.00E+00	342.57	1.86E-187
TUBA8	3.27	2.02E-08	2.68	5.48E-05
UNCX	2.95	2.02E-07	5.01	3.50E-07
Usp44	6.69	2.11E-11	4.11	2.22E-05
VAX2	8.19	9.86E-06	14.14	1.12E-06

Appendix G: Continued

Gene Symbol	n=1		n=2	
	Fold Change (<i>Tgfb3</i> ^{-/-} / <i>Tgfb3</i> ^{+/+})	p-value	Fold Change (<i>Tgfb3</i> ^{-/-} / <i>Tgfb3</i> ^{+/+})	p-value
VCAN	3.62	1.57E-150	2.42	2.78E-91
VEGFC	2.42	2.50E-75	2.00	2.18E-28
WASF3	7.81	3.28E-11	15.75	7.58E-14
WNT3	2.60	4.27E-43	2.02	3.61E-13
WNT7A	5.86	1.55E-19	3.98	1.09E-17
WNT7B	2.74	4.45E-08	3.62	2.27E-06
WSCD1	3.79	7.96E-09	6.43	2.58E-09
XIST	999.00	0.00E+00	2090.96	0.00E+00
Xlr3c	9.04	4.11E-31	6.30	6.33E-10
ZDHHC2	5.91	3.82E-102	3.20	2.46E-44
ZDHHC14	2.63	1.67E-06	2.62	6.15E-05
1010001B22Rik	-5.60	1.84E-05	-3.63	5.04E-09
1010001N08Rik	-2.19	2.60E-16	-3.40	2.98E-53
2210408F21Rik	-2.03	5.09E-04	-2.03	5.14E-09
2410017I17Rik	-9.92	2.70E-97	-6.52	1.00E-92
2610507I01Rik	-7.78	2.50E-08	-9.78	1.03E-14
8030451A03Rik	-4.07	1.42E-20	-7.17	7.45E-74
9530026P05Rik	-2.33	5.87E-04	-2.41	1.47E-11
9530082P21Rik	-27.23	3.37E-08	-21.77	3.58E-20
A130040M12Rik	-2.93	2.10E-04	-2.22	3.20E-05
A630023A22Rik	-5.45	6.25E-07	-5.43	1.27E-23
ACVR1B	-2.98	1.12E-17	-4.32	1.57E-63
ADAM12	-2.59	2.00E-45	-3.64	5.58E-163
ADAM33	-2.14	1.25E-04	-3.65	2.62E-13
ADAMTS14	-3.33	4.24E-07	-2.85	4.25E-10
ADAMTSL2	-10.50	0.00E+00	-5.83	0.00E+00
AHR	-2.02	3.00E-88	-2.24	2.37E-187
ALCAM	-2.93	4.99E-261	-2.79	0.00E+00
AMDHD1	-7.78	4.62E-14	-11.86	7.63E-45
ANGPTL7	-19.29	2.07E-72	-30.64	0.00E+00
ANKRD34A	-2.71	6.69E-06	-2.94	5.70E-13
ANTXR1	-2.09	1.07E-37	-2.47	8.04E-97
ANTXRL	-8.04	1.24E-05	-6.20	1.78E-11
APOE	-3.66	8.68E-122	-6.95	0.00E+00
ATOH8	-6.70	1.55E-38	-8.01	1.85E-104
ATP1B1	-3.86	0.00E+00	-4.56	0.00E+00
AUTS2	-4.22	1.31E-45	-4.54	2.79E-100
AVPR1A	-3.42	2.73E-42	-3.85	6.05E-110
BC023719	-3.25	1.71E-06	-5.19	1.23E-17
BCL3	-2.09	2.88E-08	-2.04	1.08E-10

Appendix G: Continued

Gene Symbol	n=1		n=2	
	Fold Change (<i>Tgfb3</i> ^{-/-} / <i>Tgfb3</i> ^{+/+})	p-value	Fold Change (<i>Tgfb3</i> ^{-/-} / <i>Tgfb3</i> ^{+/+})	p-value
BEGAIN	-10.50	1.83E-05	-2.63	5.51E-05
BHLHE41	-2.78	1.76E-19	-2.35	9.65E-30
BMF	-4.51	4.12E-04	-6.60	1.84E-13
BNIP3	-2.07	1.44E-04	-2.12	2.24E-09
C3	-2.65	2.60E-48	-3.28	6.97E-142
C1qtnf6	-2.10	5.47E-20	-2.45	5.17E-45
C1S	-2.13	1.16E-115	-3.44	0.00E+00
C2orf40	-21.78	3.89E-12	-25.63	8.73E-76
CACNA1A	-3.23	1.15E-13	-4.48	3.99E-37
CADM1	-7.03	5.81E-150	-7.47	0.00E+00
CCDC68	-3.41	2.00E-07	-5.63	2.75E-29
CCDC141	-2.03	1.39E-07	-2.96	1.52E-27
CD1D	-3.77	1.07E-06	-3.59	4.83E-15
CDYL2	-6.48	2.25E-04	-4.26	8.54E-05
CEBPD	-2.24	1.93E-32	-2.36	1.01E-76
CFH	-3.15	6.87E-60	-3.32	4.49E-165
CFI	-5.45	6.25E-07	-12.70	3.95E-37
CISH	-2.80	6.40E-22	-3.06	1.03E-47
Clca4	-10.78	3.55E-64	-8.33	3.70E-197
Clca1/Clca2	-8.43	0.00E+00	-9.07	0.00E+00
CLCN5	-2.05	2.11E-14	-2.23	6.42E-29
CLDN15	-7.43	7.24E-16	-13.13	6.83E-81
CLU	-3.74	1.29E-41	-4.26	3.52E-125
CMKLR1	-3.11	4.13E-09	-4.86	9.74E-31
CMYA5	-2.54	8.55E-04	-6.31	5.97E-17
CNKS3R3	-2.14	6.05E-16	-2.33	1.64E-42
CNRIP1	-2.68	5.38E-07	-3.79	1.55E-13
CPQ	-2.15	1.02E-08	-3.24	2.05E-35
CPXM1	-2.70	6.00E-62	-4.27	0.00E+00
CRLF2	-2.01	2.67E-35	-2.14	1.05E-96
CTSW	-2.73	1.64E-34	-3.16	9.56E-108
CXADR	-2.19	1.39E-142	-2.24	9.35E-258
Cyp2d22	-6.37	4.77E-18	-7.32	4.86E-34
DAAM2	-3.12	5.53E-22	-5.94	4.24E-120
DCN	-2.27	3.28E-60	-4.06	0.00E+00
DDC	-2.38	1.02E-06	-2.39	2.66E-18
DPEP1	-2.39	1.28E-05	-2.80	6.58E-12
DPP4	-3.01	3.13E-44	-3.55	5.77E-101
E130102H24Rik	-2.30	7.94E-04	-3.76	3.34E-20
EHD3	-5.39	4.36E-188	-9.14	0.00E+00

Appendix G: Continued

Gene Symbol	n=1		n=2	
	Fold Change (<i>Tgfb3</i> ^{-/-} / <i>Tgfb3</i> ^{+/+})	p-value	Fold Change (<i>Tgfb3</i> ^{-/-} / <i>Tgfb3</i> ^{+/+})	p-value
ELN	-3.15	2.35E-49	-7.56	0.00E+00
EMILIN1	-2.88	3.60E-43	-5.33	1.00E-150
EN1	-2.61	1.82E-17	-2.16	1.75E-28
ENTPD4	-2.06	4.54E-12	-2.14	2.08E-61
EPS8	-2.45	1.75E-52	-2.26	3.56E-93
EZR	-2.10	6.37E-317	-2.02	0.00E+00
F730043M19Rik	-2.84	7.19E-08	-2.59	1.86E-17
FADS6	-3.00	7.58E-05	-3.10	8.22E-07
FAM110C	-3.02	1.49E-57	-3.17	4.41E-134
FAM163A	-6.48	2.25E-04	-3.61	9.69E-06
FAM163B	-14.00	3.32E-04	-9.34	5.29E-17
FAM176B	-2.57	7.16E-100	-2.16	1.09E-129
FAM180A	-2.59	8.85E-52	-2.74	1.32E-194
FGF2	-3.70	4.50E-22	-2.90	1.87E-38
FGL2	-6.54	1.15E-06	-7.36	1.38E-14
FIGF	-2.29	8.85E-21	-2.50	7.65E-72
FMOD	-4.05	1.37E-283	-3.81	0.00E+00
FOLR1	-2.14	6.43E-37	-2.66	3.79E-157
GAS1	-2.57	5.06E-209	-2.47	0.00E+00
GAS7	-2.45	1.68E-04	-4.76	3.11E-22
GBP2	-42.01	9.01E-13	-118.62	2.28E-32
GBX2	-2.33	5.87E-04	-3.28	4.25E-09
GGCT	-2.30	1.38E-12	-2.23	3.77E-30
GGT5	-3.83	7.11E-31	-3.94	5.68E-64
GLI1	-3.74	7.13E-08	-4.12	1.06E-13
Gm2895	-5.20	4.23E-43	-4.16	1.17E-120
Gm10389	-3.55	2.05E-16	-3.06	3.13E-31
Gm10824	-2.81	4.24E-04	-3.81	1.44E-17
Gm15506	-13.23	4.90E-07	-5.97	4.70E-10
GMPR	-2.13	5.49E-11	-2.97	9.92E-50
GNAI1	-2.45	7.84E-12	-2.04	1.25E-11
GPNMB	-2.63	6.21E-27	-3.01	2.78E-61
GPR88	-3.56	8.65E-04	-7.74	3.41E-19
GPR153	-2.01	6.21E-08	-2.43	3.76E-17
GPSM3	-2.02	2.78E-06	-2.09	4.07E-13
Gsta4	-2.91	1.99E-15	-3.07	9.02E-32
GUCY1A3	-15.45	7.90E-77	-20.06	5.52E-163
H2-M2	-4.11	1.14E-04	-32.45	3.53E-54
H2-Q10	-3.61	4.77E-160	-6.38	0.00E+00
H3f3a/H3f3b	-2.13	6.67E-223	-3.23	0.00E+00

Appendix G: Continued

Gene Symbol	n=1		n=2	
	Fold Change (<i>Tgfb3</i> ^{-/-} / <i>Tgfb3</i> ^{+/+})	p-value	Fold Change (<i>Tgfb3</i> ^{-/-} / <i>Tgfb3</i> ^{+/+})	p-value
H6PD	-2.61	4.15E-69	-3.81	1.11E-262
HAL	-7.17	2.14E-36	-10.60	4.49E-159
HDDC3	-8.03	7.63E-43	-6.68	1.29E-75
HLA-B	-10.83	0.00E+00	-23.04	0.00E+00
HLA-DQB1	-3.38	1.72E-99	-3.19	3.13E-172
HLX	-3.01	3.92E-05	-4.35	1.71E-10
HOXB2	-5.65	1.06E-17	-5.62	2.57E-31
HOXB3	-5.11	1.46E-24	-7.00	4.29E-57
HOXB4	-2.58	4.16E-12	-3.32	1.61E-25
HOXD4	-2.11	3.07E-06	-2.07	5.52E-14
HSD11B1	-14.39	1.02E-07	-12.20	6.58E-15
ICAM5	-2.44	8.84E-05	-2.92	1.96E-11
ID1	-4.04	2.31E-298	-5.44	0.00E+00
ID3	-4.28	0.00E+00	-4.67	0.00E+00
IGFBP4	-3.57	9.89E-86	-5.12	0.00E+00
IGFBP6	-3.16	2.39E-21	-3.35	2.24E-62
IGLON5	-3.82	5.66E-15	-7.86	6.24E-39
IL13RA1	-2.06	1.75E-07	-2.39	7.35E-17
IL1RL2	-2.72	7.93E-08	-4.79	1.28E-38
IL4R	-2.73	7.91E-69	-3.66	2.30E-209
INPP5D	-9.22	5.63E-14	-9.04	3.84E-37
INPPL1	-2.25	2.09E-197	-2.44	0.00E+00
ITGA7	-3.09	4.74E-74	-3.29	6.82E-129
ITGBL1	-4.87	2.10E-19	-6.72	5.06E-48
IVL	-2.69	4.57E-26	-3.44	4.48E-84
KCNT1	-2.38	1.96E-09	-2.65	2.22E-23
KIAA1199	-2.59	2.18E-33	-3.93	3.29E-146
KIAA1324L	-6.80	3.72E-45	-9.25	6.07E-121
KLHL30	-4.41	1.75E-57	-5.69	2.69E-182
LCP1	-2.40	8.68E-15	-2.76	6.31E-42
LPAR1	-2.46	5.52E-82	-3.31	0.00E+00
LRRN4	-4.30	1.80E-214	-7.59	0.00E+00
LRTM2	-13.61	2.90E-07	-10.10	1.72E-06
LSP1	-2.08	2.46E-18	-3.28	8.55E-85
MAF	-2.05	5.85E-31	-2.20	2.37E-101
MAN1C1	-2.12	7.78E-75	-2.28	1.93E-169
MDM4	-2.14	5.21E-44	-2.03	4.85E-91
MEGF6	-6.98	2.67E-166	-8.13	0.00E+00
MFAP2	-2.35	6.83E-16	-3.95	1.09E-74
MGP	-80.95	0.00E+00	-114.50	0.00E+00

Appendix G: Continued

Gene Symbol	n=1		n=2	
	Fold Change (<i>Tgfb3</i> ^{-/-} / <i>Tgfb3</i> ^{+/+})	p-value	Fold Change (<i>Tgfb3</i> ^{-/-} / <i>Tgfb3</i> ^{+/+})	p-value
MGST1	-2.46	3.80E-90	-2.40	6.69E-152
Mirg	-2.02	4.21E-05	-2.92	4.34E-25
MMP3	-5.60	5.26E-31	-14.46	1.67E-279
MMP16	-2.38	1.20E-35	-2.40	9.76E-53
MMP19	-2.14	5.31E-09	-3.29	2.57E-52
MMRN2	-2.81	4.24E-04	-2.19	8.08E-06
MOB4	-3.61	6.18E-34	-2.02	1.50E-43
MPP1	-2.20	3.94E-43	-2.12	3.89E-71
MSRB2	-2.13	4.66E-04	-2.48	2.35E-09
MTSS1	-2.31	1.28E-22	-2.82	3.31E-81
MTUS2	-3.05	1.97E-15	-4.99	1.22E-77
MYLK3	-2.07	1.83E-07	-2.59	6.12E-19
MYLK	-2.44	3.11E-38	-2.45	3.33E-102
NAPRT1	-2.88	1.23E-06	-2.96	2.26E-11
NDRG1	-2.34	6.75E-82	-3.01	3.72E-266
Neat1	-2.68	1.50E-40	-2.88	3.66E-90
NEU3	-2.61	1.22E-28	-2.49	3.12E-44
NID2	-3.04	0.00E+00	-2.94	0.00E+00
NKD2	-2.79	4.65E-06	-3.81	5.61E-20
NLRC3	-3.22	1.69E-41	-3.44	7.82E-97
NPL	-2.37	8.60E-05	-5.78	8.94E-30
NPR1	-2.76	2.22E-35	-2.72	1.56E-70
NR1H4	-2.84	1.73E-06	-4.37	6.11E-41
NRGN	-2.70	3.16E-04	-5.63	2.12E-26
NUP210	-2.13	3.88E-10	-2.33	7.06E-19
Nup62cl	-6.13	4.69E-18	-5.05	8.15E-20
NXPH1	-2.48	1.23E-16	-2.24	3.62E-47
OLFML3	-2.01	3.53E-12	-4.51	4.94E-96
OLR1	-5.22	3.79E-14	-5.99	5.85E-30
OTUD7A	-6.22	2.92E-06	-4.98	1.96E-12
PCDH9	-3.09	3.25E-25	-2.52	2.54E-26
PCDH10	-3.67	1.07E-43	-2.18	5.00E-24
PCDH17	-14.68	4.09E-109	-14.50	4.93E-230
PDE2A	-7.49	5.24E-12	-8.23	2.05E-36
PDE3A	-14.00	3.32E-04	-18.93	4.23E-05
PDGFRA	-10.00	3.48E-72	-18.41	0.00E+00
PDLM4	-2.33	5.24E-07	-2.35	6.03E-18
PDZD2	-5.10	9.12E-113	-14.51	6.70E-07
PLEK	-3.98	2.08E-05	-3.79	2.88E-07
PLXNA4	-2.14	1.18E-36	-2.18	1.16E-67

Appendix G: Continued

Gene Symbol	n=1		n=2	
	Fold Change (<i>Tgfb3</i> ^{-/-} / <i>Tgfb3</i> ^{+/+})	p-value	Fold Change (<i>Tgfb3</i> ^{-/-} / <i>Tgfb3</i> ^{+/+})	p-value
PNLDC1	-6.51	3.37E-13	-9.61	1.31E-43
PNMAL2	-15.56	2.08E-08	-14.51	1.13E-12
PPM1N	-2.50	3.43E-05	-3.15	4.23E-16
PPP2R2B	-3.93	4.84E-35	-4.30	2.56E-82
PRPH	-2.44	2.79E-09	-3.25	3.06E-19
PRR15	-3.22	1.38E-16	-10.33	1.09E-135
PRSS12	-6.83	2.74E-22	-5.08	2.60E-43
PTN	-4.57	1.08E-15	-2.68	5.10E-21
PYCARD	-4.67	3.95E-08	-10.58	1.83E-64
RAB27B	-2.04	1.22E-05	-4.44	2.53E-40
RAB40B	-2.27	8.42E-06	-2.01	6.17E-14
RAB6B	-2.19	5.66E-07	-4.24	1.66E-31
RASL11A	-3.48	2.90E-59	-3.72	2.91E-248
RASL11B	-2.40	5.90E-51	-2.65	2.37E-148
RBM46	-7.26	5.35E-05	-3.53	2.61E-04
RBM47	-2.70	1.20E-04	-2.37	6.16E-06
Rcan2	-2.27	1.10E-20	-2.38	1.18E-41
REC8	-5.06	4.99E-04	-7.89	3.95E-11
RGS3	-3.30	7.66E-48	-4.08	1.75E-151
RGS16	-2.51	1.67E-14	-3.41	3.99E-45
RGS20	-5.45	2.90E-05	-22.72	3.68E-11
RIMS1	-3.11	2.69E-04	-3.01	7.21E-07
RORC	-4.61	3.34E-09	-6.50	3.04E-31
S100A4	-7.76	0.00E+00	-6.19	0.00E+00
SAA2	-40.45	2.75E-12	-265.00	3.81E-73
SCARB2	-2.59	0.00E+00	-2.62	0.00E+00
SEMA5A	-2.44	9.55E-06	-2.50	7.48E-09
SEMA6D	-3.06	1.42E-05	-10.10	5.15E-31
SEPP1	-2.90	9.79E-12	-5.82	4.47E-69
SERPINA3	-2.82	6.60E-18	-4.29	4.79E-92
Serpina3k	-19.45	7.87E-06	-6.31	3.87E-09
Serpinb6b	-24.12	1.79E-38	-38.04	3.49E-191
SFRP1	-5.26	1.26E-119	-4.74	1.42E-216
SFRP2	-2.77	4.27E-69	-3.28	5.04E-196
SH2D5	-8.56	2.17E-09	-7.09	7.05E-15
SLC39A4	-2.68	4.33E-13	-3.98	2.81E-40
SLC43A3	-2.44	2.06E-221	-2.54	0.00E+00
SLFN13	-2.62	5.51E-12	-4.99	6.32E-53
SLIT3	-2.50	4.87E-88	-2.50	5.59E-113
SMAD9	-5.71	3.62E-09	-3.55	1.80E-14

Appendix G: Continued

Gene Symbol	n=1		n=2	
	Fold Change (<i>Tgfb3</i> ^{-/-} / <i>Tgfb3</i> ^{+/+})	p-value	Fold Change (<i>Tgfb3</i> ^{-/-} / <i>Tgfb3</i> ^{+/+})	p-value
SMOC2	-4.87	2.07E-29	-5.86	4.82E-79
SMPDL3A	-3.33	8.36E-06	-4.30	2.12E-13
SMTNL2	-3.11	4.19E-22	-3.18	2.70E-40
SNCAIP	-2.11	3.35E-09	-2.16	5.33E-25
SNTG2	-3.76	4.38E-26	-2.24	9.90E-28
SOD3	-6.50	1.65E-31	-5.71	1.60E-73
SPP1	-6.81	7.78E-06	-5.75	4.92E-08
SPRR2G	-3.53	9.51E-07	-8.12	1.68E-106
SPRY2	-2.04	1.21E-39	-2.34	8.12E-81
ST3GAL1	-4.87	4.91E-42	-7.01	2.57E-170
STAC	-3.70	2.56E-09	-3.57	1.09E-17
STAP2	-2.01	1.43E-05	-3.10	1.33E-20
STBD1	-8.08	1.47E-178	-8.80	0.00E+00
STEAP4	-9.18	2.99E-10	-13.88	3.13E-52
SV2A	-2.63	1.28E-08	-2.62	7.26E-13
SVEP1	-4.57	8.96E-51	-4.68	9.85E-124
SYNGR1	-3.36	1.17E-71	-2.26	5.87E-51
SYNPO2	-2.43	1.80E-08	-5.42	1.75E-51
TAF5	-2.44	2.63E-17	-13.00	0.00E+00
TCF21	-4.28	2.11E-233	-5.23	0.00E+00
TEK	-5.08	3.84E-12	-7.53	3.41E-33
TF	-3.18	7.17E-71	-2.78	1.72E-135
TGFBI	-15.95	9.12E-24	-39.26	4.94E-170
TGFBR3	-2.69	1.18E-31	-4.28	2.08E-149
THR8	-3.05	3.06E-08	-2.85	6.21E-20
TLR4	-2.70	4.56E-05	-3.13	2.02E-13
TMEM108	-2.21	1.43E-44	-2.19	2.98E-82
TMEM215	-16.14	1.85E-16	-10.64	1.04E-40
TMEM176B	-2.02	5.57E-58	-2.12	2.19E-148
TNC	-4.29	0.00E+00	-6.69	0.00E+00
TNIK	-2.54	6.60E-17	-2.67	1.80E-35
TNNT2	-5.00	0.00E+00	-5.24	0.00E+00
TSPAN18	-4.18	1.90E-09	-3.00	3.64E-09
UCP2	-3.84	0.00E+00	-5.40	0.00E+00
VSTM2A	-62.24	4.16E-19	-167.84	4.79E-46
VTCN1	-7.78	2.03E-05	-4.12	3.65E-09
WBSCR17	-2.76	1.46E-10	-2.00	3.49E-09
XDH	-2.83	7.08E-58	-3.43	1.83E-198
ZFHX4	-11.28	6.56E-06	-19.35	1.56E-13
ZNF575	-2.18	9.89E-06	-2.09	3.01E-10

Appendix G: Continued

Gene Symbol	n=1		n=2	
	Fold Change (<i>Tgfb3</i> ^{-/-} / <i>Tgfb3</i> ^{+/+})	p-value	Fold Change (<i>Tgfb3</i> ^{-/-} / <i>Tgfb3</i> ^{+/+})	p-value
ZNF608	-2.19	8.18E-12	-2.04	1.64E-19
ZNF697	-2.04	4.53E-34	-2.14	4.32E-72
ZNF764	-2.50	2.34E-04	-2.13	1.09E-07

APPENDIX H

GENES >2-FOLD DYSREGULATED BETWEEN *TGFBR3^{+/+}* AND *TGFBR3^{-/-}* EPICARDIAL CELLS AFTER BMP2 INCUBATION

Gene Symbol	n=1		n=2	
	Fold Change (<i>Tgfbr3^{-/-}</i> / <i>Tgfbr3^{+/+}</i>)	p-value	Fold Change (<i>Tgfbr3^{-/-}</i> / <i>Tgfbr3^{+/+}</i>)	p-value
XIST	8672.44	0.00E+00	999.00	0.00E+00
TSIX	1488.02	0.00E+00	999.00	3.64E-84
9030619P08Rik	999.00	2.25E-17	999.00	2.34E-09
CHST7	999.00	3.03E-04	999.00	8.94E-04
Ly6a	999.00	6.56E-22	999.00	3.60E-05
RIMS2	999.00	1.75E-41	999.00	4.42E-21
Rprl2	999.00	3.62E-11	999.00	2.86E-37
Rprl3	999.00	4.33E-18	188.45	4.85E-57
CKM	999.00	7.73E-13	8.72	5.48E-06
ALX4	122.35	1.13E-38	72.13	1.94E-21
FGF10	32.24	8.58E-19	999.00	7.60E-07
SYCE1	30.77	7.07E-18	40.57	6.59E-12
CTNND2	24.91	3.12E-14	999.00	5.23E-06
CSGALNACT1	24.32	7.02E-192	14.58	6.47E-59
MFAP5	21.61	2.38E-23	4.96	3.45E-05
RIPK4	17.22	1.61E-09	27.95	3.78E-08
SYN2	16.85	1.48E-17	4.57	2.66E-09
FZD10	16.49	4.47E-09	27.05	6.98E-08
Usp44	16.12	7.43E-09	13.53	5.87E-04
BCAT1	13.96	1.91E-126	9.34	2.89E-31
PLD5	13.31	2.02E-19	28.85	2.05E-08
CTHRC1	13.24	3.48E-124	24.13	2.09E-102
COL9A2	12.46	8.70E-04	999.00	2.47E-04
DSCAML1	12.46	1.66E-09	7.89	9.34E-07
CRABP2	12.00	1.78E-93	9.39	1.18E-22
PPP2R2C	11.58	7.73E-14	4.99	5.53E-10
PVRL4	11.45	3.89E-21	8.84	2.06E-09
MS4A10	10.91	3.97E-43	5.05	4.30E-08
FAXC	10.91	3.21E-22	3.29	1.92E-05
PCOLCE2	10.72	1.92E-19	9.92	5.90E-07
Cbr2	10.70	1.45E-12	20.74	4.95E-06

Appendix H: Continued

Gene Symbol	n=1		n=2	
	Fold Change (<i>Tgfb3</i> ^{-/-} / <i>Tgfb3</i> ^{+/+})	p-value	Fold Change (<i>Tgfb3</i> ^{-/-} / <i>Tgfb3</i> ^{+/+})	p-value
Xlr3c	10.47	4.52E-32	4.36	2.35E-04
IL17RE	10.21	5.04E-31	16.83	9.50E-13
LIMCH1	10.16	5.39E-117	15.07	2.33E-81
TSHR	9.89	3.54E-05	9.02	1.73E-04
CD80	9.77	2.72E-25	33.36	9.40E-10
FAM134B	9.53	5.74E-05	8.57	3.02E-04
DSP	9.46	2.53E-22	10.25	2.15E-23
B4GALNT2	9.43	2.11E-73	9.92	1.67E-20
Klra18	9.38	1.26E-29	999.00	2.75E-06
NT5E	9.21	3.66E-14	6.01	6.92E-04
Klra4	9.18	8.42E-29	999.00	2.75E-06
GALNTL4	9.01	1.26E-31	10.37	1.58E-13
LMO7	8.71	5.99E-172	8.85	4.15E-55
IL6	8.48	1.00E-12	13.53	5.87E-04
NKX2-8	8.37	8.45E-32	11.15	4.38E-26
CYFIP2	8.36	1.46E-20	3.98	1.40E-06
CUX2	8.33	4.70E-14	4.06	6.67E-05
SEC14L5	8.30	6.32E-06	13.53	5.66E-07
HS3ST6	8.14	3.54E-15	5.41	1.73E-10
ALOX5	8.06	1.36E-22	4.96	1.53E-06
WASF3	7.98	8.96E-15	4.06	6.67E-05
PARM1	7.75	2.21E-51	5.26	6.45E-24
NFATC1	7.64	5.62E-28	5.77	4.36E-14
D730039F16Rik	7.64	8.29E-31	4.96	6.99E-08
CKMT1A/CKMT1B	7.42	4.85E-12	15.63	1.01E-11
RAI2	7.33	1.65E-10	4.85	2.48E-06
TSPAN12	7.14	1.91E-11	5.86	1.09E-04
RARRES2	7.10	7.85E-175	2.91	4.97E-16
CNKS1R1	6.89	3.12E-07	999.00	9.94E-06
MAMDC2	6.89	2.42E-25	3.04	2.68E-05
NPR2	6.84	1.23E-94	5.02	3.94E-54
ANXA8L2	6.73	2.57E-264	9.73	2.85E-218
EPB41L3	6.70	1.95E-17	2.71	4.25E-04
CGREF1	6.69	5.50E-38	8.17	1.75E-27
SPOCK2	6.69	1.46E-18	3.85	8.02E-06
SERPINE2	6.60	1.51E-176	6.25	2.41E-121
PIANP	6.59	7.79E-53	8.34	2.54E-19
SH2D4A	6.55	2.27E-53	6.49	9.69E-17

Appendix H: Continued

Gene Symbol	n=1		n=2	
	Fold Change (<i>Tgfb3</i> ^{-/-} / <i>Tgfb3</i> ^{+/+})	p-value	Fold Change (<i>Tgfb3</i> ^{-/-} / <i>Tgfb3</i> ^{+/+})	p-value
HMHA1	6.46	2.97E-25	10.14	4.55E-25
KLRG2	6.42	3.16E-28	3.25	5.09E-08
POSTN	6.41	1.73E-05	16.23	9.95E-05
ST14	6.41	9.42E-53	10.97	4.20E-54
C19orf33	6.32	4.92E-194	8.15	1.61E-73
MAB21L2	6.31	5.91E-15	5.14	2.64E-08
BAI1	6.23	9.37E-18	10.14	3.84E-17
KRT8	6.23	5.28E-28	4.13	2.69E-10
P2RX3	6.07	6.62E-29	2.57	2.40E-09
PIK5	6.04	4.24E-05	6.01	6.92E-04
CST9L	6.02	1.07E-23	4.87	2.13E-04
NIPAL4	5.97	1.86E-21	10.19	3.13E-21
SNAI3	5.86	3.11E-16	5.94	5.22E-12
SP9	5.79	1.63E-20	8.72	7.47E-35
Tnfrsf26	5.74	1.39E-141	7.60	7.20E-38
PPL	5.67	2.87E-31	5.10	2.06E-23
PPP1R16B	5.66	5.47E-11	14.73	5.90E-11
CTSC	5.62	9.75E-04	14.43	3.26E-04
GJB3	5.62	2.32E-14	4.87	2.13E-04
FLT1	5.55	3.77E-25	32.01	1.00E-17
EXOC3L2	5.55	3.26E-07	3.01	3.55E-04
ST6GAL1	5.50	4.32E-18	3.36	1.08E-04
SVOP	5.47	3.52E-101	5.35	8.17E-44
KCNC3	5.41	5.75E-25	13.93	1.70E-28
AMN	5.32	3.02E-13	9.92	6.50E-09
FGF5	5.29	8.33E-47	3.49	1.00E-06
GRHL3	5.28	4.77E-24	5.07	9.35E-18
SCN4B	5.22	2.04E-07	12.92	1.95E-09
ACOT11	5.13	5.59E-20	5.30	6.79E-14
ITGA6	5.05	2.07E-22	2.64	2.35E-14
GNA15	5.01	2.96E-19	5.57	3.78E-10
PTPRB	4.97	4.93E-14	12.77	1.73E-17
PERP	4.95	8.39E-249	4.73	4.66E-121
KIAA1467	4.93	7.46E-14	4.71	1.09E-06
COL11A1	4.92	1.90E-50	3.53	5.78E-21
WNT3	4.87	7.40E-11	8.42	2.14E-10
NOG	4.86	8.86E-248	4.30	2.88E-139
SRPX	4.81	0.00E+00	3.65	1.28E-61
ANGPTL4	4.80	2.58E-13	61.31	3.71E-18
MEIS3	4.80	3.14E-31	5.32	6.00E-17

Appendix H: Continued

Gene Symbol	n=1		n=2	
	Fold Change (<i>Tgfb3</i> ^{-/-} / <i>Tgfb3</i> ^{+/+})	p-value	Fold Change (<i>Tgfb3</i> ^{-/-} / <i>Tgfb3</i> ^{+/+})	p-value
VNN1	4.79	1.02E-100	5.14	3.23E-56
GAL3ST2	4.69	1.16E-07	7.94	3.16E-08
HCK	4.68	5.61E-16	5.47	3.07E-12
PRDM8	4.67	1.83E-11	4.16	1.56E-07
EGFL8	4.64	6.04E-294	4.13	1.34E-21
PEX5L	4.59	5.35E-13	3.94	1.61E-09
FGFBP3	4.58	3.85E-51	5.91	5.43E-19
SLC37A2	4.58	6.74E-21	5.19	3.80E-19
Serpinb9b	4.51	5.11E-68	5.82	1.49E-18
1700030C10Rik	4.42	7.60E-17	2.91	3.35E-04
LRRC3	4.40	4.11E-08	3.81	6.94E-05
TEX15	4.40	7.76E-10	3.23	1.05E-04
MYH14	4.26	3.46E-07	2.95	9.20E-05
DKKL1	4.25	1.31E-06	6.99	7.99E-06
ANKS1B	4.24	1.36E-44	2.91	2.11E-16
COL5A3	4.23	4.50E-15	3.76	5.32E-06
MMP15	4.20	8.58E-73	6.83	3.91E-72
Ces2f	4.18	7.98E-36	4.96	3.49E-13
RLN1	4.15	2.90E-04	999.00	4.70E-04
GPX3	4.13	5.09E-18	2.34	1.99E-05
LEFTY2	4.09	8.85E-10	6.99	7.99E-06
SHISA4	4.07	1.15E-305	2.42	1.09E-38
PAK6	4.05	1.49E-11	3.95	3.09E-08
SHANK2	4.05	1.24E-24	2.30	1.40E-07
C9orf116	4.02	1.16E-158	3.27	9.07E-36
WISP1	4.01	7.61E-193	6.96	3.03E-108
PROS1	3.98	1.70E-49	3.44	1.25E-18
FAM124A	3.91	3.95E-08	4.01	2.83E-05
C1orf115	3.90	2.48E-46	2.57	8.40E-07
STR6	3.89	1.55E-08	3.10	1.80E-05
Snhg9	3.87	4.67E-28	5.05	1.62E-11
CEND1	3.86	3.64E-06	13.53	5.66E-07
ENHO	3.85	9.28E-05	6.99	7.99E-06
SH3YL1	3.85	4.71E-15	5.91	2.92E-09
Fhod3	3.83	2.81E-38	4.01	4.39E-31
RBM20	3.82	3.33E-19	5.86	4.95E-17
SCN3B	3.81	1.05E-105	3.70	1.92E-47
PID1	3.80	2.77E-17	3.25	5.08E-10
TMSB10/TMSB4X	3.80	0.00E+00	2.57	0.00E+00
SOX13	3.78	8.10E-07	4.73	4.02E-06

Appendix H: Continued

Gene Symbol	n=1		n=2	
	Fold Change (<i>Tgfb3</i> ^{-/-} / <i>Tgfb3</i> ^{+/+})	p-value	Fold Change (<i>Tgfb3</i> ^{-/-} / <i>Tgfb3</i> ^{+/+})	p-value
PDGFRL	3.78	2.04E-09	4.66	9.09E-05
CPE	3.78	2.40E-192	3.42	4.36E-97
NRN1	3.73	8.70E-19	4.67	8.04E-08
PITPNM3	3.73	7.82E-06	4.12	1.58E-04
A730035I17Rik	3.73	7.82E-06	3.38	9.48E-04
PRDM6	3.70	1.07E-30	2.62	1.14E-08
SLC7A3	3.68	2.45E-34	3.70	5.11E-12
SERPINF1	3.66	2.18E-71	2.41	1.01E-17
PLTP	3.62	0.00E+00	5.42	9.40E-322
SLC17A9	3.61	7.95E-12	2.75	3.07E-05
GPC4	3.60	4.66E-50	2.17	2.06E-28
MREG	3.59	3.71E-31	3.06	1.58E-13
MATN4	3.58	2.36E-22	12.62	1.43E-22
ADRB3	3.57	1.31E-25	5.61	5.69E-20
CORO2A	3.57	2.23E-18	5.02	8.73E-17
CRIP1	3.53	0.00E+00	2.41	3.19E-118
STOX2	3.51	1.25E-23	4.81	2.67E-16
BFSP2	3.48	6.45E-14	3.43	3.56E-06
REEP2	3.47	5.36E-56	4.20	2.40E-32
CELF5	3.44	3.38E-69	2.32	1.82E-22
TNFRSF18	3.37	1.57E-67	3.55	1.66E-39
PDK4	3.37	2.41E-06	3.25	3.88E-04
Bmyc	3.35	7.25E-65	3.93	2.71E-30
REM1	3.35	1.15E-35	3.91	4.44E-05
RPRM	3.35	1.09E-69	3.70	5.87E-35
PSTPIP1	3.35	8.58E-74	3.15	1.78E-32
ANGPTL2	3.32	1.32E-30	2.71	3.77E-20
5830418P13Rik	3.30	6.62E-23	2.68	1.45E-08
PITPNC1	3.30	1.96E-39	2.61	9.79E-13
SLC29A4	3.29	7.09E-12	2.66	1.58E-04
P2RX7	3.27	2.62E-39	5.62	1.87E-39
ANKRD35	3.26	1.96E-10	4.06	8.95E-07
LTBP1	3.26	7.07E-79	3.88	1.95E-30
ABCG1	3.24	1.43E-11	4.61	3.50E-11
C13orf33	3.24	2.23E-45	2.54	1.89E-07
MMP10	3.21	1.38E-08	8.42	9.51E-06
DCXR	3.21	6.36E-219	2.51	1.76E-72
RASGRP3	3.20	2.88E-11	3.20	2.48E-04
PLEK2	3.20	8.06E-27	3.10	7.17E-08
CTSH	3.17	3.96E-28	3.83	7.50E-08

Appendix H: Continued

Gene Symbol	n=1		n=2	
	Fold Change (<i>Tgfb3</i> ^{-/-} / <i>Tgfb3</i> ^{+/+})	p-value	Fold Change (<i>Tgfb3</i> ^{-/-} / <i>Tgfb3</i> ^{+/+})	p-value
CCBE1	3.17	2.20E-62	2.20	1.84E-09
PTPRVP	3.16	2.58E-71	2.75	1.79E-43
RAP1GAP2	3.13	2.13E-04	3.25	3.88E-04
SIGLEC10	3.12	1.01E-29	2.98	1.50E-07
ARHGAP24	3.12	1.91E-12	2.31	2.22E-04
Nppb	3.09	1.13E-16	7.21	4.69E-06
ANKRD1	3.04	2.05E-174	12.87	1.44E-207
RPL22L1	3.04	2.23E-149	4.10	1.38E-17
PRRG4	3.04	2.37E-63	3.25	2.45E-21
SERPINB9	3.03	4.21E-130	2.36	6.82E-13
FSTL3	3.01	2.77E-06	2.64	9.72E-04
UCHL1	2.99	1.29E-116	5.72	3.16E-47
DES	2.99	5.24E-45	3.95	3.03E-36
ATG9B	2.98	6.72E-42	5.15	7.89E-42
C16orf89	2.98	9.53E-16	4.15	1.85E-08
LTB4R	2.98	1.37E-59	3.12	6.90E-26
PDIA5	2.94	5.16E-98	2.50	1.46E-27
KCNJ4	2.93	3.01E-08	4.21	4.50E-13
Apol10a	2.92	1.84E-23	5.71	2.23E-16
SP6	2.91	7.61E-10	3.35	7.93E-08
LMOD1	2.90	2.01E-12	4.09	2.92E-08
PVRL1	2.90	9.58E-35	2.30	5.17E-12
CD109	2.87	9.87E-167	2.64	5.72E-35
VWA7	2.87	2.01E-16	2.60	1.05E-08
HPRT1	2.84	3.42E-235	2.46	1.13E-44
Ugt1a7c	2.82	7.42E-101	3.54	1.24E-41
UGT1A6	2.81	1.33E-80	3.19	1.18E-30
CDKL2	2.81	1.73E-18	2.75	3.07E-05
FAM212B	2.81	1.39E-131	2.69	4.89E-51
COL18A1	2.80	9.81E-125	5.14	1.08E-144
HLA-DRB1	2.80	6.10E-222	3.32	1.95E-145
CYBA	2.80	9.65E-160	2.89	5.46E-31
1700003M07Rik	2.79	2.35E-14	4.43	3.30E-07
DLX2	2.79	2.71E-19	2.84	1.11E-09
PRKAA2	2.79	2.77E-16	2.67	1.17E-06
FAM129C	2.78	1.54E-04	4.25	9.94E-05
SLC2A9	2.78	3.81E-16	2.96	6.28E-08
CA12	2.78	8.19E-15	2.71	5.25E-07
UGT1A4	2.77	2.87E-64	3.71	2.31E-33
UGT1A9	2.77	2.87E-64	3.70	3.55E-33

Appendix H: Continued

Gene Symbol	n=1		n=2	
	Fold Change (<i>Tgfb3</i> ^{-/-} / <i>Tgfb3</i> ^{+/+})	p-value	Fold Change (<i>Tgfb3</i> ^{-/-} / <i>Tgfb3</i> ^{+/+})	p-value
UGT1A1	2.77	1.64E-64	3.64	8.80E-33
UGT1A3	2.77	1.11E-64	3.54	1.14E-31
FAM26E	2.74	2.14E-04	4.33	9.00E-04
SCUBE3	2.74	5.88E-13	3.00	3.28E-13
MDM2	2.72	0.00E+00	2.39	0.00E+00
SCXA/SCXB	2.71	1.95E-12	2.32	5.06E-07
NDUFA13	2.70	0.00E+00	2.86	5.67E-136
9530053A07Rik	2.69	3.85E-23	5.70	1.21E-19
EVPL	2.69	5.22E-13	2.88	1.72E-11
TM4SF1	2.67	9.81E-113	3.22	2.02E-27
WNT11	2.65	6.30E-82	4.29	1.60E-66
HEBP2	2.65	7.76E-66	2.62	1.31E-18
ABCB1	2.63	7.70E-06	3.80	6.29E-07
CCND1	2.63	0.00E+00	2.75	3.95E-124
VAMP5	2.63	1.16E-80	2.47	3.18E-22
DAPK2	2.62	6.77E-08	4.91	4.15E-07
EIF2S3	2.61	1.25E-138	3.48	9.19E-47
PRR7	2.61	1.76E-20	2.71	1.76E-09
Ces2e	2.60	1.68E-211	3.19	2.56E-122
NDUFC2	2.60	0.00E+00	2.04	1.57E-41
FBXO25	2.60	1.13E-115	2.01	1.56E-17
MESP2	2.58	3.11E-08	5.27	7.89E-11
TMEM37	2.58	4.63E-28	3.78	5.06E-14
NTN4	2.57	6.49E-12	3.31	2.82E-11
ARHGEF4	2.57	2.02E-09	3.23	3.41E-12
ITGB4	2.54	1.75E-126	5.04	1.61E-212
Peg12	2.53	3.39E-08	3.41	3.97E-04
ACPP	2.52	9.33E-07	3.85	8.02E-06
CTH	2.52	4.25E-14	3.83	7.50E-08
INHBA	2.52	1.23E-39	3.52	6.85E-25
P4HA3	2.52	4.06E-07	2.95	1.89E-06
SDC1	2.52	5.91E-230	2.62	2.22E-95
TMEM125	2.50	1.26E-06	5.59	2.91E-05
NDUFB6	2.50	3.60E-280	3.38	1.12E-81
Miat	2.49	6.18E-08	8.12	1.65E-05
GFRA2	2.49	2.90E-06	3.13	2.79E-05
COX6B2	2.49	3.72E-237	2.17	1.66E-53
2900026A02Rik	2.49	2.25E-81	2.08	1.77E-23
GLCE	2.48	1.09E-15	2.59	5.63E-04
HMCN2	2.47	2.09E-10	2.39	5.97E-06

Appendix H: Continued

Gene Symbol	n=1		n=2	
	Fold Change (<i>Tgfb3</i> ^{-/-} / <i>Tgfb3</i> ^{+/+})	p-value	Fold Change (<i>Tgfb3</i> ^{-/-} / <i>Tgfb3</i> ^{+/+})	p-value
VCAN	2.46	4.35E-07	2.86	3.53E-05
SYTL1	2.46	8.36E-27	2.45	2.25E-15
Ifi27l1	2.46	1.47E-303	2.10	1.57E-57
DUSP15	2.45	7.57E-13	2.57	5.55E-08
CYP1B1	2.44	5.39E-181	3.01	3.83E-58
Pmaip1	2.44	9.21E-164	2.90	2.13E-49
Snhg8	2.42	9.54E-236	2.22	2.84E-26
Snora24	2.42	1.16E-235	2.22	1.24E-26
SPR	2.41	1.56E-64	2.21	7.41E-19
SAPCD1	2.40	6.15E-04	4.77	1.50E-05
LAMC2	2.40	4.71E-11	3.61	1.19E-09
CXXC4	2.39	1.15E-04	5.64	1.82E-04
HYAL1	2.39	1.66E-86	3.28	1.42E-73
DGKA	2.39	3.50E-57	2.65	2.59E-41
AKR1B1	2.38	1.55E-74	2.61	5.55E-32
Gm6644	2.38	1.55E-74	2.61	5.55E-32
VAT1L	2.38	1.34E-13	2.29	1.98E-04
B4GALNT1	2.37	1.27E-05	4.41	4.48E-06
PLCXD2	2.36	7.76E-27	2.73	4.60E-18
HTRA1	2.36	1.75E-141	2.38	5.00E-70
GLDC	2.36	7.49E-18	2.21	7.48E-09
B230344G16Rik	2.35	1.75E-11	5.75	2.57E-28
PPP2R3C	2.35	2.37E-73	2.09	5.80E-08
RPS2	2.34	0.00E+00	3.82	0.00E+00
Rps28	2.34	3.76E-296	2.47	4.26E-71
RPS29	2.34	1.49E-294	2.45	3.25E-68
INHBB	2.33	1.24E-18	3.84	1.76E-31
LTB4R2	2.32	4.51E-54	3.43	2.96E-52
FKBP1B	2.32	1.48E-08	2.55	4.94E-05
SCN1B	2.32	2.18E-44	2.42	3.53E-37
MMP2	2.32	0.00E+00	2.15	1.06E-301
FAM115C	2.31	8.86E-24	2.94	5.53E-12
IMMP1L	2.31	5.82E-16	2.83	3.14E-04
GDF15	2.30	7.57E-08	4.90	2.48E-10
9230114K14Rik	2.29	7.82E-48	2.23	2.79E-06
FBXW9	2.28	2.41E-182	2.76	2.60E-87
POLR3K	2.28	2.26E-106	2.43	2.79E-27
MGLL	2.28	6.25E-159	2.18	9.43E-45
TTLL9	2.27	3.03E-05	4.24	3.07E-06
FAM132B	2.26	1.80E-22	3.56	4.21E-33

Appendix H: Continued

Gene Symbol	n=1		n=2	
	Fold Change (<i>Tgfb3</i> ^{-/-} / <i>Tgfb3</i> ^{+/+})	p-value	Fold Change (<i>Tgfb3</i> ^{-/-} / <i>Tgfb3</i> ^{+/+})	p-value
ITGB1	2.25	0.00E+00	2.22	6.25E-231
NDUFA1	2.25	1.00E-271	2.21	3.71E-44
ATP5E	2.24	0.00E+00	3.18	1.10E-78
LGALS1	2.24	0.00E+00	2.07	0.00E+00
SDC3	2.23	4.84E-04	6.61	2.43E-04
CDO1	2.23	2.01E-34	3.62	7.55E-29
MTHFS	2.23	8.68E-27	2.39	2.25E-06
CDC42BPG	2.23	6.33E-173	2.30	1.66E-106
METRNL	2.23	3.83E-162	2.08	1.08E-38
TSPAN8	2.22	6.97E-05	10.37	3.19E-05
CILP2	2.22	3.06E-05	3.68	8.25E-06
LINC00493	2.22	6.66E-23	3.28	7.81E-08
NOTCH3	2.22	1.24E-43	2.45	4.68E-49
PLEKHN1	2.22	4.50E-21	2.41	3.93E-12
1110038B12Rik	2.22	1.29E-152	2.40	1.99E-26
PMEPA1	2.19	3.22E-117	2.16	1.56E-70
PET100	2.18	2.68E-81	2.05	1.27E-13
Gm10393	2.17	3.34E-139	3.86	1.18E-80
TRIB3	2.17	1.88E-94	3.30	1.15E-31
ARF6	2.16	6.29E-47	3.70	9.77E-42
C15orf59	2.16	1.39E-12	3.63	1.89E-13
4932441J04Rik	2.16	2.59E-14	2.28	9.36E-04
MRPS14	2.16	1.04E-112	2.12	6.86E-22
DHRS9	2.15	3.74E-16	2.45	5.21E-06
GLIPR2	2.15	7.15E-81	2.19	3.36E-20
ORAOV1	2.15	1.15E-81	2.19	1.42E-23
EFNA3	2.14	3.01E-05	4.66	6.06E-12
TRIM7	2.14	8.20E-16	2.67	8.67E-16
EFS	2.14	8.52E-19	2.45	9.17E-14
DRD4	2.13	1.00E-07	2.71	6.97E-05
PIGF	2.13	3.87E-50	2.47	3.02E-19
COX17	2.13	1.95E-145	2.46	2.40E-42
CHD5	2.12	2.57E-06	3.61	1.19E-09
PLCD4	2.12	2.72E-04	2.42	5.96E-04
AIF1L	2.11	5.39E-42	4.35	4.00E-62
ATP5I	2.11	9.75E-121	2.15	7.79E-24
ISG15	2.10	0.00E+00	3.62	0.00E+00
NAT6	2.10	9.75E-58	2.80	6.45E-50
FAM176C	2.10	1.29E-05	2.52	6.95E-06
PTGR1	2.10	2.13E-48	2.24	6.94E-12

Appendix H: Continued

Gene Symbol	n=1		n=2	
	Fold Change (<i>Tgfb3</i> ^{-/-} / <i>Tgfb3</i> ^{+/+})	p-value	Fold Change (<i>Tgfb3</i> ^{-/-} / <i>Tgfb3</i> ^{+/+})	p-value
DYNLT3	2.10	9.77E-117	2.21	3.44E-23
TMEFF2	2.10	5.68E-20	2.19	1.47E-09
CDH26	2.09	1.69E-05	4.77	1.50E-05
SLC25A40	2.09	1.03E-21	2.08	3.21E-07
COX6A2	2.08	3.25E-06	35.16	2.73E-10
LEFTY1	2.08	6.78E-11	3.74	1.75E-09
SERPINI1	2.08	2.65E-04	3.70	4.57E-05
PI4K2B	2.08	2.04E-26	2.95	3.71E-20
HSDL2	2.08	2.29E-28	2.40	9.25E-12
WNT9A	2.07	6.01E-61	2.60	9.10E-57
CDKN2A	2.06	0.00E+00	2.69	0.00E+00
TPD52	2.06	2.88E-45	2.40	2.04E-20
SIVA1	2.05	9.31E-118	2.18	3.33E-42
ACER3	2.03	9.71E-38	2.72	1.01E-14
GLRX5	2.02	2.19E-23	2.73	2.14E-34
KANK3	2.01	2.03E-23	2.77	2.27E-27
ITGB5	2.00	4.20E-50	2.60	5.18E-65
RPS18	2.00	1.63E-93	2.31	2.84E-58
BTBD6	-2.01	4.66E-07	-2.18	1.62E-15
ATXN7L1	-2.01	3.05E-08	-2.33	1.51E-22
SARDH	-2.02	5.09E-22	-2.32	1.61E-54
FMNL1	-2.03	5.94E-04	-2.18	1.64E-12
SSFA2	-2.03	4.64E-32	-2.22	3.98E-62
Clca1/Clca2	-2.03	9.02E-07	-2.60	0.00E+00
INPPL1	-2.04	9.46E-181	-2.62	0.00E+00
HSPA1A/HSPA1B	-2.04	3.18E-28	-5.16	0.00E+00
STXBP6	-2.05	6.08E-05	-2.18	1.21E-21
SEMA3E	-2.05	1.81E-04	-2.31	4.71E-17
MDK	-2.05	4.40E-06	-2.53	9.30E-20
OSGIN1	-2.06	4.49E-12	-3.09	1.71E-94
NOD1	-2.08	9.01E-40	-2.01	8.49E-76
SPEF1	-2.09	3.04E-04	-2.61	4.74E-20
RNF39	-2.10	1.17E-04	-2.18	5.99E-18
IL1R1	-2.10	7.01E-27	-2.39	2.41E-108
SAA2	-2.10	4.45E-07	-2.90	7.66E-66
LAYN	-2.11	1.22E-05	-2.58	3.67E-25
ALDH1A2	-2.11	1.54E-05	-2.62	4.37E-20
CLU	-2.11	1.02E-16	-2.96	1.12E-128
INPP5A	-2.13	1.02E-21	-2.51	3.07E-54
FLI1	-2.15	4.81E-15	-2.19	7.67E-53

Appendix H: Continued

Gene Symbol	n=1		n=2	
	Fold Change (<i>Tgfb3</i> ^{-/-} / <i>Tgfb3</i> ^{+/+})	p-value	Fold Change (<i>Tgfb3</i> ^{-/-} / <i>Tgfb3</i> ^{+/+})	p-value
ENTPD4	-2.15	7.90E-24	-2.25	1.42E-68
S1PR3	-2.15	1.35E-11	-2.74	4.97E-69
ATP1B1	-2.16	6.81E-279	-2.10	0.00E+00
SLC48A1	-2.18	2.65E-94	-2.40	0.00E+00
Ifi204	-2.18	2.77E-14	-2.69	8.05E-82
NRP2	-2.18	2.17E-37	-3.00	3.50E-210
CNKS3R	-2.19	1.64E-23	-2.39	6.65E-65
TRIB1	-2.20	2.31E-17	-2.41	2.22E-57
ABCC10	-2.20	6.30E-15	-2.80	6.75E-46
FDXR	-2.22	3.14E-14	-2.10	9.28E-36
CHD6	-2.22	7.53E-05	-2.28	4.99E-08
NPR1	-2.22	1.24E-10	-2.75	8.62E-29
EPAS1	-2.22	3.17E-09	-2.95	1.31E-30
ZFP36L2	-2.23	7.76E-51	-2.81	1.89E-262
GCLC	-2.23	1.10E-10	-3.17	1.72E-44
MKI67	-2.24	2.74E-143	-2.54	0.00E+00
HDDC3	-2.24	1.92E-06	-2.79	9.75E-32
ST3GAL1	-2.25	3.25E-121	-2.33	0.00E+00
DENND4B	-2.26	1.03E-07	-2.02	2.97E-10
A730090H04Rik	-2.26	7.39E-04	-2.11	1.12E-09
9930014A18Rik	-2.27	3.99E-41	-2.06	2.25E-115
NXPH1	-2.27	8.83E-06	-2.34	5.11E-13
H6PD	-2.27	6.01E-73	-2.67	4.60E-253
PTGS1	-2.28	7.25E-67	-2.01	4.57E-141
PRKCB	-2.29	9.48E-05	-3.46	2.07E-16
ANXA11	-2.29	1.18E-06	-3.78	1.24E-22
CENPF	-2.32	8.11E-25	-2.09	4.82E-44
RAPGEFL1	-2.34	1.70E-04	-2.02	2.64E-06
GCLM	-2.34	4.46E-28	-2.54	1.31E-70
TMEM173	-2.34	1.00E-28	-3.63	1.53E-229
FAM84A	-2.35	7.43E-70	-2.60	0.00E+00
STK11IP	-2.36	4.24E-08	-2.21	1.74E-22
TUBA4A	-2.36	9.51E-18	-4.31	2.63E-174
CPQ	-2.37	1.93E-11	-2.09	7.06E-22
Gbp6	-2.39	9.16E-04	-2.21	1.58E-09
SLFN13	-2.39	3.21E-06	-3.42	5.12E-62
TULP4	-2.41	1.74E-06	-2.08	2.35E-07
SERPING1	-2.42	7.22E-227	-3.34	0.00E+00
RGS16	-2.42	5.20E-10	-4.35	5.85E-79
BBS1	-2.43	1.66E-05	-2.32	4.78E-11

Appendix H: Continued

Gene Symbol	n=1		n=2	
	Fold Change (<i>Tgfb3</i> ^{-/-} / <i>Tgfb3</i> ^{+/+})	p-value	Fold Change (<i>Tgfb3</i> ^{-/-} / <i>Tgfb3</i> ^{+/+})	p-value
AMOT	-2.44	4.87E-15	-2.35	2.89E-30
Hist1h2af	-2.46	8.09E-58	-5.06	0.00E+00
GPR146	-2.48	7.22E-11	-3.19	1.25E-43
HOXD4	-2.49	8.52E-16	-2.01	6.18E-33
Mocs1	-2.49	4.50E-26	-2.27	4.35E-74
HIST1H2AD	-2.49	9.45E-61	-2.63	1.02E-97
NETO2	-2.49	4.81E-15	-2.99	4.77E-66
ABHD15	-2.50	4.16E-04	-9.10	1.22E-05
NRIP1	-2.53	5.32E-30	-2.10	4.52E-27
SYNE2	-2.54	6.49E-300	-2.06	5.83E-236
RCOR2	-2.54	1.99E-07	-2.71	1.55E-14
PTPRZ1	-2.54	1.61E-22	-3.06	1.25E-81
MATN2	-2.55	2.29E-12	-2.53	1.60E-34
SLC16A5	-2.55	8.13E-06	-2.66	1.17E-15
MT1H	-2.56	2.90E-08	-12.82	0.00E+00
IDUA	-2.58	1.68E-07	-3.00	1.41E-21
NLGN2	-2.59	6.80E-79	-2.03	1.09E-116
C030034L19Rik	-2.59	5.44E-06	-2.12	1.13E-06
MAOA	-2.62	9.83E-82	-2.31	1.95E-251
FOXP2	-2.63	1.53E-06	-2.10	4.29E-08
IGSF3	-2.64	4.15E-30	-3.19	1.52E-147
ELMO1	-2.67	5.09E-05	-2.93	2.16E-13
STEAP4	-2.67	1.33E-09	-3.47	1.58E-55
EMILIN1	-2.67	1.27E-29	-3.57	6.90E-115
H2-T3-like	-2.68	3.71E-04	-8.50	1.38E-18
SLC43A3	-2.71	3.12E-112	-2.12	1.66E-177
USP25	-2.71	4.72E-06	-3.26	1.02E-07
CNIH2	-2.73	5.90E-06	-2.33	4.37E-08
NR4A1	-2.74	2.28E-33	-2.03	8.95E-36
ZNF503	-2.74	5.24E-33	-3.55	2.23E-120
RANBP17	-2.77	2.92E-07	-2.08	2.43E-10
BDH1	-2.77	1.26E-04	-2.29	8.93E-09
SRRM4	-2.77	8.50E-13	-2.32	8.04E-25
HIST1H2AB	-2.77	2.22E-62	-3.91	1.03E-214
SPSB1	-2.82	4.68E-54	-2.49	2.47E-101
CCNO	-2.82	9.31E-04	-4.53	9.49E-21
SHANK3	-2.83	2.26E-08	-2.38	7.99E-10
CCDC8	-2.89	4.84E-06	-2.73	2.56E-08
ADAM33	-2.90	5.26E-17	-3.73	8.32E-53
PDGFRA	-2.91	7.86E-82	-2.94	0.00E+00

Appendix H: Continued

Gene Symbol	n=1		n=2	
	Fold Change (<i>Tgfb3</i> ^{-/-} / <i>Tgfb3</i> ^{+/+})	p-value	Fold Change (<i>Tgfb3</i> ^{-/-} / <i>Tgfb3</i> ^{+/+})	p-value
EIF4G3	-2.93	3.65E-185	-2.37	8.56E-262
XDH	-2.93	1.96E-262	-3.17	0.00E+00
MERTK	-2.93	4.65E-47	-3.99	2.61E-173
HIST2H2AC	-2.97	3.13E-25	-2.01	4.32E-11
EHD3	-2.97	0.00E+00	-3.09	0.00E+00
BCL3	-2.98	5.90E-38	-2.25	1.58E-50
FAM13C	-2.99	1.51E-53	-2.06	9.08E-45
C3	-3.00	2.00E-153	-2.76	1.80E-233
HIVEP3	-3.02	5.89E-54	-2.57	1.04E-88
GBP5	-3.03	1.01E-04	-4.17	9.38E-17
ARHGAP32	-3.04	5.53E-90	-2.53	9.95E-128
PKDCC	-3.04	5.43E-23	-3.13	5.24E-63
EGR2	-3.05	4.73E-04	-2.65	5.21E-09
SH3PXD2B	-3.07	5.75E-41	-2.22	8.81E-59
SEMA6D	-3.07	3.13E-51	-2.41	2.60E-66
FXYD1	-3.07	2.42E-04	-2.45	6.98E-14
GSTT1	-3.07	1.85E-11	-2.81	1.44E-25
LIN7A	-3.14	8.76E-06	-2.60	1.95E-11
GSTM5	-3.18	4.70E-44	-4.04	3.15E-208
B3GALT1	-3.19	2.07E-05	-2.03	5.03E-07
ACTN3	-3.19	6.50E-14	-3.77	6.35E-37
H2-T3	-3.19	2.07E-05	-9.03	3.78E-20
MYLK	-3.23	2.25E-155	-2.71	1.23E-313
APOE	-3.26	1.35E-154	-7.83	0.00E+00
RORC	-3.27	7.53E-18	-2.52	7.73E-31
ANTXR1	-3.30	4.49E-95	-2.12	2.44E-89
FAM110C	-3.31	7.91E-138	-2.77	5.16E-233
NDRG1	-3.33	1.61E-134	-2.37	1.08E-205
ZFP36	-3.33	1.20E-120	-2.83	1.58E-229
ARHGEF3	-3.38	5.11E-08	-2.70	2.45E-14
SUSD2	-3.39	3.67E-12	-3.62	6.44E-34
HCN4	-3.40	3.38E-10	-3.14	1.23E-26
SLC2A13	-3.43	1.17E-07	-3.16	1.86E-11
STBD1	-3.43	4.97E-24	-5.11	8.38E-146
MPP6	-3.44	2.07E-13	-2.24	1.79E-11
CABLES1	-3.44	2.25E-07	-2.98	5.68E-09
BICC1	-3.45	0.00E+00	-2.68	0.00E+00
SCD	-3.51	1.28E-81	-2.13	6.54E-85
E130310I04Rik	-3.51	5.08E-17	-3.95	8.37E-40
AVPR1A	-3.52	2.46E-35	-2.96	2.04E-104

Appendix H: Continued

Gene Symbol	n=1		n=2	
	Fold Change (<i>Tgfb3</i> ^{-/-} / <i>Tgfb3</i> ^{+/+})	p-value	Fold Change (<i>Tgfb3</i> ^{-/-} / <i>Tgfb3</i> ^{+/+})	p-value
SEPP1	-3.64	2.43E-43	-2.85	1.03E-84
FOSB	-3.64	1.69E-08	-5.19	5.09E-41
PYCARD	-3.66	1.02E-04	-3.48	3.41E-13
H2-Q10	-3.66	8.02E-112	-7.13	6.33E-320
CHRDL1	-3.67	8.46E-06	-2.55	6.83E-11
ZKSCAN2	-3.74	3.91E-04	-2.43	4.70E-04
HLF	-3.74	4.37E-07	-2.49	4.52E-07
F730043M19Rik	-3.74	3.91E-04	-4.10	5.73E-19
CISH	-3.75	2.48E-19	-3.45	2.72E-40
DAAM2	-3.79	2.10E-24	-3.45	2.16E-63
HIST1H2BB	-3.83	6.21E-31	-2.99	1.32E-06
KALRN	-3.88	2.82E-90	-4.30	5.71E-124
PRPH	-3.92	2.65E-93	-5.77	2.09E-200
SFRP1	-3.93	8.76E-68	-2.34	6.95E-50
AUTS2	-3.93	1.80E-62	-3.12	1.19E-103
CACNA1A	-3.93	7.51E-11	-3.48	8.15E-24
NRXN2	-3.94	7.18E-05	-5.14	3.27E-26
PLEKHA6	-3.95	2.40E-102	-4.58	1.36E-09
TGM1	-3.99	1.84E-07	-3.05	4.00E-12
PPARGC1B	-4.01	4.60E-12	-2.23	2.95E-08
KIAA1324L	-4.05	6.50E-29	-3.78	5.96E-53
GGT5	-4.05	9.62E-10	-4.82	3.39E-25
TGFBI	-4.05	2.09E-26	-8.26	3.05E-256
RTN1	-4.11	7.43E-83	-2.69	2.46E-101
LGALS2	-4.11	9.78E-12	-2.85	2.26E-32
C1orf226	-4.13	5.15E-33	-3.30	4.54E-50
SEZ6L	-4.15	3.16E-13	-6.42	1.21E-35
FADS6	-4.16	1.75E-15	-2.83	9.72E-38
MGP	-4.17	0.00E+00	-3.59	0.00E+00
BMP4	-4.19	1.41E-210	-2.05	1.54E-159
PEG10	-4.19	6.07E-26	-2.20	5.40E-14
ACVR1B	-4.23	8.78E-41	-4.28	5.08E-109
PGAM2	-4.25	2.07E-12	-2.38	2.72E-14
CAPN6	-4.25	1.21E-09	-3.60	9.50E-14
RASSF4	-4.29	2.30E-08	-3.78	5.09E-23
ALPL	-4.31	1.49E-05	-2.91	1.10E-05
PCDHAC2	-4.35	7.36E-14	-2.63	1.29E-17
CDH23	-4.44	3.07E-04	-2.55	1.92E-04
IL1RL2	-4.53	1.52E-07	-6.47	2.39E-34
Rpph1	-4.63	0.00E+00	-4.29	1.40E-134

Appendix H: Continued

Gene Symbol	n=1		n=2	
	Fold Change (<i>Tgfb3</i> ^{-/-} / <i>Tgfb3</i> ^{+/+})	p-value	Fold Change (<i>Tgfb3</i> ^{-/-} / <i>Tgfb3</i> ^{+/+})	p-value
CNRIP1	-4.64	5.70E-16	-3.06	1.08E-30
ELN	-4.64	8.26E-277	-5.44	0.00E+00
RASL11A	-4.67	4.28E-242	-3.17	0.00E+00
GUCY1A3	-4.68	3.58E-101	-3.78	2.02E-265
TNC	-4.68	0.00E+00	-4.23	0.00E+00
TGM2	-4.69	0.00E+00	-2.55	0.00E+00
PDZD2	-4.71	5.15E-08	-2.42	2.73E-106
IL16	-4.74	1.65E-07	-17.50	7.75E-40
TMEM196	-4.77	5.28E-07	-3.25	1.64E-13
PDE3A	-4.99	5.84E-05	-5.87	8.33E-09
GSTA3	-5.02	2.70E-40	-3.22	2.21E-83
PLEK	-5.08	5.67E-09	-3.32	3.56E-17
HLA-B	-5.16	2.31E-27	-15.05	0.00E+00
TEK	-5.25	3.49E-24	-5.41	6.34E-51
9430069I07Rik	-5.27	6.40E-04	-4.29	2.76E-04
LRP3	-5.27	6.40E-04	-8.19	1.22E-12
CADM1	-5.29	6.76E-77	-3.58	1.15E-196
HIST1H1A	-5.32	1.47E-18	-5.83	1.80E-09
NOS1AP	-5.49	2.81E-30	-3.96	9.59E-34
TRPS1	-5.55	1.05E-05	-2.37	4.19E-05
GALNT14	-5.55	3.58E-04	-2.91	3.84E-04
TMTC1	-5.65	1.05E-09	-3.03	1.31E-13
MGAT3	-5.73	7.81E-48	-3.16	2.20E-59
H19	-5.80	6.44E-114	-2.34	6.61E-153
HIST2H3C	-5.88	7.99E-50	-2.61	2.80E-119
ZNF521	-5.89	4.98E-87	-3.00	3.16E-64
RHOBTB1	-6.17	2.05E-29	-2.90	1.46E-30
FAM189A2	-6.18	1.79E-07	-6.14	8.17E-16
BMF	-6.19	2.85E-24	-4.64	9.18E-57
Cyp2d22	-6.33	6.42E-17	-5.67	6.96E-33
TPBGL	-6.43	9.75E-11	-5.29	1.44E-30
UCP2	-6.44	3.70E-241	-9.12	0.00E+00
LINGO1	-6.51	8.46E-53	-12.31	9.98E-308
ITGB8	-6.52	5.39E-09	-3.43	1.19E-13
USH1G	-6.84	1.67E-07	-6.82	1.16E-14
HAS1	-6.91	5.07E-15	-2.32	7.97E-06
HOXB4	-7.02	4.85E-11	-4.39	1.04E-19
IGFBP5	-7.17	8.84E-47	-2.42	1.28E-43
CMYA5	-7.21	2.64E-10	-3.26	1.02E-07
DOCK10	-7.21	1.45E-12	-8.87	2.85E-18

Appendix H: Continued

Gene Symbol	n=1		n=2	
	Fold Change (<i>Tgfb3</i> ^{-/-} / <i>Tgfb3</i> ^{+/+})	p-value	Fold Change (<i>Tgfb3</i> ^{-/-} / <i>Tgfb3</i> ^{+/+})	p-value
PDE2A	-7.21	9.76E-06	-12.28	1.65E-23
HOXB3	-7.27	1.44E-11	-6.68	4.18E-36
CLDN15	-7.31	1.28E-68	-3.91	1.84E-142
CFI	-7.54	2.73E-07	-3.64	7.07E-08
PIEZO2	-7.76	2.83E-06	-3.33	1.95E-05
HOXB2	-7.76	6.37E-19	-7.53	2.56E-56
A930033H14Rik	-8.32	6.14E-04	-3.04	5.91E-06
SLC39A4	-8.40	3.45E-11	-5.85	4.50E-22
Pdlim3	-8.65	1.20E-08	-8.19	2.27E-31
AR	-8.87	3.23E-04	-28.66	1.64E-07
FGL2	-9.00	2.35E-15	-11.08	9.65E-84
CDH13	-9.02	8.70E-25	-8.40	7.48E-43
TGFB3R3	-9.27	2.19E-114	-6.44	8.81E-258
SOSTDC1	-9.43	1.69E-04	-6.14	5.21E-19
2410017I17Rik	-9.45	5.24E-43	-7.73	9.94E-77
IGLON5	-10.60	5.59E-19	-2.87	7.63E-18
SLC16A2	-10.87	1.91E-11	-5.89	7.33E-18
SYNPO2	-10.91	8.45E-26	-8.47	5.57E-72
SLC40A1	-11.65	1.22E-05	-2.03	3.73E-08
AQP1	-11.65	1.22E-05	-9.73	3.27E-14
ALDOC	-11.73	3.29E-160	-8.03	0.00E+00
8030451A03Rik	-12.20	6.29E-06	-5.69	1.52E-05
Serpinbb6b	-12.31	2.44E-25	-5.80	1.65E-86
ACSS3	-12.57	1.20E-08	-5.96	6.79E-16
PRR15	-13.31	1.64E-46	-6.44	1.46E-182
BC023719	-13.31	3.15E-09	-9.04	1.62E-24
9530082P21Rik	-13.31	1.64E-06	-18.56	3.50E-20
NR4A3	-14.42	4.85E-04	-13.06	3.48E-18
NPAS4	-15.53	2.45E-04	-2.92	1.61E-05
FAM19A2	-16.08	5.50E-08	-2.31	1.15E-05
2610507I01Rik	-16.08	5.50E-08	-8.44	9.01E-16
PCDH17	-16.35	3.48E-191	-8.56	8.82E-241
TSHZ3	-17.75	6.15E-05	-31.39	3.17E-08
HLX	-19.96	7.72E-37	-11.56	1.79E-70
Dcaf12l1	-22.18	3.77E-06	-4.10	1.91E-06
FMO2	-23.29	1.86E-06	-6.11	1.81E-16
GBP2	-28.17	8.79E-35	-22.03	2.31E-66
VSTM2A	-31.05	1.30E-08	-45.32	5.80E-55
TMEM215	-32.16	7.89E-17	-21.08	5.39E-41
SORBS2	-39.56	6.58E-31	-30.57	5.13E-104

Appendix H: Continued

Gene Symbol	n=1		n=2	
	Fold Change (<i>Tgfb3</i> ^{-/-} / <i>Tgfb3</i> ^{+/+})	p-value	Fold Change (<i>Tgfb3</i> ^{-/-} / <i>Tgfb3</i> ^{+/+})	p-value
PNLDC1	-48.80	1.29E-13	-8.12	7.73E-25
STC1	-64.70	2.53E-52	-18.02	0.00E+00
CYP4F22	-92.05	5.40E-26	-31.08	4.70E-92

REFERENCES

- Ackerman, K. G., B. J. Herron, et al. (2005). "Fog2 is required for normal diaphragm and lung development in mice and humans." PLoS Genet **1**(1): 58-65.
- Aikawa, E., P. Whittaker, et al. (2006). "Human semilunar cardiac valve remodeling by activated cells from fetus to adult: implications for postnatal adaptation, pathology, and tissue engineering." Circulation **113**(10): 1344-52.
- Akiyama, H., M. C. Chaboissier, et al. (2004). "Essential role of Sox9 in the pathway that controls formation of cardiac valves and septa." Proc Natl Acad Sci U S A **101**(17): 6502-7.
- Alfieri, C. M., J. Cheek, et al. (2010). "Wnt signaling in heart valve development and osteogenic gene induction." Dev Biol **338**(2): 127-35.
- Andres, J. L., D. DeFalcis, et al. (1992). "Binding of two growth factor families to separate domains of the proteoglycan betaglycan." J Biol Chem **267**(9): 5927-30.
- Angel, P. M., D. Nusinow, et al. "Networked-based Characterization of Extracellular Matrix Proteins from Adult Mouse Pulmonary and Aortic Valves." J Proteome Res.
- Araki, T., M. G. Mohi, et al. (2004). "Mouse model of Noonan syndrome reveals cell type- and gene dosage-dependent effects of Ptpn11 mutation." Nat Med **10**(8): 849-57.
- Attar, M. A., J. C. Salem, et al. (2012). "CNK3 and IPCEF1 produce a single protein that is required for HGF dependent Arf6 activation and migration." Exp Cell Res **318**(3): 228-37.
- Audic, S. and J. M. Claverie (1997). "The significance of digital gene expression profiles." Genome Res **7**(10): 986-95.
- Austin, A. F., L. A. Compton, et al. (2008). "Primary and immortalized mouse epicardial cells undergo differentiation in response to TGFbeta." Developmental dynamics : an official publication of the American Association of Anatomists **237**(2): 366-76.
- Azhar, M., R. B. Runyan, et al. (2009). "Ligand-specific function of transforming growth factor beta in epithelial-mesenchymal transition in heart development." Dev Dyn **238**(2): 431-42.
- Baldwin, H. S. and M. Solursh (1989). "Degradation of hyaluronic acid does not prevent looping of the mammalian heart in situ." Dev Biol **136**(2): 555-9.

- Barnett, J. V. and J. S. Desgrosellier (2003). "Early events in valvulogenesis: a signaling perspective." *Birth Defects Res C Embryo Today* **69**(1): 58-72.
- Bartram, U., D. G. Molin, et al. (2001). "Double-outlet right ventricle and overriding tricuspid valve reflect disturbances of looping, myocardialization, endocardial cushion differentiation, and apoptosis in TGF-beta(2)-knockout mice." *Circulation* **103**(22): 2745-52.
- Beg, A. A., W. C. Sha, et al. (1995). "Embryonic lethality and liver degeneration in mice lacking the RelA component of NF-kappa B." *Nature* **376**(6536): 167-70.
- Beppu, H., R. Malhotra, et al. (2009). "BMP type II receptor regulates positioning of outflow tract and remodeling of atrioventricular cushion during cardiogenesis." *Dev Biol* **331**(2): 167-75.
- Bernanke, D. H. and R. R. Markwald (1982). "Migratory behavior of cardiac cushion tissue cells in a collagen-lattice culture system." *Dev Biol* **91**(2): 235-45.
- Blobe, G. C., X. Liu, et al. (2001). "A novel mechanism for regulating transforming growth factor beta (TGF-beta) signaling. Functional modulation of type III TGF-beta receptor expression through interaction with the PDZ domain protein, GIPC." *J Biol Chem* **276**(43): 39608-17.
- Blobe, G. C., W. P. Schiemann, et al. (2001). "Functional roles for the cytoplasmic domain of the type III transforming growth factor beta receptor in regulating transforming growth factor beta signaling." *J Biol Chem* **276**(27): 24627-37.
- Bochmann, L., P. Sarathchandra, et al. (2010). "Revealing new mouse epicardial cell markers through transcriptomics." *PLoS One* **5**(6): e11429.
- Brown, C. B., A. S. Boyer, et al. (1996). "Antibodies to the Type II TGFbeta receptor block cell activation and migration during atrioventricular cushion transformation in the heart." *Dev Biol* **174**(2): 248-57.
- Brown, C. B., A. S. Boyer, et al. (1999). "Requirement of type III TGF-beta receptor for endocardial cell transformation in the heart." *Science* **283**(5410): 2080-2.
- Brutsaert, D. L., G. W. De Keulenaer, et al. (1996). "The cardiac endothelium: functional morphology, development, and physiology." *Prog Cardiovasc Dis* **39**(3): 239-62.
- Buermans, H. P., B. van Wijk, et al. (2010). "Comprehensive gene-expression survey identifies wif1 as a modulator of cardiomyocyte differentiation." *PLoS One* **5**(12): e15504.

- Burke, J. R., M. A. Pattoli, et al. (2003). "BMS-345541 is a highly selective inhibitor of I kappa B kinase that binds at an allosteric site of the enzyme and blocks NF-kappa B-dependent transcription in mice." J Biol Chem **278**(3): 1450-6.
- Butcher, J. T. and R. R. Markwald (2007). "Valvulogenesis: the moving target." Philos Trans R Soc Lond B Biol Sci **362**(1484): 1489-503.
- Butcher, J. T., R. A. Norris, et al. (2007). "Periostin promotes atrioventricular mesenchyme matrix invasion and remodeling mediated by integrin signaling through Rho/PI 3-kinase." Dev Biol **302**(1): 256-66.
- Cai, C. L., J. C. Martin, et al. (2008). "A myocardial lineage derives from Tbx18 epicardial cells." Nature **454**(7200): 104-8.
- Camenisch, T. D., D. G. Molin, et al. (2002). "Temporal and distinct TGFbeta ligand requirements during mouse and avian endocardial cushion morphogenesis." Dev Biol **248**(1): 170-81.
- Camenisch, T. D., J. A. Schroeder, et al. (2002). "Heart-valve mesenchyme formation is dependent on hyaluronan-augmented activation of ErbB2-ErbB3 receptors." Nat Med **8**(8): 850-5.
- Camenisch, T. D., A. P. Spicer, et al. (2000). "Disruption of hyaluronan synthase-2 abrogates normal cardiac morphogenesis and hyaluronan-mediated transformation of epithelium to mesenchyme." J Clin Invest **106**(3): 349-60.
- Capdevila, J., T. Tsukui, et al. (1999). "Control of vertebrate limb outgrowth by the proximal factor Meis2 and distal antagonism of BMPs by Gremlin." Mol Cell **4**(5): 839-49.
- Chakraborty, S., J. Cheek, et al. (2008). "Shared gene expression profiles in developing heart valves and osteoblast progenitor cells." Physiol Genomics **35**(1): 75-85.
- Chan-Thomas, P. S., R. P. Thompson, et al. (1993). "Expression of homeobox genes Msx-1 (Hox-7) and Msx-2 (Hox-8) during cardiac development in the chick." Dev Dyn **197**(3): 203-16.
- Cheifetz, S., T. Bellon, et al. (1992). "Endoglin is a component of the transforming growth factor-beta receptor system in human endothelial cells." J Biol Chem **267**(27): 19027-30.
- Chen, B., R. T. Bronson, et al. (2000). "Mice mutant for Egfr and Shp2 have defective cardiac semilunar valvulogenesis." Nat Genet **24**(3): 296-9.
- Chen, Y. H., M. Ishii, et al. (2008). "Msx1 and Msx2 are required for endothelial-mesenchymal transformation of the atrioventricular cushions and patterning of the atrioventricular myocardium." BMC Dev Biol **8**: 75.

- Chen, Z. F. and R. R. Behringer (1995). "twist is required in head mesenchyme for cranial neural tube morphogenesis." *Genes Dev* **9**(6): 686-99.
- Christiaen, L., A. Stolfi, et al. (2010). "BMP signaling coordinates gene expression and cell migration during precardiac mesoderm development." *Developmental biology* **340**(2): 179-87.
- Christodoulou, D. C., J. M. Gorham, et al. (2011). "Construction of normalized RNA-seq libraries for next-generation sequencing using the crab duplex-specific nuclease." *Curr Protoc Mol Biol Chapter 4*: Unit4 12.
- Christodoulou, D. C., J. M. Gorham, et al. (2011). "Quantification of gene transcripts with deep sequencing analysis of gene expression (DSAGE) using 1 to 2 microg total RNA." *Current protocols in molecular biology / edited by Frederick M. Ausubel ... [et al.] Chapter 25*: Unit25B 9.
- Christoffels, V. M., T. Grieskamp, et al. (2009). "Tbx18 and the fate of epicardial progenitors." *Nature* **458**(7240): E8-9; discussion E9-10.
- Cole, W. C. and D. G. Welsh (2011). "Role of myosin light chain kinase and myosin light chain phosphatase in the resistance arterial myogenic response to intravascular pressure." *Arch Biochem Biophys* **510**(2): 160-73.
- Combs, M. D. and K. E. Yutzey (2009). "Heart valve development: regulatory networks in development and disease." *Circ Res* **105**(5): 408-21.
- Compton, L. A., D. A. Potash, et al. (2007). "Coronary vessel development is dependent on the type III transforming growth factor beta receptor." *Circ Res* **101**(8): 784-91.
- Compton, L. A., D. A. Potash, et al. (2006). "Transforming growth factor-beta induces loss of epithelial character and smooth muscle cell differentiation in epicardial cells." *Dev Dyn* **235**(1): 82-93.
- Connolly, H. M., J. L. Crary, et al. (1997). "Valvular heart disease associated with fenfluramine-phentermine." *N Engl J Med* **337**(9): 581-8.
- Conway, S. J., D. J. Henderson, et al. (1997). "Pax3 is required for cardiac neural crest migration in the mouse: evidence from the splotch (Sp2H) mutant." *Development* **124**(2): 505-14.
- Craig, E. A., A. F. Austin, et al. (2010). "TGFbeta2-mediated production of hyaluronan is important for the induction of epicardial cell differentiation and invasion." *Exp Cell Res* **316**(20): 3397-405.
- Craig, E. A., P. Parker, et al. (2010). "Involvement of the MEKK1 signaling pathway in the regulation of epicardial cell behavior by hyaluronan." *Cell Signal* **22**(6): 968-76.

- Craig, E. A., P. Parker, et al. (2009). "Size-dependent regulation of Snail2 by hyaluronan: its role in cellular invasion." *Glycobiology* **19**(8): 890-8.
- Criswell, T. L. and C. L. Arteaga (2007). "Modulation of NFkappaB activity and E-cadherin by the type III transforming growth factor beta receptor regulates cell growth and motility." *J Biol Chem* **282**(44): 32491-500.
- Criswell, T. L., N. Dumont, et al. (2008). "Knockdown of the transforming growth factor-beta type III receptor impairs motility and invasion of metastatic cancer cells." *Cancer research* **68**(18): 7304-12.
- Cross, N. A., S. Chandrasekharan, et al. (2005). "The expression and regulation of ADAMTS-1, -4, -5, -9, and -15, and TIMP-3 by TGFbeta1 in prostate cells: relevance to the accumulation of versican." *Prostate* **63**(3): 269-75.
- de la Pompa, J. L., L. A. Timmerman, et al. (1998). "Role of the NF-ATc transcription factor in morphogenesis of cardiac valves and septum." *Nature* **392**(6672): 182-6.
- del Monte, G., J. C. Casanova, et al. (2007). "Differential Notch signaling in the epicardium is required for cardiac inflow development and coronary vessel morphogenesis." *Circulation research* **108**(7): 824-36.
- del Monte, G., J. Grego-Bessa, et al. (2007). "Monitoring Notch1 activity in development: evidence for a feedback regulatory loop." *Dev Dyn* **236**(9): 2594-614.
- DeLaughter, D. M., L. Saint-Jean, et al. (2011). "What chick and mouse models have taught us about the role of the endocardium in congenital heart disease." *Birth Defects Res A Clin Mol Teratol* **91**(6): 511-25.
- Dennis, G., Jr., B. T. Sherman, et al. (2003). "DAVID: Database for Annotation, Visualization, and Integrated Discovery." *Genome Biol* **4**(5): P3.
- DeRuiter, M. C., R. E. Poelmann, et al. (1992). "The development of the myocardium and endocardium in mouse embryos. Fusion of two heart tubes?" *Anat Embryol (Berl)* **185**(5): 461-73.
- Derynck, R. and Y. E. Zhang (2003). "Smad-dependent and Smad-independent pathways in TGF-beta family signalling." *Nature* **425**(6958): 577-84.
- Desgrosellier, J. S., N. A. Mundell, et al. (2005). "Activin receptor-like kinase 2 and Smad6 regulate epithelial-mesenchymal transformation during cardiac valve formation." *Dev Biol* **280**(1): 201-10.
- Dettman, R. W., W. Denetclaw, Jr., et al. (1998). "Common epicardial origin of coronary vascular smooth muscle, perivascular fibroblasts, and intermyocardial fibroblasts in the avian heart." *Dev Biol* **193**(2): 169-81.

- Dewulf, N., K. Verschueren, et al. (1995). "Distinct spatial and temporal expression patterns of two type I receptors for bone morphogenetic proteins during mouse embryogenesis." Endocrinology **136**(6): 2652-63.
- Dickson, M. C., H. G. Slager, et al. (1993). "RNA and protein localisations of TGF beta 2 in the early mouse embryo suggest an involvement in cardiac development." Development **117**(2): 625-39.
- Doetschman T, B. J., Runyan R, Camenisch TD, Heimark RL, Granzier HL, Conway SJ, Azhar A (2012). "Transforming growth factor beta signaling in adult cardiovascular diseases and repair." Cell and tissue research **347**(2): 539-548.
- Dupuis, L. E., D. R. McCulloch, et al. (2011). "Altered versican cleavage in ADAMTS5 deficient mice; a novel etiology of myxomatous valve disease." Developmental biology **357**(1): 152-64.
- Enard, W. (2011). "FOXP2 and the role of cortico-basal ganglia circuits in speech and language evolution." Curr Opin Neurobiol **21**(3): 415-24.
- Enciso, J. M., D. Gratzinger, et al. (2003). "Elevated glucose inhibits VEGF-A-mediated endocardial cushion formation: modulation by PECAM-1 and MMP-2." J Cell Biol **160**(4): 605-15.
- Erickson, S. L., K. S. O'Shea, et al. (1997). "ErbB3 is required for normal cerebellar and cardiac development: a comparison with ErbB2-and heregulin-deficient mice." Development **124**(24): 4999-5011.
- Ernkvist, M., N. Luna Persson, et al. (2009). "The Amot/Patj/Syx signaling complex spatially controls RhoA GTPase activity in migrating endothelial cells." Blood **113**(1): 244-53.
- Fraidenraich, D., E. Stillwell, et al. (2004). "Rescue of cardiac defects in id knockout embryos by injection of embryonic stem cells." Science **306**(5694): 247-52.
- French, C. A., M. Groszer, et al. (2007). "Generation of mice with a conditional Foxp2 null allele." Genesis **45**(7): 440-6.
- Frieden, L., Townsend, TA, Vaught, D, DeLaughter, D., Hwang, Y, Barnett, JV, Chen, J. (2010). "Regulation of heart valve morphogenesis by Eph receptor ligand, ephrin-A1. ." Developmental Dynamics in press.
- Galvin, K. M., M. J. Donovan, et al. (2000). "A role for smad6 in development and homeostasis of the cardiovascular system." Nat Genet **24**(2): 171-4.
- Garg, V., A. N. Muth, et al. (2005). "Mutations in NOTCH1 cause aortic valve disease." Nature **437**(7056): 270-4.

- Gassmann, M., F. Casagranda, et al. (1995). "Aberrant neural and cardiac development in mice lacking the ErbB4 neuregulin receptor." Nature **378**(6555): 390-4.
- Gelb, B. D. and M. Tartaglia (2006). "Noonan syndrome and related disorders: Dysregulated RAS-mitogen activated protein kinase signal transduction." Hum Mol Genet **15 Spec No 2**: R220-6.
- Gitler, A. D., Y. Zhu, et al. (2003). "Nf1 has an essential role in endothelial cells." Nat Genet **33**(1): 75-9.
- Gittenberger-de Groot, A. C., M. P. Vrancken Peeters, et al. (1998). "Epicardium-derived cells contribute a novel population to the myocardial wall and the atrioventricular cushions." Circ Res **82**(10): 1043-52.
- Gittenberger-de Groot, A. C., E. M. Winter, et al. (2010). "Epicardium-derived cells (EPDCs) in development, cardiac disease and repair of ischemia." Journal of cellular and molecular medicine **14**(5): 1056-60.
- Go, A. S., D. Mozaffarian, et al. (2013). "Heart disease and stroke statistics--2013 update: a report from the American Heart Association." Circulation **127**(1): e6-e245.
- Gonzalez-Iriarte, M., R. Carmona, et al. (2003). "Development of the coronary arteries in a murine model of transposition of great arteries." J Mol Cell Cardiol **35**(7): 795-802.
- Gordon, J. W., J. A. Shaw, et al. (2011). "Multiple facets of NF-kappaB in the heart: to be or not to NF-kappaB." Circ Res **108**(9): 1122-32.
- Goumans, M. J., G. Valdimarsdottir, et al. (2003). "Activin receptor-like kinase (ALK)1 is an antagonistic mediator of lateral TGFbeta/ALK5 signaling." Mol Cell **12**(4): 817-28.
- Goumans, M. J., G. Valdimarsdottir, et al. (2002). "Balancing the activation state of the endothelium via two distinct TGF-beta type I receptors." Embo J **21**(7): 1743-53.
- Greulich, F., C. Rudat, et al. "Mechanisms of T-box gene function in the developing heart." Cardiovasc Res **91**(2): 212-22.
- Grieskamp, T., C. Rudat, et al. (2011). "Notch signaling regulates smooth muscle differentiation of epicardium-derived cells." Circulation research **108**(7): 813-23.
- Hamburger, V. and H. L. Hamilton (1951). "A series of normal stages in development of the chick embryo." Journal of Morphology **88**(1): 49-92.

- Han, L. and A. I. Gotlieb (2011). "Fibroblast growth factor-2 promotes in vitro mitral valve interstitial cell repair through transforming growth factor-beta/Smad signaling." Am J Pathol **178**(1): 119-27.
- Hartnett, L., C. Glynn, et al. (2010). "Insulin-like growth factor-2 regulates early neural and cardiovascular system development in zebrafish embryos." Int J Dev Biol **54**(4): 573-83.
- Hauser, M. (2005). "Congenital anomalies of the coronary arteries." Heart **91**(9): 1240-5.
- Hill, C. R., N. S. Sanchez, et al. (2012). "BMP2 signals loss of epithelial character in epicardial cells but requires the Type III TGFbeta receptor to promote invasion." Cellular signalling **24**(5): 1012-22.
- Hinton, R. B., Jr., J. Lincoln, et al. (2006). "Extracellular matrix remodeling and organization in developing and diseased aortic valves." Circ Res **98**(11): 1431-8.
- Hoffman, J. I. (1968). "Natural history of congenital heart disease. Problems in its assessment with special reference to ventricular septal defects." Circulation **37**(1): 97-125.
- Hurle, J. M. and E. Colvee (1983). "Changes in the endothelial morphology of the developing semilunar heart valves. A TEM and SEM study in the chick." Anat Embryol (Berl) **167**(1): 67-83.
- Hurle, J. M., E. Colvee, et al. (1980). "Development of mouse semilunar valves." Anat Embryol (Berl) **160**(1): 83-91.
- Hurlstone, A. F., A. P. Haramis, et al. (2003). "The Wnt/beta-catenin pathway regulates cardiac valve formation." Nature **425**(6958): 633-7.
- Inai, K., R. A. Norris, et al. (2008). "BMP-2 induces cell migration and periostin expression during atrioventricular valvulogenesis." Dev Biol **315**(2): 383-96.
- Ishii, Y., R. J. Garriock, et al. (2010). "BMP signals promote proepicardial protrusion necessary for recruitment of coronary vessel and epicardial progenitors to the heart." Dev Cell **19**(2): 307-16.
- Iwamoto, R., S. Yamazaki, et al. (2003). "Heparin-binding EGF-like growth factor and ErbB signaling is essential for heart function." Proc Natl Acad Sci U S A **100**(6): 3221-6.
- Jackson, L. F., T. H. Qiu, et al. (2003). "Defective valvulogenesis in HB-EGF and TACE-null mice is associated with aberrant BMP signaling." EMBO J **22**(11): 2704-16.

- Jain, R., K. A. Engleka, et al. "Cardiac neural crest orchestrates remodeling and functional maturation of mouse semilunar valves." J Clin Invest **121**(1): 422-30.
- Jen, Y., K. Manova, et al. (1996). "Expression patterns of Id1, Id2, and Id3 are highly related but distinct from that of Id4 during mouse embryogenesis." Dev Dyn **207**(3): 235-52.
- Jiao, K., M. Langworthy, et al. (2006). "Tgfbeta signaling is required for atrioventricular cushion mesenchyme remodeling during in vivo cardiac development." Development **133**(22): 4585-93.
- Kaartinen, V., J. W. Voncken, et al. (1995). "Abnormal lung development and cleft palate in mice lacking TGF-beta 3 indicates defects of epithelial-mesenchymal interaction." Nat Genet **11**(4): 415-21.
- Kalluri, R. (2009). "EMT: when epithelial cells decide to become mesenchymal-like cells." The Journal of clinical investigation **119**(6): 1417-9.
- Kalluri, R. and R. A. Weinberg (2009). "The basics of epithelial-mesenchymal transition." The Journal of clinical investigation **119**(6): 1420-8.
- Kalman, F., S. Viragh, et al. (1995). "Cell surface glycoconjugates and the extracellular matrix of the developing mouse embryo epicardium." Anat Embryol (Berl) **191**(5): 451-64.
- Kamm, K. E. and J. T. Stull (2001). "Dedicated myosin light chain kinases with diverse cellular functions." J Biol Chem **276**(7): 4527-30.
- Katz, T. C., M. K. Singh, et al. (2012). "Distinct compartments of the proepicardial organ give rise to coronary vascular endothelial cells." Dev Cell **22**(3): 639-50.
- Kawagoe, T., S. Sato, et al. (2008). "Sequential control of Toll-like receptor-dependent responses by IRAK1 and IRAK2." Nat Immunol **9**(6): 684-91.
- Kern, C. B., W. O. Twal, et al. (2006). "Proteolytic cleavage of versican during cardiac cushion morphogenesis." Developmental dynamics : an official publication of the American Association of Anatomists **235**(8): 2238-47.
- Kern, C. B., W. O. Twal, et al. (2006). "Proteolytic cleavage of versican during cardiac cushion morphogenesis." Dev Dyn **235**(8): 2238-47.
- Keyes, W. M., C. Logan, et al. (2003). "Expression and function of bone morphogenetic proteins in the development of the embryonic endocardial cushions." Anat Embryol (Berl) **207**(2): 135-47.
- Khairy, P., J. A. Hosn, et al. (2008). "Multicenter research in adult congenital heart disease." International journal of cardiology **129**(2): 155-9.

- Kikuchi, K., V. Gupta, et al. (2011). "tcf21+ epicardial cells adopt non-myocardial fates during zebrafish heart development and regeneration." *Development* **138**(14): 2895-902.
- Kirkbride, K. C., T. A. Townsend, et al. (2008). "Bone morphogenetic proteins signal through the transforming growth factor-beta type III receptor." *J Biol Chem* **283**(12): 7628-37.
- Kitamura, K., H. Miura, et al. (1999). "Mouse Pitx2 deficiency leads to anomalies of the ventral body wall, heart, extra- and periocular mesoderm and right pulmonary isomerism." *Development* **126**(24): 5749-58.
- Komiyama, M., K. Ito, et al. (1987). "Origin and development of the epicardium in the mouse embryo." *Anat Embryol (Berl)* **176**(2): 183-9.
- Kramer, R., N. Bucay, et al. (1996). "Neuregulins with an Ig-like domain are essential for mouse myocardial and neuronal development." *Proc Natl Acad Sci U S A* **93**(10): 4833-8.
- Kraus, F., B. Haenig, et al. (2001). "Cloning and expression analysis of the mouse T-box gene Tbx20." *Mechanisms of Development* **100**(1): 87-91.
- Kretzschmar, M. and J. Massague (1998). "SMADs: mediators and regulators of TGF-beta signaling." *Curr Opin Genet Dev* **8**(1): 103-11.
- Krishnamurthy, V. K., A. M. Opoka, et al. (2012). "Maladaptive matrix remodeling and regional biomechanical dysfunction in a mouse model of aortic valve disease." *Matrix Biol* **31**(3): 197-205.
- Krug, E. L., C. H. Mjaatvedt, et al. (1987). "Extracellular matrix from embryonic myocardium elicits an early morphogenetic event in cardiac endothelial differentiation." *Dev Biol* **120**(2): 348-55.
- Kruithof, B. P., B. van Wijk, et al. (2006). "BMP and FGF regulate the differentiation of multipotential pericardial mesoderm into the myocardial or epicardial lineage." *Developmental biology* **295**(2): 507-22.
- Kruzynska-Frejtag, A., M. Machnicki, et al. (2001). "Periostin (an osteoblast-specific factor) is expressed within the embryonic mouse heart during valve formation." *Mech Dev* **103**(1-2): 183-8.
- Kwee, L., H. S. Baldwin, et al. (1995). "Defective development of the embryonic and extraembryonic circulatory systems in vascular cell adhesion molecule (VCAM-1) deficient mice." *Development* **121**(2): 489-503.
- Lai, Y. T., K. B. Beason, et al. (2000). "Activin receptor-like kinase 2 can mediate atrioventricular cushion transformation." *Dev Biol* **222**(1): 1-11.

- Lakkis, M. M. and J. A. Epstein (1998). "Neurofibromin modulation of ras activity is required for normal endocardial-mesenchymal transformation in the developing heart." *Development* **125**(22): 4359-67.
- Lampugnani, M. G., M. Resnati, et al. (1992). "A Novel Endothelial-Specific Membrane-Protein Is a Marker of Cell Cell Contacts." *Journal of Cell Biology* **118**(6): 1511-1522.
- Lavine, K. J. and D. M. Ornitz (2009). "Shared circuitry: developmental signaling cascades regulate both embryonic and adult coronary vasculature." *Circulation research* **104**(2): 159-69.
- Lebrin, F., M. J. Goumans, et al. (2004). "Endoglin promotes endothelial cell proliferation and TGF-beta/ALK1 signal transduction." *Embo J* **23**(20): 4018-28.
- Lee, J. G. and E. P. Kay (2012). "NF-kappaB is the transcription factor for FGF-2 that causes endothelial mesenchymal transformation in cornea." *Invest Ophthalmol Vis Sci* **53**(3): 1530-8.
- Lee, M. P. and K. E. Yutzey (2011). "Twist1 directly regulates genes that promote cell proliferation and migration in developing heart valves." *PLoS One* **6**(12): e29758.
- Lee, N. Y., B. Ray, et al. (2008). "Endoglin promotes transforming growth factor beta-mediated Smad 1/5/8 signaling and inhibits endothelial cell migration through its association with GIPC." *J Biol Chem* **283**(47): 32527-33.
- Lencinas, A., A. L. Tavares, et al. (2012). "Collagen gel analysis of epithelial-mesenchymal transition in the embryo heart: an in vitro model system for the analysis of tissue interaction, signal transduction, and environmental effects." *Birth Defects Res C Embryo Today* **93**(4): 298-311.
- Lepilina, A., A. N. Coon, et al. (2006). "A dynamic epicardial injury response supports progenitor cell activity during zebrafish heart regeneration." *Cell* **127**(3): 607-19.
- Lewis, E. F., L. A. Moye, et al. (2003). "Predictors of late development of heart failure in stable survivors of myocardial infarction: the CARE study." *Journal of the American College of Cardiology* **42**(8): 1446-53.
- Li, S., J. Weidenfeld, et al. (2004). "Transcriptional and DNA binding activity of the Foxp1/2/4 family is modulated by heterotypic and homotypic protein interactions." *Mol Cell Biol* **24**(2): 809-22.
- Li, S., D. Zhou, et al. (2004). "Advanced cardiac morphogenesis does not require heart tube fusion." *Science* **305**(5690): 1619-22.
- Li, S. W., D. J. Prockop, et al. (1995). "Transgenic mice with targeted inactivation of the Col2 alpha 1 gene for collagen II develop a skeleton with

- membranous and periosteal bone but no endochondral bone." *Genes Dev* **9**(22): 2821-30.
- Lie-Venema, H., I. Eralp, et al. (2008). "Periostin expression by epicardium-derived cells is involved in the development of the atrioventricular valves and fibrous heart skeleton." *Differentiation* **76**(7): 809-19.
- Liebner, S., A. Cattelino, et al. (2004). "Beta-catenin is required for endothelial-mesenchymal transformation during heart cushion development in the mouse." *J Cell Biol* **166**(3): 359-67.
- Lim, J. and J. P. Thiery (2012). "Epithelial-mesenchymal transitions: insights from development." *Development* **139**(19): 3471-86.
- Lim, S., E. Bae, et al. (2012). "TRAF6 mediates IL-1beta/LPS-induced suppression of TGF-beta signaling through its interaction with the type III TGF-beta receptor." *PLoS One* **7**(3): e32705.
- Limana, F., M. C. Capogrossi, et al. (2011). "The epicardium in cardiac repair: from the stem cell view." *Pharmacology & therapeutics* **129**(1): 82-96.
- Limana, F., A. Zacheo, et al. (2007). "Identification of myocardial and vascular precursor cells in human and mouse epicardium." *Circulation research* **101**(12): 1255-65.
- Lin, A. E., P. H. Birch, et al. (2000). "Cardiovascular malformations and other cardiovascular abnormalities in neurofibromatosis 1." *Am J Med Genet* **95**(2): 108-17.
- Lin, Y. Z., S. Y. Yao, et al. (1995). "Inhibition of nuclear translocation of transcription factor NF-kappa B by a synthetic peptide containing a cell membrane-permeable motif and nuclear localization sequence." *J Biol Chem* **270**(24): 14255-8.
- Lincoln, J., R. Kist, et al. (2007). "Sox9 is required for precursor cell expansion and extracellular matrix organization during mouse heart valve development." *Dev Biol* **305**(1): 120-32.
- Lloyd-Jones, D., R. J. Adams, et al. (2010). "Executive summary: heart disease and stroke statistics--2010 update: a report from the American Heart Association." *Circulation* **121**(7): 948-54.
- Lockhart, M., E. Wirrig, et al. (2011). "Extracellular matrix and heart development." *Birth Defects Res A Clin Mol Teratol* **91**(6): 535-50.
- Loffredo, C. A. (2000). "Epidemiology of cardiovascular malformations: prevalence and risk factors." *Am J Med Genet* **97**(4): 319-25.

- Loomes, K. M., D. B. Taichman, et al. (2002). "Characterization of Notch receptor expression in the developing mammalian heart and liver." Am J Med Genet **112**(2): 181-9.
- Lopez-Casillas, F., S. Cheifetz, et al. (1991). "Structure and expression of the membrane proteoglycan betaglycan, a component of the TGF-beta receptor system." Cell **67**(4): 785-95.
- Lopez-Casillas, F., J. L. Wrana, et al. (1993). "Betaglycan presents ligand to the TGF beta signaling receptor." Cell **73**(7): 1435-44.
- Lozano, R., M. Naghavi, et al. (2012). "Global and regional mortality from 235 causes of death for 20 age groups in 1990 and 2010: a systematic analysis for the Global Burden of Disease Study 2010." Lancet **380**(9859): 2095-128.
- Luna-Zurita, L., B. Prados, et al. (2010). "Integration of a Notch-dependent mesenchymal gene program and Bmp2-driven cell invasiveness regulates murine cardiac valve formation." The Journal of clinical investigation **120**(10): 3493-507.
- Lyons, K. M., R. W. Pelton, et al. (1990). "Organogenesis and pattern formation in the mouse: RNA distribution patterns suggest a role for bone morphogenetic protein-2A (BMP-2A)." Development **109**(4): 833-44.
- Ma, L., M. F. Lu, et al. (2005). "Bmp2 is essential for cardiac cushion epithelial-mesenchymal transition and myocardial patterning." Development **132**(24): 5601-11.
- MacGrogan, D., M. Nus, et al. "Notch signaling in cardiac development and disease." Curr Top Dev Biol **92**: 333-65.
- Major, R. J. and K. D. Poss (2007). "Zebrafish Heart Regeneration as a Model for Cardiac Tissue Repair." Drug discovery today. Disease models **4**(4): 219-225.
- Manasek, F. J. (1969). "Embryonic development of the heart. II. Formation of the epicardium." J Embryol Exp Morphol **22**(3): 333-48.
- Manasek, F. J. (1970). "Sulfated extracellular matrix production in the embryonic heart and adjacent tissues." J Exp Zool **174**(4): 415-39.
- Manasek, F. J., M. Reid, et al. (1973). "Glycosaminoglycan synthesis by the early embryonic chick heart." Dev Biol **35**(2): 332-48.
- Manner, J. (1992). "The development of pericardial villi in the chick embryo." Anat Embryol (Berl) **186**(4): 379-85.
- Manner, J. (1993). "Experimental study on the formation of the epicardium in chick embryos." Anat Embryol (Berl) **187**(3): 281-9.

- Manner, J. (1999). "Does the subepicardial mesenchyme contribute myocardioblasts to the myocardium of the chick embryo heart? A quail-chick chimera study tracing the fate of the epicardial primordium." Anat Rec **255**(2): 212-26.
- Maron, B. J. and G. M. Hutchins (1974). "The development of the semilunar valves in the human heart." Am J Pathol **74**(2): 331-44.
- Masuda, M., T. Maruyama, et al. (2010). "CADM1 interacts with Tiam1 and promotes invasive phenotype of human T-cell leukemia virus type I-transformed cells and adult T-cell leukemia cells." J Biol Chem **285**(20): 15511-22.
- Matsumoto, K., M. Shionyu, et al. (2003). "Distinct interaction of versican/PG-M with hyaluronan and link protein." J Biol Chem **278**(42): 41205-12.
- McBride, K. L., M. F. Riley, et al. (2008). "NOTCH1 mutations in individuals with left ventricular outflow tract malformations reduce ligand-induced signaling." Hum Mol Genet **17**(18): 2886-93.
- McKellar, S. H., D. J. Tester, et al. (2007). "Novel NOTCH1 mutations in patients with bicuspid aortic valve disease and thoracic aortic aneurysms." J Thorac Cardiovasc Surg **134**(2): 290-6.
- Medvedev, A. E., A. Lentschat, et al. (2002). "Dysregulation of LPS-induced Toll-like receptor 4-MyD88 complex formation and IL-1 receptor-associated kinase 1 activation in endotoxin-tolerant cells." J Immunol **169**(9): 5209-16.
- Mellgren, A. M., C. L. Smith, et al. (2008). "Platelet-derived growth factor receptor beta signaling is required for efficient epicardial cell migration and development of two distinct coronary vascular smooth muscle cell populations." Circ Res **103**(12): 1393-401.
- Mendelsohn, C., D. Lohnes, et al. (1994). "Function of the retinoic acid receptors (RARs) during development (II). Multiple abnormalities at various stages of organogenesis in RAR double mutants." Development **120**(10): 2749-71.
- Mercado-Pimentel, M. E., A. D. Hubbard, et al. (2007). "Endoglin and Alk5 regulate epithelial-mesenchymal transformation during cardiac valve formation." Dev Biol **304**(1): 420-32.
- Merki, E., M. Zamora, et al. (2005). "Epicardial retinoid X receptor alpha is required for myocardial growth and coronary artery formation." Proc Natl Acad Sci U S A **102**(51): 18455-60.
- Meyer, D. and C. Birchmeier (1995). "Multiple essential functions of neuregulin in development." Nature **378**(6555): 386-90.

- Mikawa, T. and R. G. Gourdie (1996). "Pericardial mesoderm generates a population of coronary smooth muscle cells migrating into the heart along with ingrowth of the epicardial organ." *Dev Biol* **174**(2): 221-32.
- Min, C., S. F. Eddy, et al. (2008). "NF-kappaB and epithelial to mesenchymal transition of cancer." *J Cell Biochem* **104**(3): 733-44.
- Mjaatvedt, C. H., R. C. Lepera, et al. (1987). "Myocardial specificity for initiating endothelial-mesenchymal cell transition in embryonic chick heart correlates with a particulate distribution of fibronectin." *Dev Biol* **119**(1): 59-67.
- Mjaatvedt, C. H., H. Yamamura, et al. (1998). "The Cspg2 gene, disrupted in the hdf mutant, is required for right cardiac chamber and endocardial cushion formation." *Dev Biol* **202**(1): 56-66.
- Mohamed, S. A., Z. Aherrahrou, et al. (2006). "Novel missense mutations (p.T596M and p.P1797H) in NOTCH1 in patients with bicuspid aortic valve." *Biochem Biophys Res Commun* **345**(4): 1460-5.
- Molin, D. G., U. Bartram, et al. (2003). "Expression patterns of Tgfbeta1-3 associate with myocardialisation of the outflow tract and the development of the epicardium and the fibrous heart skeleton." *Dev Dyn* **227**(3): 431-44.
- Monzani, E., R. Bazzotti, et al. (2009). "AQP1 is not only a water channel: it contributes to cell migration through Lin7/beta-catenin." *PLoS One* **4**(7): e6167.
- Moore, A. W., L. McInnes, et al. (1999). "YAC complementation shows a requirement for Wt1 in the development of epicardium, adrenal gland and throughout nephrogenesis." *Development* **126**(9): 1845-57.
- Moore, A. W., A. Schedl, et al. (1998). "YAC transgenic analysis reveals Wilms' tumour 1 gene activity in the proliferating coelomic epithelium, developing diaphragm and limb." *Mech Dev* **79**(1-2): 169-84.
- Morabito, C. J., R. W. Dettman, et al. (2001). "Positive and negative regulation of epicardial-mesenchymal transformation during avian heart development." *Developmental biology* **234**(1): 204-215.
- Morgelin, M., M. Paulsson, et al. (1995). "Evidence of a defined spatial arrangement of hyaluronate in the central filament of cartilage proteoglycan aggregates." *Biochem J* **307** (Pt 2): 595-601.
- Mylonakis, E. and S. B. Calderwood (2001). "Infective endocarditis in adults." *N Engl J Med* **345**(18): 1318-30.
- Nakajima, Y., V. Mironov, et al. (1997). "Expression of smooth muscle alpha-actin in mesenchymal cells during formation of avian endocardial cushion

- tissue: a role for transforming growth factor beta3." Dev Dyn **209**(3): 296-309.
- Newman, P. J., M. C. Berndt, et al. (1990). "Pecam-1 (Cd31) Cloning and Relation to Adhesion Molecules of the Immunoglobulin Gene Superfamily." Science **247**(4947): 1219-1222.
- Ng, C. M., A. Cheng, et al. (2004). "TGF-beta-dependent pathogenesis of mitral valve prolapse in a mouse model of Marfan syndrome." J Clin Invest **114**(11): 1586-92.
- Niessen, K., Y. Fu, et al. (2008). "Slug is a direct Notch target required for initiation of cardiac cushion cellularization." J Cell Biol **182**(2): 315-25.
- Niu, S., J. J. Bahl, et al. (1998). "Structure, regulation and function of avian glycan." J Mol Cell Cardiol **30**(3): 537-50.
- Niwa, H., J. Miyazaki, et al. (2000). "Quantitative expression of Oct-3/4 defines differentiation, dedifferentiation or self-renewal of ES cells." Nat Genet **24**(4): 372-6.
- Norris, R. A., R. A. Moreno-Rodriguez, et al. (2008). "Periostin regulates atrioventricular valve maturation." Dev Biol **316**(2): 200-13.
- Olivey, H. E., L. A. Compton, et al. (2004). "Coronary vessel development: the epicardium delivers." Trends in cardiovascular medicine **14**(6): 247-51.
- Olivey, H. E., N. A. Mundell, et al. (2006). "Transforming growth factor-beta stimulates epithelial-mesenchymal transformation in the proepicardium." Dev Dyn **235**(1): 50-9.
- Olivey, H. E. and E. C. Svensson (2010). "Epicardial-myocardial signaling directing coronary vasculogenesis." Circulation research **106**(5): 818-32.
- Ozdamar, B., R. Bose, et al. (2005). "Regulation of the polarity protein Par6 by TGFbeta receptors controls epithelial cell plasticity." Science **307**(5715): 1603-9.
- Paige, S. L., S. Thomas, et al. (2012). "A temporal chromatin signature in human embryonic stem cells identifies regulators of cardiac development." Cell **151**(1): 221-32.
- Parikh, N. I., P. Gona, et al. (2009). "Long-term trends in myocardial infarction incidence and case fatality in the National Heart, Lung, and Blood Institute's Framingham Heart study." Circulation **119**(9): 1203-10.
- Partanen, J., E. Armstrong, et al. (1992). "A Novel Endothelial-Cell Surface-Receptor Tyrosine Kinase with Extracellular Epidermal Growth-Factor Homology Domains." Molecular and Cellular Biology **12**(4): 1698-1707.

- Paruchuri, S., J. H. Yang, et al. (2006). "Human pulmonary valve progenitor cells exhibit endothelial/mesenchymal plasticity in response to vascular endothelial growth factor-A and transforming growth factor-beta2." *Circ Res* **99**(8): 861-9.
- Pentassuglia, L. and D. B. Sawyer (2009). "The role of Neuregulin-1beta/ErbB signaling in the heart." *Exp Cell Res* **315**(4): 627-37.
- Perego, C., C. Vanoni, et al. (2002). "Invasive behaviour of glioblastoma cell lines is associated with altered organisation of the cadherin-catenin adhesion system." *J Cell Sci* **115**(Pt 16): 3331-40.
- Perkins, S. J., A. S. Nealis, et al. (1989). "Immunoglobulin fold and tandem repeat structures in proteoglycan N-terminal domains and link protein." *J Mol Biol* **206**(4): 737-53.
- Person, A. D., R. J. Garriock, et al. (2005). "Frzb modulates Wnt-9a-mediated beta-catenin signaling during avian atrioventricular cardiac cushion development." *Dev Biol* **278**(1): 35-48.
- Person, A. D., S. E. Klewer, et al. (2005). "Cell biology of cardiac cushion development." *Int Rev Cytol* **243**: 287-335.
- Poelmann, R. E., A. C. Gittenberger-de Groot, et al. (1993). "Development of the cardiac coronary vascular endothelium, studied with antiendothelial antibodies, in chicken-quail chimeras." *Circ Res* **73**(3): 559-68.
- Potts, J. D., J. M. Dagle, et al. (1991). "Epithelial-mesenchymal transformation of embryonic cardiac endothelial cells is inhibited by a modified antisense oligodeoxynucleotide to transforming growth factor beta 3." *Proc Natl Acad Sci U S A* **88**(4): 1516-20.
- Potts, J. D. and R. B. Runyan (1989). "Epithelial-mesenchymal cell transformation in the embryonic heart can be mediated, in part, by transforming growth factor beta." *Dev Biol* **134**(2): 392-401.
- Rabkin-Aikawa, E., M. Farber, et al. (2004). "Dynamic and reversible changes of interstitial cell phenotype during remodeling of cardiac valves." *J Heart Valve Dis* **13**(5): 841-7.
- Rabkin, E., M. Aikawa, et al. (2001). "Activated interstitial myofibroblasts express catabolic enzymes and mediate matrix remodeling in myxomatous heart valves." *Circulation* **104**(21): 2525-32.
- Red-Horse, K., H. Ueno, et al. (2010). "Coronary arteries form by developmental reprogramming of venous cells." *Nature* **464**(7288): 549-53.
- Reese, D. E., T. Mikawa, et al. (2002). "Development of the coronary vessel system." *Circ Res* **91**(9): 761-8.

- Rensen, S. S. M., P. A. F. M. Doevendans, et al. (2007). "Regulation and characteristics of vascular smooth muscle cell phenotypic diversity." *Netherlands Heart Journal* **15**(3): 100-108.
- Ricciardelli, C., A. J. Sacco, et al. (2009). "The biological role and regulation of versican levels in cancer." *Cancer Metastasis Rev* **28**(1-2): 233-45.
- Riethmacher, D., E. Sonnenberg-Riethmacher, et al. (1997). "Severe neuropathies in mice with targeted mutations in the ErbB3 receptor." *Nature* **389**(6652): 725-30.
- Rivera-Feliciano, J., K. H. Lee, et al. (2006). "Development of heart valves requires Gata4 expression in endothelial-derived cells." *Development* **133**(18): 3607-18.
- Roberts, A. E., T. Araki, et al. (2007). "Germline gain-of-function mutations in SOS1 cause Noonan syndrome." *Nat Genet* **39**(1): 70-4.
- Roberts, K. E., J. J. McElroy, et al. (2004). "BMPR2 mutations in pulmonary arterial hypertension with congenital heart disease." *Eur Respir J* **24**(3): 371-4.
- Robiolio, P. A., V. H. Rigolin, et al. (1995). "Carcinoid heart disease. Correlation of high serotonin levels with valvular abnormalities detected by cardiac catheterization and echocardiography." *Circulation* **92**(4): 790-5.
- Rodgers, L. S., S. Lalani, et al. (2008). "Differential growth and multicellular villi direct proepicardial translocation to the developing mouse heart." *Dev Dyn* **237**(1): 145-52.
- Roger, V. L., A. S. Go, et al. (2012). "Heart disease and stroke statistics--2012 update: a report from the American Heart Association." *Circulation* **125**(1): e2-e220.
- Rosati, B., F. Grau, et al. (2006). "Regional variation in mRNA transcript abundance within the ventricular wall." *J Mol Cell Cardiol* **40**(2): 295-302.
- Roussou, D. L., C. A. Pearson, et al. (2012). "Foxp-mediated suppression of N-cadherin regulates neuroepithelial character and progenitor maintenance in the CNS." *Neuron* **74**(2): 314-30.
- Ruffell, B. and P. Johnson (2005). "Chondroitin sulfate addition to CD44H negatively regulates hyaluronan binding." *Biochem Biophys Res Commun* **334**(2): 306-12.
- Ruffell, B., G. F. Poon, et al. (2011). "Differential use of chondroitin sulfate to regulate hyaluronan binding by receptor CD44 in Inflammatory and Interleukin 4-activated Macrophages." *J Biol Chem* **286**(22): 19179-90.

- Saggin, L., S. Ausoni, et al. (1988). "Troponin-T Switching in the Developing Rat-Heart." Journal of Biological Chemistry **263**(34): 18488-18492.
- Saggin, L., L. Gorza, et al. (1989). "Troponin-I Switching in the Developing Heart." Journal of Biological Chemistry **264**(27): 16299-16302.
- Sanchez, N. S. and J. V. Barnett (2012). "TGFbeta and BMP-2 regulate epicardial cell invasion via TGFbetaR3 activation of the Par6/Smurf1/RhoA pathway." Cellular signalling **24**(2): 539-48.
- Sanchez, N. S., C. R. Hill, et al. (2011). "The cytoplasmic domain of TGFbetaR3 through its interaction with the scaffolding protein, GIPC, directs epicardial cell behavior." Dev Biol **358**(2): 331-43.
- Sanford, L. P., I. Ormsby, et al. (1997). "TGFbeta2 knockout mice have multiple developmental defects that are non-overlapping with other TGFbeta knockout phenotypes." Development **124**(13): 2659-70.
- Sato, T., M. Gotoh, et al. (2003). "Differential roles of two N-acetylgalactosaminyltransferases, CSGalNAcT-1, and a novel enzyme, CSGalNAcT-2. Initiation and elongation in synthesis of chondroitin sulfate." J Biol Chem **278**(5): 3063-71.
- Schlueter, J., J. Manner, et al. (2006). "BMP is an important regulator of proepicardial identity in the chick embryo." Developmental biology **295**(2): 546-58.
- Schroeder, J. A., L. F. Jackson, et al. (2003). "Form and function of developing heart valves: coordination by extracellular matrix and growth factor signaling." J Mol Med **81**(7): 392-403.
- Schubert, F. R., R. C. Mootoosamy, et al. (2002). "Wnt6 marks sites of epithelial transformations in the chick embryo." Mech Dev **114**(1-2): 143-8.
- Sedmera, D., T. Pexieder, et al. (2000). "Developmental patterning of the myocardium." Anat Rec **258**(4): 319-37.
- Sengbusch, J. K., W. He, et al. (2002). "Dual functions of [alpha]4[beta]1 integrin in epicardial development: initial migration and long-term attachment." J Cell Biol **157**(5): 873-82.
- Serluca, F. C. (2008). "Development of the proepicardial organ in the zebrafish." Dev Biol **315**(1): 18-27.
- Sha, W. C., H. C. Liou, et al. (1995). "Targeted disruption of the p50 subunit of NF-kappa B leads to multifocal defects in immune responses." Cell **80**(2): 321-30.

- Shapiro, I. M., A. W. Cheng, et al. (2011). "An EMT-driven alternative splicing program occurs in human breast cancer and modulates cellular phenotype." PLoS Genet **7**(8): e1002218.
- Shelton, E. L. and K. E. Yutzey (2008). "Twist1 function in endocardial cushion cell proliferation, migration, and differentiation during heart valve development." Dev Biol **317**(1): 282-95.
- Shen, R., Y. B. Ouyang, et al. (2002). "Grap negatively regulates T-cell receptor-elicited lymphocyte proliferation and interleukin-2 induction." Mol Cell Biol **22**(10): 3230-6.
- Shi, Y. and J. Massague (2003). "Mechanisms of TGF-beta signaling from cell membrane to the nucleus." Cell **113**(6): 685-700.
- Shirai, M., K. Imanaka-Yoshida, et al. (2009). "T-box 2, a mediator of Bmp-Smad signaling, induced hyaluronan synthase 2 and Tgfbeta2 expression and endocardial cushion formation." Proc Natl Acad Sci U S A **106**(44): 18604-9.
- Shull, M. M., I. Ormsby, et al. (1992). "Targeted disruption of the mouse transforming growth factor-beta 1 gene results in multifocal inflammatory disease." Nature **359**(6397): 693-9.
- Sibilia, M., B. Wagner, et al. (2003). "Mice humanised for the EGF receptor display hypomorphic phenotypes in skin, bone and heart." Development **130**(19): 4515-25.
- Singh, R., W. M. Hoogaars, et al. (2012). "Tbx2 and Tbx3 induce atrioventricular myocardial development and endocardial cushion formation." Cell Mol Life Sci **69**(8): 1377-89.
- Smith, C. L., S. T. Baek, et al. (2011). "Epicardial-derived cell epithelial-to-mesenchymal transition and fate specification require PDGF receptor signaling." Circ Res **108**(12): e15-26.
- Smith, K. A., I. C. Joziasse, et al. (2009). "Dominant-negative ALK2 allele associates with congenital heart defects." Circulation **119**(24): 3062-9.
- Smith, T. K. and D. M. Bader (2007). "Signals from both sides: Control of cardiac development by the endocardium and epicardium." Semin Cell Dev Biol **18**(1): 84-9.
- Song, L., R. Fassler, et al. (2007). "Essential functions of Alk3 during AV cushion morphogenesis in mouse embryonic hearts." Dev Biol **301**(1): 276-86.
- Sridurongrit, S., J. Larsson, et al. (2008). "Signaling via the Tgf-beta type I receptor Alk5 in heart development." Dev Biol **322**(1): 208-18.

- Stankunas, K., C. T. Hang, et al. (2008). "Endocardial Brg1 represses ADAMTS1 to maintain the microenvironment for myocardial morphogenesis." *Dev Cell* **14**(2): 298-311.
- Stennard, F. A., M. W. Costa, et al. (2005). "Murine T-box transcription factor Tbx20 acts as a repressor during heart development, and is essential for adult heart integrity, function and adaptation." *Development* **132**(10): 2451-62.
- Stephen, L. J., A. L. Fawkes, et al. (2007). "A critical role for the EphA3 receptor tyrosine kinase in heart development." *Dev Biol* **302**(1): 66-79.
- Strutz, F., H. Okada, et al. (1995). "Identification and characterization of a fibroblast marker: FSP1." *J Cell Biol* **130**(2): 393-405.
- Sugi, Y., H. Yamamura, et al. (2004). "Bone morphogenetic protein-2 can mediate myocardial regulation of atrioventricular cushion mesenchymal cell formation in mice." *Dev Biol* **269**(2): 505-18.
- Swift, M. R. and B. M. Weinstein (2009). "Arterial-venous specification during development." *Circulation research* **104**(5): 576-88.
- Tadano, M., H. Edamatsu, et al. (2005). "Congenital semilunar valvulogenesis defect in mice deficient in phospholipase C epsilon." *Mol Cell Biol* **25**(6): 2191-9.
- Tartaglia, M., K. Kalidas, et al. (2002). "PTPN11 mutations in Noonan syndrome: molecular spectrum, genotype-phenotype correlation, and phenotypic heterogeneity." *Am J Hum Genet* **70**(6): 1555-63.
- Tartaglia, M., E. L. Mehler, et al. (2001). "Mutations in PTPN11, encoding the protein tyrosine phosphatase SHP-2, cause Noonan syndrome." *Nat Genet* **29**(4): 465-8.
- Tartaglia, M., L. A. Pennacchio, et al. (2006). "Gain-of-function SOS1 mutations cause a distinctive form of Noonan syndrome." *Nat Genet*.
- Tauseef, M., N. Knezevic, et al. (2012). "TLR4 activation of TRPC6-dependent calcium signaling mediates endotoxin-induced lung vascular permeability and inflammation." *J Exp Med* **209**(11): 1953-68.
- Tevosian, S. G., A. E. Deconinck, et al. (2000). "FOG-2, a cofactor for GATA transcription factors, is essential for heart morphogenesis and development of coronary vessels from epicardium." *Cell* **101**(7): 729-39.
- Tidball, J. G. (1992). "Distribution of collagens and fibronectin in the subepicardium during avian cardiac development." *Anat Embryol (Berl)* **185**(2): 155-62.

- Tidball, J. G. (1992). "Identification and distribution of a novel, collagen-binding protein in the developing subepicardium and endomyxium." J Biol Chem **267**(29): 21211-9.
- Timmerman, L. A., J. Grego-Bessa, et al. (2004). "Notch promotes epithelial-mesenchymal transition during cardiac development and oncogenic transformation." Genes Dev **18**(1): 99-115.
- Tjew, S. L., K. L. Brown, et al. (2005). "Expression of N-acetylglucosamine 6-O-sulfotransferases (GlcNAc6STs)-1 and -4 in human monocytes: GlcNAc6ST-1 is implicated in the generation of the 6-sulfo N-acetyllactosamine/Lewis x epitope on CD44 and is induced by TNF-alpha." Glycobiology **15**(7): 7C-13C.
- Tomanek, R. J., A. Sandra, et al. (2001). "Vascular endothelial growth factor and basic fibroblast growth factor differentially modulate early postnatal coronary angiogenesis." Circ Res **88**(11): 1135-41.
- Townsend, T. A., J. Y. Robinson, et al. (2011). "BMP-2 and TGFbeta2 shared pathways regulate endocardial cell transformation." Cells Tissues Organs **194**(1): 1-12.
- Townsend, T. A., J. Y. Robinson, et al. (2011). "Endocardial cell epithelial-mesenchymal transformation requires Type III TGFbeta receptor interaction with GIPC." Cellular signalling **24**(1): 247-56.
- Townsend, T. A., J. L. Wrana, et al. (2008). "Transforming growth factor-beta-stimulated endocardial cell transformation is dependent on Par6c regulation of RhoA." J Biol Chem **283**(20): 13834-41.
- Tran, D. D., C. A. Corsa, et al. (2011). "Temporal and spatial cooperation of Snail1 and Twist1 during epithelial-mesenchymal transition predicts for human breast cancer recurrence." Mol Cancer Res **9**(12): 1644-57.
- Trapnell, C., L. Pachter, et al. (2009). "TopHat: discovering splice junctions with RNA-Seq." Bioinformatics **25**(9): 1105-11.
- Troyanovsky, B., T. Levchenko, et al. (2001). "Angiomotin: an angiostatin binding protein that regulates endothelial cell migration and tube formation." J Cell Biol **152**(6): 1247-54.
- Vallabhapurapu, S. and M. Karin (2009). "Regulation and function of NF-kappaB transcription factors in the immune system." Annu Rev Immunol **27**: 693-733.
- van Wijk, B., Q. D. Gunst, et al. (2012). "Cardiac regeneration from activated epicardium." PLoS One **7**(9): e44692.

- Verstrepen, L., T. Bekaert, et al. (2008). "TLR-4, IL-1R and TNF-R signaling to NF-kappaB: variations on a common theme." Cell Mol Life Sci **65**(19): 2964-78.
- Vetter, G., A. Le Bechec, et al. (2009). "Time-resolved analysis of transcriptional events during SNAI1-triggered epithelial to mesenchymal transition." Biochem Biophys Res Commun **385**(4): 485-91.
- Vieira, J. M. and P. R. Riley (2011). "Epicardium-derived cells: a new source of regenerative capacity." Heart **97**(1): 15-9.
- Viragh, S. and C. E. Challice (1981). "The origin of the epicardium and the embryonic myocardial circulation in the mouse." Anat Rec **201**(1): 157-68.
- von Gise, A. and W. T. Pu (2012). "Endocardial and epicardial epithelial to mesenchymal transitions in heart development and disease." Circ Res **110**(12): 1628-45.
- Vrljicak, P., A. C. Chang, et al. (2010). "Genomic analysis distinguishes phases of early development of the mouse atrio-ventricular canal." Physiol Genomics **40**(3): 150-7.
- Vrljicak, P., R. Cullum, et al. (2012). "Twist1 transcriptional targets in the developing atrio-ventricular canal of the mouse." PLoS One **7**(7): e40815.
- Wang, B., J. Weidenfeld, et al. (2004). "Foxp1 regulates cardiac outflow tract, endocardial cushion morphogenesis and myocyte proliferation and maturation." Development **131**(18): 4477-87.
- Wang, J., S. Sridurongrit, et al. (2005). "Atrioventricular cushion transformation is mediated by ALK2 in the developing mouse heart." Dev Biol **286**(1): 299-310.
- Wang, L., E. R. Hauser, et al. (2007). "Peakwide mapping on chromosome 3q13 identifies the kalirin gene as a novel candidate gene for coronary artery disease." Am J Hum Genet **80**(4): 650-63.
- Wang, Q., R. S. Reiter, et al. (2001). "Comparative studies on the expression patterns of three troponin T genes during mouse development." Anatomical Record **263**(1): 72-84.
- Wang, X. F., H. Y. Lin, et al. (1991). "Expression cloning and characterization of the TGF-beta type III receptor." Cell **67**(4): 797-805.
- Wei, Q., N. R. Manley, et al. (2011). "Whole mount *in situ* hybridization of E8.5 to E11.5 mouse embryos." J Vis Exp(56).
- Wessels, A. and J. M. Perez-Pomares (2004). "The epicardium and epicardially derived cells (EPDCs) as cardiac stem cells." Anat Rec A Discov Mol Cell Evol Biol **276**(1): 43-57.

- Wiater, E., C. A. Harrison, et al. (2006). "Identification of distinct inhibin and transforming growth factor beta-binding sites on betaglycan: functional separation of betaglycan co-receptor actions." J Biol Chem **281**(25): 17011-22.
- Wilm, B., A. Ipenberg, et al. (2005). "The serosal mesothelium is a major source of smooth muscle cells of the gut vasculature." Development **132**(23): 5317-28.
- Wilting, J., K. Buttler, et al. (2007). "The proepicardium delivers hemangioblasts but not lymphangioblasts to the developing heart." Developmental biology **305**(2): 451-9.
- Wirrig, E. E., B. S. Snarr, et al. (2007). "Cartilage link protein 1 (Crtl1), an extracellular matrix component playing an important role in heart development." Dev Biol **310**(2): 291-303.
- Wu, B., Z. Zhang, et al. (2012). "Endocardial cells form the coronary arteries by angiogenesis through myocardial-endocardial VEGF signaling." Cell **151**(5): 1083-96.
- Yang, J. T., H. Rayburn, et al. (1995). "Cell adhesion events mediated by alpha 4 integrins are essential in placental and cardiac development." Development **121**(2): 549-60.
- You, H. J., T. How, et al. (2009). "The type III transforming growth factor-beta receptor negatively regulates nuclear factor kappa B signaling through its interaction with beta-arrestin2." Carcinogenesis **30**(8): 1281-7.
- Yu, H., P. M. Smallwood, et al. (2010). "Frizzled 1 and frizzled 2 genes function in palate, ventricular septum and neural tube closure: general implications for tissue fusion processes." Development **137**(21): 3707-17.
- Yu, S., D. Crawford, et al. (2011). "The chemokine receptor CXCR7 functions to regulate cardiac valve remodeling." Dev Dyn **240**(2): 384-93.
- Yutzey, K. E., M. Colbert, et al. (2005). "Ras-related signaling pathways in valve development: ebb and flow." Physiology (Bethesda) **20**: 390-7.
- Zanin, M. K., J. Bundy, et al. (1999). "Distinct spatial and temporal distributions of aggrecan and versican in the embryonic chick heart." Anat Rec **256**(4): 366-80.
- Zeisberg, M. and E. G. Neilson (2009). "Biomarkers for epithelial-mesenchymal transitions." The Journal of clinical investigation **119**(6): 1429-37.
- Zhao, Q., A. J. Beck, et al. (2011). "Developmental ablation of Id1 and Id3 genes in the vasculature leads to postnatal cardiac phenotypes." Dev Biol **349**(1): 53-64.

- Zheng, Y., S. Vertuani, et al. (2009). "Angiomotin-like protein 1 controls endothelial polarity and junction stability during sprouting angiogenesis." Circulation research **105**(3): 260-70.
- Zhou, B., L. B. Honor, et al. (2011). "Adult mouse epicardium modulates myocardial injury by secreting paracrine factors." The Journal of clinical investigation **121**(5): 1894-904.
- Zhou, B., Q. Ma, et al. (2009). "Fog2 is critical for cardiac function and maintenance of coronary vasculature in the adult mouse heart." J Clin Invest **119**(6): 1462-76.
- Zhou, B., Q. Ma, et al. (2008). "Epicardial progenitors contribute to the cardiomyocyte lineage in the developing heart." Nature **454**(7200): 109-13.